ICARIA
Improving climate resilience of critical assets

www.icaria-project.eu

D1.2 CLIMATE PROJECTIONS AND HAZARD SCENARIOS

This project has received funding from the European Union's Horizon Europe research and innovation programme under grant agreement No. 101093806. The publication reflects only the authors' views and the European Union is not liable for any use that may be made of the information contained therein.

D1.2 ICARIA Climate projections and hazard scenarios

Summary

Deliverable D1.2, named "ICARIA Climate projections and hazard scenarios", outlines the work performed and results in T1.2 for the three case studies, namely the Metropolitan Area of Barcelona, the Salzburg Region, and the South Aegean Region. This document summarizes T1.2 activities such as input datasets like ERA5-Land reanalysis, weather observations for climate characterization, or the employment of various global and regional climate models for statistical and dynamical downscaling to generate local climate change projections. The document also takes hazards identified and defines indicators and extreme events through co-design and partner discussions.
Results, covering main climate variables and associated indicators, are extensively discussed for both statistical and dynamical downscaling methodologies. The outputs demonstrate reliable performance across simulated scenarios, projecting a warmer future with heightened heatwaves and altered rainfall patterns, carrying significant societal impacts. The document ensures the credibility of findings by appropriately assessing and explaining uncertainties. The overall discussion emphasizes coherent changes in mean climate and extreme events, aligning with current warming trends. The comprehensive approach provides a robust understanding of potential future climate scenarios and their potential consequences on the specified regions, setting this document therefore the basis of all the different climate inputs required for the following tasks and the proper consecution of the ICARIA project.

Deliverable number	Work package	
D1.2	WP1	
Deliverable lead beneficiary	**Deliverable author(s)**	**Contributor(s)**
FIC	César Paradinas Blázquez (FIC) Marianne Bügelmayer-Blaschek (AIT)	Lorena Galiano Sánchez (FIC) Darío Redolat Negro (FIC) Carlos Prado López (FIC) Kristofer Hasel (AIT) Johann Züger (AIT) Jasmin Lampert (AIT) Pascal Thiele (AIT) María Guerrero Hidalgo (CETAQUA) Alberto Couce Rodriguez (CETAQUA)
Internal reviewer(s)	**External reviewer(s)**	
Thanasis Sfetsos (DEMOKRITOS) Nadia Pol (DEMOKRITOS)	Jordi Cunillera i Grañó (SMC)	
Planned delivery date	**Actual delivery date**	
30/04/2024	30/04/2024	
Dissemination level	**x PU = Public** □ PP = Restricted to other programme participants □ RE = Restricted to a group specified by the consortium. □ CO = Confidential, only for members of the consortium	

Document history			
Date	**Version**	**Author(s)**	**Comments**
11/12/2023	1.0	César Paradinas Blázquez (FIC) Marianne Bügelmayer-Blaschek (AIT)	Draft version of the deliverable's structure and methodology.
02/02/2024	1.1	César Paradinas Blázquez (FIC) Darío Redolat Negro (FIC) Lorena Galiano Sánchez (FIC) Carlos Prado López (FIC) María Guerrero Hidalgo (CETAQUA) Alberto Couce Rodriguez (CETAQUA)	Draft version of the deliverable's contents from FIC and CETAQUA.
27/02/2024	1.2	Thanasis Sfetsos (DEMOKRITOS)	Internal review of methodology and FIC's contents in the deliverable. All suggestions have been considered.
19/04/2024	1.3	Marianne Bügelmayer-Blaschek (AIT) Kristofer Hasel (AIT) Johann Züger (AIT) Jasmin Lampert (AIT) Pascal Thiele (AIT)	Draft version of the deliverable's contents from AIT.
24/04/2024	1.4	Thanasis Sfetsos (DEMOKRITOS) Nadia Pol (DEMOKRITOS)	Internal review of AIT's contents in the deliverable and the whole document. All suggestions have been considered.
25/04/2024	1.5	César Paradinas Blázquez (FIC) Lorena Galiano Sánchez (FIC) Darío Redolat Negro (FIC) Carlos Prado López (FIC) Marianne Bügelmayer-Blaschek (AIT) Kristofer Hasel (AIT) Johann Züger (AIT) Jasmin Lampert (AIT) Pascal Thiele (AIT) María Guerrero Hidalgo (CETAQUA) Alberto Couce Rodriguez (CETAQUA)	Cleaned verDsion with inputs from all required partners and internal review considered.
29/04/2024	1.6	Jordi Cunillera i Grañó (SMC)	External review of the deliverable. All suggestions have been considered.
30/04/2024	1.7	César Paradinas Blázquez (FIC) Marianne Bügelmayer-Blaschek (AIT)	Final version of the deliverable. All suggestions have been considered and applied.

Table of contents

List of Figures

List of Tables

List of Acronyms and Abbreviations

AEMet	Agencia Estatal de Meteorología
AIT	Austrian Institute of Technology
AMB	Area Metropolitana de Barcelona (Metropolitan Area of Barcelona)
AMO	Atlantico Multidecadal Oscillation
BCASA	Barcelona Cicle de l'Aigua
CC	Climate Change
CCF	Climate Change Factor
CLM	Climate Limited-area Modelling-Community
CM	Climate Model
CS	Case Study
CDO	Climate Data Online (NOAA)
CMIP	Coupled Model Intercomparison Project
C3S	Copernicus Climate Change Service (C3S) programme
DWD	German Meteorological Service (Deutscher WetterDienst)
ECMWF	European Centre for Medium-Range Weather Forecasts
ENSO	El-Niño Southern Oscillation
ESM	Earth System Models, run in the CMIP experiments.
ERA5	Latest version of the ECMWF Re-Analysis, providing hourly data on many atmospheric, land-surface and sea-state parameters together with estimates of uncertainty.
ERA5-Land	ECMWF Re-Analysis dataset providing a consistent view of the evolution of land variables over several decades.
FIC	Fundación para la Investigación del Clima
FTP	File Transfer Protocol
GCM	Global Climate Model
HI	Heat Index
HNMS	Hellenic National Meteorological Service
ICARIA	Improving Climate Resilience of Critical Assets
IDF	Intensity-Duration-Frequency
IPCC	The Intergovernmental Panel on Climate Change
ML-OE	ML-Optimized Ensemble
MSL	Mean Sea Level
NetCDF	Network Common Data Form
NOAA	National Oceanic and Atmospheric Administration
NOA	National Observatory of Athens
RCM	Regional Climate Models
RCP	Representative Concentration Pathway
RH	Relative Humidity

SAR	South Aegean Region
SLZ	Salzburg Region
SMC	Servei Meteorologic de Catalunya
SPEI	Standard Precipitation Evapotranspiration Index
SPI	Standard Precipitation Index
SSO	Specific Sub-Objectives
SSP	Shared Socio-Economic Pathway
PdE	Puertos del Estado
UHI	Urban Heat Island
UNFCC	United Nations Framework Convention on Climate Change
UTCI	Universal Thermal Confort Index
WCRP	World Climate Research Programme
WGCP	Working Group on Coupled Modeling
WP	Work Package
WRF	Weather Research and Forecasting
WMO	World Meteorological Organization
ZAMG	Austrian Central Institute for Meteorology and Geodynamics (Zentralanstalt für Meteorologie und Geodynamik)

Executive summary

One of the main problems that climate change poses for the future, and even current human activities and well-being at the European level, is the impact it may have on the main sectors of economic activity and the critical infrastructure built around them. To meet this challenge as the climate emergency becomes already a reality, it is necessary to have good quality, updated state-of-the-art local-scale future climate information to enable the necessary measures to be taken to better adapt to the expected climate impacts. Climate change impact analysis is one of the strengths of ICARIA, displayed in one of the main and specific objectives detailed in ICARIA's project, the obtaining and delivery of updated local climate change projections, explained in the Specific Sub-Objective 2 (SSO2 - Obtaining tailored scenarios for the case studies regions). To cover and justify this aim, this D1.2 deliverable provides detailed information on the outputs of ICARIA's task T1.2 "Climate scenario building".

This document explains throughout its extension the different datasets used to perform the needed activities contemplated in T1.2, such as the use of ERA5-Land reanalysis and weather observations for climate characterization and verification procedures, or the different global and regional climate models utilized. These different input sources are used to generate the local climate change projections through a two-methods approach, by a statistical and a dynamical downscaling of different CMIP6 models, using both or just one method depending on the case study; methodologies which are correspondingly explained for the sake of clarity. This downscaling includes the analysis and interpretation of a set of main climate variables, like temperature, wind, rainfall or relative humidity. However, ICARIA's main concern recalls the effects of climate hazards on the Metropolitan Area of Barcelona, the Salzburg Region and the South Aegean Region, for which it is required to define and project into the future a set of indicators and extreme events that would help with the modelling in WP2. These indicators are therefore defined in this document after a co-design and discussion amongst the partners involved.

After all the necessary methodological explanations, at the end of the document, it is possible to find a detailed discussion of all the results coming from both main climate variables and their linked indicators and hazards. These results are discussed for both methodologies used and detailed in each of the case studies considered. Verification of outputs shows an adequate performance of both methodologies, and that results are trustworthy for all simulated scenarios, with uncertainties being properly assessed and explained. Both mean climate and extreme events simulations project coherent changes with the current warming trends, depicting a much warmer future where high temperatures and heat waves will cause severe impacts on society, and rainfall patterns will change towards more sparse and extreme events.

1. Introduction

This document presents the *climate projections and hazard scenarios* developed within the ICARIA project, which has received funding from the European Union's Horizon Europe Research and Innovation program under Grant Agreement number 101093806. Specifically, this document corresponds to Deliverable 1.2 and is one of the results of Task 1.2 - Climate scenario building (WP1 - Project framework, climate scenarios and modelling inputs).

1.1. ICARIA in short

The number of climate-related disasters has been progressively increasing in the last two decades and this trend could be drastically exacerbated in the medium- and long-term horizons according to climate change projections. It is estimated that, between 2000 and 2019, 7,348 natural hazard-related disasters such as heat waves, forest fires, droughts, floods, or storms caused 2.97 trillion US$ losses and affected 4 billion people worldwide. These estimates include compound and cascading events whose increasing frequency is a direct expression of ongoing climate change and related global warming (UNDRR, 2020; IPCC, 2021). For the future, by mid-century, the world stands to lose around 10% of total economic value from climate change if the temperature increases stay on the current trajectory, and both the Paris Agreement and 2050 net-zero emissions targets are not met (Guo *et al.,* 2021).

In this framework, the **ICARIA Project** (Improving ClimAte Resilience of crItical Assets) has the overall objective of promoting the definition and the use of a holistic asset-level modelling framework to achieve a better understanding of climate-related impacts produced by complex interactions, characterised by compound events and cascading effects, and the possible risk reduction provided by suitable, sustainable, and cost-effective adaptation solutions.

Special regard is devoted to critical assets and services that are particularly susceptible to climate change as its local effects can lead to significant increases in the cost of potential losses for unplanned outages and failures, as well as maintenance – unless an effort is undertaken in making these risk receptors more resilient. Therefore, ICARIA aims to understand how climate might affect the life-cycle costs of these assets and services in the coming decades and to ensure that, whenever possible, investments in adaptation solutions are made upfront to face these changes. This requires planning that considers a comprehensive multi-hazard risk/impact assessment and the uncertainties associated with climate change, rather than reliance on models solely based on past events and single climate hazards (Barr & Nider, 2015).

To achieve this goal, ICARIA has identified has identified three Strategic Sub-Objectives (SSO) that are directly linked to the activities held in WP1 from which two T1.2 tackles

- SSO2 - Obtaining tailored scenarios for the case studies regions;
- SSO3 - Quantify uncertainty and manage data gaps through model input requirements and innovative methods.

1.2. Objective and Structure of the Deliverable 1.2

In the current context where the changing climate determines a different future to be considered, weather and climate-related information become one of the core inputs of ICARIA. This information ought to be viable, accurate and reliable to guarantee that the best information is used as input for the project's outcomes. This ensures that the project's results are based on the best data available and can effectively support effective decision-making amidst the dynamics of a changing climate. During this first part of the ICARIA project, T1.2 was aimed at producing up-to-date climate information, obtaining and providing post-processed local-scale climate scenarios for the three case study regions, with their projected changes up to the year 2100, plus information on climate-related hazards from regional downscaled climate change projections. This work allows T1.2 to determine future variations in the main climate variables, with a special focus on extreme events frequency and intensity (e.g. heavy rains, drought, storm winds, storm surges, heatwaves). These outputs are of vital importance for ICARIA since they will construct the basis of the current and future climate conditions that will structure and feed the coming tasks.

The present D1.2 document summarises these aforementioned results and the work needed for them to be obtained, having as the main objective to provide a comprehensive overview of the methodologies, datasets, and results, focusing on the expected climate dynamics and their related impact projection according to the hazard changes estimated. This primary objective of explaining the intricate processes undertaken to characterize climate inputs for ICARIA will help set the floor for their appropriate use in the next WPs. Some of the other objectives of this document are related to understanding and projecting climate impacts.

- It delves into the utilization of specific datasets, such as ERA5-Land reanalysis and weather observations, forming the foundation for the analysis of climate conditions in Task 1.2.
- The focus extends to elucidating the application of global and regional climate models, detailing techniques like statistical and dynamical downscaling. This provides insights into how these models contribute to the generation of local climate change predictions.
- Acknowledging the importance of anticipating climate hazards, the document concentrates on defining indicators and extreme events. These definitions result from collaborative discussions among project partners, ensuring a comprehensive understanding of potential risks.
- The core of the document is dedicated to presenting results from climate projections, with a meticulous analysis covering main climate variables like temperature, wind, rainfall, and relative humidity. This analysis extends to examining associated indicators and hazards, with a focus on specific case studies, namely, the Metropolitan Area of Barcelona, the Salzburg Region, and the South Aegean Region.

This deliverable is a critical component in advancing ICARIA's understanding of regional climate change and its potential repercussions. In order to achieve its objectives, the document is structured in a way that aims to flow from the input needed to start, going through the core of the methodologies applied or the analysis work undergone in ICARIA, and ending as the last step with the results.

- **Input data**
    - Explanation of the datasets used, such as the role of ERA5-Land reanalysis and weather observations.

    - Discussion on the chosen models in climate characterization.
- **Future climate information**
    - Detailed insights into the statistical and dynamical downscaling methods, elucidating their individual contributions and the criteria guiding their selection.
    - Comprehensive explanation of the comparison of both methods applied in the study.
- **Climate variables and hazards**
    - Presentation of the collaborative process employed in defining indicators and extreme events, and the rationale behind them and their relevance to the specified regions.
    - Definition in detail of each indicator and where they apply regarding Trials and Mini-Trials.
- **Discussion of results**
    - Thorough analysis of the outcomes derived from the projections.
    - Discussion of main climate variables, indicators, and hazards, with a focus on case studies for the Metropolitan Area of Barcelona, the Salzburg Region, and the South Aegean Region.
- **Conclusions**
    - Summarization of key findings.
    - Implications of the results for the ICARIA project and broader implications for understanding regional climate dynamics.

In addition, in the Annexes it can be found for more information:

- **Data Management Statement**, with information on all used and produced datasets.
- **Verification and Uncertainty Assessment**:
    - Examination of the methodologies used to verify the outputs of both methodologies and its results. Impact on the uncertainty chain considered for final climate outcomes.
- **Definition of considered climate change indicators**

This structured approach ensures a clear and comprehensive exploration of the methodologies and results encompassed in Task 1.2, contributing significantly to ICARIA's overarching goals in climate research and impact projection.

2. Input data

The work that has taken place during T1.2 to obtain future climate projections as output needs to be fed with a multiple set of data depending on the needs of each of the two downscaling methodologies that have been applied for ICARIA. This section will summarize this input information depending on the time scale that it covers and the purpose it has served. Mainly, two types of data are considered, that that covers or studies the historic climate, and the one that is used to peek at how climate change will affect past climate towards the future.

2.1. Past climate information

In order to analyze and understand where we are coming from, it is necessary to study and acknowledge what the climate has been like in the past and present days. The main purpose of this is to characterize the past climate and establish what was it like when most of present infrastructures and services were designed and built up, what were they designed to be resilient to; previously recorded extreme situations that led to damages and the definition of what today is categorized as hazard. This climate baseline is what is taken as a comparison point, established now for this ICARIA project in the years 1986-2014. Furthermore, in climate science, 30 years are considered to depict the mean climate state to smoothen short-term variability, as defined by the World Meteorological Organization (WMO[1]).

Past information, as gained through observations and reanalysis data, is used for verification purposes, checking when put in contrast to historical simulations how climate models behave, but also to feed statistical downscaling procedures. There are two main sources to obtain this information: reanalysis and weather observations.

2.1.1. Reanalysis

The most reliable validation for surface meteorological and climatological variables comes from data recorded by either manual or automatic stations, which are weather observations. Nevertheless, there are instances where the spatial distribution or temporal coverage of these stations is inadequate, leading to inconsistencies and inhomogeneities. Furthermore, it is important to note that observations present single-point conditions that can, but do not have to represent its surroundings. Recognizing these limitations, within ICARIA it was chosen to also use reanalysis data for verification and training purposes, as they offer improved spatial-temporal coherence and physical consistency.

Climate reanalysis combines numerical weather models with assimilated observations, furnishing numerical and physical representations of recent climate conditions. These encompass estimates of atmospheric variables like air temperature, pressure, and wind at various levels, as well as surface variables such as rainfall, soil moisture content, ocean-wave height, and sea-surface temperature. Offering temporal and spatial coverage across the entire globe, these estimates span multiple decades or more (source: ECMWF[2]).

[1] https://community.wmo.int/en/wmo-climatological-normals
[2] https://www.ecmwf.int/en/research/climate-reanalysis

Since the case studies within ICARIA (Barcelona Metropolitan Area, South Aegean Region, Salzburg) are located inland or in coastal areas, not covering marine areas, the chosen atmospheric reanalysis for ICARIA is the European reanalysis ERA5-Land. This selection is based on several considerations: 1) it is developed by the European Centre for Medium-Range Weather Forecasts (ECMWF), whose primary operational area aligns with the geographical scope of ICARIA and is renowned for delivering top-notch weather forecasts, 2) it represents the latest version of the European reanalysis, boasting enhanced spatial and temporal resolution compared to its predecessors, and 3) it is freely accessible for download through the Copernicus program's Climate Change Service (C3S, 2019)

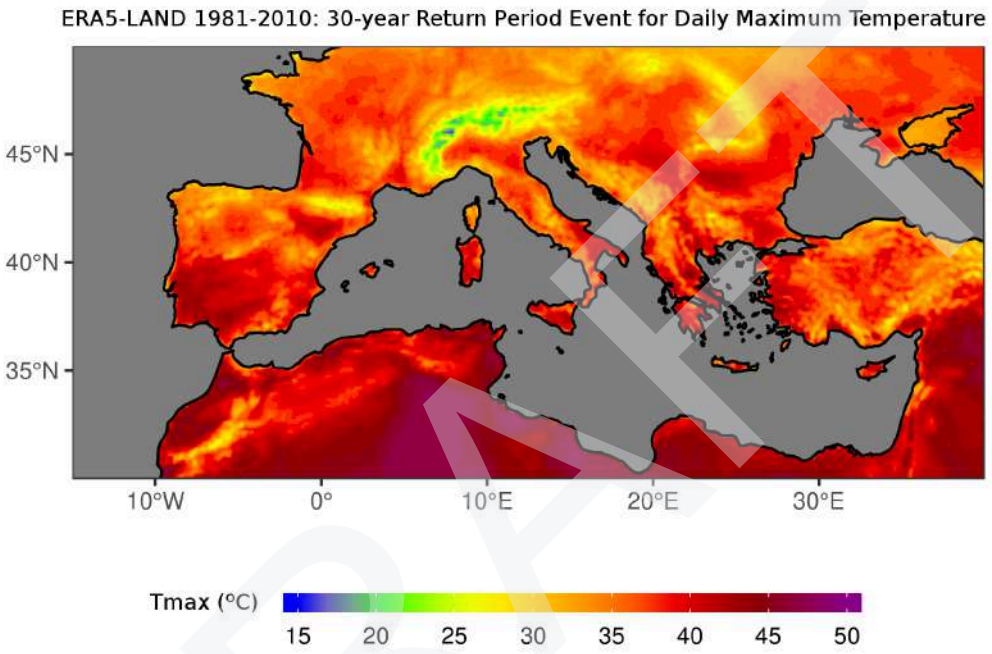

Figure 1. Example of the spatial representation of ERA5-Land reanalysis, representing a 30-year return period event for daily maximum temperature. (Source: C3S)

ERA5-Land is the most recent reanalysis developed by the ECMWF. Released in July 2019, it provides hourly data with a temporal coverage that goes from 1950 to the present day (with a delay of about three months relative to the actual date), and it is still being expanded backwards as climate and computational science progresses. It only covers land terrain, but worldwide and with a global grid of 0.1°x 0.1 spatial resolution (9km approx. at mid-latitude).

From all the variables available to download, only some of them were first identified to be used; mostly those related to the usual atmospheric observations needed from weather stations: 2m Air Temperature, Dew point Temperature, Total Precipitation, U Component of the Wind, V Component of the Wind.

Table 1. Variables and their main characteristics selected from ERA5-Land.

Variable	Daily scale	Comments
Hourly temperature	-Maximum temperature -Minimum temperature -Mean temperature	Hourly temperature values allow us to obtain with great detail not only maximum and minimum daily temperature but also to obtain mean daily temperature with more significance than when obtained only with max and min values.

Hourly dew point temperature	-Maximum relative humidity -Minimum relative humidity -Heat Index	Dew point Temperature is a variable that points at which temperature value the atmosphere would reach saturation and its moisture would start condensing in droplets. Therefore, it is an indicator of the net content of moisture of the atmosphere, being useful to get the Specific Humidity (q); moreover, the closest this value is to the actual temperature, the higher that Relative Humidity (RH) will be.
Hourly precipitation	24-h accumulation of precipitation	Precipitation hourly values have been aggregated at daily intervals to obtain the 24-h accumulation of precipitation for each day to obtain total precipitation for each point and the maximum precipitation accumulated. Precipitation units were adapted from "m" to "mm" for a more intuitive use.
Hourly wind (U and V components)	Maximum daily mean wind	In the case of wind, ERA5-Land available hourly data corresponds to both U and V wind components with the hourly mean values. Both components have been composed at hourly intervals according to the following rule: Wind = $\sqrt{(U^2 + V^2)}$ since U and V are vectorial components of the wind module.

2.1.2. Weather observations

As a basis for local point data, surface observations were gathered for all of ICARIA's pilot areas. This involved creating a comprehensive database with long-standing weather observations (ideally 30 years, or for verification purposes, at least 2.000 registers), thanks to the collaboration with various meteorological national centers or the open-access policies developed by them. In the cases where no data was freely available, other sources were sought such as historical records of WMO or those from the National Oceanic and Atmospheric Administration (NOAA) through its CDO[3] tool, where over 80,000 worldwide quality-controlled Weather Station summaries are freely available; this resource proves to be invaluable in regions lacking their weather information or where data is unavailable for various reasons.

Figure 2. Example of European stations' distribution of daily data summaries freely available at NOAA's CDO tool. No data on Spain, but several can be retrieved for Salzburg and South Aegean case studies.

[3] https://www.ncdc.noaa.gov/cdo-web/

To ensure data quality, observed data underwent thorough evaluation and treatment, with tests for inhomogeneities, outliers, anomalies or trend changes, discarding entries that did not meet minimum quality requirements. The outcome is a high-quality observed database for study areas where observed information could be collected. For more details about these procedures and quality results, please refer to **Annex 2**.

Hereafter there is a resume of the weather observations retrieved for each CS, their number, location and respective source.

The Barcelona Metropolitan Area (Area Metropolitana de Barcelona -AMB-)

For the case study of AMB there are several sources of information available since in this area there are different entities at the local, regional and national scale collaborating in monitoring the weather. After tight collaboration and support of these entities for ICARIA and other research activities, observed data for AMB and its watersheds were sought from four distinct sources (refer to Figures X and X). These sources include the Spanish Meteorological Agency (AEMet, *Agencia Estatal de Meteorología*), Catalan Meteorological Service (SMC, *Servei Meteorologic de Catalunya*), Spanish State Ports (PdE, *Puertos del Estado*), and Barcelona Cicle de l'Aigua (BCASA).

1. AEMet has provided daily data for the Ter-Llobregat system, which is the hydrological area of influence of Barcelona, also covering the AMB. These data cover precipitation, temperature, relative humidity and wind.
2. SMC has provided on-demand precipitation, temperature, relative humidity and wind hourly data for the metropolitan area, plus sub-hourly rainfall measurements.
3. PdE provides data freely on its website. Hourly data on waves and daily data on sea level were retrieved in this case.
4. BCASA data provided during the RESCCUE project for hourly precipitation for the AMB were reused.

A summary of the available stations and the data sources is shown in Table 2, including temporal resolution and number of stations. It must be noted that the final number of useful stations shown in that table is calculated after all quality tests have been passed.

Table 2. Stations provided for the meteorological variables to study for AMB and its watersheds (Ter and Llobregat river basins). The variable name, its temporal resolution, the original number of provided stations, the final number of useful stations and the data source are shown.

Variable	Temporal resolution	Number of provided stations	Number of useful stations	Source
Precipitation	Hourly	92	79	SMC
Precipitation	1-minute	12	12	SMC
Temperature	Hourly	90	75	SMC
Wind (mean & gust)	Hourly	52	44	SMC
Relative Humidity	Hourly	84	79	SMC
Precipitation	Daily	95	95	AEMet
Temperature	Daily	78	78	AEMet
Wind (mean & gust)	Daily	14	13	AEMet
Relative Humidity	Daily	87	34	AEMet
Precipitation	Hourly	26	26	BCASA
Waves	Hourly	11	11	PdE
Sea level	Daily	1	1	PdE

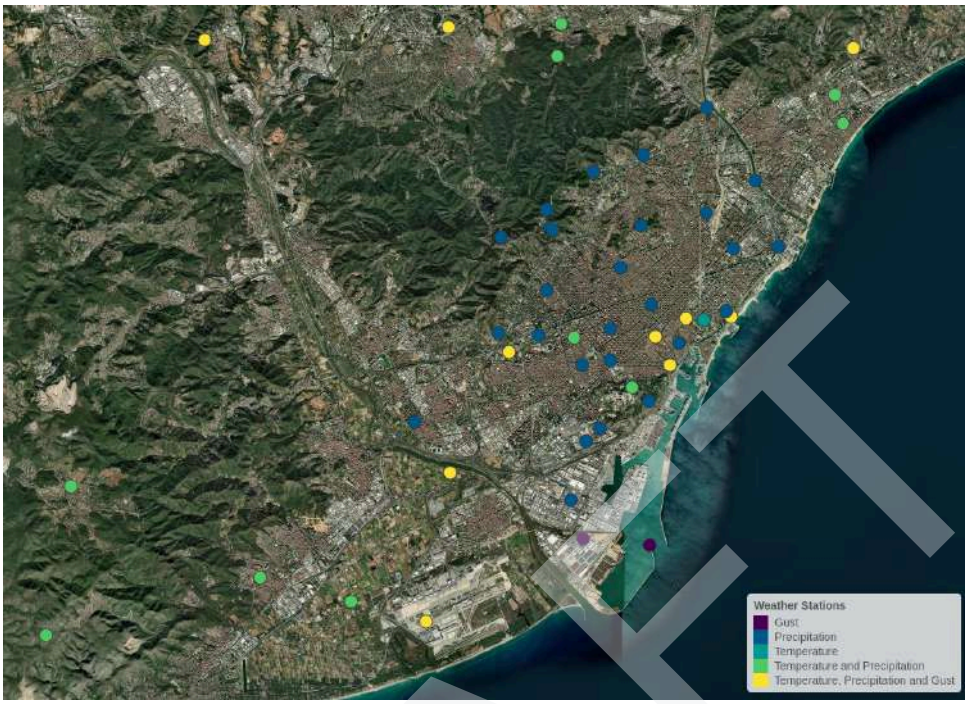

Figure 3. AMB CS stations' distribution for AMB area, depending on the types of variables collected.

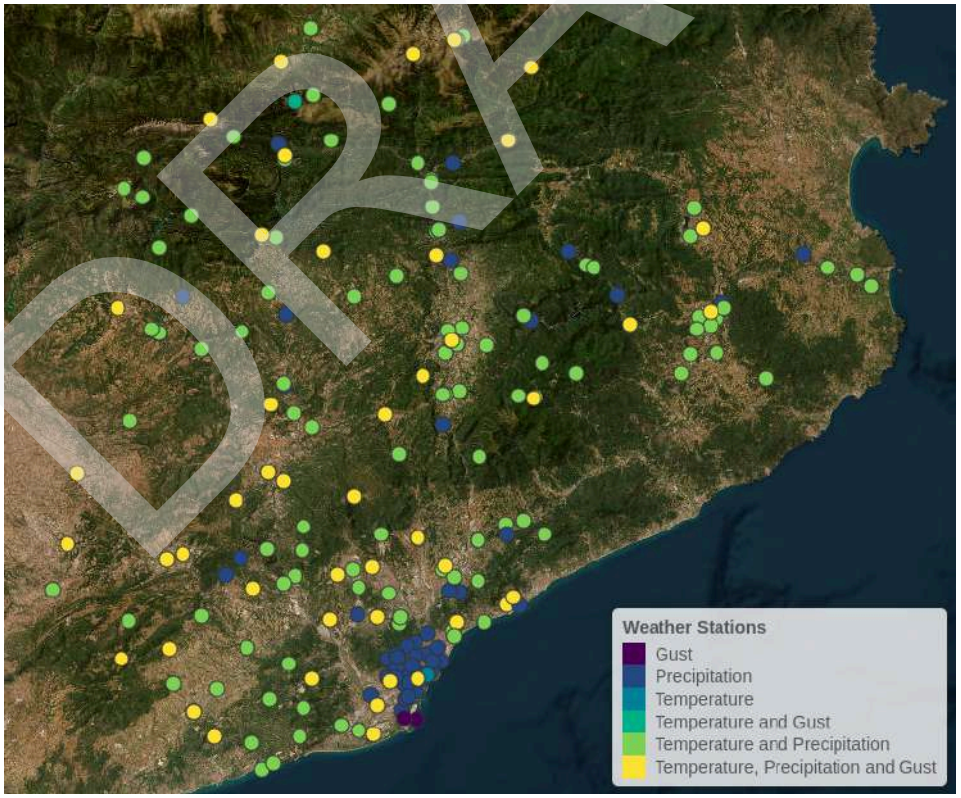

Figure 4. AMB CS stations' distribution for river watersheds considered, depending on the types of variables collected.

The South Aegean Region

For the SAR case study the available information was scarcer, but still different sources of information were considered. The data for weather observations come from two main sources, the official Hellenic National Meteorological Service (HNMS, or EMY after Εθνική Μετεωρολογική Υπηρεσία) and the weather portal Meteo.gr[4].

1. HNMS data is not freely available on their website, so data was retrieved from NOAA's CDO tool, both from their Daily Summaries and the WMO data. Daily data for temperature, precipitation, wind and RH were obtained for the SAR areas of study.
2. Meteo.gr is a portal that encompasses all the professional and official weather stations managed by the National Observatory of Athens (NOA[5]). This high-quality data was retrieved from monthly summaries and assembled together at a daily scale for temperature, precipitation, wind and RH variables.

A summary of the available stations and the data sources is shown in Table 3, including temporal resolution and number of stations. It must be noted that the final number of useful stations shown in that table is calculated after all quality tests have been passed.

Table 3. Stations provided for the meteorological variables to study for SAR. The variable name, its temporal resolution, the original number of provided stations, the final number of useful stations and the data source are shown.

Variable	Temporal resolution	Number of provided stations	Number of useful stations	Source
Precipitation	Daily	8	3	HNMS (NOAA)
Temperature	Daily	8	6	HNMS (NOAA)
Wind	Daily	8	7	HNMS (NOAA)
Relative Humidity	Daily	8	8	HNMS (NOAA)
Precipitation	Daily	2	2	HNMS (WMO)
Temperature	Daily	2	2	HNMS (WMO)
Precipitation	Daily	9	9	Meteo.gr (NOA)
Temperature	Daily	9	9	Meteo.gr (NOA)
Wind (mean & gust)	Daily	9	9	Meteo.gr (NOA)
Relative Humidity	Daily	9	8	Meteo.gr (NOA)

[4] https://meteo.gr/about-meteo.cfm
[5] https://www.noa.gr/

Figure 5. SAR stations' distribution for Syros and Naxos islands, depending on the types of variables collected.

Figure 6. SAR stations' distribution for Kos and Rhodes islands, depending on the types of variables collected.

The Salzburg Region

Regarding the SLZ case study, there was plenty of available information covering the whole region in an open-access way, so, therefore, its obtaining was easier than in other cases. Besides, despite being SLZ region a large one to study and with enough data from the Austrian side, due to its location very close to the German border, also data from the German institute was considered to enrich the possible outcomes of the project. Therefore, for SLZ, two different data sources were considered to cover this case's needs: weather data from the Austrian Central Institute for Meteorology and Geodynamics (ZAMG, after *Zentralanstalt für Meteorologie und Geodynamik*), and also from the neighbouring German Weather Service (DWD, from *Deutscher Wetterdienst*).

1. ZAMG data is freely available on their website through an intuitive GIS platform. Data was downloaded covering sub-daily data for temperature, precipitation, wind and dew point variables.
2. DWD data is also available for public download from their server using an FTP interface. Through these means, sub-daily data was collected for temperature, precipitation, wind and RH variables.

A summary of the available stations and the data sources is shown in Table 4, including temporal resolution and number of stations. It must be noted that the final number of useful stations shown in that table is calculated after all quality tests have been passed.

Table 4. Stations provided for the meteorological variables to study for SLZ. The variable name, its temporal resolution, the original number of provided stations, the final number of useful stations and the data source are shown.

Variable	Temporal resolution	Number of provided stations	Number of useful stations	Source
Precipitation	Hourly	47	44	ZAMG
Temperature	Hourly	47	43	ZAMG
Mean wind	Hourly	48	44	ZAMG
Wind gust	Hourly	3	3	ZAMG
Dew point	Hourly	45	44	ZAMG
Precipitation	Hourly	14	14	DWD
Temperature	Hourly	14	14	DWD
Mean wind	Hourly	2	2	DWD
Wind gust	Hourly	2	2	DWD
Relative Humidity	Hourly	14	14	DWD

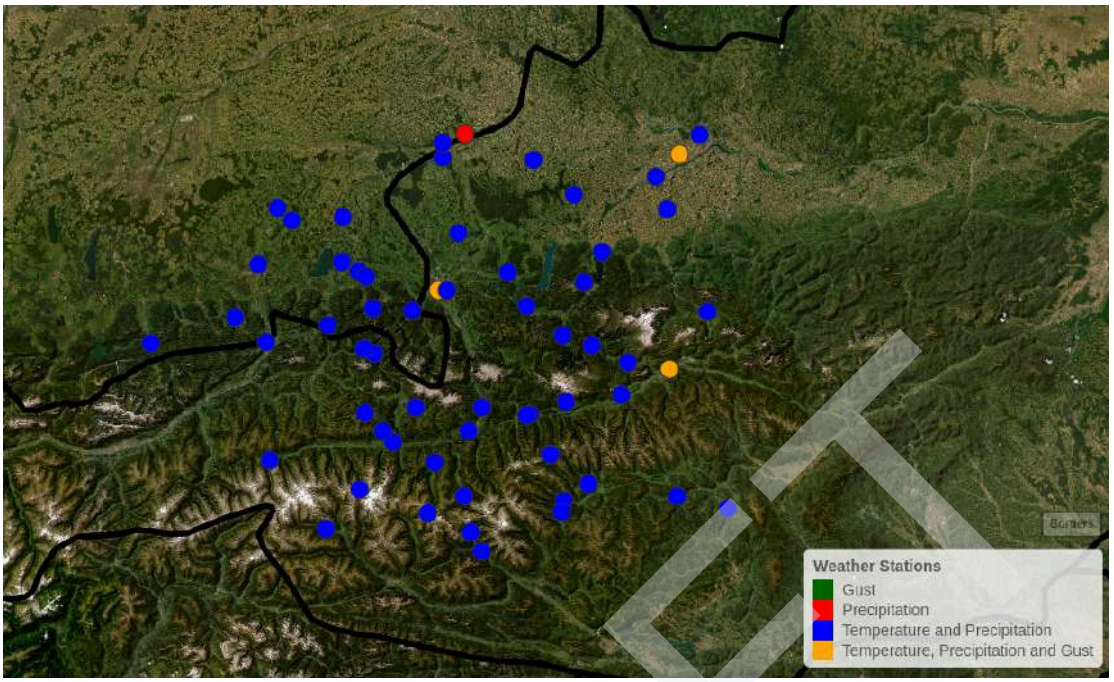

Figure 7. SLZ stations' distribution, depending on the types of variables collected.

2.2. Future climate information

2.2.1. The IPCC 6th report. CMIP6, ESMs and SSPs

The Intergovernmental Panel on Climate Change (IPCC) plays a crucial role in coordinating global efforts related to climate change. As a United Nations body, it produces comprehensive reports encompassing scientific, technical, and socio-economic information pertinent to understanding human-induced climate change risks, potential impacts, and adaptation/mitigation options. These reports significantly inform the United Nations Framework Convention on Climate Change (UNFCCC), the principal international treaty addressing climate change, which aims to stabilize greenhouse gas concentrations to prevent detrimental interference with the climate system. Widely recognized as an authoritative source, the IPCC has already published its Sixth Assessment Report (AR6[6]); endorsed by leading climate scientists and governments, it consolidates advancements and studies from the scientific community.

This IPCC's AR6 sets the basis for the state-of-the-art regarding climate change science. It works with the last version of the Global Climate Models (GCMs), clustered within the Coupled Model Intercomparison Project (CMIP[7], Eyring et al., 2016). The CMIP is a cooperative initiative aimed at enhancing our understanding of climate change. Established in 1995 by the Working Group on Coupled Modeling (WGCM) under the World Climate Research Programme (WCRP), CMIP has significantly contributed to comprehending historical, present, and future climate changes within a multi-model framework. It establishes standardized experiment protocols, forcings, and outputs. Implemented in successive phases, CMIP not only drives improvements in climate models but also supports global and national climate change assessments. In its latest (sixth) phase, CMIP has seen advancements up to the latest Earth System Models (ESMs) and also introduced new emission scenarios tailored to evolving needs for adaptation and mitigation strategies in the context of climate change.

ESMs are coupled atmosphere-land-ocean (both hydro and cryosphere) general circulation models representing all components of the climate system and including the representation of the carbon cycle, allowing the interactive calculation of atmospheric CO2 or compatible emissions. It can also include other components like. chemistry of the atmosphere or dynamic vegetation for example, which is mostly solved through static input data (e.g. leaf area index per month).

[6] https://www.ipcc.ch/assessment-report/ar6/
[7] https://wcrp-cmip.org/cmip-phase-6-cmip6/

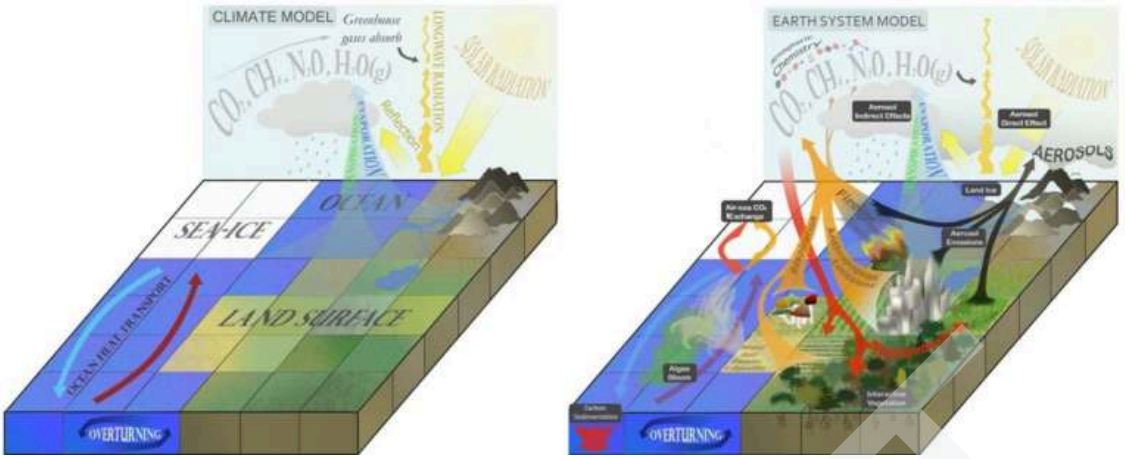

Figure 8. Key features of climate models and earth system models: ESMs gain complexity by considering the biological and chemical processes that feedback into the physics of climate. Source: ©2013 Nature Education.

Climate models utilize concentration scenarios derived from emissions scenarios to project future climate outcomes. Emissions scenarios depict plausible future substance emissions, like greenhouse gases and aerosols, based on factors like demographic, socio-economic development, land-use changes and technological evolution. The resulting climate scenarios from models offer plausible and simplified representations of future climate conditions, driven by internally coherent physical relationships. These scenarios are explicitly designed to explore the potential consequences of human-induced climate change, serving as input for impact models.

As was aforementioned, this recent CMIP6 has revamped the consideration of future GHG concentration scenarios, replacing CMIP5's Representative Concentration Pathways (RCPs) with the Shared Socioeconomic Pathways (SSPs). **The SSP approach displays a step forward from the RCPs as they provide a "story" on how society can evolve to the emission scenarios. Furthermore, the new generation of GCMs (CMIP6) provides a higher sensitivity, and higher spatial resolution and displays more severe impacts of climate change as anticipated by CMIP5**. Besides, within the IPCC report AR6 (Masson-Delmotte et al., 2021) it is also reported that CMIP6 models not only have higher spatial resolutions than previous CMIP generations, but also show an increased ability to represent atmospheric circulation patterns. Therefore, there is a general understanding that using CMIP6 data provides additional information and should be used for further studies or risk assessments (see also EU-Taxonomy regulation, Annex A).

The SSPs are scenarios of global socioeconomic changes projected up to 2100 that describe alternative socioeconomic developments. Each of the SSPs describes a potential line of evolution for humankind regarding different pathways like radiative forcing induced through the mitigation policies adopted, the adaptation strategies followed, the social concept for human development (peace, war, sustainability, fossil fuel extraction, economic inequality...). These potential pathways will define the way that the climate will behave in the future (Figure 9).

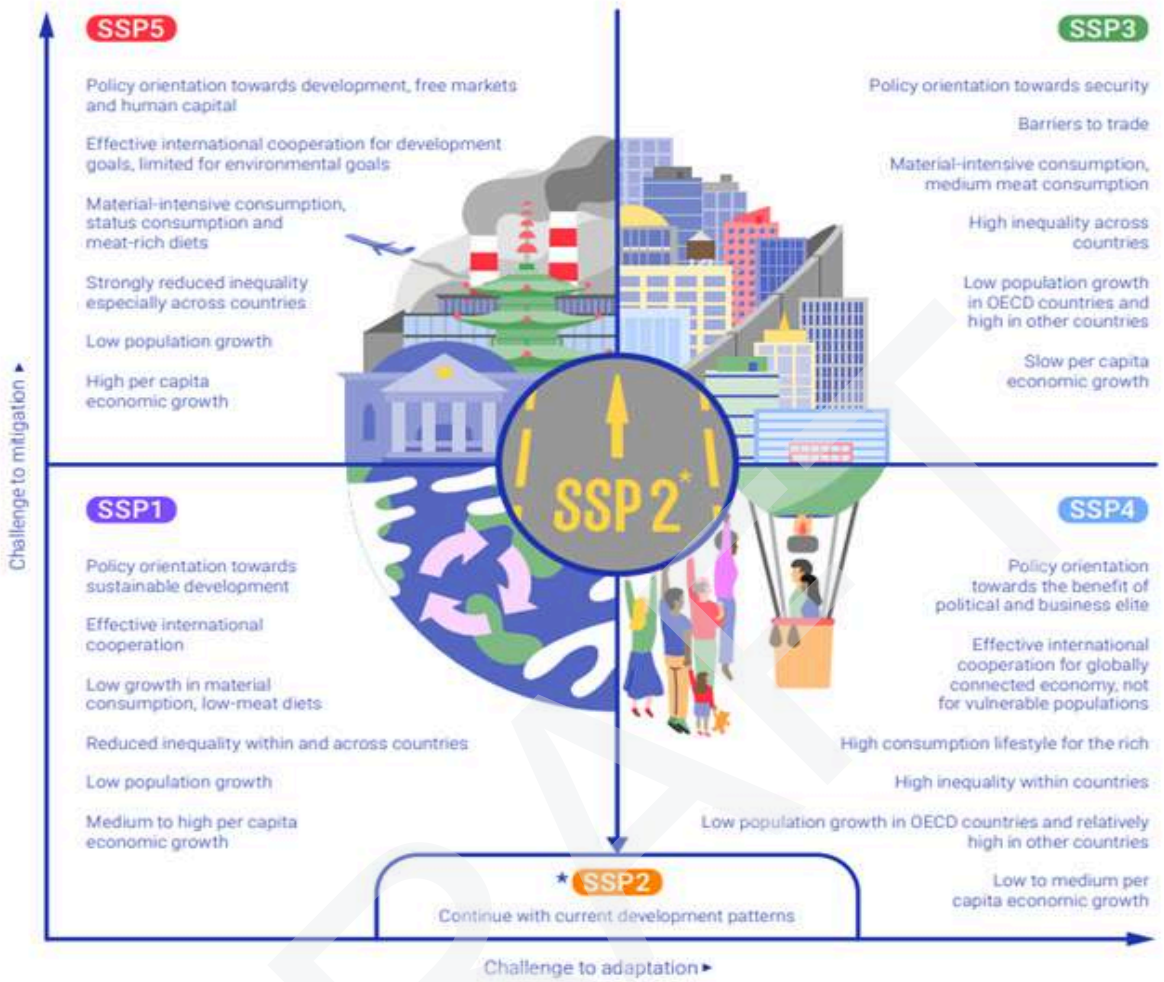

Figure 9. Shared Socioeconomic Pathways (in the figure, OECD stands for Organizations of Economic Co-operation and Development). Source: figure adapted from O'Neill et al., 2017.

CMIP6 has established SSP1-2.6, SSP2-4.5, SSP3-7.0, and SSP5-8.5 as the main scenarios, also referred to as Tier 1. Unlike CMIP5 (RCP 4.5 and RCP 8.5), CMIP6 extends Tier 1 from 2 to 4 scenarios. In contrast to CMIP5 and RCPs, the improved CMIP6, following the Tier 1 SSPs, exhibit a more extensive spread in anticipated global mean temperatures thanks to a better understanding of the global climate system. These SSPs project temperatures surpass the range covered by the RCP ensemble (Meinshausen et al., 2019). Figure 10 visually depicts the temperature variations associated with different SSPs, facilitating comparison with the RCPs.

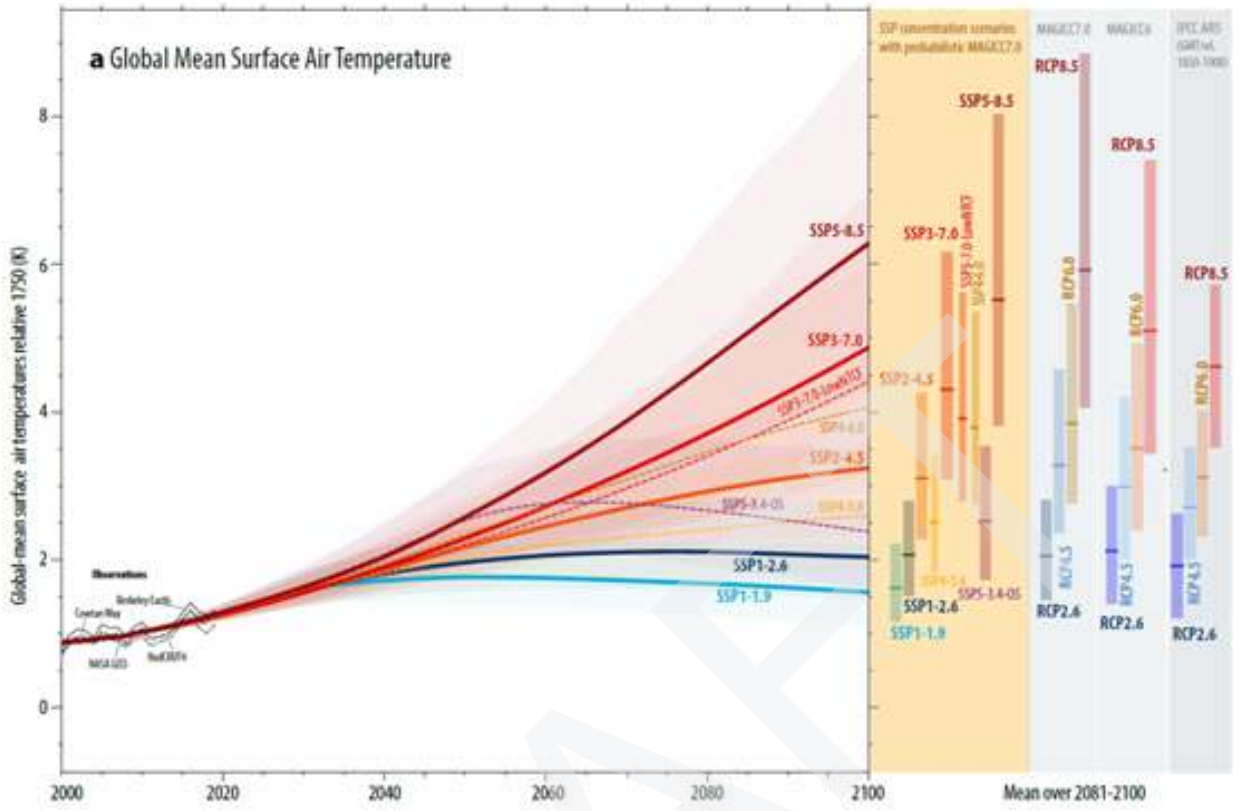

Figure 10: Comparison of illustrative projections of global mean surface temperature in the SSP and RCP scenarios. Global mean temperatures are shown relative to pre-industrial levels (1750), normalized to 0.92°C over the period 1995-2014. Time series for the period 2000-2100 are shown for the nine SSPs relative to 1750, with bold solid lines indicating the highest priority SSP scenarios and thin dashed lines indicating other so-called "level 2" scenarios. The shaded areas indicate the 5% to 95% confidence intervals for each scenario. Bar graphs illustrate the mean 2081-2100 relative to 1750 for the nine SSPs (yellow shaded area with bar graphs), and the RCP scenarios, using the same MAGICC7.0 configuration (light gray bar shaded area on the left) and an earlier MAGICC6 configuration used at the time of IPCC AR5 (light gray area on the right). Also shown is the likely range of temperature increase averages according to IPCC AR5 for that period, based on multiple lines of evidence (set of dark gray shaded bars on the right). Observational data for global mean surface temperatures, normalized over the same 1986-2005 period, are shown for Berkeley Earth (solid black), Cowtan & Way (Cowtan & Way, 2014) (long dashes), HadCRUT4 (Morice et al., 2012; Brohan et al., 2006) (small dashes), and NASA GISS (Lenssen et al., 2019) (dashes). Source: Meinshausen et al., 2019.

2.2.2. CMIP6 Global Climate Models

Following prior scientific recommendations, ICARIA's climate information is already based on CMIP6 models and incorporating in its workflow the current SSPs. Therefore, the presented high-resolution future climate projections display a unique dataset. These models will provide the scenarios to be considered within the Risk Assessment and the design and development of all adaptation measures coming as ICARIA outcomes.

As will be explained in the next section of this document, ICARIA follows a strong scientific approach by incorporating two different downscaling methodologies (statistical and dynamical) as a way to provide enough reliable climate information that allows a good understanding and representation of uncertainties related to climate projections.

Nevertheless, these two approaches take as a primary input the same source of information: GCMs coming from the latest CMIP6. As a way to create the best possible evaluation of uncertainty, an ensemble approach is followed, and a total of 10 different CMIP6 models have been retrieved (10 models at a daily scale give us enough information for quantifying their intrinsic uncertainty in projecting changes). Each model has its particularities, so a thorough analysis of each model and documentation available was performed to select the 10 best ones for the European area of interest taken as a case study in ICARIA. The same analysis period was considered, from 01/01/1950 to 31/12/2014 and the 4 Tier 1 SSPs (ssp126, ssp245, ssp370 and ssp585) ranging from 01/01/2015 to 31/12/2100. The relation of the selected models is detailed in Table 5:

Table 5. Information about the 10 climate models belonging to the 6 Coupled Model Intercomparison Project (CMIP6) corresponding to the IPCC AR6. Models were retrieved from the Earth System Grid Federation (ESGF) portal in support of the Program for Climate Model Diagnosis and Intercomparison (PCMDI).

CMIP6 MODELS	Resolution	Responsible Centre	References
ACCESS-CM2	1,875º x 1,250º	Australian Community Climate and Earth System Simulator (ACCESS), Australia	Bi, D. et al (2020)
BCC-CSM2-MR	1,125º x 1,121º	Beijing Climate Center (BCC), China Meteorological Administration, China.	Wu T. et al. (2019)
CanESM5	2,812º x 2,790º	Canadian Centre for Climate Modeling and Analysis (CC-CMA), Canadá.	Swart, N.C. et al. (2019)
CMCC-ESM2	1,000º x 1,000º	Centro Mediterraneo sui Cambiamenti Climatici (CMCC).	Cherchi et al, 2018
CNRM-ESM2-1	1,406º x 1,401º	CNRM (Centre National de Recherches Meteorologiques), Meteo-France, Francia.	Seferian, R. (2019)
EC-EARTH3	0,703º x 0,702º	EC-EARTH Consortium	EC-Earth Consortium. (2019)
MPI-ESM1-2-HR	0,938º x 0,935º	Max-Planck Institute for Meteorology (MPI-M), Germany.	Müller et al., (2018)
MRI-ESM2-0	1,125º x 1,121º	Meteorological Research Institute (MRI), Japan.	Yukimoto, S. et al. (2019)
NorESM2-MM	1,250º x 0,942º	Norwegian Climate Centre (NCC), Norway.	Bentsen, M. et al. (2019)
UKESM1-0-LL	1,875º x 1,250º	UK Met Office, Hadley Centre, United Kingdom	Good, P. et al. (2019)

3. Future climate information generation

3.1. ICARIA approach. Downscalings and uncertainty analysis.

When talking about the generation of climate information for projects that focus on climate risk and impact assessments as ICARIA, one of the main concerns that both climate scientists (as information providers) and sectoral partners or decision-makers (as information receivers) have to deal with is the inherent uncertainty of climate data. Climate Models (CMs), as stated above, are numerical models that represent the climate system with varying degrees of complexity and are based on the physical, chemical and biological properties of its components, their interactions and feedback processes. Therefore, each CM, depending on its inner architecture, simulates past and possible future climate states in a unique way, which translates into a degree of uncertainty depending on the CM selected. Additionally, the climate system has inherent inner variability due to the different time scales of the components involved (e.g. atmosphere days, ocean years) and related impacts on weather patterns, as well as other patterns such as ENSO or AMO. This is the reason why a 30-year period is selected for climate analysis. Furthermore, CMs simulate broad atmospheric circulation well but lack the resolution (around 100 km) for smaller-scale local phenomena. To address this limitation, downscaling techniques are employed, and this treatment of CMs further incorporates more uncertainty into the equation. Apart from model and climate-related variability and uncertainties, the emission scenarios used for driving future climate projections (SSPs) represent possible evolutions that cause possible climate states, adding another level of complexity and uncertainty in the interpretation and communication of climate model results and related (local) impacts.

Efforts within the scientific community focus on addressing and quantifying uncertainties in climate simulations. The main way to address this is the ensemble strategy[8], where either the same model is initialized with slightly different conditions or different models are used for computing the same SSP scenario, both approaches being done for CMIP6, thus combinations of models/SSPs/horizons for consistent projections are available (see past Figure 10). This approach displays the different outcomes and impacts for future climate states, clearly displaying the spread within the model simulations. Often the medians and quantiles are applied to gain a better knowledge and reduce uncertainty, enhancing the understanding of future climates for specific locations. Different procedures can then be applied from the ensemble outcome to further reduce the uncertainty (Wilcke et al. 2016), like selecting different ranges of change.

In this sense, ICARIA has tried to tackle this uncertainty issue not only with the common (yet necessary and efficient) ensemble approach, but also not sticking to one but considering the two main sources of generation of information at the local scale available: dynamical and statistical downscaling. ICARIA has incorporated into its procedures these two downscaling methods that have worked in parallel during T1.2. Each of them assesses its own uncertainty with inner processes of verification through the use of different procedures and statistics, ensuring that the methodology introduces the least amount of uncertainty into the outcomes, thus reducing this factor of the equation (see **Annex 3** for more detail). Once they are put together, this enlarges the perspective with two different sources, assessing therefore at the same time their uncertainty and the way it translates into future projections. Furthermore, the

[8] https://climateinformation.org/knowledge-base/why-use-a-model-ensemble2/

chosen approach enables the better representation of variability and possible future states while being time efficient.

About their characteristics, in brief; statistical downscaling obtains empirical relationships between large-scale variables from GCMs and high-resolution (surface) variables, allowing us to obtain very local results (like in a village) with less error than the dynamical one. Dynamical downscaling, on the other hand, increases the resolution of the GCMs over the region of interest with RCMs, taking into account local characteristics and altering physical processes, allowing us to obtain results in areas (like watersheds) where there are no observed data as well as a better representation of atmospheric processes. A more detailed summary of the pros and cons of each method can be found in Table 6.

Table 6: Differences between dynamical and statistical downscaling. (Patz, et al., 2005)

Dynamic Down scaling	**Benefits**	• Simulates climate mechanisms • No *apriori* assumptions about how current and future climate are related • 'State of the art science' tools • Continually advancing computers are making RCMs faster and cheaper to run • Encourages collaborations between climate scientists
	Draw backs	• Expensive, in terms of computer resources and professional expertise • Results may be sensitive to uncertain parameterisations • Biases in the GCM (providing boundary conditions) may propagate to regional scale • Output from models may not be in a format well-suited to analysis—additional data processing often required
	Appli cations	• Studies associated with climate extremes and non-linear variability, as health • Data-poor areas • Connecting outcomes with climate processes • Include land-use impacts on climate or health outcomes
Statistical Down scaling	**Benefits**	• Much cheaper in terms of computational time. • Builds on the statistical expertise common among researchers. • May correct for biases in GCM. • Allows for the assessment of climate results over a range of GCMs and emission scenarios.
	Draw backs	• Assumes relationships between local and large-scale climate remain constant • Does not capture climate mechanisms • Not well suited to capturing variance or extreme events. • Very localized information
	Appli cations	• Climate means, and variability with some limitations • Data-rich regions, especially Northern Hemisphere mid-latitudes • Compare present with projected climate in a consistent framework • Test a range of inputs • Variable scales, down to individual measurement sites

It could then be said that having similar results from both methodologies at the same location cast reliability onto ICARIA's main climate outcomes, allowing case studies and other partners to use trustworthy information on their respective tasks. If they largely differ, this has to be taken into account since it means that the future state is highly uncertain and depends on the model used. Further, this could relate to cascading uncertainties that could develop throughout the rest of the project. In the next sections, a more in-depth description of each one will be done for the statistical (FICLIMA) and dynamical (AIT) methodologies.

It must be noted that, due to ICARIA's schedule and the time needs of the dynamical downscaling, this is only performed for SAR and SLZ CS, whereas AMB will only count on statistical results.

For the presentation of the results concerning future climate projections in ICARIA, a three-time-periods strategy has been taken to represent them depending on the fairness in time: **short-term (2021-2050), mid-term (2041-2070) and long-term (2071-2100)**. The baseline (or historic period) is aligned with the IPCC AR6 also considering CMIP6 historical experiments, being set to the **1981-2010** 30-year period.

3.2. Statistical downscaling - FICLIMA

The statistical downscaling methodology applied in ICARIA by FIC, named FICLIMA (Ribalaygua et al. 2013), consists of a two-step analogue/regression statistical method which has been used in national and international projects with good verification results (i.e.: Monjo et al. 2016). The first step (see Figure 11) is common for all simulated climate variables and it is based on an analogue stratification (Zorita et al. 1993). An analogue method was applied based on the hypothesis that 'analogue' atmospheric patterns (predictors) should cause analogue local effects (predictands), which means that the number of days that were most similar to the day to be downscaled was selected. The similarity between any two days was measured according to three nested synoptic windows (with different weights) and four large-scale fields using a pseudo-Euclidean distance between the large-scale fields used as predictors. For each predictor, the weighted Euclidean distance was calculated and standardised by substituting it with the closest percentile of a reference population of weighted Euclidean distances for that predictor. This method is a good method for reproducing nonlinear relationships between predictors and the predictands, but it could not be used to simulate values outside of the range of observed values. In order to overcome this problem and obtain a better simulation, a second step was required.

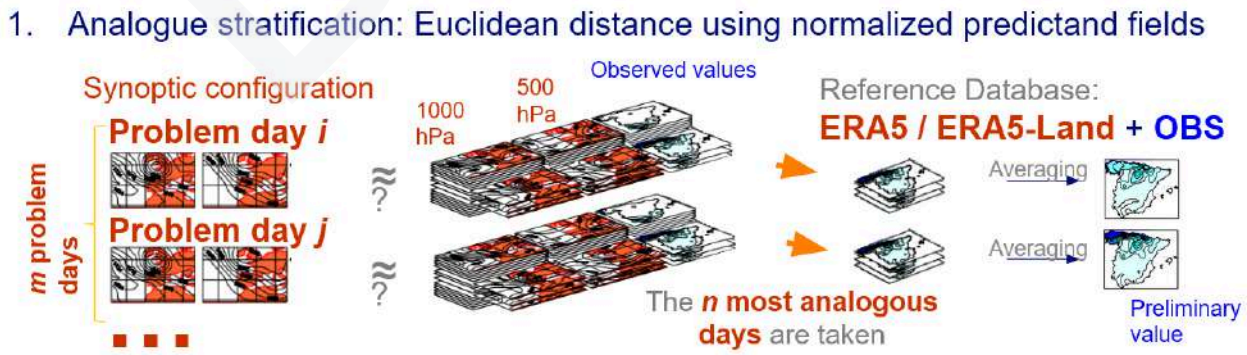

Figure 11. Key features of the first step of the FICLIMA statistical downscaling.

For this second step (see Figure 12), the procedures applied depend on the variable of interest. To determine the temperature, multiple linear regression analysis for the selected number of most analogous days was performed for each station and for each problem day. From a group of potential predictors, the linear regression selected those with the highest correlation, using a forward and backward stepwise approach.

For precipitation, a group of m problem days (we use the whole days of a month) is downscaled. For each problem day we obtain a "preliminary precipitation amount" averaging the rain amount of its n most analogous days, so we can sort the m problem days from the highest to the lowest "preliminary precipitation amount". For assigning the final precipitation amount, all amounts of the m×n analogous days are sorted and clustered in m groups. Every quantity is finally assigned, orderly, to the m days previously sorted by the "preliminary precipitation amount".

For wind or relative humidity, the second step is a transfer function between the observed probability distribution and the simulated one using the averaged values from the n = 30 analogous days. Particularly, a parametric bias correction was performed to the time series obtained from the analogue stratification (first step). In order to estimate the improvement of this procedure, the bias correction was also applied to the direct model outputs.

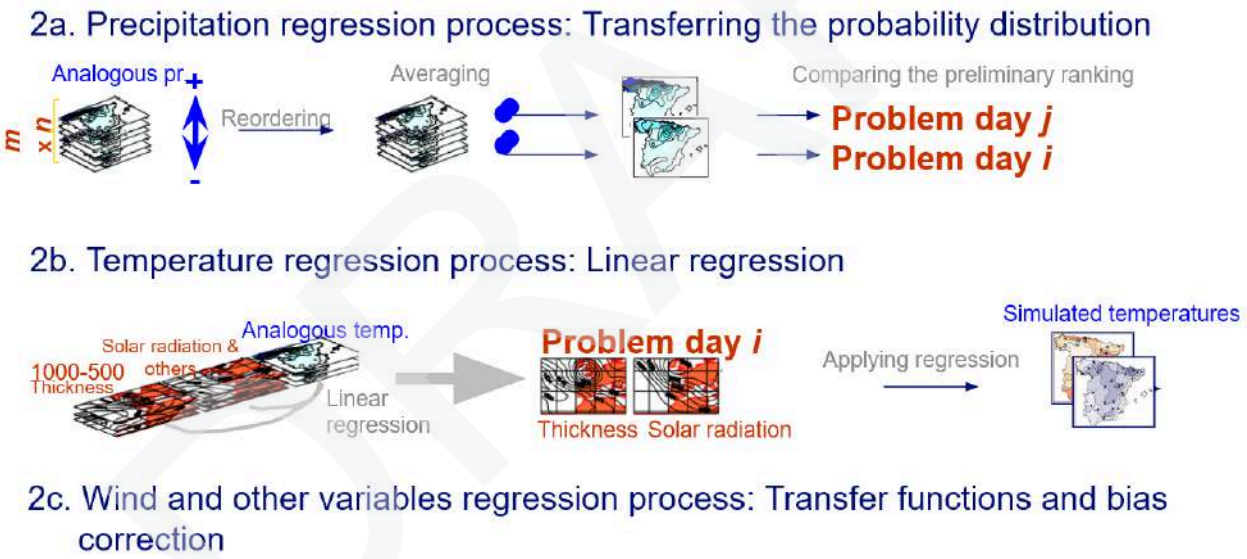

Figure 12. Key features of the second step of the FICLIMA statistical downscaling, with graphic details of the work done for each type of variable.

This second step done at a daily scale with an inner thorough verification procedure is essential and the main differentiating process of FICLIMA method. It extends beyond mean values to include extremes and covers all time scales, including daily intervals. With the verification it can be proven If the method correctly simulates changes from one day to the next, indicating an effective capture of the underlying physical connections between predictors and predictands. These physical links remain relatively consistent, even in the face of climate change (as opposed to purely empirical relationships that might shift). In essence, this approach theoretically addresses the primary challenge in statistical downscaling known as the non-stationarity problem. This problem questions the stability of predictor/predictand relationships established in the past, probing whether these relationships will persist in the future.

3.3. Dynamical downscaling - Regional Climate Models

General Circulation - or Global Climate Models (GCMs) represent all components of the climate system (atmosphere, ocean, land, ice sheets) and their interactions and thus display a great tool for analysing past and future climate conditions. To integrate all components and still have meaningful computation times, the current spatial resolutions of GCMs are in the order of ~80 - 200 km. Therefore, one temperature, precipitation etc. value representing the mean of the gridcell (e.g. 80 km x 80km) is received. To overcome the coarse spatial resolution, regional climate models (RCMs) have been used for dynamical downscaling intensively over the past. Their spatial resolution is in the range of 2 - 25 km and temporal resolution is often hourly. RCMs are initialised by GCMs, meaning that the boundary conditions are provided by the GCMs and only atmospheric processes are explicitly resolved for the respective domains. Within RCMs local characteristics such as topography, land-use, vegetation type etc. are represented with greater spatial detail, emphasising their impact on physical processes. These processes are represented within the climate models through so-called schemes (e.g. microphysics schemes which resolve the physical processes and **parameterizations** related to cloud formation and large-scale precipitation patterns). Depending on the spatial resolution of the applied models, physical processes can either be resolved or need to be parameterized if they are subgrid-scale (e.g. convective processes are only resolved explicitly at resolutions < 4km, Prein et al., 2015).

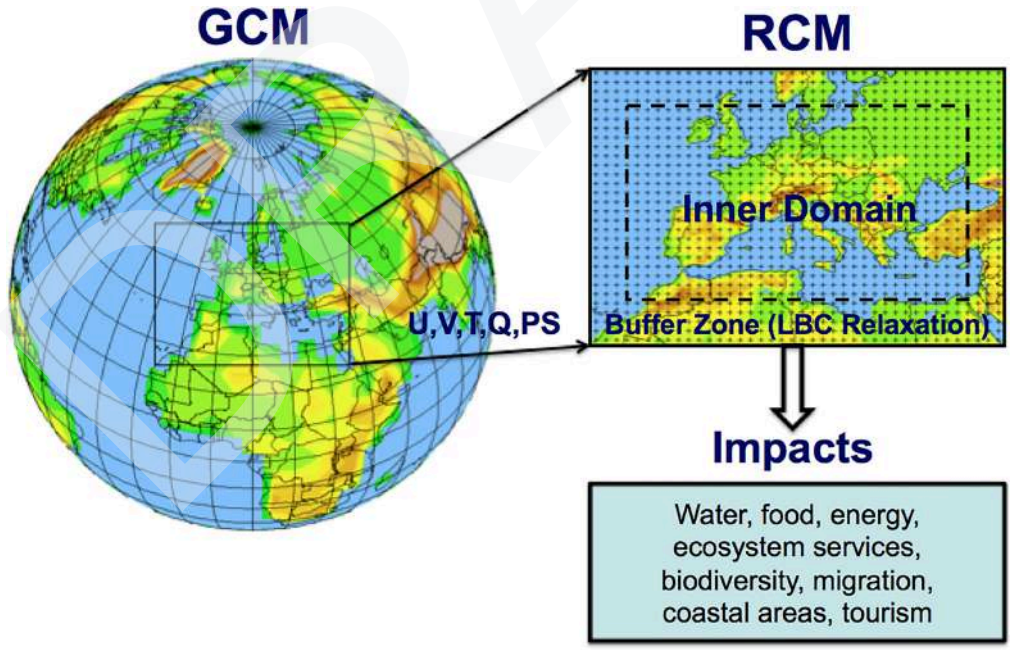

Figure 13: Schematic depiction of regional climate modelling and application to VIA studies. VIA = vulnerability, impacts, and adaptation; RCM = regional climate model; GCM = global climate model. Source: Giorgi, F. 2019.

Within ICARIA, two different RCMs were initialized with two GCMs for the SSP scenarios SSP126 and SSP585 to account for uncertainties within the models and better depict the variability within possible future climate conditions (Table 7).

First, the CCLM domains, set-up and status of simulations are depicted, afterwards the same is done for WRF.

Table 7. GCMs and RCMs used and applied for the dynamical downscaling in ICARIA.

GCM	RCM
EC-Earth3-Veg (Dröscher et al., 2021)	COSMO-CLM (CCLM, Rockel et al., 2008)
MPI-ESM1-2-HR (Müller et al., 2018)	WRF (Skamarock et al., 2019)

The produced dataset of dynamically downscaled climate projections depicts valuable insights into future climate states at a high resolution. As it is based on CMIP6 model data, it is one of the first openly available. As Central Europe is covered by two RCMs at a spatial resolution of 12 - 15km2, the benefit of this data goes far beyond the project and the case studies. Furthermore, setting up long term climate simulations at the very high resolution of 2 - 5 km² (even convection permitting) offers valuable insights of great importance.

However, the (computational) resources needed for dynamical downscaling are extensive and are unfortunately prone to issues. Failure of hardware has caused a delay in finalizing the simulations, as well as the complexity of convection permitting simulations (CCLM). The status of the simulations at time of deliverable:

Table 8. Current status of simulations at the time of deliverable is:

Domain	CCLM historical ERA5	CCLM - SSP126	CCLM- SSP858	WRF historical ERA5	WRF - SSP126	WRF - SSP858
Europe	1981 - 2010	1981 - 2100	1981 - 2100	1981 - 2010	1981 - 2100	1981 - 2100
SBG	1981 - 2010	1981 - 2100	1981 - 2100	1981 - 2010	1981 - 2100	1981 - 2100
AEG		1981 - 2060*	1981 - 2060*	1981 - 2010	1981 - 2100	1981 - 2100

* these runs are still being finalized. Their delay doesn't impact the project's overall approach as their results will be ready for hazard models within WP4 in time.

3.3.1. CCLM simulations ICARIA

The chosen climate model COSMO-CLM Version 4.8_19 (Roeckel et al., 2008, Doms et al., 2011) is a mesoscale non-hydrostatic regional climate model, maintained and further developed by the COSMO Consortium, an open international network of scientists of the Climate Limited-area Modelling-Community (CLM-community, www.clm-community.eu) based on the weather prediction model COSMO (Steppeler et al., 2003) of the Deutscher Wetterdienst. It is based on the primitive equations specifying the compressible flow in a moist atmosphere and physical processes like radiation, turbulence, land surface processes and convection are represented. Further, the governing equations are integrated using the mode-splitting approach to split up the equations into a longer model time step for processes on larger time scales such as advection and the tendencies from the physical parameterizations, and into a short time step for the fast sound wave processes (Baldauf et al., 2011).

Within CCLM the following domains were simulated at the specified spatial resolution:

0.1° (~12km): 0.02° (~2km): 0.02° (~2km):

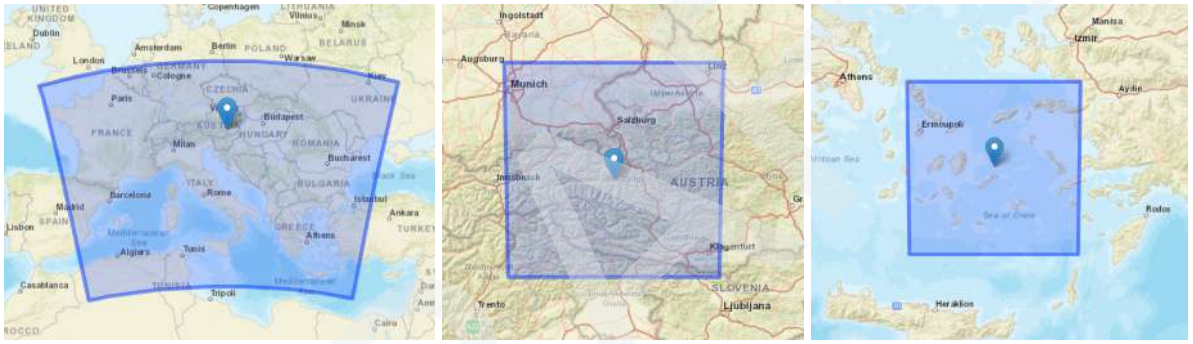

Figure 14: CCLM simulation domains within ICARIA

All simulations have hourly output and are performed until 2100. The AMB area was not simulated due to time constraints and the fact that it is covered within the KNOWING[9] project.

The following **namelist parameters** applied were:

- 2 time-level Runge-Kutta scheme: 3rd-order Runge-Kutta scheme used by Wicker and Skamarock (2002)
- Smagorinsky diffusion
- horizontal advection: Bott 2nd order finite-volume scheme with Strang splitting
- semi-Lagrangian advection of the moisture variables
- scheme for horizontal diffusion: Monotonic 4th-order linear scheme with orographic limiter
- grid scale precipitation: Graupel scheme with prognostic cloud water, cloud ice, and graupel
- Vertical Turbulent Diffusion: old ijk-behaviour of the turbulence scheme
- include horizontal turbulent diffusion: Prognostic TKE-based scheme
- parameterization for evaporation of bare soil, BATS version
- parameterization for transpiration by vegetation, BATS version

[9] https://knowing-climate.eu/

- diagnosis of snow-cover fraction: parameterization depending on soil water equivalent
- subgrid-scale convection
- convection parameterization: Shallow convection based on Tiedtke
- include lake processes

The numerical models used for **dynamical downscaling** compute the atmospheric state and its change at each model internal timestep, therefore, all parameters needed for these physical processes are part of the modelling equations and, depending on the settings, can also be part of the output. For instance, the **output file of WRF/CCLM contains ~100-400 parameters**. A list of the **most relevant output parameters** for each output timestep (hourly) are:

2D (x,y): 10m wind, humidity, 2m temperature, surface pressure, cloud cover, precipitation, minimum/maximum temperature, incoming radiation
3D (x,y,z): wind, temperature, pressure, humidity, cloud cover in different heights

3.3.2. WRF simulations ICARIA

The second model applied is the commonly used WRF model (version 4.3.3), a state-of-the-art mesoscale numerical weather prediction system designed for both atmospheric research and operational forecasting applications. It features two dynamical cores, a data assimilation system, and a software architecture supporting parallel computation and system extensibility. The model serves a wide range of meteorological applications across scales from tens of meters to thousands of kilometers. It is jointly developed by various institutions and allows the user to choose from different physical parameterization schemes. The domains simulated by WRF are displayed in Figure 15.

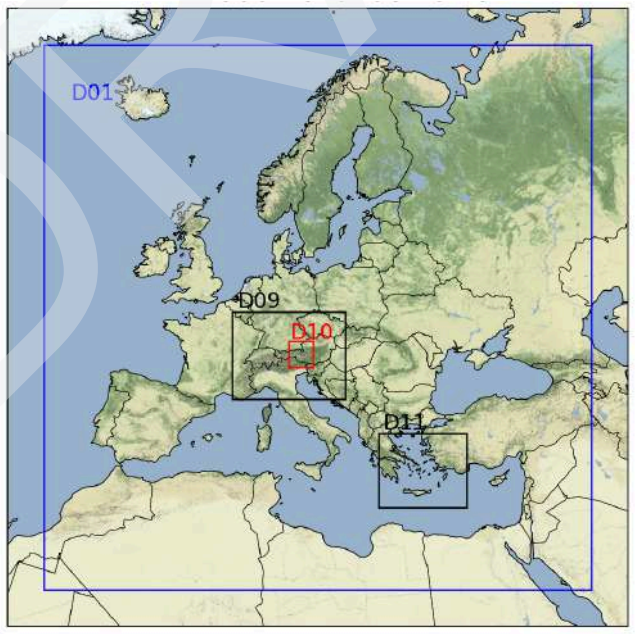

Figure 15: WRF domains: spatial resolution D01: 15 x 15km2, D09 & D11: 5 x 5km2, D10: for specific events at 1km2

For the simulations performed within ICARIA, the following namelist parameter settings were chosen for all case studies:

- microphysics: new Thompson scheme with ice, snow and graupel processes suitable for high-resolution simulations.
- long- and shortwave radiation: new version of RRTM added in Version 3.1. It includes the MCICA method of random cloud overlap.. Since V4.2, the CO2 value is replaced by a function of the year: CO2(ppm) = 280 + 90 exp (0.02*(year-2000)), which has about 4% of error for 1920s and 1960s, and about 1 % after year 2000 when compared to observed values
- Land surface: Noah-MP (multi-physics) Land Surface Model: uses multiple options for key land-atmosphere interaction processes. Noah-MP contains a separate vegetation canopy defined by a canopy top and bottom with leaf physical and radiometric properties used in a two-stream canopy radiation transfer scheme that includes shading effects.
- planetary boundary layer: Mellor-Yamada Nakanishi and Niino Level 2.5 PBL (5). Predicts sub-grid TKE terms.
- cumulus parameterization: Grell Freitas scheme that tries to smooth the transition to cloud-resolving scales

The numerical models used for **dynamical downscaling** compute the atmospheric state and its change at each model internal timestep, therefore, all parameters needed for these physical processes are part of the modelling equations and, depending on the settings, can also be part of the output. For instance, the **output file of WRF/CCLM contains ~100-400 parameters**. A list of the **most relevant output parameters** for each output timestep (hourly) are:

2D (x,y): 10m wind, humidity, 2m temperature, surface pressure, cloud cover, precipitation, minimum/maximum temperature, incoming radiation

3D (x,y,z): wind, temperature, pressure, humidity, cloud cover in different heights

3.4. AI weighting

State-of-the-Art: AI-based ensemble weighting

To improve the accuracy of model predictions, meteorologists combine different models. Within the ensemble, different models can be assigned with a weight to consider regional characteristics and to correct for model bias Merrifield et al. (2020). The weighting scheme is typically provided by experienced meteorologists, but recently AI-based methods have been explored. So far, only a limited amount of literature exists on ML-enhanced ensemble weighting, particularly within the meteorological and geophysical domains. Consequently, ML-aided weighting for ensemble forecasting remains largely unexplored, presenting a promising method for future research. To date, only two notable contributions have been identified in this area.

Sun et al. (2021) introduced an ML-Optimized Ensemble (ML-OE) method to forecast the seasonal occurrence of tropical cyclones. Assuming linearity between the statistical models, the authors performed a simple least squares regression problem augmented by regularization terms. Additionally, to directly solve the inversion problem, they employed a simple gradient descent scheme for the linear regression problem. Different ensemble subsets were considered as well. In certain cases, the authors found that an ML-OE leads to a better or similar prediction accuracy than the simple averaging scheme. Most notably, the ML approach demonstrated superior accuracy for poorly resolved response variables, surpassing individual model predictions and average ensemble forecasts.

In contrast to this approach, the ensemble weighting method presented by Sengupta et al. (2020) is a deep learning approach. There, a Bayesian neural network was constructed to weight an ensemble of models predicting the monthly average total ozone column. Bayesian networks model train parameters of probability density distribution instead of scalar weights. This offers, due to the inherent statistical nature, interpretability and UQ capabilities. By integrating prior knowledge through data transformation and network design, Sengupta et al. exemplified a physics-informed ML scheme. Their approach enables the capture of spatio-temporally varying model accuracy, thereby enhancing ensemble forecast performance.

Methodology

In order to find the optimal weighting between the 2 GCM and 2 RCM models, we will follow a classical machine learning workflow, i.e. we will:

- Define a research question
- Select which data is used for training, validation and testing
- Decide about the input and target parameters
- Choose a model architecture
- Train and validate a first model and fine-tune if necessary
- Evaluate the model performance

Research Question and Metrics

Which combination of physical models is optimal for predicting a single parameter such as e.g. temperature or a set of e.g. temperature, pressure, humidity and wind in the specified spatiotemporal domains? Can ML-based weighting schemes match, or even outperform, state-of-the-art non-ML weighting schemes?

It is essential to define here according to which metrics we consider the model weights found as optimal. A useful approach could be to use for this the meteorological verification e.g. with respect to the ERA5 reanalysis.

Considered spatiotemporal domain

In order to cover both regions of interest, i.e. the Salzburg area and the Aegean region, and to capture also large-scale weather effects, we will focus on middle Europe. The considered time frame for model training should be limited to the one considered for the developed GCM and RCM models.

Selection of data for training, validation and testing

The data available comprises the model output from 2 GCMs and 2 RCMs, with spatial resolutions ranging from 100 km to 2-12 km. The GCMs provide daily output, while the RCMs offer hourly output. Each model provides an output for approximately 380 parameters for each time step. Together, with the domain experts we will decide which subset of parameters is essential for answering the research question and whether all time steps should be considered. This input parameter reduction and input feature importance analysis can also be achieved or supported by traditional dimensionality reduction methods such as the principal component analysis. This subset is then considered as the input parameters for the machine learning model. The target output is four values lying on a four-dimensional simplex, with additional constrain that sum up to one. These four outputs are associated with weights attributed to the four physical models for the climate projection. We will further investigate how the output can be reshaped to allow for both geographic and temporal diverging weight sampling. We expect a sensible trade-off between enhanced performance and computational cost.

Physics-informed ML methods in the form of knowledge-driven data-transformation should also be applied. Following the example of Slater et al. (2023), the time arrow can be transformed to a helix, which captures annual periodicity and allows the quicker emergence of seasonal effects without losing the information of long-term climate trends.

While the exact temporal extension of training, validation and testing set needs to be determined, we require a significant overlap between the testing set of the ML approach and the traditional approach, to address the above-defined research questions.

Model architecture and loss function

The general proposition is that we start with as simple model as possible and increase the complexity if required. Due to the data availability supervised and unsupervised ML methods can be applied. The ML architecture used by Sengupta et al. is based on a Bayesian Neural Network. The input to the network consists of the spatiotemporal domain considered in the respective climate projection scenario. Here, it is ensured that geolocation (coordinates) do not contain any discontinuities and that the temporal input reflects cyclic behaviour to account for seasonality. Additionally, all data are scaled to ensure numerical consistency. The output is fed forward through several fully connected Bayesian layers. The connections between the nodes of the neural network are modelled as normal distributions. The training consists of finding the optimal parameter space of means and variances to optimize the underlying loss function, i.e., to find the best prediction of past climate with weighted climate models. Due to the high dimensionality of the problem, not every inference strategy can be used. The authors propose, therefore, maximum a posteriori sampling. Under certain assumptions, this is equivalent to minimizing a computable loss function, which is discussed below.

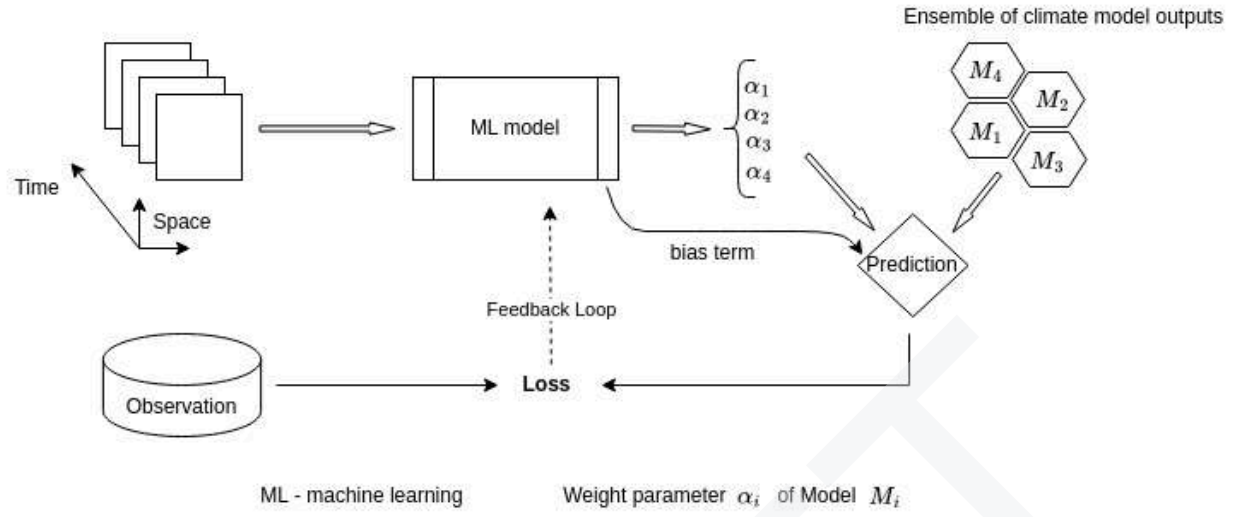

Figure 16: sketch of ML modelling approach

Sampled values from the last layer in the network are subjected to a softmax activation function to obtain the target physical model weights. The choice of the softmax function is important but not unique; it ensures, on one hand, that all weights lie in the interval [0,1], and on the other hand, that the sum of all weights equals one. In addition to the weights, a bias term and a heteroscedastic aleatoric noise are retrieved from the network. The climatological prediction consists then of the sum over weighted physical models, corrected by the bias and noise term. The loss function used in the training process consists of several terms. The first one is the square distance between climatological prediction and recorded climate data, scaled by the respective variance term. The second and third terms are derived from the inference strategy and essentially minimize the uncertainty of the sampling distributions while converging towards the mean parameterizing the normal distribution.

Due to the availability of the code on GitHub, and the thoughtful design, we propose a similar approach while also exploring different ML techniques. As for Sengupta et al., the high dimensionality of the input and output space is a limiting and time-consuming factor in applying different ML strategies, which is a challenge that will be addressed throughout.

Model performance evaluation

To assess the effectiveness of the ML weighting strategy, we will compare it against simple baselines, such as individual model performance or an evenly distributed weight allocation among the models. Additionally, we will define various spatiotemporal subsets to evaluate the significance of each model in different regions. This analysis will provide valuable insights that can be reviewed, verified, and discussed by climatologists within the consortium, potentially enhancing our understanding of model performances in specific regions. As the model expands to assign weights for different meteorological variables across space and time, the performance analysis can be extended to the predicted variables. The final validation process will involve a validation by meteorological experts.

3.5. Comparison of both methodologies.

The characteristics of the applied methodologies (statistical and dynamical) have been described above and display the base for future comparison within the two regions covered by both, SLZ and SAR. Further, the GCMs used for dynamical downscaling were also part of the ensemble of the statistical one, which is crucial.

The approach behind the comparison is to depict the strengths and weaknesses of both, maybe also depending on the specific region so not uniformly applicable but rather dependent on f.i. available observation data, land use and land cover, topography etc. - characteristics of the investigated region impacting the quality of the projections.

The fact that within one project consortium experts of both "worlds" are present is rare and offers great potential. Thus, the output of statistical downscaling (spatial extrapolated fields and point point locations) will be compared to the dynamical downscaled output fields and similarities, as well as discrepancies assessed. Additionally, the characteristics of compound events in both methods will be analysed to assess if their occurrence or intensities depend on the chosen method (for two GCMs both methods are available).

3.6. Next steps after D1.2: local downscaling of SSP scenarios; ARSINOE methodology

The objectives of this section are to set the basis of the methodology that will be applied later on in ICARIA to define and detail SSP projections to the adequate territorial reality as well as to include SSP scenarios into a local/region scale projection model.

To achieve these objectives a method using projected land use maps has been selected. This would allow it to more accurately represent the territorial reality of the selected climate projections by including SSP (Shared Socioeconomic Pathways) narratives in the projections. It means adjusting the potential socioeconomic outcomes to a more precise assessment of the impacts evaluated in the ICARIA project.

The proposed method is inspired by the ARSINOE[10] project method of socioeconomic downscaling and the work of (Huber García et al., 2018). This method is based on downscaling the selected SSP for the case studies using present and future projections of local land use and GDP information.

The first step requires the appropriate selection and characterization of the Shared Socioeconomic Pathways (SSP) of interest. It is proposed to select the main SSP considered as representatives of the circumstances of the case study. Another factor to characterise and select the correct SSP is considering various adaptation strategic plans for each case study. This helps to standardise the criteria used to select the SSP and increase awareness of the potential results, thereby evaluating the accuracy of this method.

[10] https://arsinoe-project.eu

All the ARSINOE case studies selected the SSP1-26 and SSP3-70:SSP1-26, considered an optimal choice since its lower boundary remains within (or at least close to) the scenario proposed by the EU-Green Deal targets. The SSP3-70 was recently considered as an upper boundary climate and socioeconomic future that (i) contrasts the "green" scenario and thus opens/covers a broad feature space of possible pathways; (ii) is fairly close in warming potential to the CMIP5 RCP8.5; (iii) is scientifically new (one of the pilots) and publishable". The objective of this phase is then to choose the SSP that best suits the future socioeconomic scenarios for each case study. With that being said the SSPs selected for the current project are yet to be determined.
A second step would be to select the different factors/descriptors to characterise the different scenarios. These criteria consider two important approaches:

1. A qualitative selection of factors/descriptors that would establish the partial relations between the possible results in both scenarios.
2. A quantitative estimation of the parameters that describe the previous factors is used to characterise the SSP to be able to include them in the aforementioned projections.

These factors/descriptors are chosen through the consensus of a set of multidisciplinary experts considering strategic plans, data availability in the different study cases, and other criteria that are found relevant within the literature. A selection of the parameters that are going to be included in the projection model will also be carried out based on the state of the art and availability.

Once these scenarios have been described and characterised, the following step is setting up a model that allows to project the change of a desirable characteristic. The model considers the effects of the previously chosen parameters to constrain the possible outcomes of our simulation inside the limits of the chosen SSP.

There are existing GIS-based models, like the CLUEMONDO or iCLUE (Verweij et al. (in prep.)), proposed in the ARSINOE project, that will be evaluated to be applied in ICARIA for land use time-scaled projections. These tools help to incorporate local SSP into the outcome of the projections. These models require the following inputs:

1. Evaluation of the Factors/Descriptors chosen as Drivers regarding the variation in land use.
2. Evaluation results of the land use variation (change detection). Historic land use maps (i.e: CORINE European project maps).
3. An estimation of the easy-of-change value for each of the land uses in each case study area. This value will be used to fine-tune the model outcomes and calculate the probability of an area changing its land use.
4. Land use demands.
5. A base map from the first point of the time series.

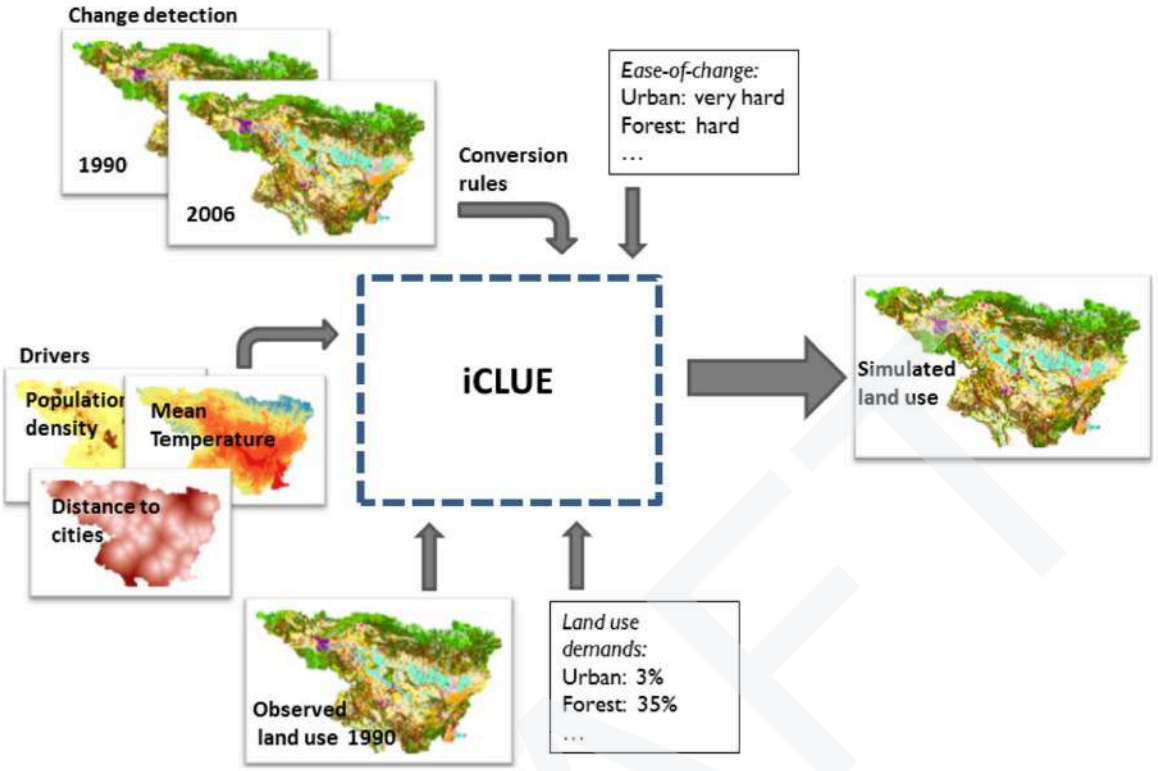

Figure 17: iCLUE model inputs. Source : (Huber Garcia et al 2018)

This model will calculate the probability of a land use change to occur in a location using three main variables:

1. Ease-of-Change
2. Suitabilities for each type of land use by selecting the most significant drivers using a stepwise regression model to estimate the overall suitability for each land sector
3. Overall land use demands

The model will use these probabilities to generate land use map projections. Given that this method will apply to the chosen SSPs, there will ultimately be one map for each scenario. Upon completion of these simulations, the next step involves evaluating the quality of the simulations. When examining the results of the CLUEMONDO or iCLUE model, the following aspects must be considered:

1. Persistence simulated correctly (correct rejections)
2. Persistence simulated as change (false alarms)
3. Change simulated as the change to wrong category (wrong hits)
4. Change simulated correctly (hist)
5. Change simulated as persistence (misses)

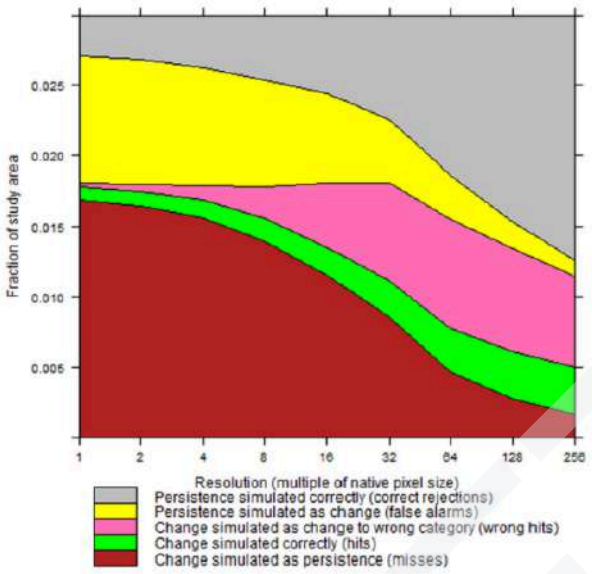

Figure 18: Validation results at multiple resolutions. Source : (Huber Garcia et al 2018).

Once it has been stated that the quality of the simulations is satisfactory, it will be possible to proceed with the use of these projected maps to estimate certain characteristics of interest, such as water demand, for the drought's impact assessments, or the estimated flood damages. This follows the method used in (Huber Garcia et al., 2018).

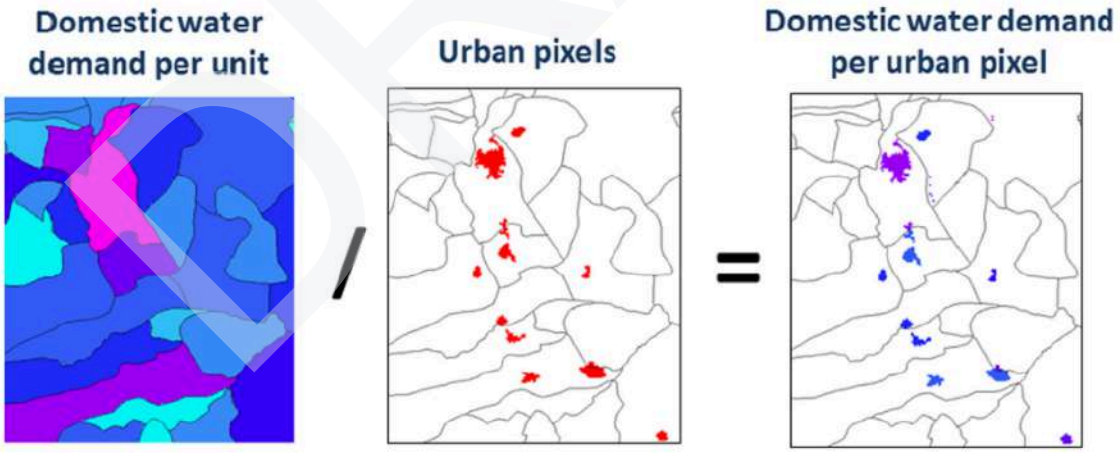

Figure 19: Validation results at multiple resolutions. Source : (Huber Garcia et al 2018).

The applied method overlapped the layer of domestic water demand per unit above the projected urban pixels layer, being able to estimate afterwards the domestic water demand per urban pixel area.

This kind of estimation is particularly useful for ICARIA's trial assessments since it would allow comparison between present scenarios and the results obtained from both projected scenarios.

Although the proposed method does not focus on impact assessment, it can be adapted to compare adaptation scenarios in the ICARIA project, establishing tailored socioeconomic projections.

Several indicators can be used to provide relevant information from which to assess the impact of the different hazards. They will be linked to the land use information from the iCLUE or CLUEMONDO model coming from the aforementioned authors (Huber García et al.,2018 and Verweij et al. (in prep.)), to provide more accurate information to reflect better the different possible outcomes taking into account the effect of the socioeconomic scenarios selected.

4. Climate variables and hazards

4.1. Climate variables

In order for the partners in T1.2 to start developing the future climate projections to be used during ICARIA, it was necessary to first determine the climate variables that would need to be modelled. These main climatic variables (or drivers) will depict the potential and likely conditions of the future climate, and will suppose the basis for obtaining the rest of the indicators that derive from hazards for the case studies. However, for them to be defined, the process ought to be done the other way round; this is, prior identification of hazards detected in the case studies should be done, and with them an analysis of what variables cause them is performed. This task was partially done during the proposal stage of ICARIA, and fully rounded through the collaboration of stakeholders mainly in T1.1 and summarized in D1.1.

Therefore, the main climatic drivers were identified according to the potential hazards enumerated in D1.1 for each CS. Their importance level was estimated considering each hazard risk as established by CS, also considering if they belong to the Trial or Mini-trial phase of the ICARIA project. The climate variables identified here, shown in Table 9, correspond to the final outcome that will be delivered and both displayed in results and used for the posterior indicators; variables needed for their calculation depend on each methodology (statistical or dynamical), and these considerations are exclusive to their procedures and therefore not detailed here.

Table 9. Climate variables related to the identified potential hazards and their importance according to the Trial or Mini-trial previous evaluation (see D1.1).

Variables	Identified hazards	AMB		SLZ		SAR	
		Trial	Mini-trial	Trial	Mini-trial	Trial	Mini-trial
Temperature (max, min and mean)	Heatwave, drought, forest fire		X		X	X	
Precipitation	Flooding, drought	X		X			X
Wind (mean and gust)	Storm winds, heatwave, drought, forest fire		X	X		X	
Relative Humidity	Drought, heatwave,forest fire		X		X	X	
Sea level	Storm surges	X					X
Wave height (significant and maximum)	Storm surges	X					X

4.2. Hazards and extreme events indicators

Following the previous section, the identification of hazards (D1.1) achieved by the CS and the climate variables obtained allowed for a more detailed discussion of the specific indicators for extreme climate events that could, directly or through cascading effects, produce the apparition of those feared hazards. The identification and/or definition of these indicators is key in order to develop their corresponding projections for future changes and assess this way the expected impacts and vulnerabilities regarding ICARIA's CS. The definition of extreme events indicators is crucial for ICARIA as it feeds other related tasks from WP1 and WP2, more specifically T1.1 (impact modelling), T2.1 (hazard dynamics) and T2.2 (multi-hazard modelling). With this aim, several online meetings were held amongst ICARIA's technical partners and also each case facilitator, gathering in the end: FIC, AIT, AQUATEC, UNEXE, DEMOKRITOS, PLINIVS, UNINA, and indirectly AMB and representatives from SLZ and SAR.

These meetings allowed for a thorough technical discussion and the comparison of different needs and contexts which led to an effort made by ICARIA to synthesize and establish common indicators for the project. These gathered the needs of each case study but also prioritized the best scientific approach to stay within the "extreme" climate definition, so that they could apply to all three CS and also be replicated elsewhere, easing ICARIA's work through a common approach for the hazard modelling. This was the ideal scheme, but given the different climates considered in ICARIA and the diverse resilience that their inhabitants have to certain climate conditions, some indicators are case-specific under a direct request from the CS.

In any case, a threefold approach was taken to identify and define the agreed indicators.

- Some of the indicators, due to their nature (like extreme rainfall or wind), were defined upon a certain amount of Return Periods (RP) whose changes would be evaluated in the future, assessing therefore potential increases or decreases in the intensity. These RP were established as 1, 2, 5, 10, 20, 50, 100 and 500 years. Their calculation was, from the statistical downscaling, based on the best fit to 2, 3 and 4-parametric versions of Gamma, Weibull, Classical Gumbel, Reverse Gumbel and Modified Log-logistic distributions (Monjo et al. 2014, 2016). Within the dynamical downscaling the change in intensities for the different RPs is estimated.

- Other indicators were approached defining or combining quantiles that, being based on the respective climate, would be thus escalable. This is the case for Heatwaves or Cold days.

- The rest of the indicators were taken from already existing definitions applied worldwide with multiple applications, like Tropical Nights, SPEI or FWI.

For the sake of simplicity and clarity, a summary table of all the indicators agreed upon is facilitated below in Table 10 and Table 11. For a more detailed description of each indicator and the mathematical basis behind it, please refer to **Annex 4**.

Table 10. Summary of selected thermal and precipitation indicators, grouped aligned with the main hazards they feed. "nd" = number of days; "ne" = number of events.

Index/name	Short description	Source	Variable	Units	Threshold
Thermal indicators					
TX90 / TX10	Warm/cold days	Zhang et al. (2011)	TX	nd	90 / 10%
HD	Heat day	ICARIA	TX	nd	> 30 °C
EHD	Extreme heat day	ICARIA	TX	nd	> 35 °C
TR	Tropical nights	Zhang et al. (2011)	TN	nd	> 20 °C
EQ	Equatorial nights	AEMet 2020, ICARIA	TN	nd	> 25 °C
IN	Infernal nights	ICARIA	TN	nd	> 30 °C
FD	Frost days	Zhang et al. (2011)	TN	nd	< 0 °C
Max consec	Max spell length for above thermal indicators	ICARIA	-	nd	-
Nº events	Number of above thermal indicators events	ICARIA	-	ne	> 3 days
TXm	Mean maximum temperatures	ICARIA	TX	°C	-
TNm	Mean minimum temperatures	ICARIA	TN	°C	-
TM	Mean temperatures	ICARIA	TA	°C	-
HWle	Heatwave length	ICARIA	TX	nd	3d > 95% TX
HWim/HWix	Mean and maximum heatwave intensity	ICARIA	TX	°C	3d > 95% TX
HWf	Heatwave frequency	ICARIA	TX	ne	3d > 95% TX
HWd	Heatwave days	ICARIA	TX	nd	3d > 95% TX
HI - P90	Heat Index (percentile 90)	NWS (1994)	TX, RH	°C	TX>27 °C, HR> 40%
UTCI	Universal Thermal Climate Index	Bröde et al. (2012)	TA RH, W	-	-
UHI	Isla de calor (BCN) anual y estacional	AMB, Metrobs 2015	T	°C	TM1-TM2 > 0 °C
Precipitation indicators					
R20	Number of heavy precipitation days	Zhang et al. (2011)	P	nd	>20 mm
R50, R100	Days with extreme heavy rain	AMB et al. (2017)	P	nd	>50mm >100mm
Ra	Yearly and seasonal rainfall relative change	ICARIA	P	mm	≥ 0.1mm
IDF - CCF	IDF Curves - Climate Change Factor	Arnbjerg-Nielsen (2012)	P	-	≥ 0.1mm
Forest fire indicators					
Mean FWI	Mean Canadian FWI in fire season	Stock, B.J. et al. (1989)	RHn, TX, P, W	.	June-September
Very High FWI	Very High Canadian FWI	Stock, B.J. et al. (1989)	RHn, TX, P, W	nd	FWI > 38

Table 11. Summary of selected drought, oceanic and wind indicators, grouped aligned with the main hazards they feed. "nd" = number of days; "ne" = number of events.

Index/name	Short description	Source	Variable	Units	Threshold
Drought indicators					
CDDx	Maximum dry spell duration	Zhang et al. (2011)	P	nd	< 1 mm
CDDm	Mean dry spell duration	Zhang et al. (2011)	P	nd	< 1 mm
SPI	SPI of 1, 3, 6, 12, 24 & 36 months	McKee et al. (1993)	P, TA	-	≥ 0.1mm
SPEI	SPEI of 1, 3, 6, 12, 24 & 36 months	Vicente-Serrano et al. (2010)	P, TA	-	≥ 0.1mm
Oceanic indicators					
SS	Storm surge	Bryant et al. (2016)	MT	cm	-
OW	Significant/maximum wave height	ICARIA	WH	m	-
Wind indicators					
EWG	Extreme wind gusts	ICARIA	W	km/h	-

Legend:
WH: Wave Height P: precipitation W: Wind MSL: mean sea level MT: meteorological tide

5. Discussion of results

This section presents the outcomes of the ICARIA project's downscaling methods, which offers a detailed glimpse into future climate change scenarios for the three considered case studies. As was aforementioned, ICARIA has used a twofold approach to obtaining climate input with two different downscaling processes. Through rigorous analysis, the two studies have generated insights into anticipated shifts in climate variables and specific indicators. From temperature projections to precipitation trends and extreme indicators like heatwaves or extreme rainfall days, the analysis offers valuable insights into potential future climatic conditions. These findings shed light on the nuanced shifts anticipated in our environment, providing crucial information for ICARIA's policymakers, researchers, and stakeholders alike. Exploring these results is expected to deepen our understanding of the potential impacts of climate change on various aspects of our planet, paving the way for informed decision-making and proactive adaptation strategies.

5.1. Statistical downscaling outputs

Throughout this section, a detailed discussion of results from FICLIMA downscaling will be done. This discussion will be split into three parts, one per CS, and in each one a more specific summary will be performed to briefly explain the outcomes of each group of variables and indicators. This will depict what the future climate, along with each considered SSP, may look like in the future compared to the one we grew and lived in. After the discussion, a thorough analysis of the outcomes is summarized and presented in a table for a quick review of expected results for each indicator and each SSP and period considered.

5.1.1. Discussion for the Barcelona Metropolitan Area - AMB

IMPORTANT: *In this section are discussed the results for the AMB area, considering all the stations (AEMet, SMC and BCASA) falling within the administrative region. Changes will be mainly discussed in what refers to changes in* ***median values****; due to the geographical heterogeneity (shore and inland, valley and mountain) of stations, some indicators might be registered or expected in the future in some points, but might not be explicitly mentioned. A more detailed summary with uncertainty thresholds is done in the next 5.1.2 section. All summary figures will be shared and available to partners for detailed consultation, and the posterior spatial treatment (TIF) of results might help in identifying in ICARIA's DSS, once made available, the particularities of results in the geographical extension of the CS.*

—

Based on the locally generated climate change scenarios for this case study, and following what was expected in the current warming scenario, temperature rises are anticipated across all scenarios, timeframes, and seasons. However, and linked to the non-linear behaviour of rainfall with warming scenarios, no notable alterations in precipitation are foreseen across any scenario. As a wrap-up, an uptick in aridity is almost certainly linked to rising temperatures, particularly during the summer months.

Thermal indicators

Regarding the group of variables and indicators linked to temperature, as they were defined in the previous 4.2 section, results show an absolutely clear trend towards increasing temperature in the future, with worse scenarios as we consider worse SSPs.

About the temperature variable, **maximum temperature** increases are expected to range from 1.7 to 2-3 degrees Celsius by mid-century considering median values as depicted in future scenarios, and from 2.5 up to 4.5 by the end of the century in the SSP2-4.5 and SSP5-8.5 respectively (see Figure 20 as example). The mean annual temperature and minimum annual temperature are expected to increase approximately the same as the maximum temperatures in absolute values. Great significant rises are expected in all scenarios, periods of the year, and time horizons.

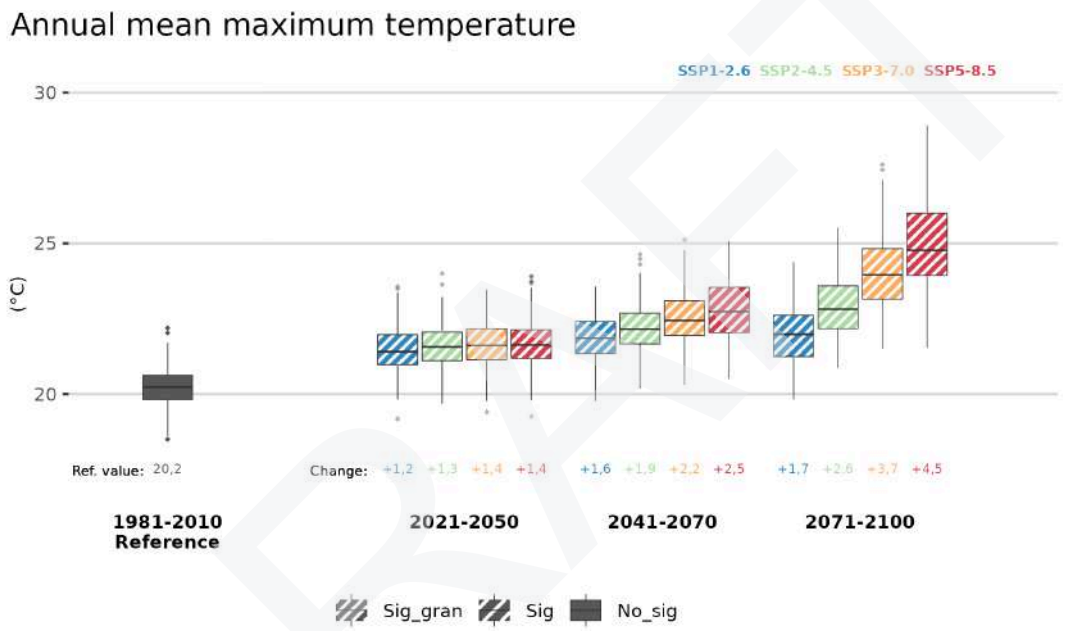

Figure 20. Expected evolution of mean maximum temperature for AMB stations.

Taking percentiles, **Cold/Warm days** (P10/P90 of maximum temperature, respectively) are expected to notably decrease/increase in the future, since taking the historic period as a reference in a percentile indicator causes that a warming climate boosts the number of days above P90 and reduces those below P10. Changes show that from the reference ~34 days/year, Cold days will reduce by 50-60% at mid-century, and about 75-90% by 2100. Warm days on the contrary would double (+100% or +35 days) by mid-century and increase about 150-200% (60-88 days) by 2100.

The change in maximum temperature will lead to changes in the indicators defined from it. As a matter of fact, Heat Day (Tx > 30ºC) and Extreme Heat Day (Tx>35ºC) will significantly sharply increase. **Heat days**, according to projections, would go in AMB from 19 historic days to a range of 50 to 70 days a year by 2050, and of more than 90-100 days by 2100 in worst-case scenarios (see Figure 21). **Extreme Heat days** would follow this trend, even being truly rare nowadays in AMB due to the tempering effect of the

Mediterranean (0.2 historic days a year), a warming sea would lose that effect, and AMB would see a significant increase of +5 days in average by mid-century and +20-30 by late-century in worst cases.

The increase in minimum temperatures will lead to a significant large decrease in the number of **frost days** during winter by the end of the century, from a historical median of 7 days to a reduction by half or even the totality of days in worst-case scenarios (SSP3-7.0 and 5-8.5). This change in minimum temperature is also expected during the summer season, and will also lead to significant increases in the occurrence of **tropical nights** (Tmin>20ºC) in all scenarios and time horizons, with a stronger and larger trend the closer to the end of the century. Historic values fall around 48 nights (median), and significant increases are already expected in the earliest time period (around +29 in consensus), increasing steeply up from +36 to even around +80 in worst cases, being expected therefore even ⅓ or more of nights (up to 150) per year above 20ºC by the year 2100 (Figure 22). This trend translates too to equatorial nights (Tmin >25ºC) and infernal nights (Tmin >30ºC)**. Equatorial nights** were barely suffered in AMB in past times (~1 night), but will follow the tropical night trend with increases of +5 nights before 2050, and from +10 in a more optimistic scenario (SSP1-2.6) up to even +60 nights in SSP5-8.5. **Infernal nights** were not registered yet, but from mid-century some stations are expected to start suffering them, and regarding the median by the end of the century 4 infernal nights are expected to happen every year, with values of +10 in some areas.

Aside from the previous discussion, and in order to better understand and assess further impacts of previous indicators, two derivatives were applied, calculating the maximum number of consecutive days of each previous indicator, and also the number of events (considered as ⩾3 consecutive days) expected throughout the year. Regarding **maximum consecutive days**, **Heat Day** could go from a typical 8-day streak in historic times to around 20 days by 2050 or more than 55 days by 2100. **Extreme Heat Days**, practically not seen, could chain 3 up to more than 13 days in a row by late-century. **Frost days** will practically disappear, while **Tropical Nights** could go from a current streak of 28 days up to an average of 60 up to 120 tropical nights in a row in the worst case. **Equatorial nights** and **Infernal nights** haven't happened consecutively, but could appear around 20 consecutive nights by mid-century or from 25 to even 60 by late-century for equatorial nights, while infernal nights are not expected to happen in a row until the end of the century (up to 3 days). Concerning the **number of events**, **Heat Day** would go from a reference of 1.5 events a year to 3 during the century (the increase is expected in the number of consecutive days). The same happens for **Extreme Heat Day**, with almost 1 up to 2 events a year by 2100. About **Frost days**, there was no event in the past and none is still expected in the future. **Tropical night** events were about 3 per year, and no change is expected (in the number, but yes in the duration of them). **Equatorial night** events were not registered in median (some stations have them though), but could appear in general by mid-century and about 1-2 by late-century. No **infernal night** events are expected so far.

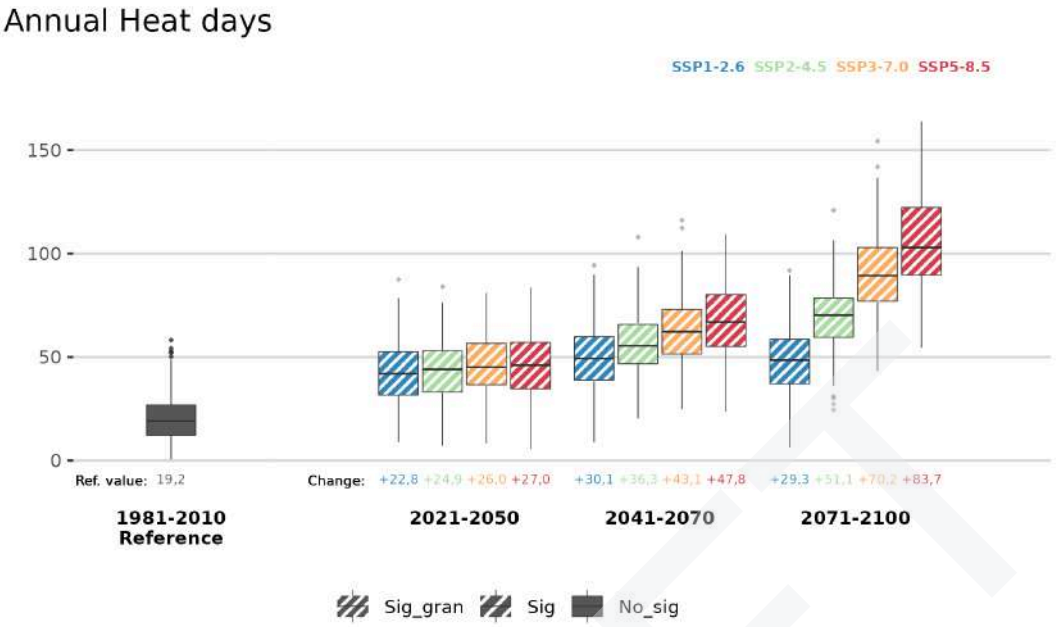

Figure 21. Expected evolution of heat days for AMB stations.

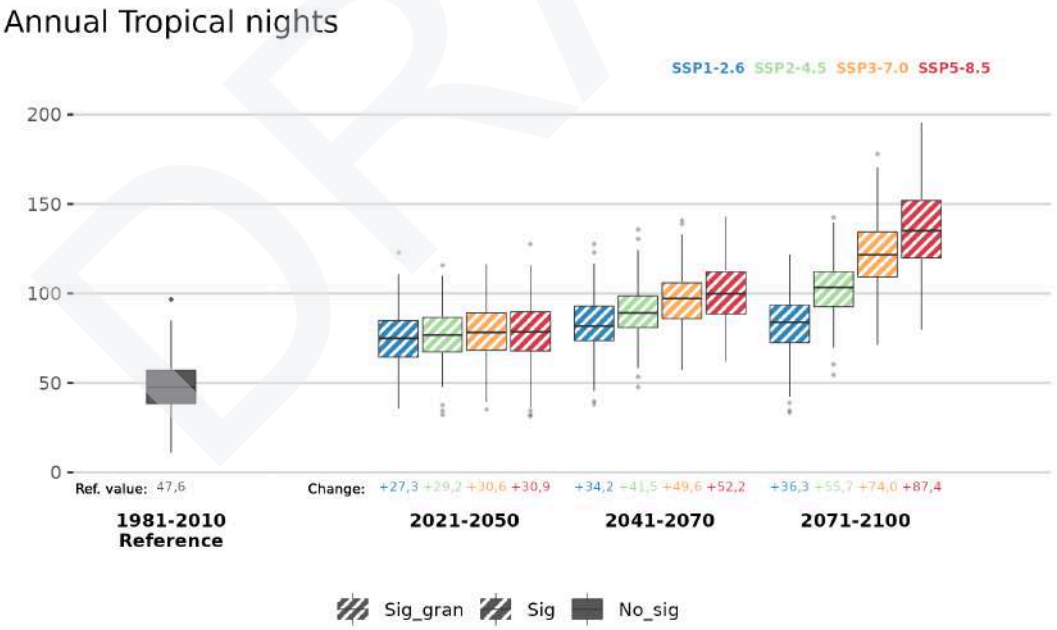

Figure 22. Expected evolution of tropical nights for AMB stations.

Additionally,, the increase in temperatures will affect the occurrence of extreme weather events such as **heat waves**, which are one of the more impactful events due to their effects on human health, infrastructure or the environment. Therefore, the length, intensity, and frequency of heat waves must be analysed to characterize these extreme weather events. The heat wave definition was created for ICARIA considering several climate and scientific conditions, and ended up being: *a temperature-related episode of at least three consecutive days where the weather observations considered register maximum temperatures above the 95% percentile of their daily maximum temperature records for the months of June to September of the 1981-2010 period.*

Heat wave impacts are expected to increase significantly since the projections indicate a very relevant rise in the intensity, length, and number of events in most scenarios by mid-century and end-century.

Coming from a definition based on percentiles, it is expected, and it is seen, that for the historical period the **number of heat wave** events is ~0.5. This is especially relevant to assess the magnitude of the change. By mid-century, the number of expected heat wave events increases to +3 on an average year, and up to +4 in the median by late-century from the SSP2-4.5 to SSP5-8.5 (Figure 23). The **average heat wave length** is expected to go from 4 days in past times up to 7-10 by mid-century, and increase significantly in the most pessimistic scenarios by late-century, with an average duration 10-14 days in moderate scenarios up to 19 days per event in the SSP5-8.5 (Figure 24). Also, increments are expected in the **maximum heat wave intensity**, set in the median at 33.4ºC for the AMB. By the early-century no significant change is expected, but by the mid-century and late-century, the change is around +1ºC up to +2.4ºC in most pessimistic scenarios. The annual number of days that agree with the definition of maximum temperatures higher than the 95th percentile but skipping the 3-row days (named **heat wave days**) would also significantly rise from a historic 3.5 days to more than 20 (up to 40) by 2050, or even to 20 up to 80 by 2100.

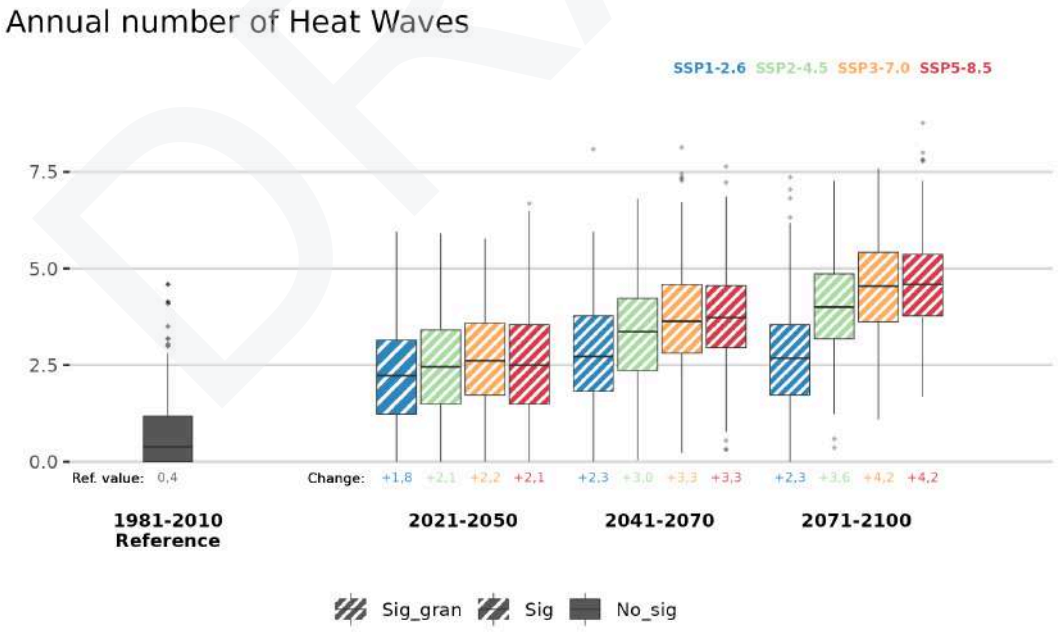

Figure 23. Expected evolution of the number of heat waves for AMB stations.

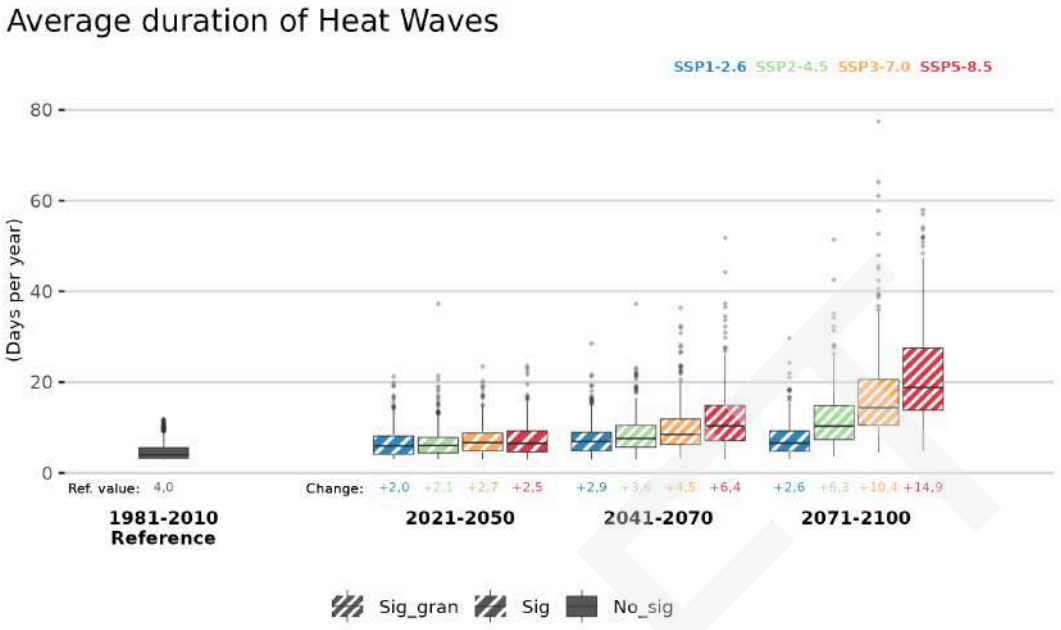

Figure 24. Expected evolution of the duration of heat waves for AMB stations.

For the case of the AMB, some tailored variables have been calculated on-demand, mainly about thermal comfort. One of them is the commonly used **Heat Index (HI)**, which results from a combination of temperature and RH about certain thresholds and represents the body's thermal sensation at some point. Heat Index represents that for certain T/RH values, the heat stress that a body can suffer, dangerous at some point, has nothing to do with the actual temperature that is being recorded.

For the AMB, reference HI oscillates around 31.5ºC, and is expected to significantly increase in the future due to rising temperatures and the constant input of humidity from an even warmer Mediterranean. In this regard, increases of +2.5-5ºC are foreseen by mid-century, while further rises of +5-9ºC in worst-case scenarios are feasible by late-century (refer to Figure 25 for more detail).

Another one, just for the AMB case, is the **UTCI.** The UTCI index shows a significant increase in its values in the last half period of the twenty one century. It needs to be remarked that, unlike for HI where there is a threshold for the calculation (Tx>25ºC), the UTCI has been obtained for all year-long, and so values don't seem to be so extreme as if they were obtained just for summer months. Also, the lack of temporal resolution limits the ability of the index to analyse the thermal stress typical of the summer months, and which is evident during the central hours of the day (high humidex factor). However, the increments analysed can be used to analyse future changes with a high level of confidence (Figure 26). UTCI will range from its historical mean value of 13.1ºC, up to values between 15 and 19ºC in the last quarter of this century.

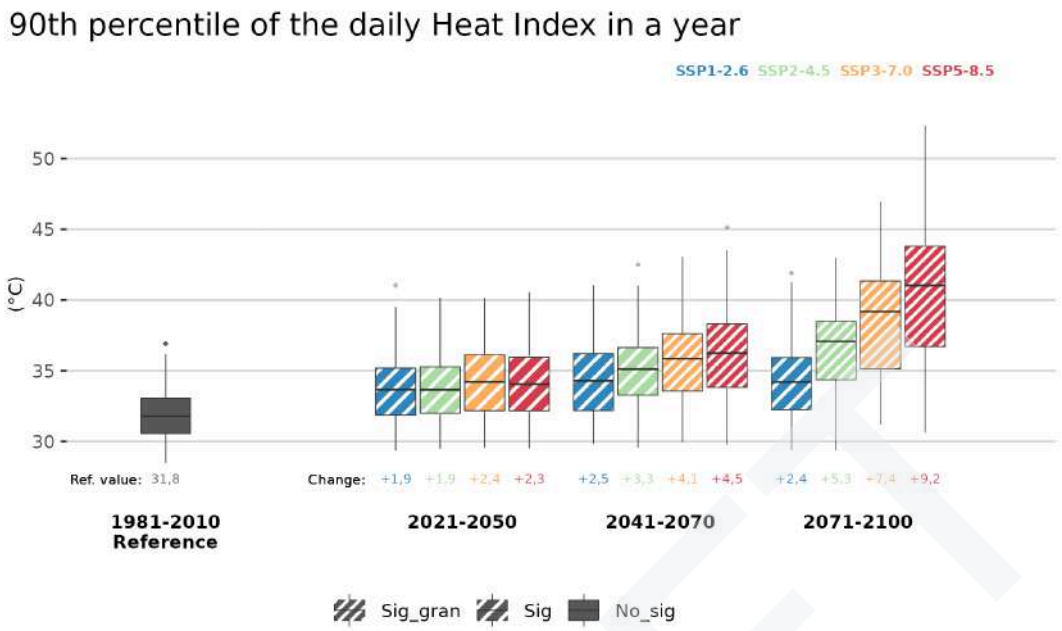

Figure 25. Expected evolution of the percentile 90 of Heat Index for AMB stations.

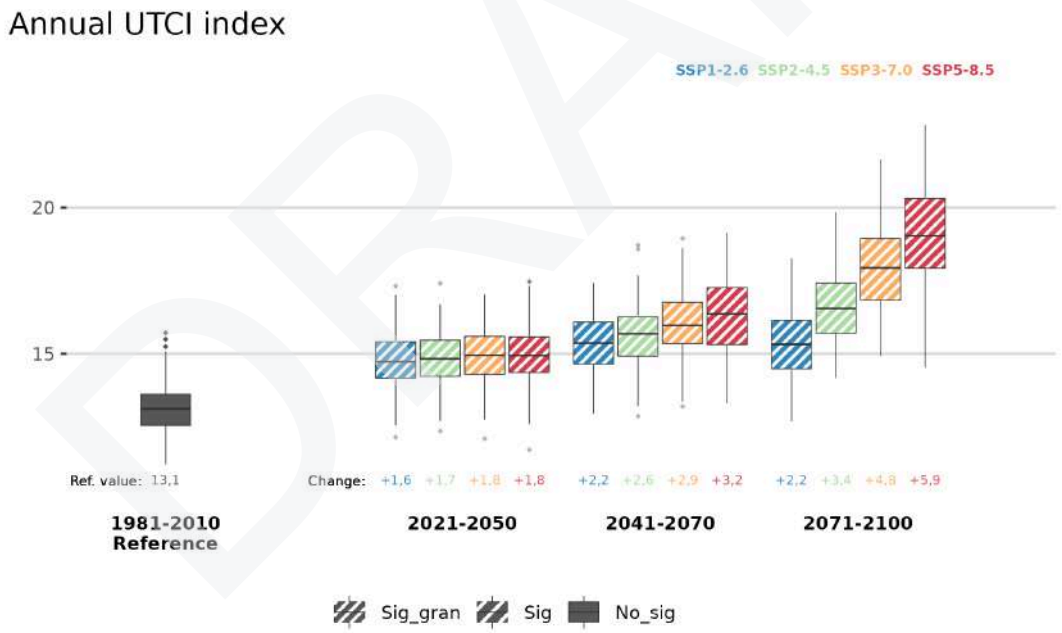

Figure 26. Expected evolution of UTCI index for AMB observatories.

Another indicator in this regard is the **Urban Heat Island effect** indicator, which was obtained from an already existing methodology comparing *Barcelona Vila Olímpica* and *Barcelona Airport* stations. In this

case, Figure 27 shows differences between these two stations with each point referring to one year within the period plotted instead of one station. Historical data shows a UHI of around 2.2ºC, while projected changes foresee an expected significant slight decrease in UHI, with reductions of around -0.5ºC by 2050 and of even -1ºC by 2100 in SSP3-7.0 and SSP5-8.5. These changes are also seen in seasonal UHI; the strongest UHI is that of winter, with a historical value of 2.8ºC, but will see the weakest reduction, of around -0.5ºC (coherent with winter UHI). The strongest reduction is expected in summer, with a historical value of 1.9ºC and a reduction of -1º even up to >-2.4ºC in SSP3.70 and SSP5.85, which would suggest a reverse situation with rural areas warmer than urban ones, an interesting result prone to discussion. This could be explained by changes in the behaviour of minimum temperatures in the outskirts maybe due to a reduction in the cooling effect in rural coastal areas of a much warmer Mediterranean. Another factor is the reduction of human activities in Barcelona city centre in part due to a decrease in the population, as also explained in *Martin-Vide, J., & Moreno-Garcia, M. C. (2020)*. or in AEMet[11].

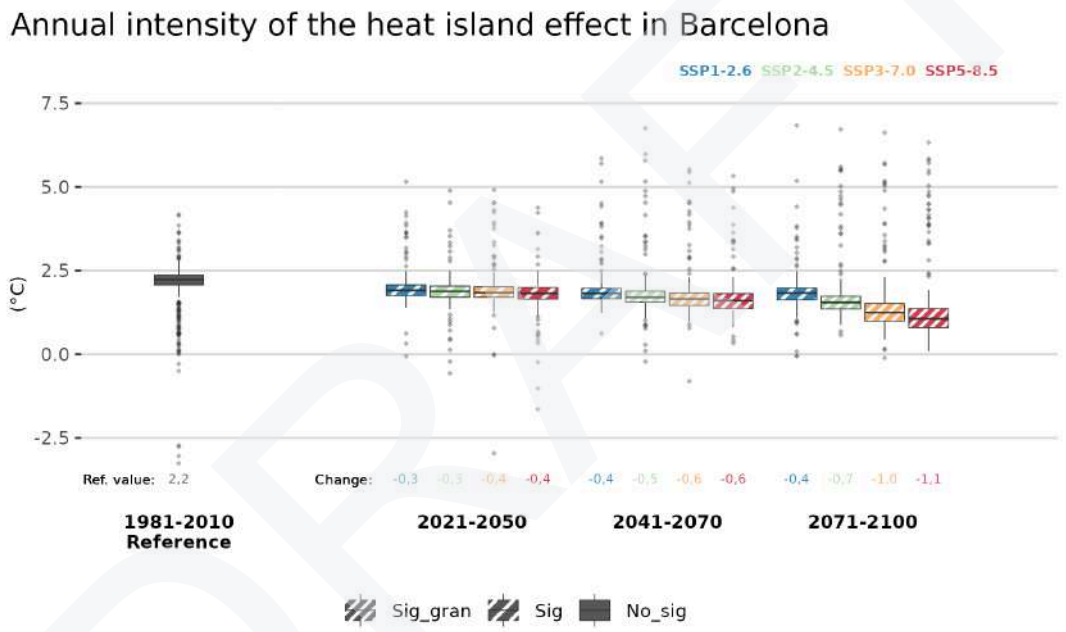

Figure 27. Expected evolution of annual mean UHI for AMB (Vila Olímpica - Airport).

[11]https://aemetblog.es/2020/09/27/el-cambio-climatico-aumentara-la-intensidad-de-las-islas-de-calor/

Precipitation indicators

Regarding precipitation indicators, different ones have been obtained depending on the needs of the AMB CS. In this regard, some indicators were designed to measure changes in annual precipitation while other indicators were more focused on extreme rainfall events. In this sense, in summary, no significant change is expected in yearly precipitation so far nor in days above specific extreme thresholds, but an increase in precipitation intensity at the sub-hourly scale is foreseen.

In more detail, about annual precipitation indicators, **yearly cumulative precipitation** as well as **seasonal cumulative precipitation** do not display any changes towards the future, as can be seen in Figure 28. Small increases or decreases appear, but are not significant enough to be considered due to the uncertainty seen.

In what refers to extreme rainfall events, some indicators of these events are obtained for **days above 20, 50 and 100mm**. In the three cases, the changes with respect to historical observed days (6, 1 and 0.1 respectively) are not significant enough to be considered.

Studying sub-daily precipitation also allows us to know the behaviour of rainfall at these time scales, which in Mediterranean climates often poses the biggest threats for extremely torrential downpours. In this regard, **IDF curves and CCF index** were obtained for sub-hourly rain at 1, 2, 5, 10, 20, 50, 100 and 500 years respectively.

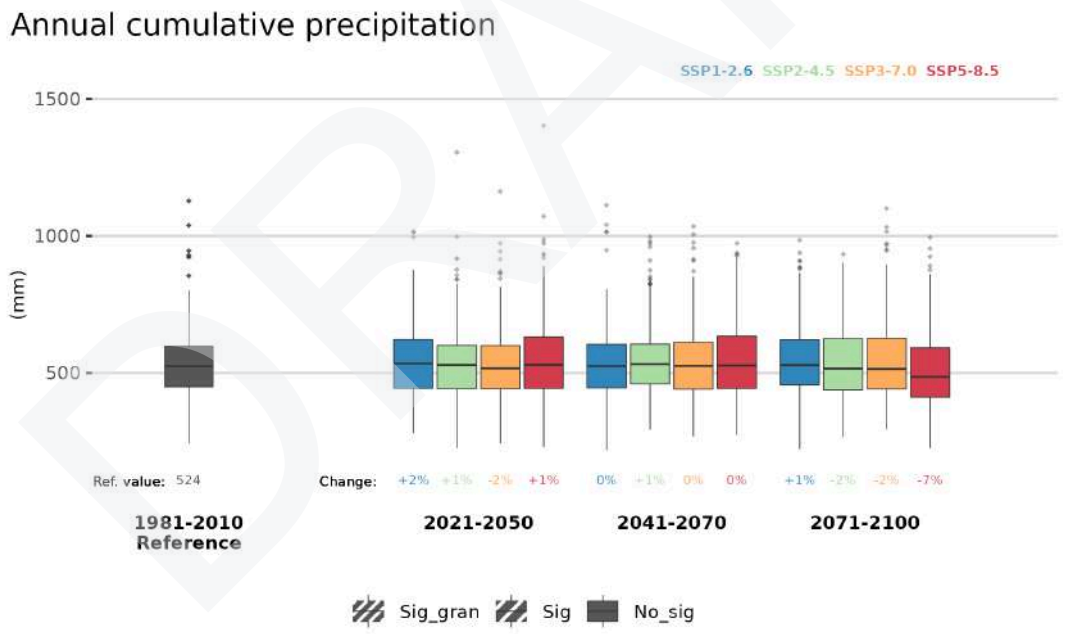

Figure 28. Expected evolution of the relative change in annual cumulative precipitation for AMB stations.

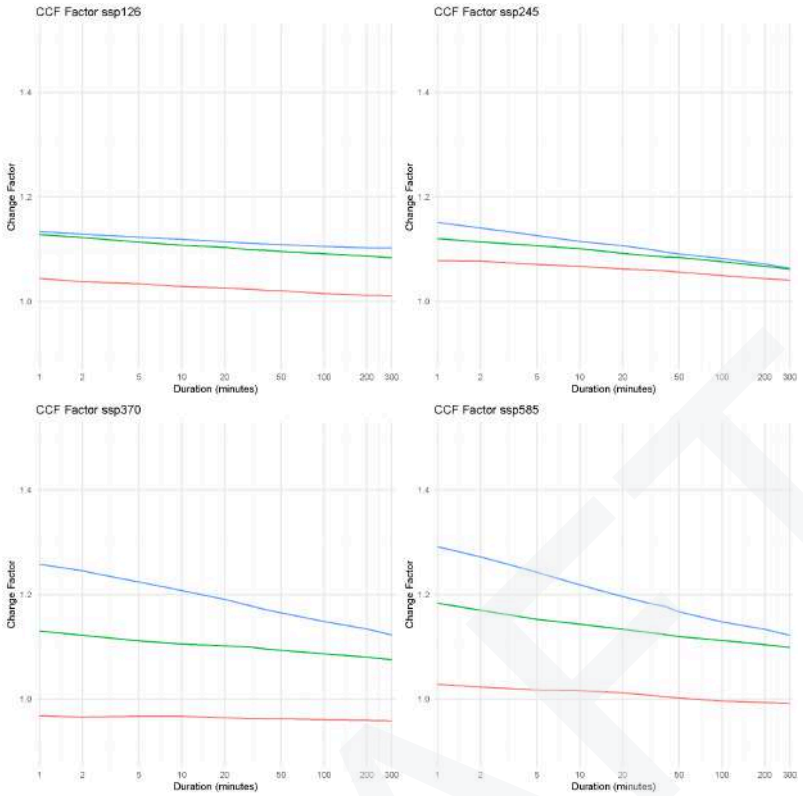

Figure 29. Example of the CCF for AMB. Y-axis represents the CCF, X-axis the duration in minutes. Each line represents the CCF for a specific period (15-40, 41-70, 71-00 for the red, green and blue respectively).

Results for CCF (which encompasses IDF as well), shown in Figure 29, are interpreted as values greater than 1 indicating an increase in the IDF rates. As the forecast examples show, they are expected especially in the worst-case scenarios (SSP3-7.0 and 5-8.5), and significantly in the low duration scales (<10 min in the X axis) and for the last period of the century (2071-2100 or the blue lines). This translates as changes foreseen of about +15-25% in the intensity of rainfall. Although positive CCF values are observed in Barcelona, the increase in drought duration in Southern Europe may partially counteract the increase in the maximum water-air capacity itself, especially in the lowest return periods, resulting in lower CCF values.

Drought indicators

In what concerns to drought, two types of indicators were agreed on in their calculation, those related to dry days (dry spell duration), and those with anomalies in precipitation/evapotranspiration (SPI & SPEI). The first type was defined as a "dry day" a day with precipitation registered below 1mm, and two indicators were calculated: mean length of dry spell and maximum length of dry spell. About the **Mean length of dry spell**, for the AMB the historical yearly value was around 10 days, with no significant changes expected in the future with the exception of SSP3-7.0 and SSP5-8.5 by the end of the century, with slight significant increases of +1-2 days. Regarding the **Maximum length of dry spell**, the historical reference value is 38 days, and although small increments are foreseen in the future, none of them is significant except for SSP5-8.5 in late-century, with a +4.7 change.

Figure 30. Expected evolution of a 36-month length SPEI Thornthwaite indicator for AMB stations.

Regarding the SPI and SPEI indexes; due to their definition, historic value is always set to 0, and expected changes differ from one to another. For **SPI**, no significant changes are expected by mid or late century in any scenario or time period since no significant change in mean accumulated precipitation is foresight in this regard. However, for **SPEI**, since it includes changes in temperature for the estimation of evapotranspiration, changes are do expected. Following an increase in temperature and no changes in rainfall, SPEI values are projected to decrease significantly for all time periods and scenarios, more steeply towards the end of the century, with decreases from -1 down to -3 in SPEI-12, and from -1.5 down to almost -4 for SSP5-8.5 in SPEI-36 (Figure 30). Similar reductions are expected in other monthly-aggregated SPEI (1,3,6,24).

Forest fire indicator

For the case of the hazards concerning forest fires, the FWI was used as an indicator to evaluate the likelihood of extreme forest fires developing when started. This index merges different conditions of humidity, temperature and wind to asses the evolution of fires. In this regard, projections show that the **mean FWI between June and September** (risk season) for the AMB is about 16 in historic period, and all scenarios agree in future increments in this value, of around +1-2 depending on the scenario, with a significant increase of around +2-4 by 2100 (Figure 31). For the extremest situations, the **number of days with FWI>38** (Very High risk) is set at 7.5 in the past, and will increase around +2-3 days up to a significant +6 for worst case scenarios by 2100.

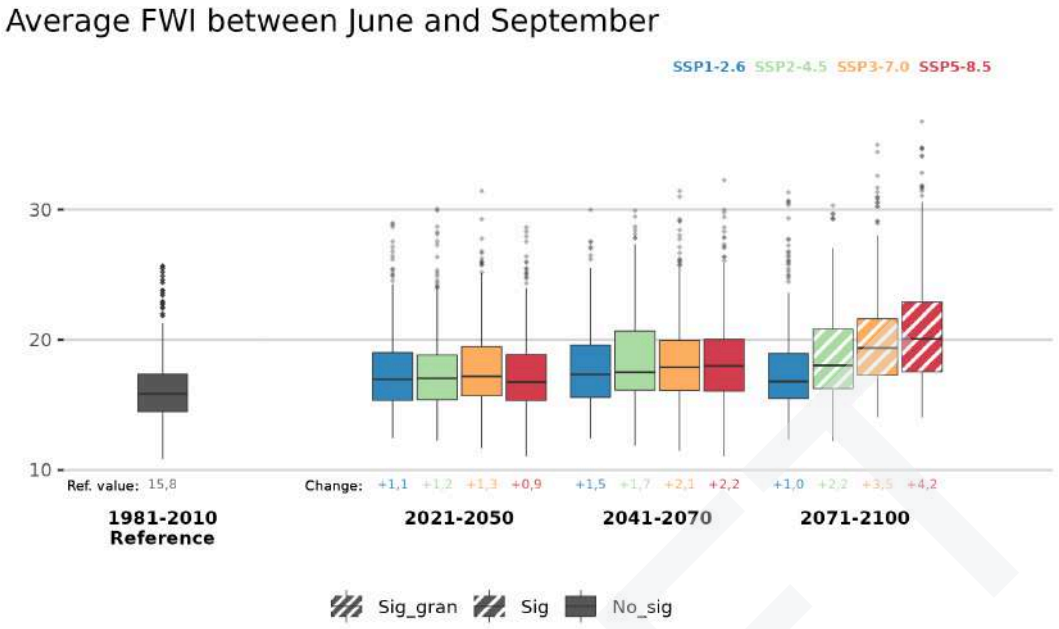

Figure 31. Expected evolution of mean FWI between June and September for AMB stations.

Oceanic indicators

Regarding **storm surges**, the results show no changes or even a decrease in the meteorological tide for some of the scenarios compared to the historical period (1981-2010) (Figure 32). However, some peculiarities of these projections should be pointed out. As specified below in Annex 4, the storm surge is calculated by decomposing the total sea level into three components: the astronomical tide, the mean sea level, and the meteorological tide. This example does not take into account the rise in sea level or the harmonics of the astronomical tide, but it does take into account the synoptic storm surge or the meteorological tide, which is expected to decrease (especially in the worst case). This can be explained by the decrease in the number of synoptic or large-scale storms in the Mediterranean basin (movement of the jet stream towards northern latitudes), although the decrease is not particularly remarkable (decreases from 10 to 20% could be expected) and they can be overcompensated by the rise in **mean sea level** (see Figure 33) or the significant wave height, among other factors. This is compatible with a future scenario in which most of the days are expected to have less wind and consequently fewer waves, and at the same time more very windy peaks as a result of deeper convective storms, Medicanes or Derechos. Therefore, the pattern of expected variations must take into account the high uncertainty cascade effect produced by the accumulation of uncertainty from the different sources (observations + method + models).

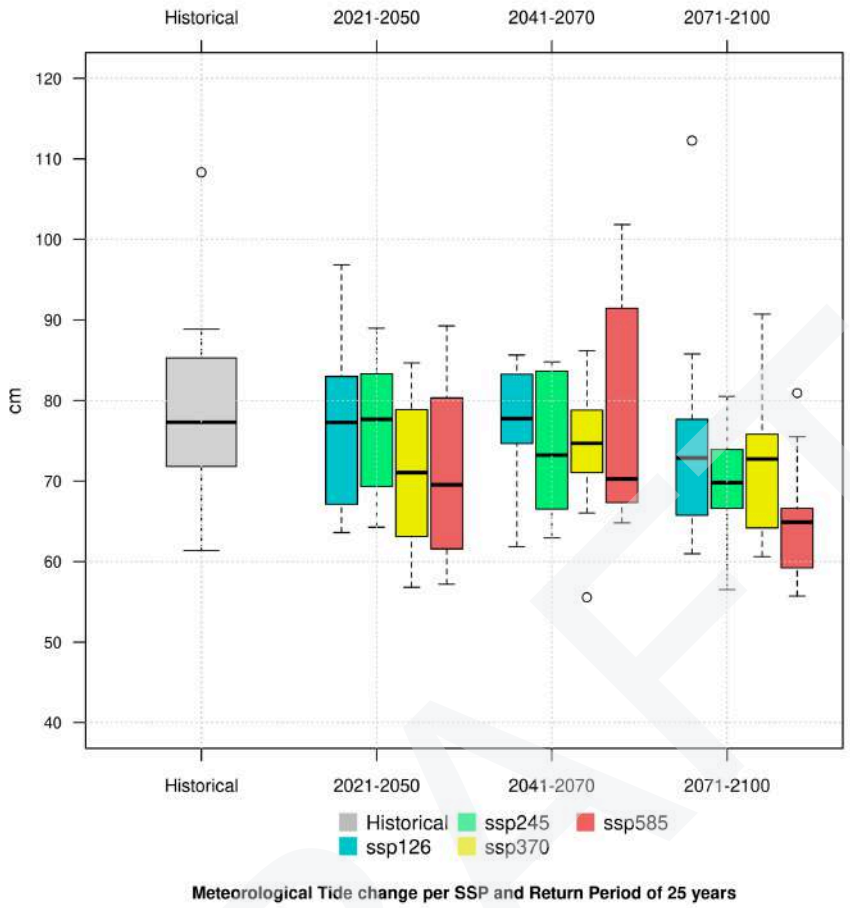

Figure 32. AMB storm surge projections (in cm) for each SSP and a return period of 25 years considering all CMIP6 models.

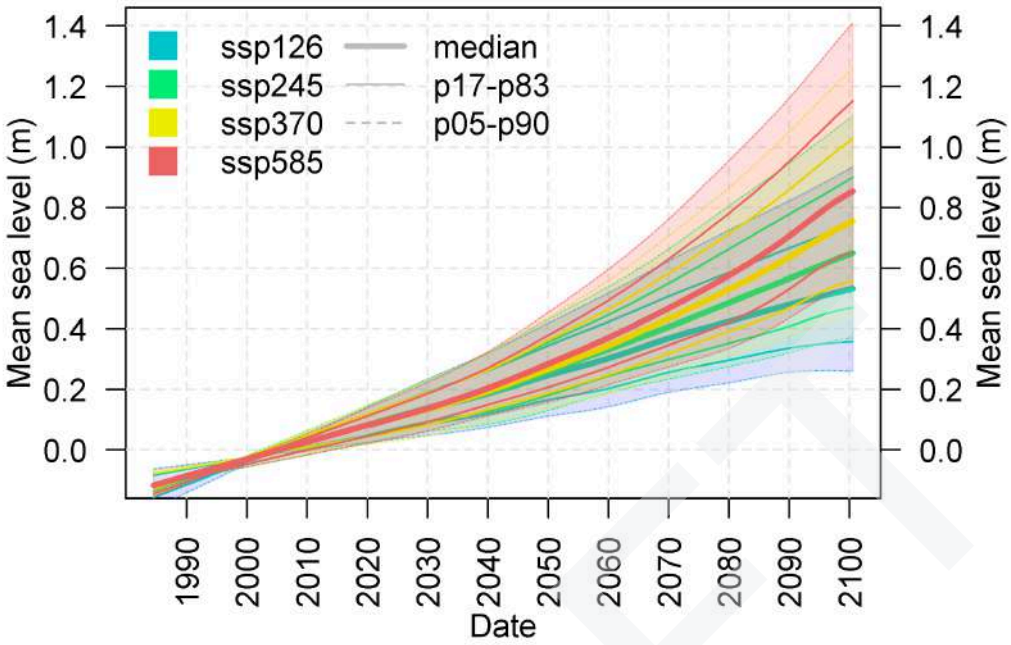

Figure 33. AMB Mean sea level projections (in meters) for each SSP considering all CMIP6 models.

The **Maximum Wave Height** is not expected to change significantly in the future. This null variation is especially obvious in the first three scenarios (SSP1-2.6, SSP2-4.5 and SSP3-7.0). Just a lighter decrease can be appreciated in the worst-case scenario (SSP5-8.5) for the median of all cases (Figure 34), for similar reasons as the meteorological tide previously mentioned.

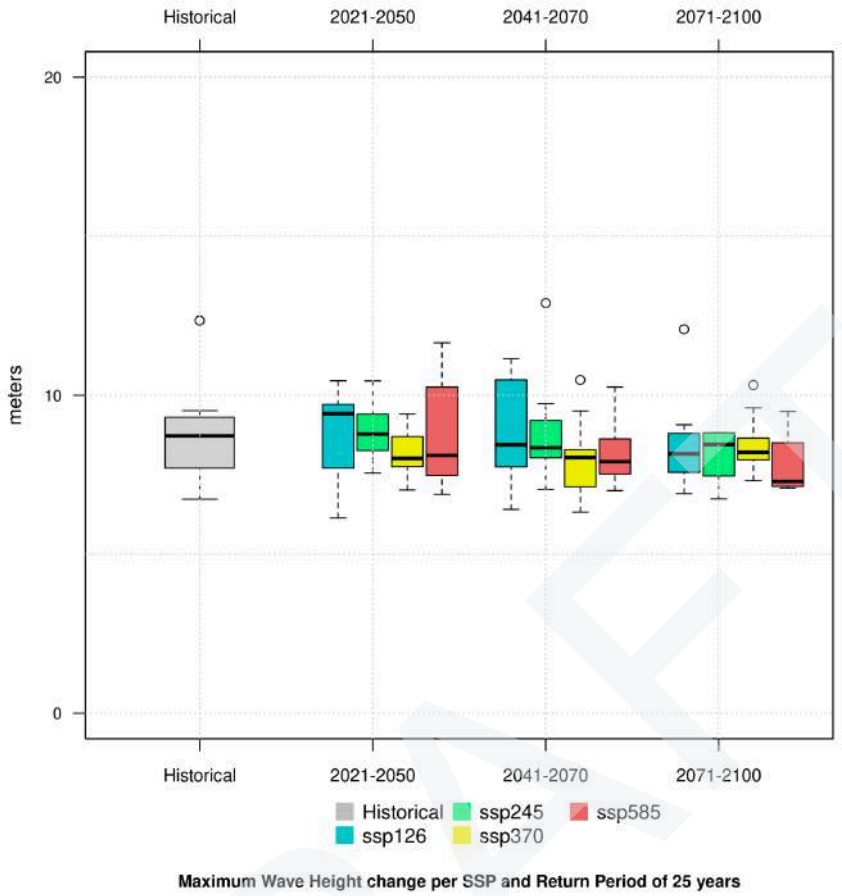

Figure 34. AMB Maximum Wave Height projections (in meters) for each SSP and a return period of 25 years considering all CMIP6 models.

The situation of the **Significant Wave Height** projections is pretty similar. In fact, the statistical variations of their significant portions (percentiles 25 to 75) are negligible for the whole models and scenarios. Just for the scenario SSP5-8.5 can be interpreted as a future decrease but lighter than other variables such as meteorological tide or maximum wave height.

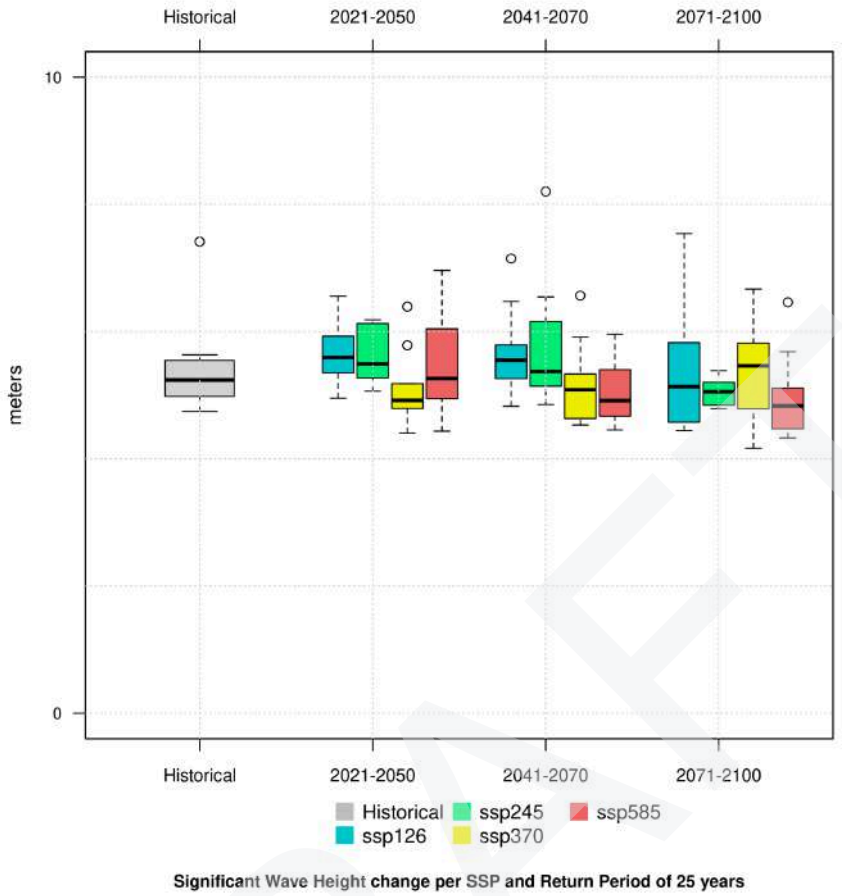

Figure 35. AMB Significant Wave Height projections (in meters) for each SSP and a return period of 25 years considering all CMIP6 models.

Wind indicator

Wind is one of the most difficult meteorological variables to be studied when dealing with future climate change variations. Due to its own nature, a result of multiple factors such as orography, local thermal variations, pressure gradients, or other weather phenomena, the future study of wind is not as straightforward as temperature could be, and future changes in pressure centres and other atmospheric patterns that determine wind's strength and direction is still today prone to high uncertainties. Besides, the remarkable lack of wind observations or their poor quality with respect to those from temperature or precipitation also hinders the procedures in statistical downscaling. On the other hand, as it can be seen in Annex 4 (Table A3.1), only 5 (out of 7) models have passed validation tests for the methodology and are used to produce these outcomes. It is good advice to take into account the aforementioned difficulty of working with the wind when interpreting the next results.

In this sense, wind gusts have been modelled for the future since it is a variable that poses a higher risk and interest for ICARIA, and is included in other multiple indicators. The future evolution is studied for

percentiles since it doesn't respond to a normal distribution and mean values are meaningless. For the AMB, Percentile 99, as well as other percentiles (P80, P90 or P100) don't seem to show any change in its expected behaviour in the future.

If we translate this into return periods, we can observe little variation in all scenarios. In general, there is a consensus that the maximum gusts will generally decrease (Figure 36), considering the limitations of the method itself, and as previously mentioned for the storm surge. Despite this, in the intermediate scenarios there is the possibility of observing an increase in maximum gusts. This is more evident in higher return periods.

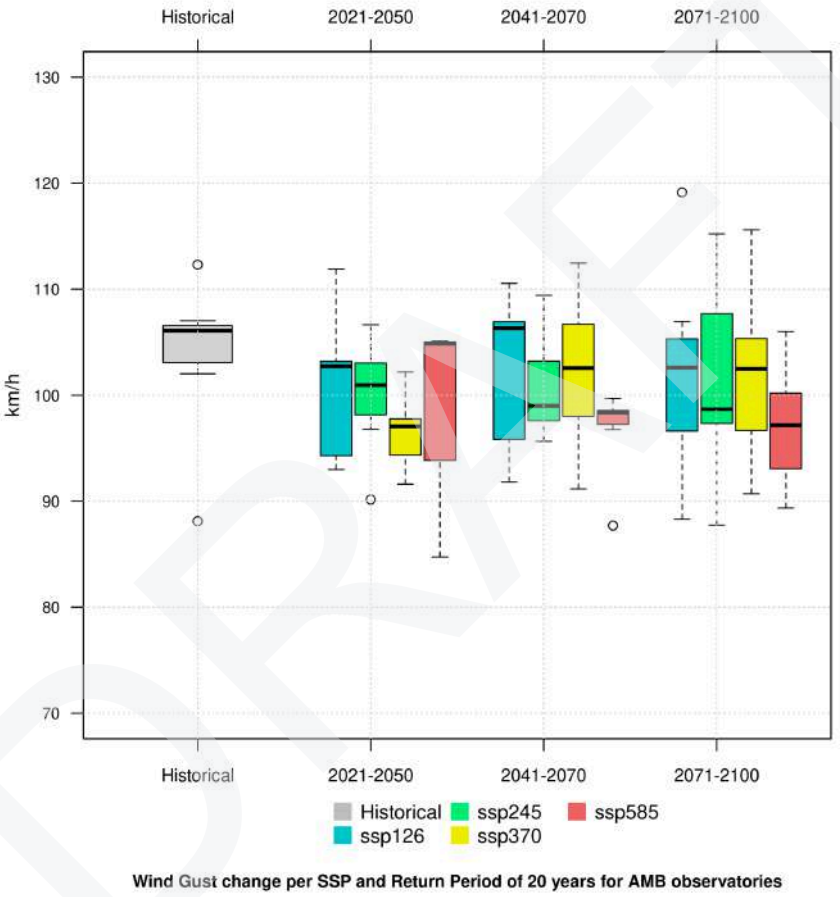

Figure 36. Results for RP of 20 years for wind gust projections and AMB stations.

5.1.2. Summary of results for the Barcelona Metropolitan Area - AMB

Table 12-1. Summary table for expected changes in future thermal climate variables and extreme indicators from FICLIMA statistical downscaling in AMB. Changes are expressed as the difference in "median(percentile 10/percentile 90)" of future expected values for each SSP and time period with respect to the historical median reference value for the period 1981-2010. Units are expressed in the INDEX column (nd = number of days, ne = number of events).

INDEX	81-10	2021-2050				2041-2070				2071-2100			
	HIST.	1-2.6	2-4.5	3-7.0	5-8.5	1-2.6	2-4.5	3-7.0	5-8.5	1-2.6	2-4.5	3-7.0	5-8.5
Thermal indicators													
TX90 (nd)	33.8	+24.1 (16.1/31.9)	+27.0 (18.9/34.8)	+26.3 (18.2/34.1)	+26.2 (18.1/34.0)	+37.6 (29.5/45.4)	+44.4 (34.3/52.2)	+51.0 (39.9/58.8)	+56.2 (44.1/64.0)	+38.2 (29.9/46.0)	+58.0 (47.9/67.8)	+74.8 (63.7/85.6)	+88.3 (77.2/99.1)
TX10 (nd)	34.2	-9.4 (-13.5/-5.6)	-10.2 (-14.3/-6.1)	-10.6 (-14.6/-5.8)	-12.5 (-17.7/-7.1)	-15.6 (-20.4/-11.2)	-17.4 (-22.0/-12.8)	-20.5 (-25.3/-15.7)	-21.7 (-27.3/-16.1)	-17.2 (-22.3/-12.4)	-22.7 (-27.3/-18.2)	-28.0 (-33.2/-22.8)	-30.1 (-35.3/-24.9)
HD (nd)	19.2	+22.8 (15.2/29.8)	+24.9 (17.3/31.1)	+26.4 (19.0/33.7)	+27.0 (18.8/33.4)	+30.1 (18.6/42.2)	+36.3 (24.1/48.8)	+43.1 (29.8/56.6)	+47.8 (34.4/61.4)	+29.3 (17.9/41.7)	+51.1 (33.2/69.5)	+70.2 (47.4/93.3)	+83.7 (58.9/108.8)
Max cons HD (nd)	8.1	7.6 (+4.4/+12.0)	+7.3 (+4.0/+11.7)	+9.0 (+5.6/+14.0)	+8.1 (+4.8/+12.5)	+14.7 (+9.4/+21.7)	+16.9 (+11.6/+24.2)	+22.2 (+16.4/+30.)	+25.9 (+20.4/+34.)	+12.2 (+7.0/+18.4)	+28.2 (+22.0/+37.)	+48.4 (+39.6/+62.)	+63.7 (+54.2/+78.)
Nº event. HD (ne)	1.7	+1.1 (+0.6/+1.7)	+1.3 (+0.8/+1.9)	+1.2 (+0.7/+1.8)	+1.3 (+0.8/+1.9)	+1.5 (+1.0/+2.1)	+1.9 (+1.4/+2.5)	+2.0 (+1.5/+2.6)	+2.0 (+1.5/+2.6)	+1.7 (+1.2/+2.3)	+1.9 (+1.4/+2.5)	+2.1 (+1.6/+2.7)	+2.0 (+1.5/+2.6)
EHD (nd)	0.2	+1.2 (+0.7/+1.8)	+1.0 (+0.5/+1.6)	+1.4 (+0.9/+2.0)	+1.1 (+0.6/+1.7)	+2.5 (+1.9/+3.1)	+4.0 (+3.2/+4.8)	+5.7 (+4.7/+6.7)	+7.2 (+6.2/+8.2)	+2.1 (+1.4/+2.8)	+8.2 (+6.7/+9.7)	+20.5 (+18.0/+23.)	+31.6 (+29.1/+34.1)
Max cons EHD (nd)	0.1	+0.7 (+0.2/+1.2)	+0.6 (+0.1/+1.1)	+0.8 (+0.3/+1.3)	+0.8 (+0.3/+1.3)	+1.3 (+0.6/+2.0)	+1.9 (+0.9/+2.9)	+2.8 (+1.3/+4.3)	+3.4 (+2.0/+4.8)	+1.2 (+0.5/+1.9)	+3.6 (+2.2/+5.0)	+8.8 (+4.9/+13.7)	+13.9 (+7.4/+20.4)

Nº event. EHD (ne)	0.0	+0.1 (+0.0/+0.2)	+0.1 (+0.0/+0.2)	+0.1 (+0.0/+0.2)	+0.1 (+0.0/+0.2)	0.2 (+0.2/+0.3)	+0.4 (+0.3/+0.5)	+0.5 (+0.2/+0.8	+0.7 (+0.3/+1.0)	+0.2 (+0.1/+0.3)	+0.8 (+0.6/+1.0)	+1.7 (+1.3/+2.1)	+2.5 (+2.1/+3.0)
TR (nd)	47.6	+27.0 (15.0/39.0)	+29.2 (17.0/41.0)	+30.6 (18.0/41.0)	+30.9 (18.0/41.5)	+34.2 (22.0/46.0)	+41.5 (29.0/53.0)	+49.6 (37.0/61.0)	+52.2 (39.0/64.0)	+36.3 (24.0/48.0)	+55.7 (43.0/67.0)	+74.0 (57.0/86.0)	+87.4 (69.0/100)
Max cons TR (nd)	28.3	+19.1 (+8.2/+32.4)	+22.9 (+11.4/+37.7)	+21.3 (+9.8/+34.4)	+23.0 (+11.2/+36.1)	+31.3 (+18.4/+46.)	+38.3 (+23.4/+54.)	+43.5 (+27.4/+60.)	+49.2 (+33.2/+66.)	+33.1 (+25.1/+43.)	51.5 (+33.3/+73.)	+69.4 (+48.4/+94.)	+84.4 (+63.4/+110.)
Nº event. TR (ne)	2.4	+0.5 (0.1/1.0)	+0.4 (0.0/0.9)	+0.5 (0.1/1.1)	+0.3 (0.0/0.8)	+0.4 (0.0/0.9)	+0.5 (0.1/1.0)	+0.5 (0.1/1.1)	+0.5 (0.1/1.0)	+0.5 (0.1/1.0)	+0.5 (0.1/1.0)	+0.5 (0.1/1.1)	+0.3 (0.0/0.8)
EQ (nd)	0.7	+4.7 (+3.6/+5.8)	+4.8 (+3.6/+5.8)	+5.7 (+3.8/+6.2)	+5.5 (+3.8/+6.0)	+10.1 (+8.5/+12.0)	+14.6 (+12.5/+17.0)	+20.1 (+17.9/+23.)	+23.1 (+19.9/+26.)	+9.6 (+7.4/+12.1)	+26.1 (+22.9/+30.)	+47.2 (+26.0/+60.)	61.4 (+47.2/+75.)
Max cons EQ (nd)	0.5	+2.8 (+0.6/+5.0)	+2.4 +0.4/+4.4)	+3.6 (1.6/+5.8)	+3.1 (+1.1/+5.3)	+6.3 (+3.1/+9.5)	+8.2 (+4.8/+11.6)	+12.0 (+7.5/ +16.4)	+14.7 (+9.3/+18.1)	+5.6 (+2.4/+8.8)	+16.2 (+11.8/+20.6)	+32.7 (+26.3/+39.)	+45.7 (+39.3/+52.)
Nº event. EQ (ne)	0.0	+0.5 (+0.1/+0.9)	+0.5 (+0.1/+0.9)	+0.5 (+0.1/+0.9)	+0.5 (+0.1/+0.9)	+0.8 (+0.6/+1.2)	+1.0 (+0.5/+1.5)	+1.2 (+0.7/+1.7)	+1.4 (+1.1/+1.8)	+0.8 (+0.3/+1.1)	+1.5 (+1.1/+1.9)	+2.0 (+1.5/+2.5)	+2.3 (+1.8/+2.8)
IN (nd)	0.0	0.0 (0.0/0.0)	0.0 (0.0/0.0)	0.0 (0.0/0.0)	0.0 (0.0/0.0)	0.0 (0.0/0.0)	0.0 (0.0/0.0)	0.0 (0.0/0.0)	0.0 (0.0/0.1)	0.0 (0.0/0.0)	0.0 (0.0/0.0)	+1.4 (0.0/+5.0)	+4.2 (0.0/+12.0)
Max cons IN (nd)	0.0	+0.0 (-0.0/+0.3)	+0.0 (0.0/+0.4)	+0.0 (+0.0/+0.5)	+0.0 (+0.0/+0.6)	+0.0 (0.0/+0.4)	+0.0 (+0.0/+0.6)	+0.0 (+0.0/+0.1)	+0.0 (+0.0/+1.0)	+0.0 (+0.0/+0.4)	+0.0 (+0.0/+1.2)	+0.9 (+0.0/+2.2)	+2.6 (+0.5/+7.2)
Nº event. IN (ne)	0.0	0.0 (0.0/0.0)	0.0 (0.0/0.0)	0.0 (0.0/0.0)	0.0 (0.0/0.0)	0.0 (0.0/0.0)	0.0 (0.0/0.0)	0.0 (0.0/0.0)	0.0 (0.0/0.0)	0.0 (0.0/0.0)	0.0 (0.0/0.0)	+0.1 (0.0/0.1)	+0.4 (0.0/0.4)
FD (nd)	7.2	-2.6 (-3.3/-2.0)	-3.0 (-2.3/-3.7)	-2.8 (-3.5/-2.2)	-3.7 (-4.4/-3.1)	-3.9 (-4.4/-3.1)	-4.5 (-5.2/-3.8)	-0.05 (-5.4/-3.8	-5.4 (-6.2/-4.8)	-4.5 (-5.2/-3.8)	-5.5 (-6.2/-4.8))	-6.6 (-7.2/-5.9)	-6.9 (-7.2/-6.2)
Max cons FD (nd)	2.9	-1.0	-1.1	-1.1	-1.3	-1.6	-1.6	-1.7	-2.0	-1.6	-2.0	-2.5	-2.7

		(-2.1/-0.5)	(-2.2/-0.1)	(-2.4/-0.2)	(-2.3/-0.9)	(-2.7-0.6)	(-3.1/-0.9)	(-3.8/-1.6)	(-3.2/-1.8)	(-2.5/-1.3)	(-2.8/-1.6)	(-2.9/-2.0)	(-2.9/-2.4)
Nº event. FD (nd)	0.6	-0.2 (0.0/-0.1)	-0.2 (0.0/-0.1)	-0.2 (0.0/-0.1)	-0.2 (0.0/-0.1)	-0.3 (-0.5/-0.1)	-0.4 (-0.5/-0.2)	-0.4 (-0.5/-0.2)	-0.5 (-0.5/-0.3)	-0.4 (-0.6/-0.2)	-0.5 (-0.6/-0.3)	-0.6 (-0.6/-0.4)	-0.6 (-0.6/-0.5)

Table 12-2. Summary table for expected changes in future thermal climate variables and extreme indicators from FICLIMA statistical downscaling in AMB. Changes are expressed as the difference in "median(percentile 10/percentile 90)" of future expected values for each SSP and time period with respect to the historical median reference value for the period 1981-2010. Units are expressed in the INDEX column (nd = number of days, ne = number of events).

INDEX	81-10	2021-2050				2041-2070				2071-2100			
	HIST.	1-2.6	2-4.5	3-7.0	5-8.5	1-2.6	2-4.5	3-7.0	5-8.5	1-2.6	2-4.5	3-7.0	5-8.5
Thermal indicators													
TXm (ºC)	20.2	+1.2 (+0.4/+1.6)	+1.3 (+0.5/+1.9)	+1.4 (+0.5/+1.9)	+1.4 (+0.5/+1.9)	+1.6 (+0.9/+2.2)	+1.9 (+1.2/+2.7)	+2.2 (+1.5/+3.0)	+2.5 (+1.8/+3.2)	+1.7 (+1.0/+2.6)	+2.6 (+1.9/+3.7)	+3.7 (+2.9/+4.5)	+4.5 (+3.7/+5.3)
TNm (ºC)	16.2	+1.0 (+0.4/+1.6)	+1.1 (+0.5/+1.9)	+1.1 (+0.5/+1.9)	+1.1 (+0.5/+1.9)	+1.6 (+0.9/+2.2)	+1.9 (+1.2/+2.7)	+2.2 (+1.5/+3.0)	+2.5 (+1.8/+3.2)	+1.7 (+1.0/+2.6)	+2.6 (+1.9/+3.7)	+3.7 (+2.9/+4.5)	+4.5 (+3.7/+5.3)
TM (ºC)	12.2	+1.0 (+0.4/+1.6)	+1.1 (+0.5/+1.9)	+1.1 (+0.5/+1.9)	+1.1 (+0.5/+1.9)	+1.6 (+0.9/+2.2)	+1.9 (+1.2/+2.7)	+2.2 (+1.5/+3.0)	+2.5 (+1.8/+3.2)	+1.7 (+1.0/+2.6)	+2.6 (+1.9/+3.7)	+3.7 (+2.9/+4.5)	+4.5 (+3.7/+5.3)
HWIe (nd)	4.0	+2.0 (+0.8/ +3.5)	+2.1 (+0.9 / +3.2)	+2.7 (+1.8 / +3.5)	+2.5 (+1.5 / +4.0)	+2.9 (+1.9 / +3.6)	+3.6 (+2.5 / +4.5)	+4.5 (+3.3 / +5.4)	+6.4 (+5.0 / +7.8)	+2.6 (+1.6 / +3.3)	+6.3 (+4.8 / +7.7)	+10.4 (+8.8 / +12.0)	+14.9 (+13.2 / +16.6)
HWix (ºC)	33.4	+0.3 (+0.0/-0.6)	+0.2 (+0.0/-0.4)	+0.4 (+0.2/-0.7)	+0.4 (+0.2/-0.7)	+0.6 (+0.3/-1.0)	+0.8 (+0.4/-1.2)	+0.9 (+0.5/-1.4)	+1.1 (+0.6/-1.7)	+0.5 (+0.2/-0.9)	+1.2 (+0.7/-1.8)	+1.9 (+1.2/-2.6)	+2.4 (+1.5/-3.3)
HWf (ne)	0.4	+1.5 (1.0/2.1)	+2.3 (1.7/3.0)	+2.3 (1.7/3.6)	+2.3 (1.7/3.6)	+3.0 (2.4/3.8)	+3.6 (3.0/4.4)	+3.3 (2.4/4.4)	+3.3 (2.6/4.5)	+3.3 (2.7/4.1)	+3.3 (2.7/4.1)	+4.2 (3.1/5.1)	+4.2 (3.6/5.0)
HWd (nd)	3.6	10.4 (+8.3/+13.0)	+11.3 (+9.2/+14.1)	+13.0 (+10.9/+15.9)	+11.8 (+9.7/+14.6)	+21.3 (+12.2/+25.9)	+26.5 (+17.4/+35.3)	+33.8 (+24.7/+47.6)	+38.4 (+25.3/+52. 2)	+18.3 (+16.2/+28.9)	+42.3 (+29.2/+54.1)	+63.3 (+51.2/+79.1)	+79.0 (+62.2/+96.1)
HI-P90 (ºC)	31.8	+1.9 (+0.5/+3.5)	+1.9 (+0.5/+2.9)	+2.4 (+0.8/+4.3)	+2.3 (+0.8/+4.0)	+2.5 (+1.0/+4.3)	+3.3 (+1.8/+5.1)	+4.1 (+2.6/+6.0)	+4.5 (+3.0/+6.4)	+2.4 (+0.9/+4.2)	+5.3 (+3.7/+7.2)	+7.4 (+5.8/+9.2)	+9.2 (+7.6/+11.0)

UTCI (ºC)	13.1	+1.6 (+1.1/+1.8)	+1.7 (+1.1/+2.1)	+1.8 (+1.1/+2.1)	+1.8 (+0.9/+2.2)	+2.2 (+1.6/+2.8)	+2.6 (+2.0/+3.0)	+2.9 (+2.3/+3.2)	+3.2 (+2.4/+4.0)	+2.2 (+1.4/+3.0)	+3.4 (+2.8/+4.8)	+4.8 (+3.8/+5.9)	+5.9 (+4.8/+7.4)
UHI (ºC)	2.2	-0.2 (-0.3 / -0.1)	-0.3 (-0.4 / -0.2)	-0.4 (-0.5 / -0.3)	-0.5 (-0.6 / -0.4)	-0.5 (-0.7 / -0.3)	-0.7 (-0.9 / -0.5)	-0.9 (-1.1 / -0.7)	-1.1 (-1.3 / -0.9)	-0.8 (-1.0 / -0.6)	-1.0 (-1.2 / -0.8)	-1.2 (-1.4 / -1.0)	-1.4 (-1.6 / -1.2)

Table 13. Summary table for expected changes in future precipitation climate variables and extreme indicators from FICLIMA statistical downscaling in AMB. Changes are expressed as the difference in "median(percentile 10/percentile 90)" of future expected values for each SSP and time period with respect to the historical median reference value for the period 1981-2010. Units are expressed in the INDEX column (nd = number of days, ne = number of events).

INDEX	81-10	2021-2050				2041-2070				2071-2100			
	HIST.	1-2.6	2-4.5	3-7.0	5-8.5	1-2.6	2-4.5	3-7.0	5-8.5	1-2.6	2-4.5	3-7.0	5-8.5
Precipitation indicators													
R20 (nd)	6.0	+0.2 (0/-0.1)	+0.1 (0/-0.1)	-0.2 (0/-0.4)	+0.1 (0/-0.1)	+0.1 (0/-0.1)	+0.2 (0/-0.1)	-0.2 (0/-0.4)	+0.1 (0/-0.1)	+0.2 (0/-0.1)	+0.1 (0/-0.1)	-0.2 (0/-0.4)	-0.4 (0/-0.1)
R50 (nd)	1.1	+0.2 (-0.1/+0.3)	+0.1 (-0.1/+0.3)	+0.0 (-0.2/+0.3)	+0.1 (-0.1/+0.3)	+0.2 (-0.1/+0.3)	+0.2 (-0.1/+0.3)	+0.2 (-0.2/+0.3)	+0.2 (-0.1/+0.3)	+0.1 (-0.1/+0.3)	+0.2 (-0.2/+0.3)	+0.3 (-0.1/+0.3)	+0.2 (-0.2/+0.3)
R100 (nd)	0.1	+0.1 (0.0/+0.2)	+0.1 (0.0/+0.2)	+0.1 (0.0/+0.2)	+0.1 (0.0/+0.2)	+0.1 (0.0/+0.2)	+0.1 (0.0/+0.2)	+0.1 (0.0/+0.3)	+0.1 (0.0/+0.3)	+0.1 (0.0/+0.2)	+0.1 (0.0/+0.2)	+0.1 (0.0/+0.3)	+0.1 (0.0/+0.2)
Ra (mm,%)	524	+2% (0%/3%)	+1% (-1%/2%)	-2% (0%/1%)	+1% (0%/3%)	+0% (0%/3%)	+1% (0%/2%)	+0% (-1%/2%)	+0% (0%/3%)	+1% (0%/2%)	-2% (-2%/3%)	-2% (-2%/3%)	-7% (-9%/1%)
IDF - CCF 100y (mm/h, %)	208	-4% (-24%/10 %)	+3.5% (-13%/13 %)	-14.5% (-23%/22 %)	-4.2% (-19%/20 %)	+8% (-25%/21 %)	-0% (-23%/25 %)	+6.5% (-17%/26 %)	+6.5% (-13%/32 %)	+4% (-28%/17 %)	+3% (-12%/33 %)	10% (-5%/63 %)	17% (-6%/51 %)
Forest fire indicators													
Mean FWI	15.8	+0.8 (-1.2/+2.5)	+0.9 (-1.2/+2.6)	+1.3 (-0.9/+3.2)	+0.8 (-1.1/+2.3)	+1.5 (-1.0/+3.4)	+1.7 (-0.9/+4.5)	+2.1 (-0.9/+4.0)	+2.2 (-1.0/+4.1)	+1.0 (-1.2/+2.6)	+2.2 (+0.4/+4.5)	+3.5 (+0.8/+5.0)	+4.2 (+1.0/+6.4)
FWI>38 (nd)	7.5	+1.5 (-0.3/+2.5)	+1.0 (-0.3/+4.2)	+2.2 (-0.4/+4.8)	+1.2 (-0.4/+3.0)	+1.8 (-0.2/+3.3)	+3.0 (-0.1/+5.5)	+2.5 (-0.1/+5.2)	+3.0 (-0.2/+6.5)	+1.8 (-0.2/+3.3)	+3.2 (-0.1/+7.0)	+4.0 (-0.0/+12)	+6.0 (+0.5/+19)

Table 14. Summary table for expected changes in future wind climate variables and drought indicators from FICLIMA statistical downscaling in AMB. Changes are expressed as the difference in "median(percentile 10/percentile 90)" of future expected values for each SSP and time period considered with respect to the historical median reference value for the period 1981-2010. Units are expressed in the INDEX column (nd = number of days, ne = number of events).

INDEX	81-10	2021-2050				2041-2070				2071-2100			
	HIST.	1-2.6	2-4.5	3-7.0	5-8.5	1-2.6	2-4.5	3-7.0	5-8.5	1-2.6	2-4.5	3-7.0	5-8.5
Drought indicators													
CDDx (nd)	38.1	+0.4 (+0.1/+0.7)	+0.0 (+0.0/+0.0)	+0.7 (+0.4/+1.0)	+0.5 (+0.2/+0.8)	+1.2 (+0.6/+1.8)	+1.8 (+1.0/+2.6)	+1.9 (+1.1/+2.7)	+2.9 (+1.9/+3.9)	+0.5 (+0.2/+0.8)	+2.5 (+1.2/+3.8)	+3.3 (+2.0/+4.6)	+4.7 (+3.4/+6.0)
CDDm (nd)	10.2	+0.1 (+0.0/+0.2)	+0.2 (+0.1/+0.3)	+0.4 (+0.2/+0.6)	+0.2 (+0.0/+0.4)	+0.2 (+0.0/+0.4)	+0.5 (+0.2/+0.7)	+0.7 (+0.4/+1.0)	+0.7 (+0.4/+1.0)	+0.3 (+0.0/+0.6)	+0.8 (+0.4/+1.2)	+1.2 (+0.8/+1.8)	+1.8 (+1.2/+2.4)
SPI-36	0.0	+0.3 (+0.1/+0.5)	+0.2 (+0.0/+0.4)	+0.1 (-0.1/+0.3)	+0.4 (+0.2/+0.6)	+0.1 (+0.1/+0.5)	+0.2 (+0.0/+0.4)	+0.1 (-0.1/+0.3)	+0.2 (+0.2/+0.6)	+0.3 (+0.1/+0.5)	+0.2 (+0.0/+0.4)	+0.1 (-0.1/+0.6)	+0.4 (+0.2/+0.5)
SPEI-36	0.0	-0.8 (-1.6/-0.0)	-1.0 (-1.8/-0.2)	-1.0 (-1.8/-0.2)	-0.9 (-1.7/-0.1)	-1.6 (-2.8/-0.4)	-1.6 (-2.4/-0.8)	-2.0 (-2.9/-1.1)	-2.2 (-3.3/-1.3)	-1.4 (-2.2/-0.6)	-2.4 (-3.2/-1.6)	-3.1 (-4.0/-2.2)	-3.8 (-4.7/-2.9)
Oceanic indicators													
SS-25y (cm, %)	79	-7% (-27/13)	-5% (-22/27)	-12% (-23/12)	-5% (-21/8)	-4% (-18/22)	-4% (-12/2)	0% (-33/11)	-3% (-17/23)	-6% (-17/9)	-12% (-21/-1)	-11% (-20/5)	-14% (-34/-7)
OW-MWH -25y (m, %)	8.77	-2% (-16/+18)	+4% (-9/+13)	-6% (-18/+8)	-4% (-12/+1)	+1% (-14/+25)	0% (-10/+17)	-8% (-16/-12)	-5% (-13/+5)	-4% (-15/+16)	-5% (-13/+2)	+2% (-18/+11)	–8% (-25/+7)

OW-SWH -25y (m, %)	5.41	-2% (-20/+16)	+3% (-10/+14)	-7% (-18/+7)	-3% (-16/+9)	+3% (-14/+25)	+5% (-14/+14)	-6% (-14/+14)	-2% (-20/+9)	+5% (-19/+16)	-4% (-10/+2)	5% (-16/+13)	-5% (-24/+6)
Wind indicators													
EWG (km/h,%)	65	-2% (-14/+6)	-2% (-13/+5)	-5% (-14/-3)	-3% (-10/+8)	+2% (-14/+8)	-1% (-8/+6)	+1% (-11/+9)	-8% (-12/-7)	-1% (-11/+10)	-2% (-8/+8)	-1% (-9/+6)	-9% (-15/-2)

5.1.3. Discussion for the South Aegean Region - SAR

IMPORTANT: *In this section, it is discussed the results for the SAR area, considering all the stations (HNMS-NOAA and NOA-MeteoGR) falling within the administrative region covering the four islands of interest. Changes will be mainly discussed in what refers to changes in* ***median values****; due to the geographical heterogeneity (shore and inland, coast and mountain) of stations, some indicators might be registered or expected in the future in some points, but might not be explicitly mentioned. A more detailed summary with uncertainty thresholds is done in the next 5.1.4 section. All summary figures will be shared and available to partners for detailed consultation, and the posterior spatial treatment (TIF) of results might help in identifying in ICARIA's DSS, once made available, the particularities of results in the geographical extension of the CS.*

—

In accordance with the climate change scenarios tailored for this specific case study, and aligning with projected trends in the current warming scenario, temperature increases are anticipated across all scenarios, timeframes, and seasons. However, due to the complex relationship between precipitation patterns and warming scenarios, significant alterations in rainfall are not expected across any scenario. In summary, an escalation in aridity is highly likely to accompany rising temperatures, especially during the summer season.

Thermal indicators

In relation to the cluster of variables and indicators associated with temperature, as delineated in the preceding section 4.2, the findings distinctly indicate a consistent trajectory towards elevated temperatures in the future, with more adverse scenarios corresponding to higher Shared Socioeconomic Pathways (SSPs).

Concerning the temperature variable specifically, projections indicate that **maximum temperatures** are poised to increase by approximately 1.5 to 2.5 degrees Celsius by mid-century, based on median values outlined in future scenarios. By the end of the century, under SSP2-4.5 and SSP5-8.5 scenarios, these increases could range from 2.5 up to 4.3 degrees Celsius, as illustrated in Figure 37. Similar increments are anticipated for mean and minimum annual temperatures relative to maximum temperatures. Substantial and noteworthy elevations are anticipated across all scenarios, seasonal periods, and timeframes.

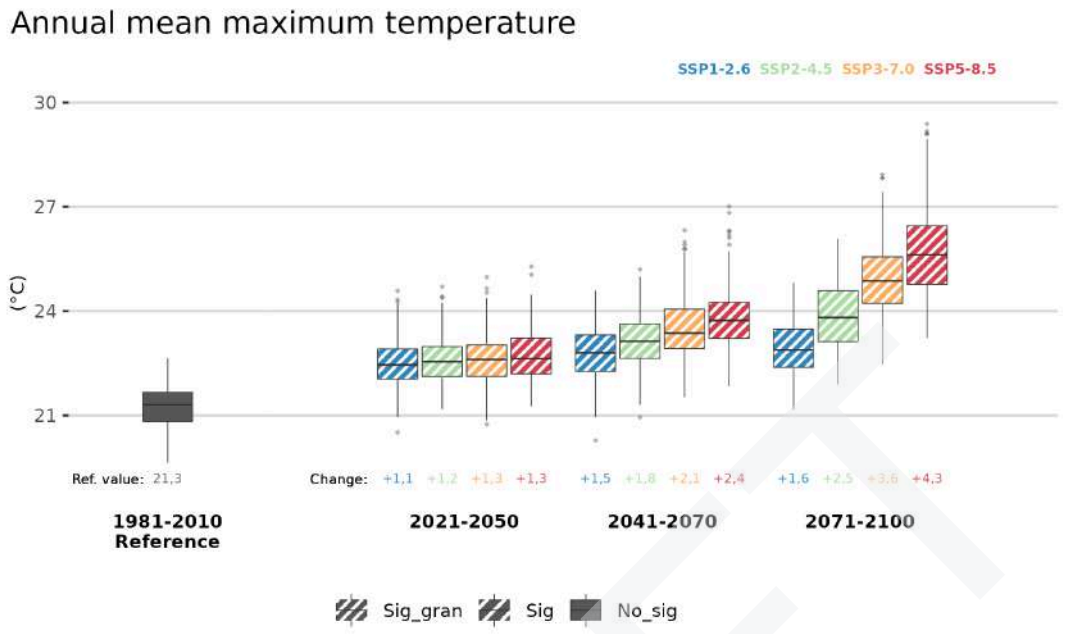

Figure 37. Expected evolution of mean maximum temperature for SAR stations.

Considering percentiles, there is an anticipated notable decrease/increase in **Cold/Warm days** (P10/P90 of maximum temperature, respectively) in the future. This is because using a percentile indicator based on historical data as a reference point in a warming climate leads to an increase in the number of days exceeding P90 and a decrease in those falling below P10. Projections indicate that **Cold days**, which currently stand at approximately ~34 days/year, are expected to decrease by 50-60% by mid-century and by about 75-90% by 2100. Conversely, **Warm days** are projected to double (+100% or +35 days) by mid-century and increase by about 150-200% (50-83 days) by 2100.

The changes in maximum temperature will consequently impact the indicators derived from it. Specifically, Heat Days (Tx > 30ºC) and Extreme Heat Days (Tx > 35ºC) are expected to see significant increases. **Heat days**, based on projections, are forecasted to increase from the historical average of 33 days to a range of 60 to 80 days per year by 2050 in the AMB region and to exceed 70-100 days annually in worst-case scenarios by 2100 (refer to Figure 37). **Extreme Heat days** would follow a similar trend. Although currently less common in the SAR region, with just 2.9 days per year, changes in sea surface temperatures and air patterns could result in a notable average increase of +7 days by mid-century and a further increase to 10 up to 32 days by the late-century in worst-case scenarios.

The rise in minimum temperatures is expected to result in the near disappearance of **frost days** during winter. Frost days, which are currently extremely rare in the Aegean region, with a median of just 0.4 days (inland high stations record around 3-4 days), are projected to dwindle to zero in most stations by 2050, with practically no frost days anticipated across all stations by 2100. This warming trend in minimum temperatures extends to the summer season as well, leading to significant increases in the occurrence of tropical nights (Tmin > 20ºC) across all scenarios and time horizons, particularly towards the end of the

century. The SAR area already experiences a high number of **tropical nights** due to warm sea surface temperatures year-round and its small island geography, with historic values averaging around 110 nights. Substantial increases are anticipated even in the earliest time periods (approximately +17 nights on average), with projections indicating a steep rise to between +26 and up to +64 nights in the worst-case scenarios, potentially resulting in a third or more of nights (up to 165) per year exceeding 20°C by 2100 (refer to Figure 39). This trend extends to equatorial nights (Tmin > 25°C) and infernal nights (Tmin > 30°C) as well. **Equatorial nights**, already present in the SAR region at approximately 14 days annually, are expected to follow the trend of tropical nights, with increases ranging from +14 nights before 2050 to between +27 and up to +82 nights by 2100 across different scenarios. **Infernal nights**, which have been almost non-existent thus far (averaging 0.4 nights per year), are projected to become more common from mid-century onwards, with a median expectation of 4 infernal nights annually by the end of the century, potentially reaching up to +15 nights in certain areas.

In addition to the preceding discussion, and to gain deeper insights into the potential impacts of the aforementioned indicators, two derived metrics were employed: the calculation of the maximum number of consecutive days for each indicator, and the frequency of events (defined as periods lasting ⩾3 consecutive days) expected throughout the year. In terms of **maximum consecutive days**, **Heat Days** may extend from the typical 12-day streak observed historically to around 20 days by 2050, or even surpass 40 days by 2100. **Extreme Heat Days** could occur consecutively for 5 to over 10 days by the end of the century. **Frost days** are predicted to virtually disappear, while **Tropical Nights** could increase from the current streak of 83 days to an average of 120 to 150 consecutive nights in the worst-case scenario. **Equatorial nights**, which have previously lasted for 7 consecutive days, could extend to approximately 25 consecutive nights by mid-century, or even from 37 to 70 nights by the end of the century. **Infernal nights**, however, are not anticipated to occur consecutively until the late 21st century, with durations ranging from 4 to 7 days.

Regarding the **number of events**, **Heat Days** are projected to increase from approximately 3 events per year to 4.5 events over the course of the century, primarily driven by the rise in consecutive days. **Extreme Heat Days**, which were previously absent, may occur almost once or twice a year by 2100. **Frost days**, which had no occurrences in the past, are not expected to occur in the future either. The frequency of **Tropical Nights** events, averaging around 3 per year historically, is anticipated to remain stable, although their duration may increase. **Equatorial night** events, with one event recorded on average, could potentially increase to 1.5-2 events by mid-century. Meanwhile, only around 1 event of **infernal nights** may occur by the end of the century.

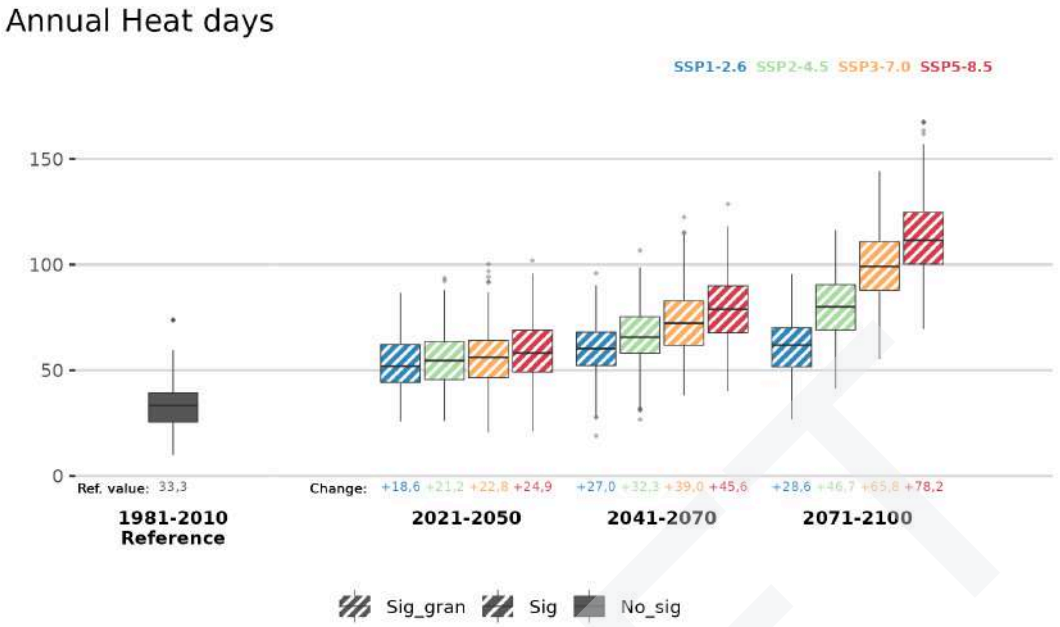

Figure 38. Expected evolution of annual heat days for SAR stations.

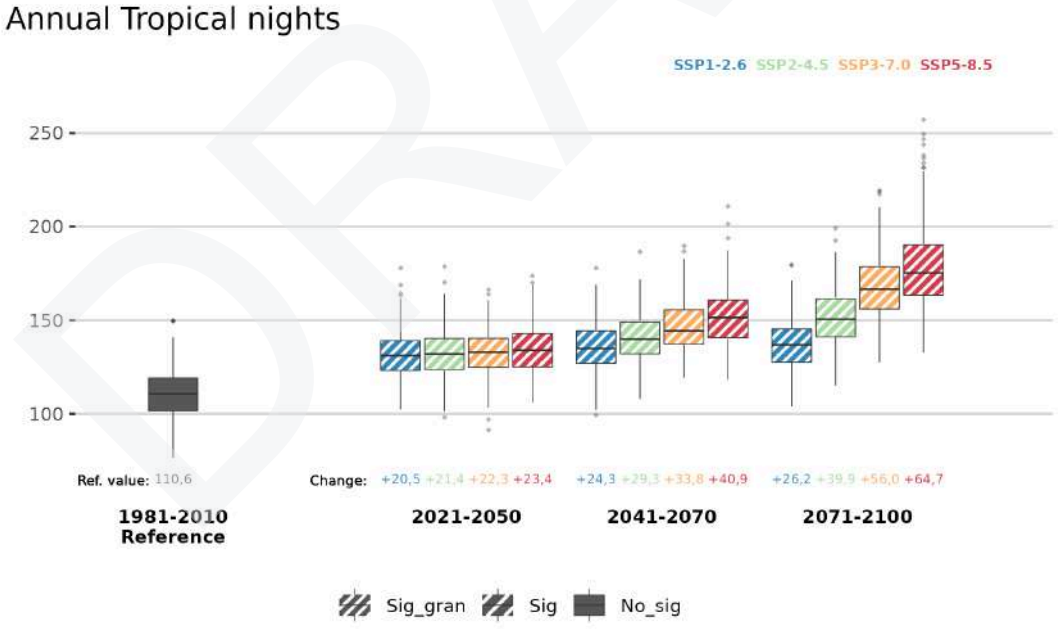

Figure 39. Expected evolution of tropical nights for SAR stations.

Moreover, in addition to the aforementioned points, rising temperatures will impact the occurrence of extreme weather phenomena, notably **heat waves**, which have substantial implications for human health, infrastructure, and the environment. Therefore, it is imperative to analyze the duration, intensity, and frequency of heat waves to characterize these extreme events. The definition of a heat wave was established within the framework of ICARIA, considering various climate and scientific criteria. *a temperature-related episode of at least three consecutive days where the weather observations considered register maximum temperatures above the 95% percentile of their daily maximum temperature records for the months of June to September of the 1981-2010 period.*

Projections suggest a significant increase in the intensity, duration, and frequency of heat waves across most scenarios by mid-century and beyond. Historically, the average **number of heat wave** events was approximately 0.6. By mid-century, this figure is expected to rise by 3 to 4 events on average annually, and up to 5 events in the median by the end of the century, under scenarios ranging from SSP2-4.5 to SSP5-8.5 (see Figure 40).

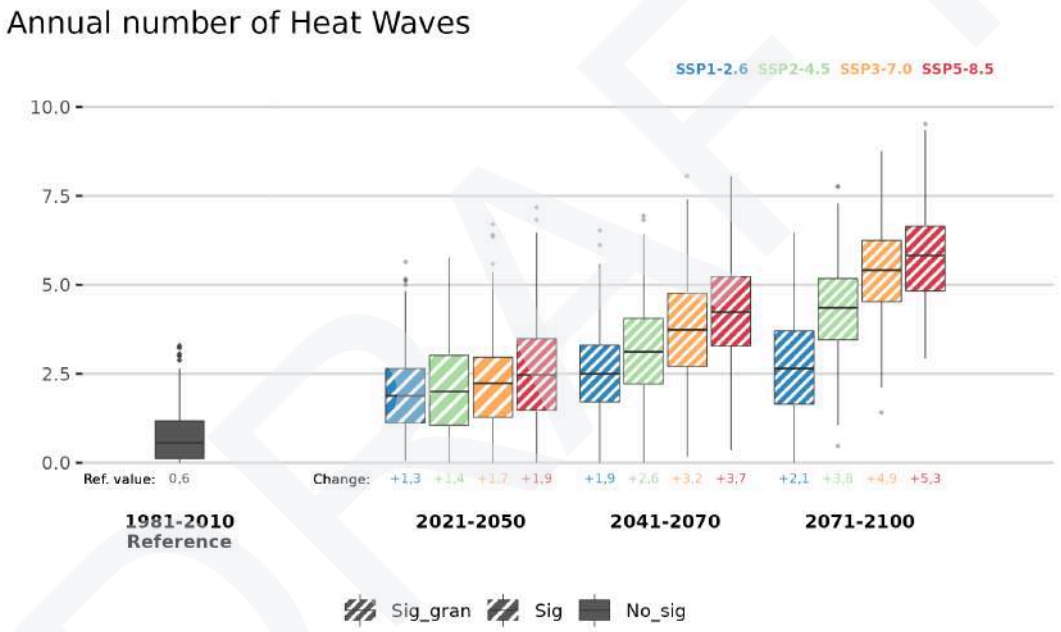

Figure 40. Expected evolution of tropical nights for SAR stations.

The **average heat wave length** is anticipated to increase from 3.8 days historically to 5.5-6 days by mid-century. By late-century, under the most pessimistic scenarios, a significant rise is projected, with durations averaging 7-9 days in moderate scenarios and up to 11 days per event in the SSP5-8.5 (refer to Figure 41). Moreover, the **maximum heat wave intensity** is expected to increase, with median values reaching 35.2ºC for the AMB. While no significant change is anticipated by early-century, projections indicate an increase of around +1ºC to +2.4ºC by mid-century and late-century, particularly in the most pessimistic scenarios. Additionally, the annual count of **heat wave days**—defined as days exceeding the 95th percentile of maximum temperatures but excluding consecutive 3-day events—is poised to rise significantly. Historic figures of 4.9 days are expected to surge to over 23 (up to 32) by 2050 and potentially reach 35 to 70 by 2100.

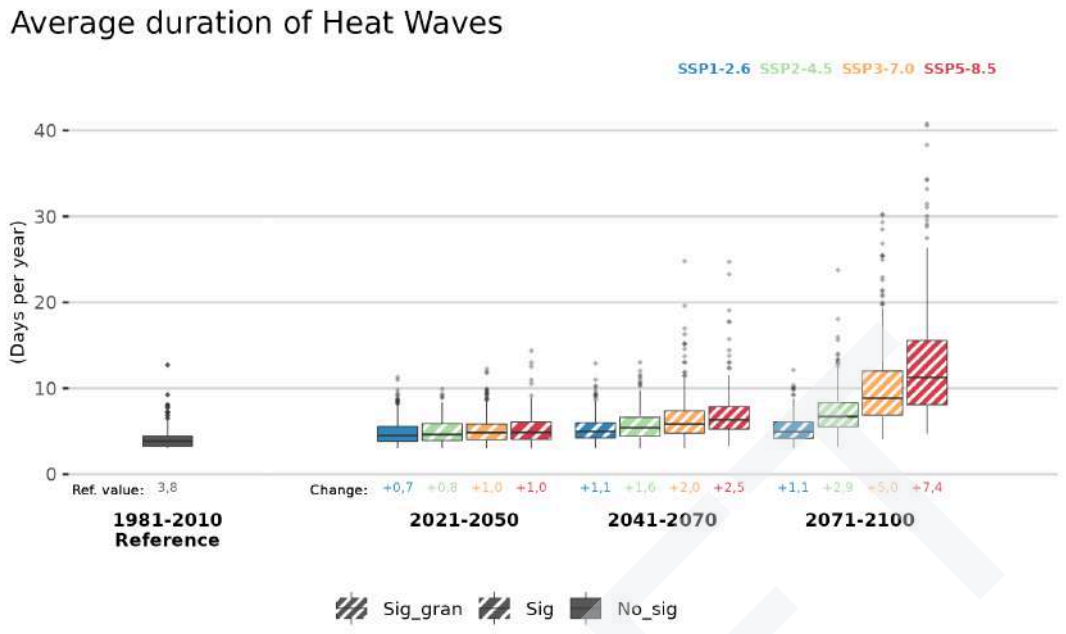

Figure 41. Expected evolution of tropical nights for SAR stations.

Customized variables have been computed for SAR, some concerning thermal comfort. Among them is the widely-used **Heat Index (HI)**, derived from a blend of temperature and relative humidity (RH) across specific thresholds, reflecting the body's thermal perception at a given moment. The Heat Index elucidates that under certain T/RH conditions, the heat stress experienced by the body, potentially perilous, diverges from the actual recorded temperature.

For SAR, the reference HI typically hovers around a notable 36.9ºC and is anticipated to undergo substantial and significant escalation in the future. This projection stems from a discernible and robust trend of escalating temperatures, coupled with the continuous infusion of humidity from an increasingly warmer Aegean Sea. Consequently, increases ranging from +4-6ºC are projected by mid-century. Further elevations of +5 up to an extraordinary +12ºC (potentially yielding a median HI of 48ºC) in worst-case scenarios are plausible by late-century (see Figure 42 for additional insight).

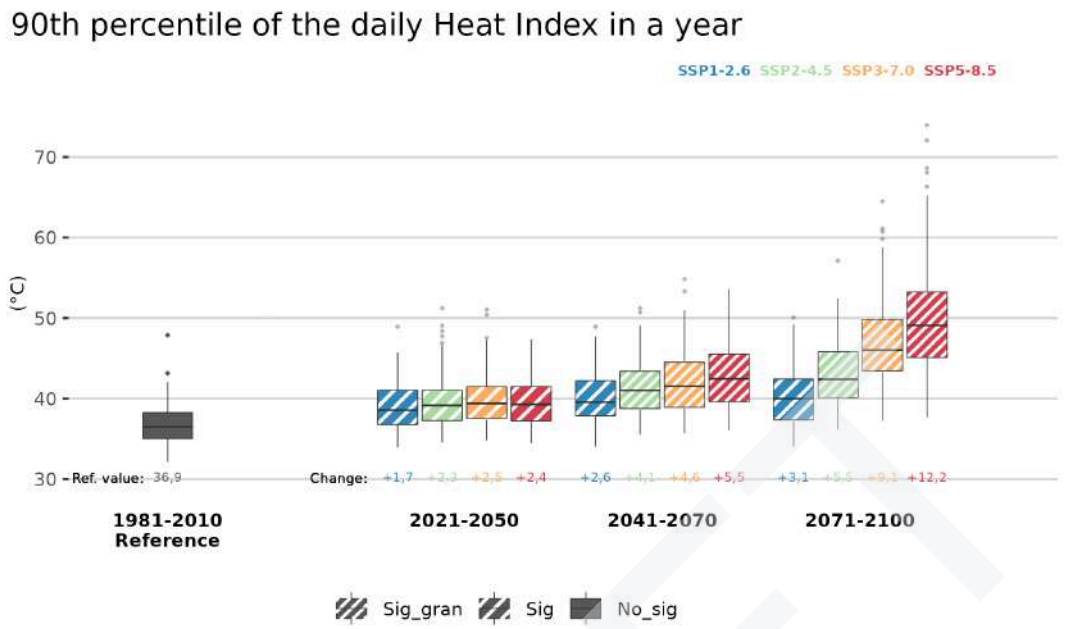

Figure 42. Expected evolution of the percentile 90 of Heat Index for SAR stations.

Precipitation indicators

Concerning precipitation indicators, a variety of metrics have been derived to suit the requirements of the SAR CS. Some were tailored to gauge shifts in annual precipitation, while others targeted extreme rainfall occurrences. Overall, no substantial alterations are anticipated in annual precipitation or in days exceeding specific extreme thresholds.

In greater detail, analyses of annual precipitation metrics, encompassing **yearly cumulative and seasonal cumulative precipitation**, reveal no notable shifts in the foreseeable future, as depicted in Figure 43. Although reductions are projected across various scenarios (up to -12% by 2100), the associated uncertainties preclude considering these changes as significant.

Regarding extreme rainfall events, indicators tracking **days surpassing thresholds of 20, 50, and 100mm** were examined. In all cases, the anticipated changes compared to historical observations (6.8, 1.5, and 0.3 days, respectively) are practically negligible and fail to reach significance.

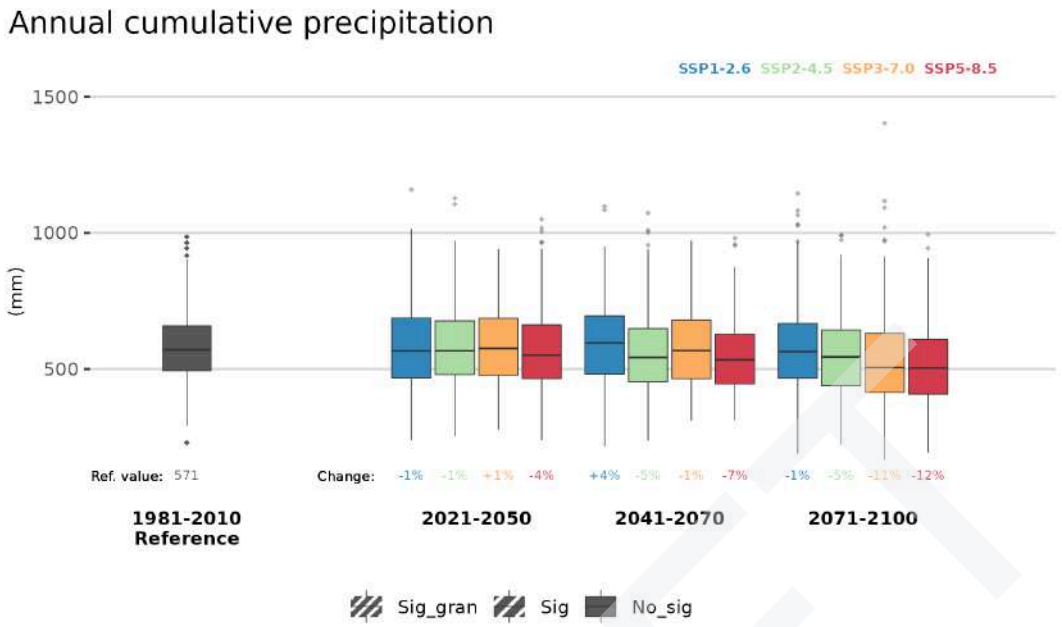

Figure 43. Expected evolution of annual cumulative precipitation for SAR stations.

Drought indicators

Concerning drought assessment, two categories of indicators were established: those focused on dry periods (dry spell duration) and those analyzing anomalies in precipitation/evapotranspiration (SPI & SPEI). Dry days were defined as those with recorded precipitation below 1mm, leading to the calculation of two indicators: mean length of dry spell and maximum length of dry spell. About the **Mean length of dry spells,** historically, the SAR experienced an average of around 13 dry days per year, with minimal anticipated changes in the future except for SSP3-7.0 and SSP5-8.5 scenarios by the century's end, showing slight but significant increases of approximately +3 days. Regarding the **maximum length of dry spells**, the historical reference value stands at 116 days, with marginal increases projected in the future, except for SSP3-7.0 and SSP5-8.5 by late-century, where a change of approximately +16 days is expected.

As for the SPI and SPEI indexes, historic values are consistently set to 0 due to their definitions. Expected changes vary between the two indices. For **SPI-36**, no significant alterations are projected by mid or late-century across scenarios, except for SSP5-8.5 by 2100, indicating a -0.8 change. This is attributed to minimal shifts in mean accumulated precipitation. Conversely, for **SPEI**, which considers temperature changes for evapotranspiration estimation, alterations are expected. With rising temperatures and stagnant or declining rainfall patterns, significant decreases in SPEI values are forecasted for all timeframes and scenarios, particularly towards the century's end. Projections indicate reductions ranging from -2 to -3.4 in SPEI-12 and from -3 to nearly -4.6 for SSP5-8.5 in SPEI-36 (refer to Figure 44). Similar declines are anticipated in other monthly-aggregated SPEI indices (1,3,6,24).

Figure 44. Expected evolution of 36-month length SPEI Thornthwaite for SAR stations.

Forest fire indicator

For the case of the hazards concerning forest fires, the FWI was used as an indicator to evaluate the likelihood of extreme forest fires developing when started. This index merges different conditions of humidity, temperature and wind to assess the evolution of fires. In this regard, projections show that the **mean FWI between June and September** (risk season) for the SAR is about 21.5 in historic period, and all scenarios agree in future significant increments in this value, of around +3-6 depending on the scenario, larger with worse SSPs and the further we go through the century (Figure 45). For the extremest situations, the **number of days with FWI>38** (Very High risk) is set at 18 in the past, and will increase around +5-7 days by 2050 up to a significant +7-11 for worst case scenarios by 2100.

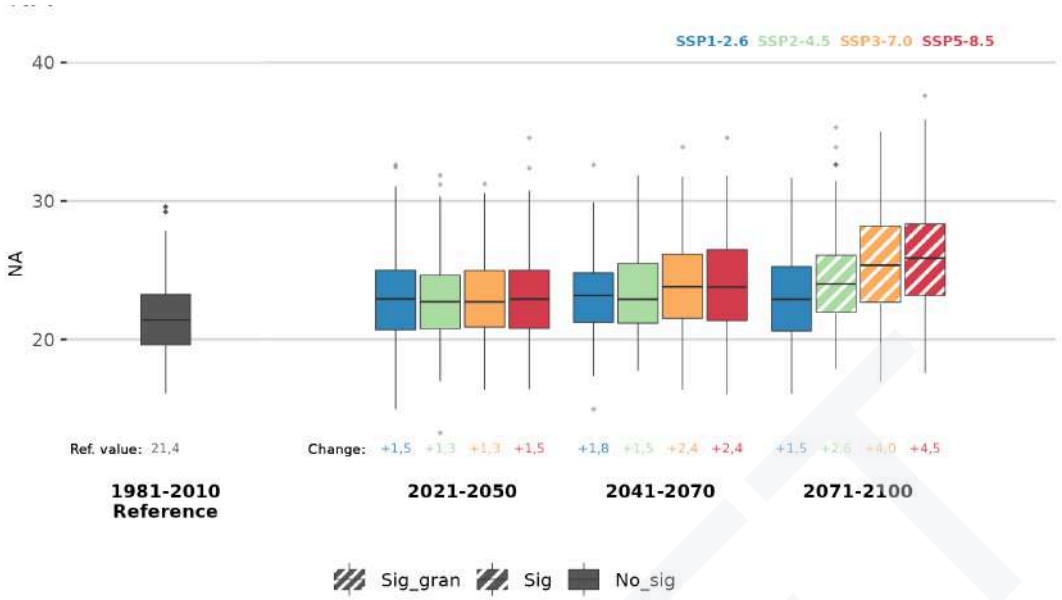

Figure 45. Expected evolution of mean FWI between June and September for SAR stations.

Wind indicator

Wind is one of the most difficult meteorological variables to be studied when dealing with future climate change variations. Due to its own nature, a result of multiple factors such as orography, local thermal variations, pressure gradients, or other weather phenomena, the future study of wind is not as straightforward as temperature could be, and future changes in pressure centres and other atmospheric patterns that determine wind's strength and direction is still today prone to high uncertainties. Besides, the remarkable lack of wind observations or their poor quality with respect to those from temperature or precipitation also hinders the procedures in statistical downscaling. It is good advice to take into account the aforementioned difficulty of working with the wind when interpreting the next results.

In this sense, wind gusts have been modelled for the future since it is a variable that poses higher risks and interest for ICARIA, and is included in other multiple indicators. The future evolution is studied for percentiles since it doesn't respond to a normal distribution and mean values are meaningless. For the SAR, Percentile 99, as well as other percentiles (P80, P90 or P100) don't seem to show any change in its expected behaviour in the future.

There are few variations in terms of maximum wind gusts (Figure 46). In general, all models and scenarios contemplate slight decreases for the Aegean Sea, but this does not include the possibility of an increase in severe phenomena such as medicanes or severe storms, which the current climate models do not yet model correctly.

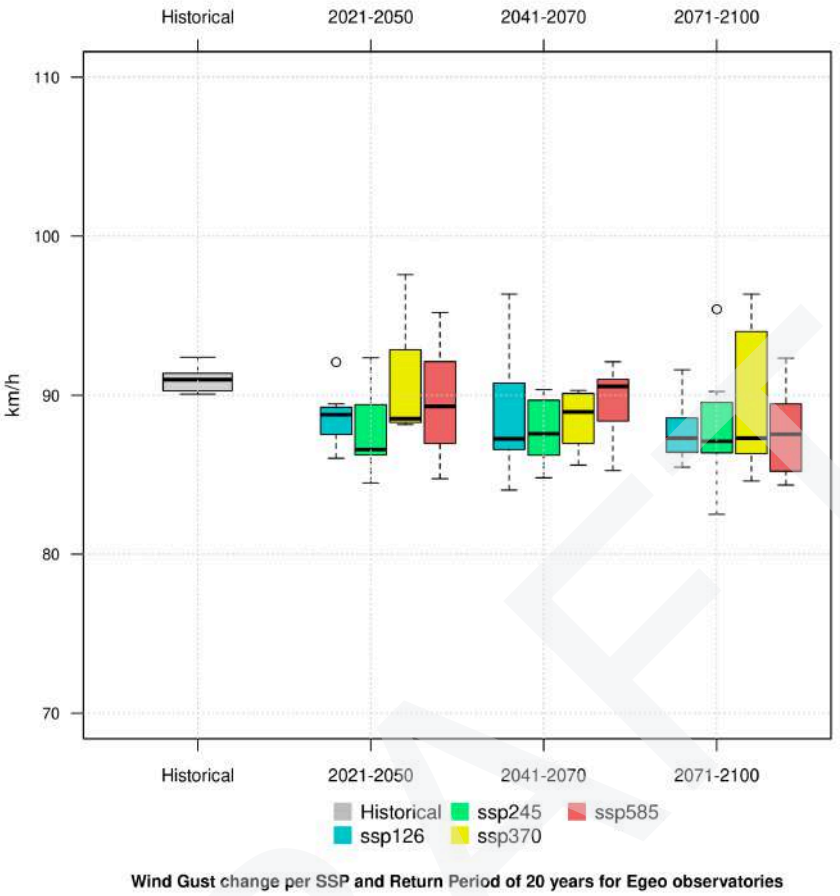

Figure 46. Results for wind gust projections for Return Period of 20 years and for SAR stations.

5.1.4. Summary of results for the South Aegean Region - SAR

Table 15-1. Summary table for expected changes in future thermal climate variables and extreme indicators from FICLIMA statistical downscaling in SAR. Changes are expressed as the difference in "median(percentile 10/percentile 90)" of future expected values for each SSP and time period with respect to the historical median reference value for the period 1981-2010. Units are expressed in the INDEX column (nd = number of days, ne = number of events).

INDEX	81-10	2021-2050				2041-2070				2071-2100			
	HIST.	1-2.6	2-4.5	3-7.0	5-8.5	1-2.6	2-4.5	3-7.0	5-8.5	1-2.6	2-4.5	3-7.0	5-8.5
Thermal indicators													
TX90 (nd)	35.9	+18.1 (+10.2/+28.4)	+19.4 (+11.3/+30.7)	+18.6 (+10.7/+29.0)	+22.7 (+14.8/+33.0)	+32.1 (+24.2/+42.4)	+33.7 (+25.8/+44.0)	+32.4 (+24.5/+42.7)	+50.5 (+42.6/+61.8)	+43.8 (+35.9/+54.1)	+52.4 (+44.5/+63.7)	+71.9 (+64.0/+83.2)	+83.0 (+75.1/+94.3)
TX10 (nd)	33.0	-10.3 (-13.9/-6.7)	-10.4 (-12.2/-8.6)	-8.6 (-10.4/-6.8)	-10.5 (-13.7/-7.3)	-13.5 (-15.3/-11.7)	-16.4 (-18.2/-14.6)	-18.4 (-20.2/-16.6)	-19.7 (-21.5/-17.9)	-15.7 (-17.5/-13.9)	-20.4 (-22.2/-18.6)	-24.7 (-26.5/-22.9)	-26.9 (-28.7/-25.1)
HD (nd)	33.3	+18.6 (+12.5/+22)	+21.2 (+13.5/+25.1)	+22.8 (+14.6/+25.1)	+24.9 (+17.0/+30)	+27.0 (+17.5/+42.3)	+32.3(+22.8/+47)	+39.0 (+29.5/+54)	+45.61 (+35.1/+61.1)	+28.6 (+18.1/+43.6)	+46.7 (+36.2/+57)	+65.8 (+55.3/+76)	+78.2 (+68.7/+88)
Max cons HD (nd)	11.9	+7.0 (+4.6/+14.2)	+7.6 (+5.2/+15.0)	+7.7 (+5.3/+15.1)	+8.5 (+5.3/+16.1)	+13.2 (+8.8/+22.4)	+17.2 (+12.8/+26)	+20.7 (+16.3/+30)	+25.6 (+21.2/+35)	+14.8 (+10.4/+24)	+28.3 (+22.9/+40)	+43.4 (+37.9/+56)	+57.6 (+52.2/+70)
Nº event. HD (ne)	2.8	+0.8 (+0.2/+1.6)	+0.8 (+0.3/+1.8)	+0.9 (+0.4/+1.8)	+1.0 (+0.5/+1.8)	+1.4 (+0.7/+2.2	+1.6 (+1.0/+2.4	+1.8 (+1.2/+2.8)	+1.8 (+1.2/+2.8)	+1.4 (+0.7/+2.2)	+1.7 (+0.9/+2.5)	+1.8 (+1.1/+2.6)	+1.6 (+1.0/+2.4)
EHD (nd)	2.9	+2.4 (+0.9/+4.9)	+2.1 (+0.8/+4.7)	+2.7 (+0.9/+5.0)	+2.8 (+0.9/+4.9)	+4.9 (+2.6/+6.3)	+6.3 (+3.8/+8.4)	+9.0 (+5.0/+11.8)	+10.3 (+6.4/+13.5)	+4.9 (+2.6/+6.3)	+11.8 (+6.7/+14.5)	+22.2 (+12.5/+31.9)	+31.9 (+20.2/+42)
Max cons EHD (nd)	1.2	+1.1 (+0.3/+2.2)	+0.9 (+0.1/+2.0)	+1.3 (+0.5/+2.5)	+1.3 (+0.5/+2.5)	+2.2 (+1.2/+3.3)	+3.0 (+2.0/+4.1)	+3.9 (+2.9/+5.0)	+4.6 (+3.6/+5.7)	+2.1 (+1.1/+3.2)	+5.1 (+4.1/+6.2)	+9.3 (+8.3/+10.4)	+12.5 (+11.5/+13.6)

Nº event. EHD (ne)	0.2	+0.2 (+0.0/+0.4)	+0.1 (-0.1/+0.3)	+0.2 (+0.0/+0.4)	+0.2 (+0.0/+0.4)	+0.4 (+0.1/+0.7)	+0.5 (+0.2/+0.8)	+0.6 (+0.3/+0.9)	+0.8 (+0.4/+1.2)	+0.4 (+0.1/+0.8)	+1.0 (+0.5/+1.8)	+1.8 (+0.8/+2.5)	+2.5 (+1.1/+3.2)
TR (nd)	110.6	+20.5 (+12.1/+29.9)	+21.4 (+13.1/+29.6)	+22.3 (+14.5/+31.3)	+23.4 (+15.1/+33.9)	+24.3 (+16.3/+33.1)	+29.3 (+21.3/+38.1)	+33.8 (+25.8/+43)	+40.4 (+33.5/+50)	+26.2 (+18.2/+35.)	+39.9 (+27.9/+52.)	+56.0 (+44.0/+68)	+64.7 (+52.7/+77.5)
Max cons TR (nd)	83.0	+20.8 (+14.2/+30.1)	+22.0 (+15.4/+31.3)	+22.0 (+15.4/+31.3)	+24.6 (+17.0/+33)	+32.0 (+24.4/+42)	+36.2 (+28.6/+46)	+42.1 (+34.5/+53)	+47.0 (+39.4/+57)	+32.1 (+22.4/+43)	+47.2 (+37.4/+57)	+61.9 (+54.3/+72)	+70.7 (+63.1/+81.0)
Nº event. TR (ne)	3.1	-0.2 (-0.3/+0.1)	-0.2 (-0.4/+0.1)	-0.3 (-0.5/+0.1)	-0.3 (-0.6/+0.2)	-0.4 (-0.5/+0.1)	-0.5 (-0.8/+0.1)	-0.4 (-0.7/+0.1)	-0.5 (-0.8/0.0)	-0.4 (-0.7/+0.2)	-0.4 (-0.6/+0.1)	-0.4 (-0.6/0.0)	-0.3 (-0.6/+0.2)
EQ (nd)	14.5	+14.3 (+11.9/+17.1)	+13.9 (+11.4/+16.7)	+15.9 (+13.4/+19.1)	+17.5 (+15.0/+20.	+27.1 (+23.6/+31.1)	+33.2 (+29.7/+37)	+39.6 (+35.9/+44)	+45.9 (+42.2/+50)	+27.8 (+24.2/+31.7)	+49.2 (+45.6/+53)	+69.3 (+65.7/+73)	+82.6 (+79.0/+86)
Max cons EQ (nd)	6.8	+7.5 (+6.0/+9.0)	+7.6(+6.0/ +9.1)	+8.4 (+6.4/+9.6)	+8.8 (+6.9/+9.9)	+13.1 (+10.0/+18.)	+18.8 (+12.0/+25.)	+22.7 (+15.0/+32)	+28.1 (+20.0/+45)	+15.6 (+12.0/+19.0)	+30.5 (+20.0/+43)	+49.9 (+40.0/+56)	+64.1 (+50.0/+80)
Nº event. EQ (ne)	1.2	+0.9 (+0.2/+1.6)	+0.9 (+0.2/+1.7)	+1.0 (+0.3/+1.9)	+1.1 (+0.4/+2.0)	+1.5 (+0.5/+2.3)	+1.7 (+0.6/+2.5)	+1.9 (+0.7/+2.7)	+2.0 (+0.8/+2.8)	+1.5 (+0.6/+2.4)	+1.9 (+0.7/+2.7)	+1.9 (+0.8/+2.8)	+2.0 (+0.9/+2.9)
IN (nd)	0.4	+0.5 (+0.1/+0.9)	+0.5 (+0.1/+0.9)	+0.8 (+0.4/+1.4)	+0.7 (+0.3/+0.9)	+1.2 (+0.6/+1.8)	+1.9 (+0.9/+2.8	+2.6 (+1.2/+3.0)	+3.4 (+2.2/+4.6)	+1.4 (+0.8/+2.2)	+3.9 (+2.4/+5.4)	+9.2 (+6.0/+12.4)	+14.8 (+9.4/+18.2)
Max cons IN (nd)	0.2	+0.2 (0.0/+0.5)	+0.2 (0.0/+0.5)	+0.3 (0.0/+0.5)	+0.3 (0.0/+0.5)	+0.5 (0.1/0.8)	+0.8 (0.3/1.2)	+1.2 (0.5/1.6)	+1.6 (0.5/3.6)	+0.5 (0.1/1.8)	+1.8 (0.5/4.6)	+4.6 (1.8/7.2)	+7.2 (3.6/10.8)
Nº event. IN (ne)	0.0	+0.1 (+0.0/+0.2)	+0.1 (+0.0/+0.2)	+0.1 (+0.0/+0.2)	+0.1 (+0.0/+0.2)	+0.1 (+0.0/+0.3)	+0.2 (+0.1/+0.3)	+0.3 (+0.2/+0.4)	+0.3 (+0.2/+0.5)	+0.2 (+0.1/+0.3)	+0.4 (+0.2/+0.4)	+0.8 (+0.4/+1.2)	+1.2 (+0.6/+1.8)
FD (nd)	0.4	-0.3 (-0.4/-0.1)	-0.2 (-0.4/0.0)	-0.2 (-0.4/-0.0)	-0.2 (-0.4/-0.2)	-0.4 (-0.4/-0.2)	-0.4 (-0.4/-0.3)	-0.4 (-0.4/-0.2)	-0.4 (-0.4/-0.2)	-0.4 (-0.4/-0.3)	-0.4 (-0.4/-0.3)	-0.4 (-0.4/-0.4)	-0.4 (-0.4/-0.4)

Max cons FD (nd)	0.3	-0.2 (-0.3/0.0)	-0.2 (-0.3/0.0)	-0.2 (-0.3/+0.1)	-0.2 (-0.3/0.0)	-0.2 (-0.3/-0.1)	-0.2 (-0.3/-0.2)	-0.3 (-0.3/-0.2)	-0.3 (-0.3/-0.2)	-0.2 (-0.3/-0.1)	-0.3 (-0.3/-0.2)	-0.3 (-0.3/-0.3)	-0.3 (-0.3/-0.3)
Nº event. FD (nd)	0.0	0.0	0.0	0.0	0.0	0.0	0.0	0.0	0.0	0.0	0.0	0.0	0.0

Table 15-2. Summary table for expected changes in future thermal climate variables and extreme indicators from FICLIMA statistical downscaling in SAR. Changes are expressed as the difference in "median(percentile 10/percentile 90)" of future expected values for each SSP and time period with respect to the historical median reference value for the period 1981-2010. Units are expressed in the INDEX column (nd = number of days, ne = number of events).

INDEX	81-10	2021-2050				2041-2070				2071-2100			
	HIST.	1-2.6	2-4.5	3-7.0	5-8.5	1-2.6	2-4.5	3-7.0	5-8.5	1-2.6	2-4.5	3-7.0	5-8.5
Thermal indicators													
TXm (ºC)	21.3	+1.1 (+0.4/+1.7)	+1.2 (+0.4/+1.7)	+1.3 (+0.4/+1.9)	+1.3 (+0.5/+2.1)	+1.5 (+0.8/+2.3)	+1.8 (+1.4/+2.6)	+2.1 (+1.3/+3.0)	+2.4 (+1.6/+3.5)	+1.6 (+1.0/+2.5)	+2.5 (+1.8/+3.6)	+3.6 (+2..9/+4.7)	+4.3 (+3.4/+5.4)
TNm (ºC)	15.8	+1.0 (+0.4/+1.7)	+1.0 (+0.4/+1.7)	+1.0 (+0.4/+1.7)	+1.0 (+0.4/+1.9)	+1.5 (+0.8/+2.3)	+1.8 (+1.4/+2.6)	+2.0 (+1.1/+2.9)	+2.4 (+1.6/+3.5)	+1.5 (+1.1/+2.3)	+2.4 (+1.7/+3.4)	+3.4 (+2.6/+4.5)	+4.2 (+3.1/+5.2)
TM (ºC)	18.6	+1.0 (+0.4/+1.7)	+1.0 (+0.4/+1.7)	+1.0 (+0.4/+1.7)	+1.1 (+0.5/+1.8)	+1.5 (+0.8/+2.3)	+1.8 (+1.4/+2.6)	+2.1 (+1.3/+3.0)	+2.4 (+1.6/+3.5)	+1.6 (+1.0/+2.5)	+2.5 (+1.8/3.6)	+3.5 (+2.7/+4.6)	+4.3 (+3.4/+5.4)
HWIe (nd)	3.8	+0.7 (+0.0/+1.0)	+0.8 (+0.2/+1.2)	+1.0 (+0.3/+1.6)	+1.0 (+0.3/+1.8)	+1.1 (+0.2/+2.2)	+1.6 (+0.5/+2.7)	+2.0 (+0.7/+3.3)	+2.5 (+1.0/+4.0)	+1.1 (+0.2/+2.2)	+2.9 (+1.2/+4.6)	+5.0 (+2.5/+7.5)	+7.4 (+4.0/+10.8)
HWix (ºC)	35.2	+0.2 (+0.4/+0.6)	+0.1 (+0.4/+1.1)	+0.3 (+0.8/+1.8)	+0.2 (+0.9/+2.3)	+0.4 (+0.6/+1.2)	+0.6 (+1.1/+2.2)	+0.8 (+1.8/+3.3)	+0.9 (+2.3/+4.4)	+0.4 (+0.6/+1.2)	+1.1 (+1.6/+3.2)	+1.8 (+2.7/+4.8)	+2.3 (+3.8/+6.4)
HWf (ne)	0.6	+1.3 (+0.4/+2.2)	+1.4 (+0.2/+2.0)	+1.7 (+0.3/+2.3)	+1.9 (+0.4/+2.5)	+1.9 (+1.2/+3.1)	+2.6 (+1.8/+3.8)	+3.2 (+2.4/+4.4)	+3.7 (+2.9/+5.0)	+2.1 (+1.4/+3.3)	-3.8 (-4.6/-2.9)	+4.9 (+4.1/+5.9)	+5.3 (+4.5/+6.3)
HWd (nd)	4.9	+6.5 (+4.9/+8.1)	+6.2 (+4.4/+8.3)	+7.9 (+5.5/+10.4)	+7.8 (+5.4/+10.3)	+13.5 (+5.1/+21.3)	+17.7 (+7.9/+25.0)	+23.8 (+12.9/+31.7)	+27.3 (+15.7/+35.1)	+13.7 (+4.8/+21.5)	+31.1 (+18.7/+37.1)	+49.4 (+35.1/+63.7)	+63.1 (+48.3/+77.1)
HI-P90 (ºC)	36.9	+1.7 (+0.5/+2.3)	+2.3 (+0.5/+2.9)	+2.5 (+0.9/+3.6)	+2.4 (+0.9/+3.3)	+2.6 (+1.1/+3.8)	+4.1 (+2.8/+6.0)	+4.6 (+2.5/+6.3)	+5.5 (+3.4/+7.2)	+3.1 (+1.8/+4.5)	+5.5 (+3.4/+7.2)	+9.1 (+6.2/12.5)	+12.2 (+8.8/16.1)

Table 16. Summary table for expected changes in future precipitation climate variables and extreme indicators from FICLIMA statistical downscaling in SAR. Changes are expressed as the difference in "median(percentile 10/percentile 90)" of future expected values for each SSP and time period with respect to the historical median reference value for the period 1981-2010. Units are expressed in the INDEX column (nd = number of days, ne = number of events).

INDEX	81-10	2021-2050				2041-2070				2071-2100			
	HIST.	1-2.6	2-4.5	3-7.0	5-8.5	1-2.6	2-4.5	3-7.0	5-8.5	1-2.6	2-4.5	3-7.0	5-8.5
Precipitation indicators													
R20 (nd)	6.8	+0.1 (0.3/-0.2)	+0.1 (0.3/+0.3)	+0.1 (0.3/+0.2)	+0.1 (-0.3/+0.2)	+0.2 (-0.4/+0.3)	+0.2 (-0.4/+0.2)	+0.1 (-0.4/+0.2)	-0.1 (-0.4/+0.2)	+0.1 (-0.4/+0.2)	-0.1 (-0.5/+0.2)	-0.4 (-0.7/+0.2)	-0.6 (-0.8/+0.2)
R50 (nd)	1.5	+0.1 (0.0/-0.2)	+0.2 (+0.1/+0.3)	+0.1 (0.0/+0.2)	+0.1 (0.0/+0.2)	+0.2 (+0.1/+0.3)	+0.1 (0.0/+0.2)	+0.3 (0.0/+0.2)	+0.1 (0.0/+0.2)	+0.1 (0.0/+0.2)	+0.1 (0.0/+0.2)	+0.1 (0.0/+0.2)	+0.2 (0.0/+0.2)
R100 (nd)	0.3	+0.1 (0.0/-0.1)	+0.1 (0.0/-0.1)	+0.1 (0.0/-0.1)	+0.1 (0.0/-0.1)	+0.1 (0.0/-0.1)	+0.1 (0.0/-0.1)	+0.1 (0.0/-0.1)	+0.1 (0.0/-0.1)	+0.1 (0.0/-0.1)	+0.1 (0.0/-0.1)	+0.1 (0.0/-0.1)	+0.1 (0.0/-0.1)
Ra (mm,%)	571	0% (-10%/+7%)	0% (-8%/+6%)	-1% (-9%/+11%)	+2% (-9%/+11%)	-1% (-5%/+14%)	-5% (-12%/+11%)	+1% (-12%/14%)	-6% (-12%/+5%)	-1% (-8%/+10%)	-5% (-12%/+8%)	-11% (-22%/+2%)	-12% (-23%/+2%)
Forest fire indicators													
Mean FWI	21.5	+1.4 (-1.0/+3.4)	+0.9 (-0.1/+4.0)	+1.2 (-1.0/+3.2)	+1.4 (-0.4/+3.2)	+1.8 (-0.4/+3.5)	+1.5 (-0.4/+4.0)	+2.4 (-0.1/+4.5)	+2.4 (-0.2/+4.7)	+1.5 (-0.8/+2.7)	+2.6 (+0.6/+4.0)	+4.0 (+1.2/+6.4)	+4.5 (+1.3/+6.5)
FWI>38 (nd)	18	+3.0 (+2.5/+5.2)	+2.0 (+1.2/+3.8)	+3.0 (+2.3/+5.0)	+3.0 (+2.3/+5.0)	+5.0 (+3.3/+7.5)	+5.0 (+3.1/+8.1)	+6.0 (+4.1/+9.8)	+7.0 (+4.3/+10.5)	+4.0 (+2.5/+6.8)	+7.0 (+4.3/+10.2)	+10.0 (+6.2/+14.8)	+11.0 (+6.8/+15.5)

Table 17. Summary table for expected changes in future wind climate variables and drought indicators from FICLIMA statistical downscaling in SAR. Changes are expressed as the difference in "median(percentile 10/percentile 90)" of future expected values for each SSP and time period considered with respect to the historical median reference value for the period 1981-2010. Units are expressed in the INDEX column (nd = number of days, ne = number of events).

INDEX	81-10	2021-2050				2041-2070				2071-2100			
	HIST.	1-2.6	2-4.5	3-7.0	5-8.5	1-2.6	2-4.5	3-7.0	5-8.5	1-2.6	2-4.5	3-7.0	5-8.5
Drought indicators													
CDDx (nd)	116.4	+3.9 (+2.8/+5.0)	+3.7 (+2.6/+4.8)	+4.5 (+3.4/+5.6)	+5.4 (+4.3/+6.5)	+6.1 (+4.0/+8.2)	+7.0 (+5.0/+9.1)	+10.5 (+8.4/+12.6)	+10.8 (+8.7/+12.9)	+6.7 (+4.0/+8.3)	+12.9 (+9.0/+16.1)	+14.8 (+12.7/+16.9)	+18.2 (+16.1/+20.3)
CDDm (nd)	13.0	+0.3 (+0.1/+0.5)	+0.5 (+0.2/+0.8)	+0.6 (+0.3/+0.9)	+0.5 (+0.2/+0.8)	+0.7 (+0.3/+1.1)	+1.2 (+0.5/+1.7)	+1.1 (+0.4/+1.6)	+1.7 (+0.8/+2.3)	+1.0 (+0.4/+1.5)	+1.5 (+0.7/+2.0)	+3.1 (+1.8/+4.3)	+3.7 (+2.3/+5.1)
SPI-36	0.0	+0.1 (-0.6/+0.4)	+0.1 (-0.5/+0.4)	+0.1 (-0.4/+0.3)	+0.0 (-0.6/+0.4)	+0.2 (-0.8/+0.4)	-0.2 (-1.0/+0.3)	+0.1 (-0.6/+0.3)	-0.4 (-0.8/+0.2)	-0.1 (-0.4/+0.3)	-0.4 (+0.8/+0.2)	-0.6 (+1.5/+0.1)	-0.8 (-1.6/-0.1)
SPEI-36	0.0	-1.3 (-2.0/-0.5)	-1.6 (-2.1/-0.6)	-1.4 (-2.0/-0.6)	-1.7 (-2.6/-0.4)	-1.6 (-2.6/-0.7)	-2.3 (-2.9/-1.8)	-2.5 (-2.8/-1.9)	-2.9 (-3.6/-2.2)	-2.0 (-2.6/-1.4)	-3.0 (-3.6/-2.3)	-4.0 (-4.7/-3.0)	-4.6 (-5.4/-4.0)
Wind indicators													
EWG (km/h)	68	-2% (-10/+3)	-1% (-7/+7)	-1% (-9/+5)	0% (-9/+8)	-1% (-8/+5)	-2% (-9/+2)	-2% (-10/+2)	0% (-8/+5)	-3% (-9/+3)	-2% (-11/+6)	-1% (-8/+5)	-3% (-9/+5)

5.1.5. Discussion for the Salzburg Region - SLZ

IMPORTANT: *In this section, it is discussed the results for the SLZ area, considering all the stations (ZAMG and DWD) falling within the region of interest covering the Salzburg city and its administrative area in the Alps, as well as the close-by German region of Upper Bavaria. Changes will be mainly discussed in what refers to changes in* ***median values****; due to the geographical heterogeneity, mainly due to height differences (valley and high-mountain) of stations, some indicators might be registered or expected in the future in some points, but might not be explicitly mentioned. A more detailed summary with uncertainty thresholds is done in the next 5.1.6 section. All summary figures will be shared and available to partners for detailed consultation, and the posterior spatial treatment (TIF) of results might help in identifying in ICARIA's DSS, once made available, the particularities of results in the geographical extension of the CS.*

–

Drawing from the locally generated climate change scenarios tailored for this case study, temperature escalation is envisaged across all scenarios, timeframes, and seasons. Particularly in SLZ, the geographical positioning (latitude, central Europe, and north of the Alps) suggests a probable surge in water availability in the atmosphere, owing to a warmer climate. This, in turn, is anticipated to influence precipitation estimates significantly. Projections indicate upticks in both average and extreme rainfall occurrences, culminating in a climate characterized by heightened warmth and moisture.

Thermal indicators

Concerning the suite of variables and indicators associated with temperature, as delineated in the preceding section 4.2, findings unequivocally illustrate a trajectory towards escalating temperatures in forthcoming years, exacerbated in more adverse SSP scenarios.

In terms of temperature variables, median projections suggest **maximum temperature** hikes ranging from 2.0 to 3.7 degrees Celsius by mid-century, with more dire scenarios projecting increases from 3.2 to 5.7 degrees Celsius by the century's end under SSP2-4.5 and SSP5-8.5, respectively (refer to Figure 47 for illustration). Notably, both mean annual temperature and minimum annual temperature are anticipated to rise proportionally to maximum temperatures in absolute terms. Substantial and statistically significant upticks are anticipated across all scenarios, seasons, and temporal horizons.

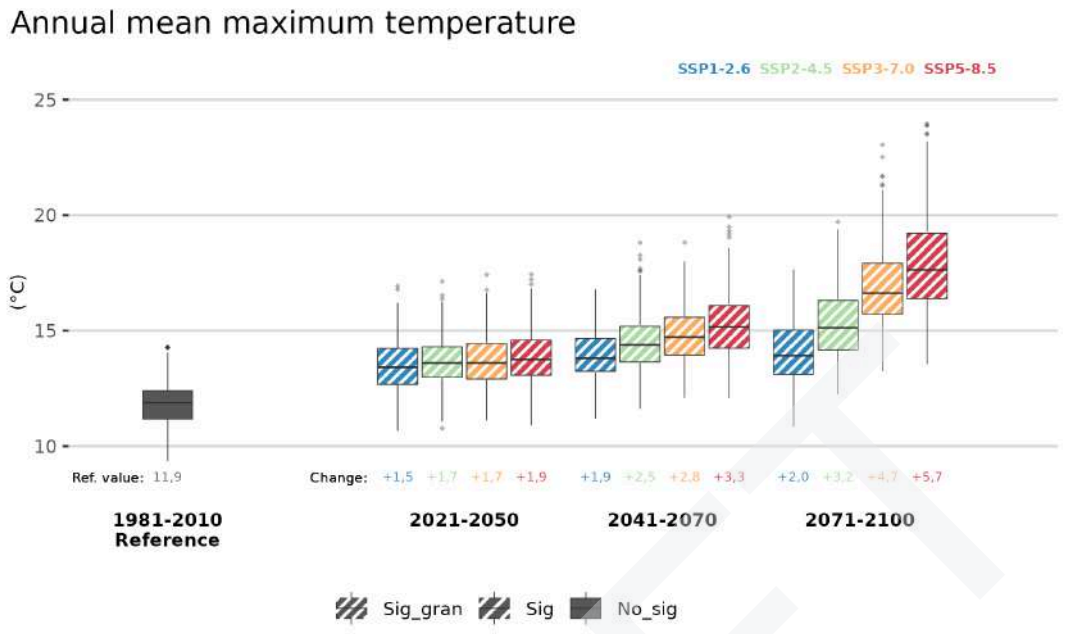

Figure 47. Expected evolution of the mean maximum temperature for SLZ stations.

Taking percentiles, **Cold/Warm days** (P10/P90 of maximum temperature, respectively) are expected to notably decrease/increase in the future, since taking the historic period as a reference in a percentile indicator causes that a warming climate boosts the number of days above P90 and reduces those below P10. Changes show that from the reference ~34 days/year, Cold days will reduce by 50-60% at mid-century, and about 60-80% by 2100. Warm days on the contrary would double (+100% or +40 days) by mid-century and increase about 150-200% (65-78 days) by 2100.

The change in maximum temperature will lead to changes in the indicators defined from it. As a matter of fact, Heat Day (Tx > 30ºC) and Extreme Heat Day (Tx>35ºC) will significantly sharply increase. **Heat days**, not so common in SLZ due to the area's climate with a median of 5.4 historic days, would increase to a range of 20 to 30 days a year by 2050, and of more than 25-50 days by 2100 in worst-case scenarios (see Figure 47). **Extreme Heat days** would follow this trend, even being exceptionally rare nowadays in SLZ, with just some records in very few stations (median of 0.0). These days would see a significant increase passing mid-century of +2-4 days on average and +4-15 by late-century.

The increase in minimum temperatures will lead to a significant large decrease in the number of **frost days**. Frost nights are a regular event in SLZ climate during winter months and even other seasons, with 122 average nights per year in the area. The decrease by the middle of the century is expected by around -25% (-35 nights), increasing by late-century to -33/-66% (from -44 up to -70 nights) in worst-case scenarios (SSP3-7.0 and 5-8.5). This change in minimum temperature is also expected during the summer season, and will also lead to the regular appearance of **tropical nights** (Tmin>20ºC), a pretty rare situation in SLZ region nowadays, with around 1.5 nights per year if so. Significant increases are already expected in the earliest time period, increasing steeply up to from +4-7 nights by 2050 and to even around +17-28 in worst cases by 2100 (Figure 49). This trend translates too to equatorial nights (Tmin

>25ºC) and infernal nights (Tmin >30ºC), both practically non-existent in this area**. Equatorial nights** and **Infernal nights** would go from 0 to around 1-2.5 nights and 0.5 by 2100 respectively.

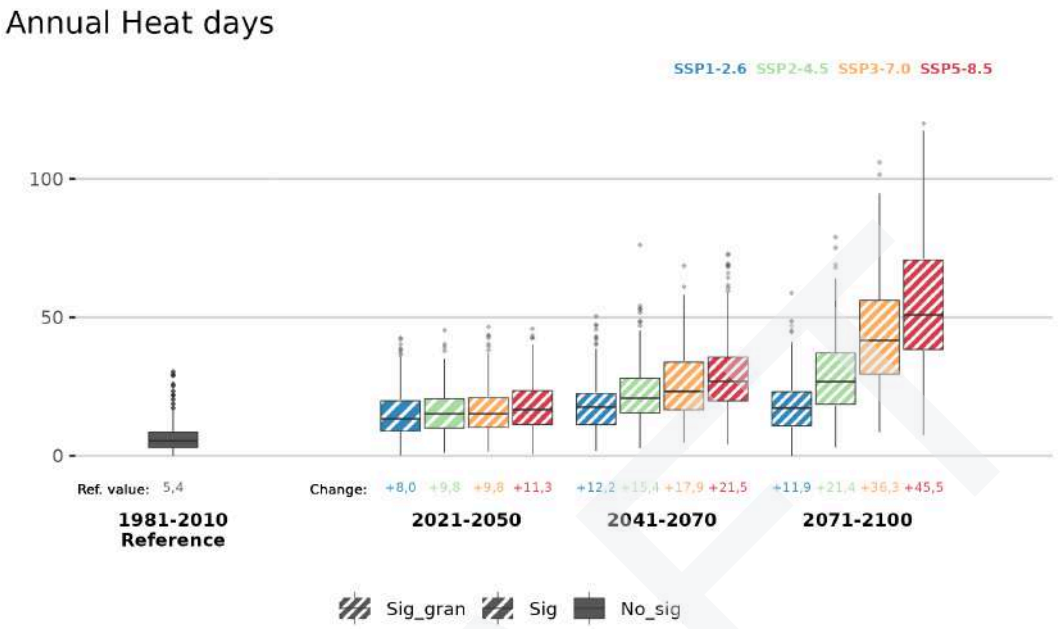

Figure 48. Expected evolution of the annual number of heat days for SLZ stations.

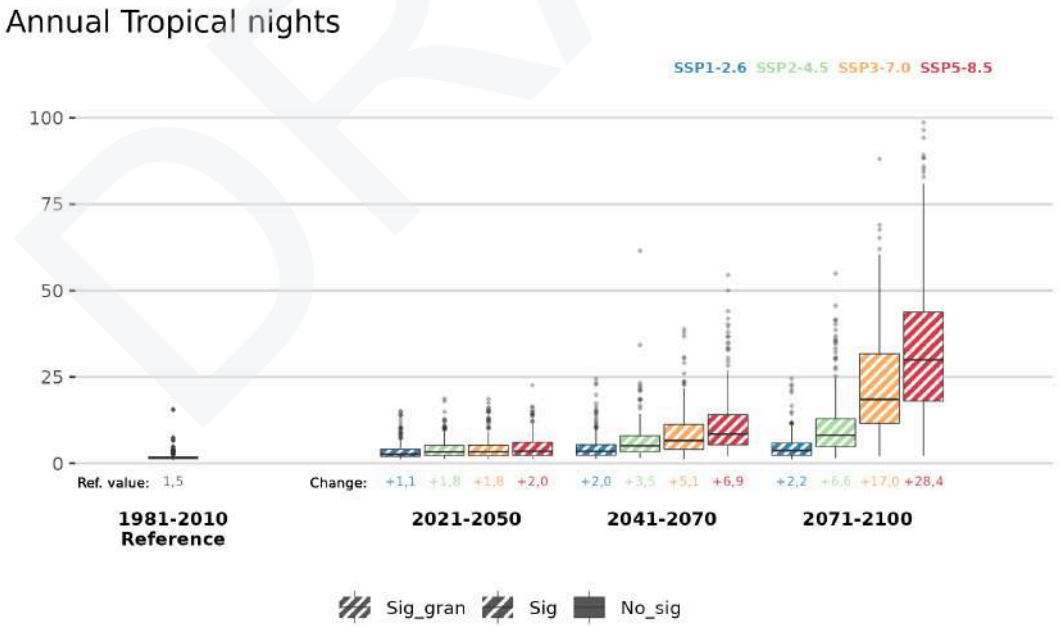

Figure 49. Expected evolution of the number of tropical nights for SLZ stations.

Aside from the previous discussion, and in order to better understand and assess further impacts of previous indicators, two derivatives were applied, calculating the maximum number of consecutive days of each previous indicator, and also the number of events (considered as ⩾3 consecutive days) expected throughout the year. Regarding **maximum consecutive days**, **Heat Day** could go from a typical 2.5-day streak in historic times to around 5-7 days by 2050 or more than 7-14 days by 2100. **Extreme Heat Days**, practically not seen, could chain 2 up to more than 5 days in a row by late-century. **Frost days** will reduce significantly, from 36 nights in a row historically to around 20 by 2050 or 15 by 2100. Warm nights would increase, with **Tropical Nights** going from non-existent to 7-11 nights in a row in the worst case by 2100. **Equatorial nights** and **Infernal nights** are not expected to chain significantly in the future. Concerning the **number of events**, **Heat Day** would go from a reference 0.3 events a year to 2-4 during the century (the increase is expected in the number of consecutive days). The same happens for **Extreme Heat Day**, with almost 1 event a year by 2100. About **Frost days**, 7.7 events were registered on average in past times, with decreases foreseen of -1.5 to -3.5 by 2100. **Tropical night** events would go from none to 2 by 2100, while no event is expected for **Equatorial nights** or **infernal nights** so far.

Additionally,, the increase in temperatures will affect the occurrence of extreme weather events such as **heat waves**, which are one of the more impactful events due to their effects on human health, infrastructure or the environment. Therefore, the length, intensity, and frequency of heat waves must be analysed to characterize these extreme weather events. The heat wave definition was created for ICARIA considering several climate and scientific conditions, and ended up being: *a temperature-related episode of at least three consecutive days where the weather observations considered register maximum temperatures above the 95% percentile of their daily maximum temperature records for the months of June to September of the 1981-2010 period.*

Heat wave impacts are expected to increase significantly since the projections indicate a very relevant rise in the intensity, length, and number of events in most scenarios by mid-century and end-century.

Emerging from a percentile-based definition, historical records indicate approximately 0.5 **heatwave events** on average. This historical context underscores the significance of gauging the scale of change. Projections suggest a notable escalation in heatwave occurrences, with an increase of around 3 events per year on average by mid-century, surging to 4 to 6 events per year by late-century across SSP2-4.5 to SSP5-8.5 scenarios (see Figure 50).

The **average length of heatwaves** is expected to extend from 3.5 days historically to 5-6 days by mid-century, with a substantial increase in the most pessimistic SSP5-8.5 scenarios, where durations could reach 6-8 days (Figure 51). Furthermore, intensification is projected in the **maximum heatwave intensity**, initially set at a median of 31.2ºC for SLZ. Although early-century changes are anticipated to be negligible, by mid-century and late-century, intensities could elevate by approximately +1.5ºC to +3.0ºC in the most pessimistic scenarios.

Anticipated changes also extend to the annual count of days meeting the definition of **heatwave days**, experiencing temperatures exceeding the 95th percentile but excluding consecutive occurrences. This count is poised to surge from a historical 5 days to over 20 (up to 30) by 2050, potentially escalating to 30 to 60 days by 2100.

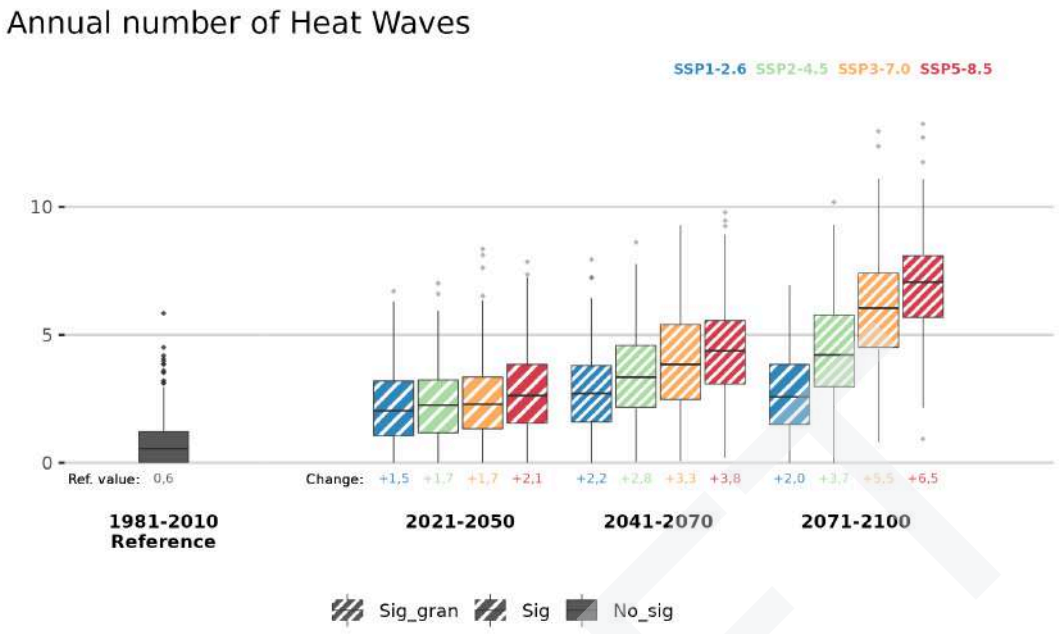

Figure 50. Expected evolution of the annual number of heat waves for SLZ stations.

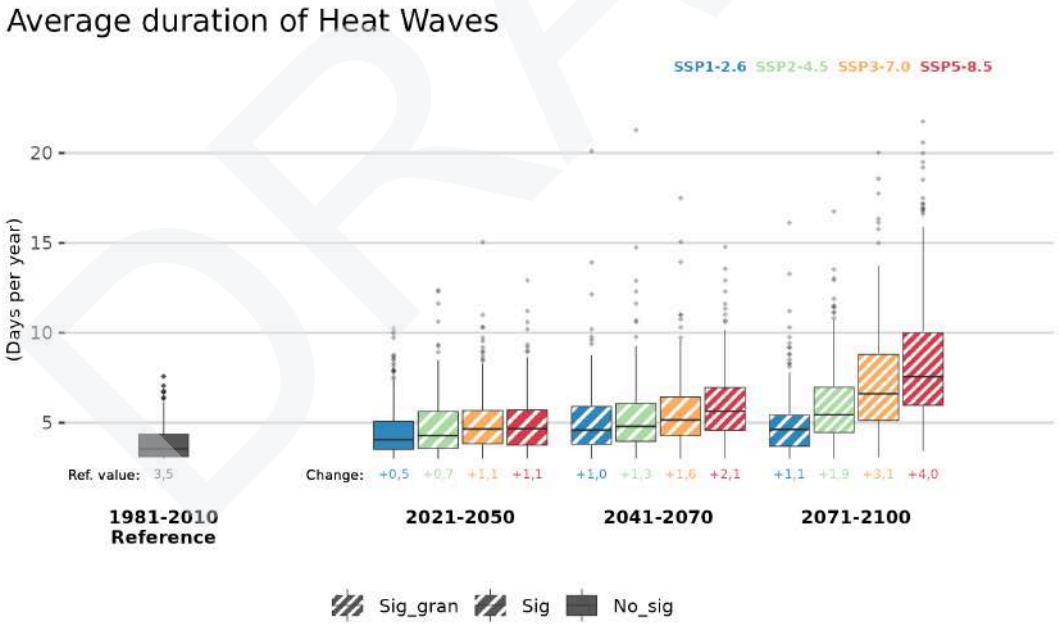

Figure 51. Expected evolution of the average duration of heat waves for SLZ stations.

Some indicators are often used to characterize thermal comfort, which is the case for the commonly used **Heat Index (HI)**, which results from a combination of temperature and RH about certain thresholds and represents the body's thermal sensation at some point. Heat Index represents that for certain T/RH values, the heat stress that a body can suffer, dangerous at some point, has nothing to do with the actual temperature that is being recorded.

For SLZ, reference measured HI oscillates around 31.4ºC, and is expected to significantly increase in the future due to rising temperatures and a typical moist environment, especially during summer, which is the wettest season in SLZ and will see an increase in rainfall.. In this regard, increases of +2-3ºC are foreseen by mid-century, while further rises of +4-7ºC in worst-case scenarios are feasible by late-century (refer to Figure 52 for more detail).

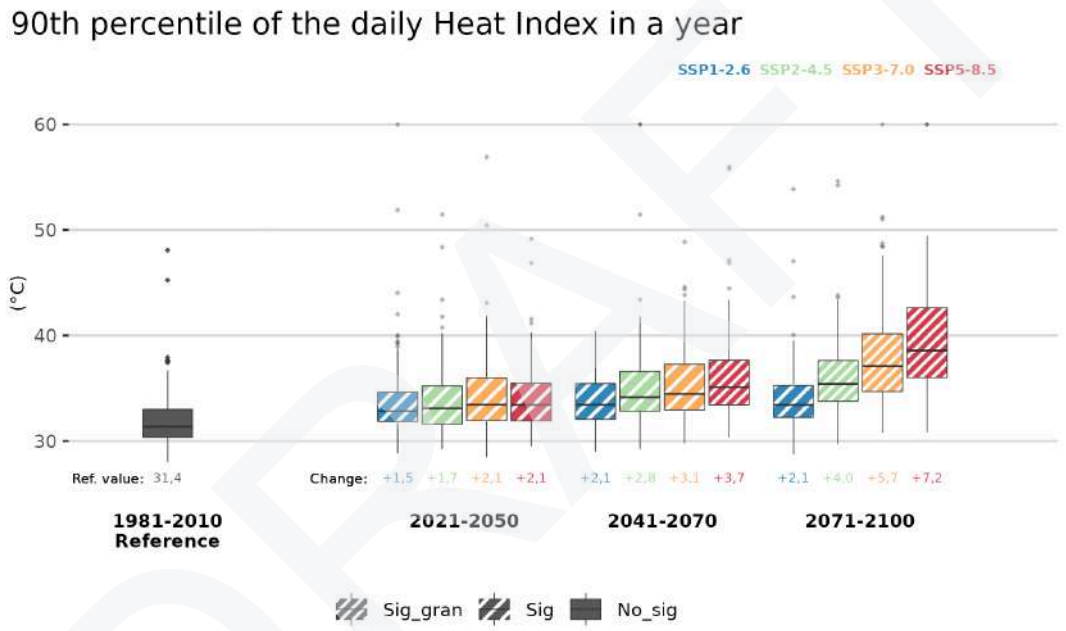

Figure 52. Expected evolution of the percentile 90 of Heat Index for SLZ stations.

Precipitation indicators

Regarding precipitation indicators, different ones have been obtained depending on the needs of the SLZ CS. In this regard, some indicators were designed to measure changes in annual precipitation while other indicators were more focused on extreme rainfall events. In this sense, in summary, no significant change is expected in yearly precipitation so far nor in days above specific extreme thresholds, but an increase in precipitation intensity at the sub-hourly scale is foreseen.

In more detail, about annual precipitation indicators, **yearly cumulative precipitation** as well as **seasonal cumulative precipitation** display significant changes towards the future, as can be seen in Figure 53. Increases are expected from mid-century, of about +10% by 2050 and larger up to +11% even +20% in SSP5-8.5. This is linked to a warmer atmosphere holding more moisture, and thanks to SLZ location in an area prone to low-pressure systems and thunderstorms all year long, climate change would affect the region towards a wetter climate.

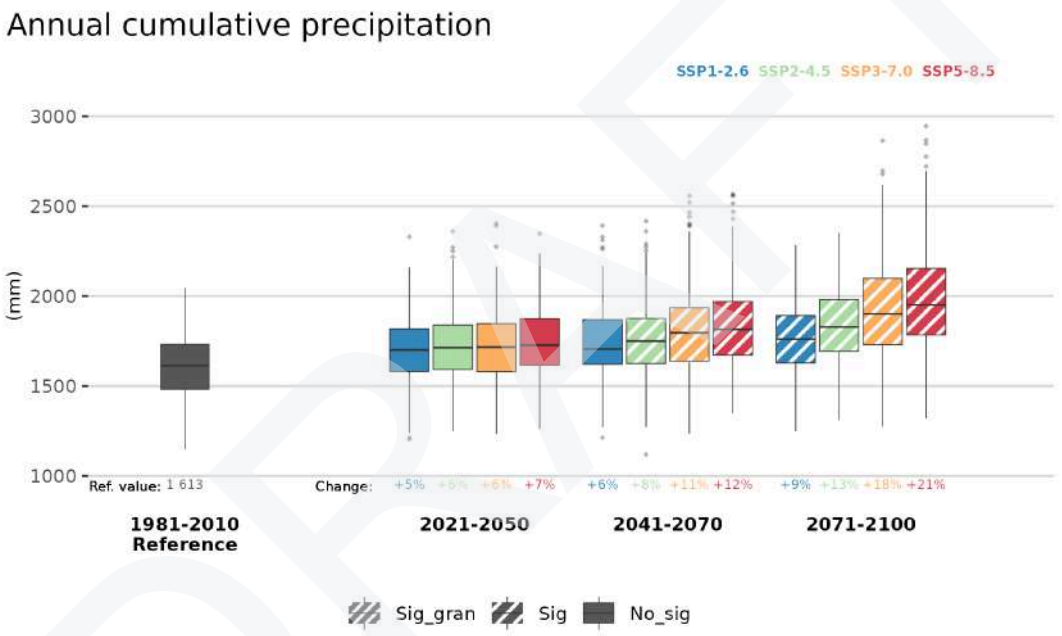

Figure 53. Expected evolution of annual cumulative precipitation for SLZ stations.

In what refers to extreme rainfall events, some indicators of these events are obtained for **days above 20, 50 and 100mm**. In the three cases, the changes with respect to historical observed days (20.8, 3.3 and 0.2 respectively) are significant increases following what was previously discussed. For >20mm days (Figure 54), increases in +4-7 days by 2100 is expected, with +1-3 days and +0.5 days for >50mm and >100mm respectively.

Studying sub-daily precipitation also allows us to know the behaviour of rainfall at these time scales. Continental climate does not see too many downpours out of summer, but future climate will increase the likelihood of these events, posing a big threat for extremely torrential downpours. In this regard, **IDF curves and CCF index** was obtained for sub-hourly rain at 1, 2, 5, 10, 20, 50, 100 and 500 years respectively.

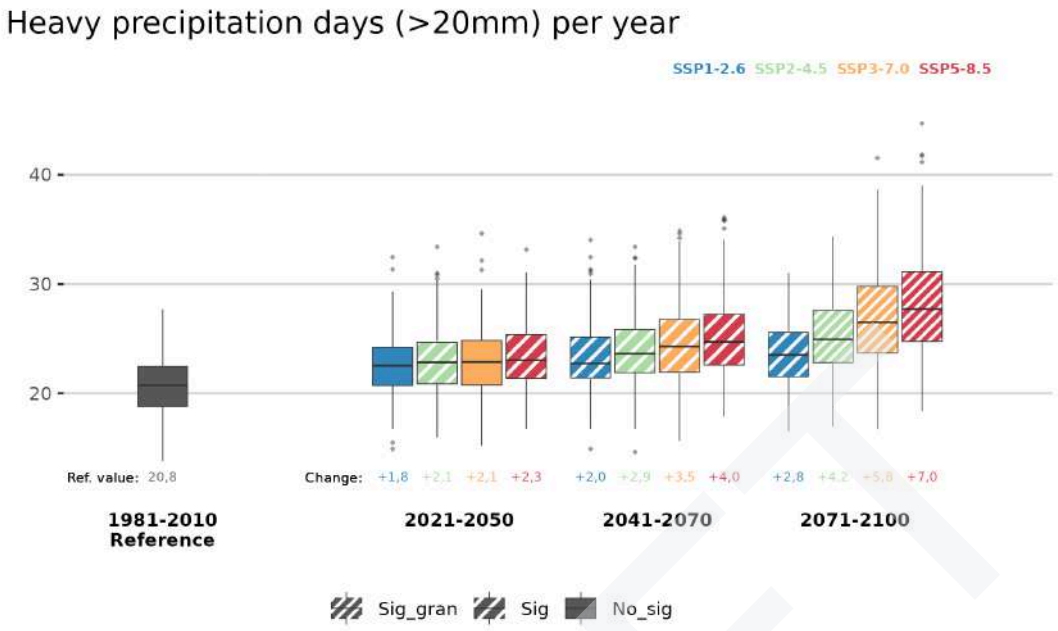

Figure 54. Expected evolution of precipitation days with >20mm accumulations for SLZ stations.

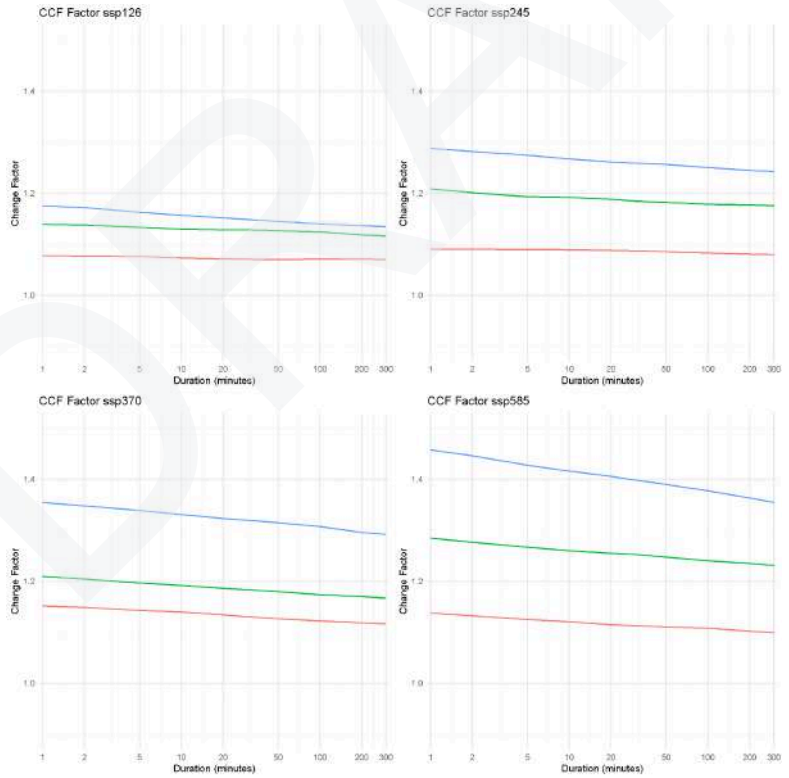

Figure 55. Example of the CCF for Salzburg region. Y axis represents the CCF, X axis the duration in minutes. Each line represents the CCF for a specific period (15-40, 41-70, 71-00 for the red, green and blue respectively).

Results for CCF (which encompasses IDF as well), shown in Figure 55, are interpreted as values greater than 1 indicating an increase in the IDF rates. As the forecast examples show, they are expected especially in the worst-case scenarios (SSP3-7.0 and 5-8.5), and significantly in the low duration scales (<10 min in the X axis) and for the last period of the century (2071-2100 or the blue lines). This translates as changes foreseen of about +20-40% in the intensity of rainfall.

Regarding its behavior among the case studio areas, it can be observed that for the Salzburg region the values are slightly higher than those observed for the case of the Metropolitan Area of Barcelona (AMB) with rate values above 1.5 in the warmest scenarios. This is consistent with the fact that the maximum water-air capacity is expected to increase more in Central Europe than in the Mediterranean region. Although positive CCF values are observed in Barcelona, the increase in drought duration in Southern Europe may partially counteract the increase in the maximum water-air capacity itself, especially in the lowest return periods, resulting in lower CCF values.

Drought indicators

In what concerns to drought, two types of indicators were agreed on in their calculation, those related to dry days (dry spell duration), and those with anomalies in precipitation/evapotranspiration (SPI & SPEI). For the first type, it was defined as a "dry day" a day with precipitation registered below 1mm, and two indicators were calculated: mean length of dry spell and maximum length of dry spell. About the **Mean length of dry spell**, for SLZ the historical yearly value was around 3.8 days, with no significant changes expected in the future at all. Regarding the **Maximum length of a dry spell**, the historical reference value is 17.6 days, and again no change whatsoever is foreseen for the future.

Regarding the SPI and SPEI indexes; due to their definition, historic value is always set to 0, and expected changes differ from one to another. For **SPI**, and associated with a significant expected increase in precipitation in the future, significant increments are expected by mid or late century in any scenario or time period, about +1-1.5 by 2050 and a more important +2-3 by 2100 (Figure 56). However, for **SPEI**, since it includes changes in temperature for the estimation of evapotranspiration, changes are not expected. Following an increase in temperature and increments in rainfall, SPEI values are projected to remain similar (more heat will contribute to evapotranspirate the extra rainfall expected) for all time periods and scenarios. Similar results are expected in other monthly-aggregated SPI and SPEI (1,3,6,12, 24).

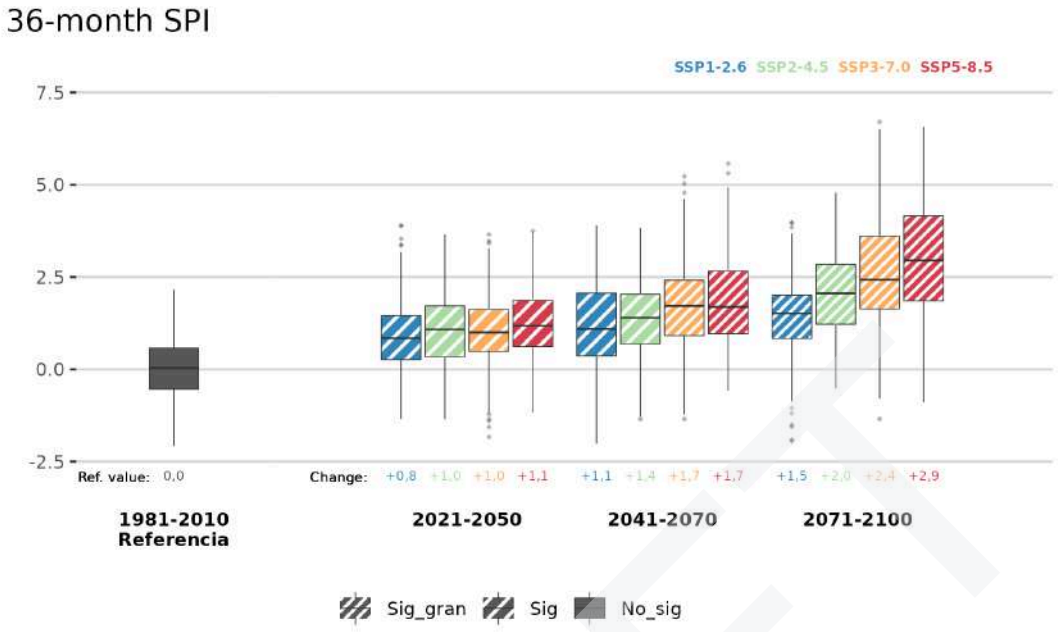

Figure 56. Expected evolution of 36-month length SPI for SLZ stations.

Wind indicator

Wind is one of the most difficult meteorological variables to be studied when dealing with future climate change variations. Due to its own nature, a result of multiple factors such as orography, local thermal variations, pressure gradients, or other weather phenomena, the future study of wind is not as straightforward as temperature could be, and future changes in pressure centres and other atmospheric patterns that determine wind's strength and direction is still today prone to high uncertainties. Besides, the remarkable lack of wind observations or their poor quality with respect to those from temperature or precipitation also hinders the procedures in statistical downscaling. On the other hand, as it can be seen in Annex 4 (Table A3.1), only 6 (out of 7) models have passed validation tests for the methodology and are used to produce these outcomes. It is good advice to take into account the aforementioned difficulty to work with the wind when interpreting the next results.

In this sense, wind gust has been modelled for the future since it is a variable that poses a higher risks and interest for ICARIA, and is included in other multiple indicators. The future evolution is studied for percentiles since it doesn't respond to a normal distribution and mean values are meaningless. For SLZ, Percentile 99, as well as other percentiles (P80, P90 or P100) don't' seem to show any change in its expected behaviour in the future. Remarkable outliers are seen corresponding to stations located in high-mountain areas.

In Salzburg, a slight downward trend is observed during the first half of the twenty-first century, however, there is a general consensus that there will be little variation during the second half of the century (Figure 57).

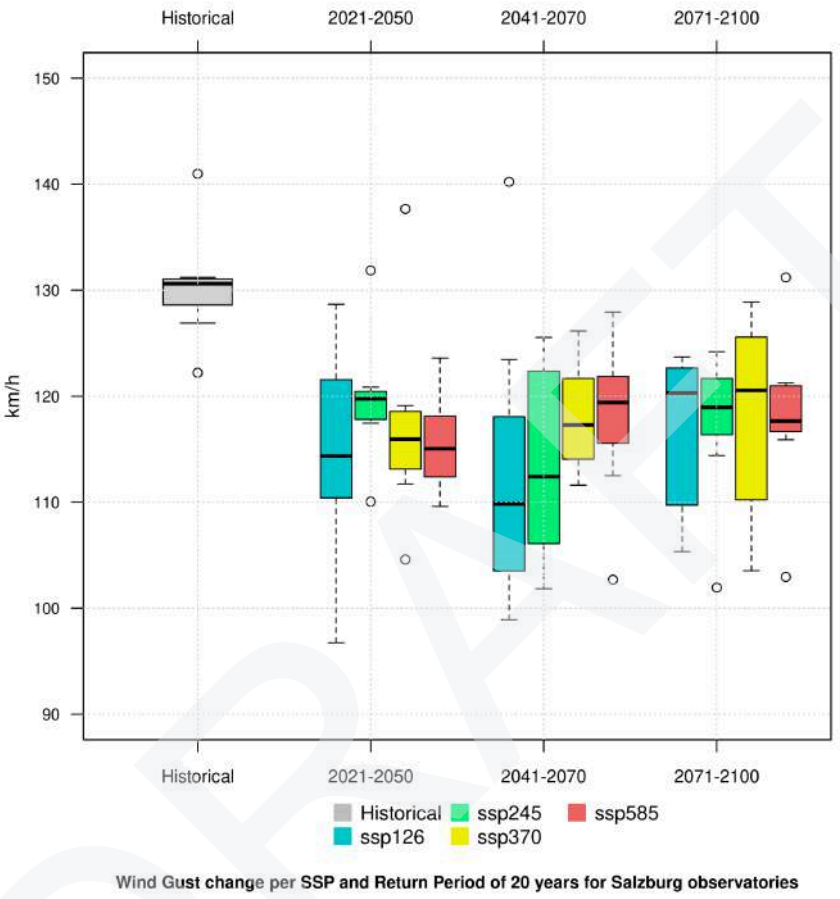

Figure 57. Results for wind gust projections for Return Period of 20 years and for SLZ stations.

5.1.6. Summary of results for the Salzburg Region - SLZ

Table 18-1. Summary table for expected changes in future thermal climate variables and extreme indicators from FICLIMA statistical downscaling in SLZ. Changes are expressed as the difference in "median(percentile 10/percentile 90)" of future expected values for each SSP and time period with respect to the historical median reference value for the period 1981-2010. Units are expressed in the INDEX column (nd = number of days, ne = number of events).

INDEX	81-10	2021-2050				2041-2070				2071-2100			
	HIST.	1-2.6	2-4.5	3-7.0	5-8.5	1-2.6	2-4.5	3-7.0	5-8.5	1-2.6	2-4.5	3-7.0	5-8.5
Thermal indicators													
TX90 (nd)	34.6	+19.5 (+10.5/+32)	+18.5 (+9.5/+31.5)	+18.3 (+9.3/+31.3)	+20.4 (+11.4/+33.4)	+29.4 (+20.4/+42)	+34.2 (+25.2/+47)	+40.3 (+31.3/+53)	+45.6 (+36.6/+58)	+30.5 (+21.5/+43)	+46.9 (+37.9/+61)	+64.8 (+55.8/+78)	+78.3 (+69.3/+91)
TX10 (nd)	33.7	-7.9 (-12.2/+1.9)	-9.0 (-12.3/+0.2)	-8.6 (-14.7/+2.7)	-11.6 (-18.3/-3.1)	-12.8 (-20.2/-2.4)	-15.1 (-22.7/-7.1)	-16.4 (-25.4/-9.2)	-19.7 (-27.7/-11.4)	-13.9 (-22.4/-5.4)	-18.7 (-27.2/-9.3)	-24.9 (-33.4/-16.3)	-27.9 (-36.6/-19.1)
HD (nd)	5.4	+8.0 (+4.1/+11.3)	+9.8 (+4.9/+13.1)	+9.8 (+5.2/+13.1)	+11.3 (+5.1/+14.2)	+27.8 (+17.5/+42.3)	+32.3 (+22.8/+47)	+39.0 (+29.5/+54)	+45.6 (+35.1/+61.1)	+11.9 (+6.2/+18.1)	+21.4 (+12.8/+34.1)	+36.3 (+28.5/+48)	+45.5 (+34.4/+65)
Max cons HD (nd)	2.4	+1.6 (+0.7/+3.5)	+1.6 (+0.6/+4.0)	+2.0 (+0.6/+4.1)	+1.6 (+0.7/+3.5)	+2.7 (+1.0/+4.3)	+3.5 (+1.7/+5.7)	+4.3 (+2.0/+5.3)	+5.3 (+2.6/+7.2)	+2.6 (+1.0/+4.7)	+4.7 (+2.2/+8.3)	+8.3 (+4.3/+12.2)	+12.2 (+5.3/+16.2)
Nº event. HD (ne)	0.3	+0.7 (+0.2/+1.2)	+0.8 (+0.3/+1.3)	+0.8 (+0.3/+1.3)	+0.8 (+0.3/+1.3)	+1.3 (+0.7/+1.8)	+1.8 (+1.2/+2.3)	+1.9 (+1.3/+2.4)	+2.4 (+1.8/+3.0)	+1.3 (+0.7/+1.8)	+2.2 (+1.6/+2.7)	+3.6 (+2.9/+4.2)	+4.2 (+3.5/+4.8)
EHD (nd)	0.0	+0.4 (+0.0/+1.0)	+0.7 (+0.2/+1.4)	+0.6 (+0.1/+1.3)	+0.5 (+0.0/+1.2)	+1.0 (+0.5/+2.0)	+2.0 (+1.0/+3.1)	+3.1 (+1.8/+4.3)	+3.8 (+2.4/+5.4)	+1.2 (+0.6/+3.6)	+3.6 (+2.2/+9.7)	+9.7 (+6.5/+20.4)	+15.4 (+10.7/+29.1)
Max cons EHD (nd)	0.0	+0.3 (+0.0/+0.8)	+0.6	+0.5	+0.4 (+0.0/+0.8)	+0.7	+1.2	+1.6	+2.0	+0.9	+1.8	+3.9	+5.2

			(+0.2/+1.2)	(+0.1/+1.0)		(+0.3/+1.4)	(+0.5/+2.0)	(+0.7/+2.7)	(+0.9/+3.4)	(+0.4/+1.8)	(+0.8/+3.0)	(+1.6/+6.4)	(+2.4/+8.4)
Nº event. EHD (ne)	0.0	+0.0 (0.0/0.0)	+0.0 (0.0/0.0)	+0.0 (0.0/0.0)	+0.0 (0.0/0.0)	+0.0 (0.0/+0.2)	+0.0 (0.0/+0.2)	+0.1 (0.0/+0.3)	+0.2 (+0.0/+0.8)	+0.0 (0.0/+0.2)	+0.2 (+0.0/+0.8)	+0.8 (+0.2/+1.5)	+1.5 (+0.8/+2.2)
TR (nd)	1.5	+0.9 (+0.3/+2.0)	+1.8 (+0.5/+3.7)	+1.8 (+0.4/+3.5)	+2.0 (+0.4/+3.6)	+2.0 (+1.2/+4.2)	+3.5 (+2.3/+6.6)	+5.1 (+3.7/+8.6)	+6.9 (+5.2/+11.4)	+2.2 (+1.4/+4.6)	+6.6 (+4.7/+11.7)	+17.0 (+12.1/+29.1)	+28.4 (+18.2/+43)
Max cons TR (nd)	0.4	+0.5 (+0.2/+1.0)	+0.7 (+0.3/+1.3)	+0.7 (+0.3/+1.3)	+0.6 (+0.2/+1.0)	+1.1 (+0.6/+2.0)	+1.8 (+0.8/+3.2)	+2.4 (+1.0/+4.4)	+3.3 (+1.8/+5.4)	+1.3 (+0.8/+2.4)	+3.2 (+1.8/+5.4)	+7.3 (+3.8/+12.2)	+11.6 (+6.0/+18.6)
Nº event. TR (ne)	0.1	+0.0 (0.0/0.0)	+0.0 (0.0/+0.1)	+0.0 (0.0/+0.1)	+0.0 (0.0/+0.1)	+0.1 (0.0/+0.2)	+0.2 (0.0/+0.3	+0.3 (+0.1/+0.5)	+0.5 (+0.2/+0.8)	+0.1 (0.0/+0.2)	+0.5 (+0.2/+0.8)	+0.9 (+0.4/+1.4)	+2.2 (+1.0/+3.4)
EQ (nd)	0.6	+0.3 (+0.1/+0.5)	+0.3 (+0.1/+0.5)	+0.3 (+0.1/+0.5)	+0.3 (+0.1/+0.5)	+0.4 (+0.2/+0.6)	+0.5 (+0.3/+0.7)	+0.6 (+0.3/+0.9)	+0.7 (+0.4/+1.0)	+0.5 (+0.3/+0.7)	+0.7 (+0.4/+1.0)	+1.4 (+0.7/+2.3)	+2.3 (+1.2/+3.2)
Max cons EQ (nd)	0.1	+0.1 (0.0/-0.1)	+0.1 (0.0/-0.1)	+0.1 (0.0/-0.1)	+0.1 (0.0/-0.1)	+0.1 (0.0/-0.1)	+0.2 (+0.0/+0.3)	+0.2 (+0.1/+0.3)	+0.3 (+0.2/+0.5)	+0.1 (+0.0/+0.2)	+0.2 (+0.1/+0.3)	+0.6 (+0.4/+1.1)	+1.2 (+0.7/+1.8)
Nº event. EQ (ne)	0.1	+0.0 (0.0/0.0)	+0.0 (0.0/0.0)	+0.0 (0.0/0.0)	+0.0 (0.0/0.0)	+0.0 (0.0/0.0)	+0.0 (0.0/0.0)	+0.0 (0.0/0.0)	+0.0 (0.0/+0.1)	+0.0 (0.0/0.0)	+0.0 (0.0/+0.1)	+0.1 (0.0/+0.2)	+0.1 (0.0/+0.4)
IN (nd)	0.1	+0.1 (0.0/+0.1)	+0.1 (0.0/+0.1)	+0.1 (0.0/+0.1)	+0.1 (+0.1/+0.1)	+0.2 (+0.2/+0.4)	+0.3 (+0.1/+0.4)	+0.3 (+0.1/+0.4)	+0.4 (+0.3/+0.4)	+0.2 (+0.2/+0.4)	+0.4 (+0.3/+0.6)	+0.7 (+0.5/+0.9)	+0.8 (+0.6/+1.1)
Max cons IN (nd)	0.0	+0.0 (0.0/+0.1)	+0.0 (0.0/+0.1)	+0.0 (0.0/+0.2)	+0.0 (0.0/+0.1)	+0.0 (0.0/+0.1)	+0.1 (0.0/+0.3)	+0.1 (+0.1/+0.3)	+0.1 (0.0/+0.3)	+0.0 (0.0/+0.1)	+0.1 (0.0/+0.3)	+0.2 (+0.2/+0.4)	+0.2 (+0.2/+0.6)
Nº event. IN (ne)	0.0	+0.0 (0.0/+0.1)	+0.0 (0.0/+0.1)	+0.0 (0.0/+0.1)	+0.0 (0.0/+0.1)	+0.0 (0.0/+0.1)	+0.0 (0.0/+0.1)	+0.0 (0.0/+0.1)	+0.0 (0.0/+0.1)	+0.0 (0.0/+0.1)	+0.0 (0.0/+0.1)	+0.1 (+0.1/+0.1)	+0.1 (+0.1/+0.1)
FD (nd)	122.2	-16.3 (-26.9/-14.4)	-17.6 (-31.2/-5.4)	-16.6 (-32.1/-2.8)	-21.1 (-36.7/-7.9)	-25.9 (-41.5/-22.5)	-32.6 (-48.2/-22.2)	-36.4 (-52.0/-30)	-43.4 (-58.0/-34.1)	-29.7 (-43.5/-20.5	-43.9 (-59.0/-34.1)	-59.2 (-74.8/-43.9)	-70.5 (-86.1/-54.2)

										)			
Max cons FD (nd)	36.1	-5.9 (-11.4/2.3)	-6.3 (-12.0/3.1)	6.7 (-0.2/14.5)	-7.4 (-12.8/0.4)	-9.3 (-15.1/0.8)	11.8 (-3.3/20.8)	13.3 (-1.2/24.2)	-15.2 (-20.7/-7.7)	-11.0 (-16.6/0.2)	-14.8 (-20.3/-7.2)	-19.8 (-25.5/-13.1)	-23.3 (-28.8/-16.8)
Nº event. FD (nd)	7.7	-0.7 (-1.3/0.6)	-0.6 (-1.7/+0.6)	-0.6 (-1.7/+0.6)	-0.7 (-1.3/+0.6)	-0.9 (-1.3/+0.2)	-0.9 (-1.3/1.8)	-1.3 (-2.1/-0.3)	-1.7 (-2.6/-0.7)	-1.2 (-2.0/-0.2)	-1.8 (-2.6/-0.4)	-2.6 (-3.6/-1.8)	-3.6 (-5.0/-2.4)

Table 18-2. Summary table for expected changes in future thermal climate variables and extreme indicators from FICLIMA statistical downscaling in SLZ. Changes are expressed as the difference in "median(percentile 10/percentile 90)" of future expected values for each SSP and time period with respect to the historical median reference value for the period 1981-2010. Units are expressed in the INDEX column (nd = number of days, ne = number of events).

INDEX	81-10	2021-2050				2041-2070				2071-2100			
	HIST.	1-2.6	2-4.5	3-7.0	5-8.5	1-2.6	2-4.5	3-7.0	5-8.5	1-2.6	2-4.5	3-7.0	5-8.5
Thermal indicators													
TXm (ºC)	11.9	+1.5 (+0.9/+2.1)	+1.7 (+0.9/+2.1)	+1.7 (+1.0/+2.2)	+1.9 (+1.1/+2.4)	+1.9 (+1.4/+2.5)	+2.5 (+1.9/+3.1)	+2.8 (+2.2/+3.4)	+3.3 (+2.7/+3.9)	+2.0 (+1.5/+2.6)	+3.2 (+2.6/+3.8)	+4.7 (+4.1/+5.3)	+5.7 (+5.1/+6.3)
TNm (ºC)	3.2	+1.2 (+0.8/+1.8)	+1.3 (+0.8/+1.8)	+1.2 (+0.8/+1.8)	+1.4 (+0.8/+2.0)	+1.8 (+1.2/+2.3)	+2.4 (+1.7/+2.7)	+2.6 (+1.8/+3.1)	+3.0 (+2.5/+3.8)	+2.0 (+1.6/+2.4)	+3.1 (+2.1/+3.5)	+4.3 (+3.8/+4.6)	+5.3 (+4.6/+5.8)
TM (ºC)	7.5	+1.3 (+0.8/+1.8)	+1.3 (+0.8/+1.8)	+1.3 (+0.8/+1.8)	+1.5 (+1.0/+2.0)	+1.9 (+1.4/+2.5)	+2.4 (+1.8/+2.9)	+2.7 (+2.0/+3.3)	+3.2 (+2.6/+4.1)	+2.0 (+1.6/+2.5)	+3.1 (+2.3/+3.7)	+4.6 (+4.0/+5.1)	+5.6 (+5.0/+6.2)
HWIe (nd)	3.5	+0.4 (+0.1/+0.7)	+0.6 (+0.2/+0.9)	+0.9 (+0.3/+1.2)	+0.7 (+0.2/+1.0)	+1.0 (+0.4/+1.3)	+1.3 (+0.5/+1.6)	+1.6 (+0.6/+1.9)	+2.1 (+0.9/+3.0)	+1.1 (+0.4/+1.4)	+1.9 (+0.8/+2.8)	+3.1 (+1.1/+4.0)	+4.0 (+1.4/+5.0)
HWIx (ºC)	31.2	+0.6 (0.0/1.4)	+0.7 (0.1/1.5)	+0.6 (0.0/1.4)	+0.5 (0.0/1.2)	+0.7 (0.1/1.5)	+1.1 (0.3/2.1)	+1.5 (0.5/2.7)	+1.8 (0.8/3.1)	+0.8 (0.2/1.7)	+1.7 (0.6/3.1)	+2.6 (1.0/4.0)	+3.1 (1.4/4.6)
HWf (ne)	0.6	+1.3 (+0.2/+2.8)	+1.4 (+0.2/+2.9)	+1.4 (+0.2/+2.9)	+1.4 (+0.2/+2.9)	+2.2 (+0.9/+3.7)	+2.8 (+1.4/+4.3)	+3.3 (+1.7/+4.8)	+3.8 (+2.4/+5.3)	+2.0 (+0.8/+3.5)	+3.7 (+2.3/+5.2)	+5.5 (+3.9/+7.1)	+6.5 (+4.9/+8.1)
HWd (nd)	5.1	+7.4 (+4.2/+12.6)	+8.9 (+5.4/+14.3)	+8.7 (+5.3/+14.0)	+9.1 (+5.2/+14.5)	+14.4 (+8.1/+22.3)	+18.5 (+10.9/+28.1)	+20.7 (+12.4/+31.4)	+26.7 (+18.3/+38)	+13.9 (+7.6/+21.7)	+25.6 (+17.2/+35.8)	+44.0 (+28.2/+59)	+56.5 (+38.4/+74.1)
HI-P90	31.4	+1.4	+1.4	+1.7	+1.7	+2.1	+2.8	+3.1	+3.7	+2.1	+4.0	+5.7	+7.2

(ºC)		(+0.6/+2.1)	(+0.7/+2.1)	(+0.7/+2.4)	(+0.6/+2.1)	(+1.3/+3.1)	(+1.8/+4.0)	(+2.1/+4.0)	(+2.7/+4.7	(+1.3/+3.1)	(+2.8/+5.2)	(+4.2/+7.2)	(+5.7/+8.7)

Table 19. Summary table for expected changes in future precipitation climate variables and extreme indicators from FICLIMA statistical downscaling in SLZ. Changes are expressed as the difference in "median(percentile 10/percentile 90)" of future expected values for each SSP and time period with respect to the historical median reference value for the period 1981-2010. Units are expressed in the INDEX column (nd = number of days, ne = number of events).

INDEX	81-10	2021-2050				2041-2070				2071-2100			
	HIST.	1-2.6	2-4.5	3-7.0	5-8.5	1-2.6	2-4.5	3-7.0	5-8.5	1-2.6	2-4.5	3-7.0	5-8.5
Precipitation indicators													
R20 (nd)	20.8	+1.5 (+0.5/+2.5)	+1.6 (+0.5/+2.5)	+1.8 (+1.0/+3.0)	+1.9 (+1.0/+3.5)	+2.0 (+1.0/+3.0)	+2.9 (+2.0/+4.0)	+3.5 (+2.5/+5.0)	+4.0 (+3.0/+5.5)	+2.8 (+2.0/+4.0)	+4.2 (+3.0/+5.5)	+5.8 (+4.0/+7.5)	+7.0 (+5.0/+9.0)
R50 (nd)	3.3	+0.6 (+0.0/+1.2)	+0.6 (+0.0/+1.2)	+0.6 (+0.2/+1.4)	+0.8 (+0.3/+1.6)	+1.0 (+0.4/+1.6)	+1.2 (+0.6/+1.8)	+1.4 (+0.6/+2.0)	+1.6 (+0.8/+2.6)	+1.0 (+0.4/+1.6)	+1.6 (+0.8/+2.4)	+2.3 (+1.0/+3.2)	+2.9 (+1.2/+4.0)
R100 (nd)	0.2	+0.1 (0.0/-0.2)	+0.1 (0.0/-0.2)	+0.1 (0.0/-0.2)	+0.2 (+0.1/-0.3)	+0.2 (0.1/-0.3)	+0.2 (0.1/-0.3)	+0.3 (+0.2/-0.4)	+0.3 (+0.2/-0.4)	+0.2 (0.1/-0.3)	+0.3 (+0.2/-0.4)	+0.5 (+0.3/-0.6)	+0.6 (+0.4/-0.7)
Ra (mm,%)	1613	+5% (+2%/+9%)	+5% (+2%/+9%)	+6% (+3%/+10%)	+6% (+3%/+10%)	+6% (+3%/+10%)	+8% (+4%/+13%)	+11% (+6%/+16%)	+12% (+7%/+17%)	+9% (+5%/+14%)	+13% (+7%/+19%)	-18% (-23%/-13%)	+21% (+14%/+27%)
IDF - CCF 100y	57	+1% (-4%/13%)	+8% (-4%/14%)	+13% (-8%/16%)	+7% (-9%/14%)	+12% (3%/20%)	+18% (2%/31%)	+19% (1%/32%)	+24% (1%/37%)	+16% (0%/23%)	+22% (7%/33%)	+30% (11%/46%)	+36% (11%/47%)

Table 20. Summary table for expected changes in future wind climate variables and drought indicators from FICLIMA statistical downscaling in SLZ. Changes are expressed as the difference in "median(percentile 10/percentile 90)" of future expected values for each SSP and time period considered with respect to the historical median reference value for the period 1981-2010. Units are expressed in the INDEX column (nd = number of days, ne = number of events).

INDEX	81-10	2021-2050				2041-2070				2071-2100			
	HIST.	1-2.6	2-4.5	3-7.0	5-8.5	1-2.6	2-4.5	3-7.0	5-8.5	1-2.6	2-4.5	3-7.0	5-8.5
Drought indicators													
CDDx (nd)	17.6	-0.1 (-0.3/+0.2)	-0.8 (1.0/+0.6)	-0.7 (-1.0/+0.8)	-0.1 (-0.3/+0.2)	-0.3 (-0.4/+0.2)	+0.1 (-0.2/+0.2)	-0.3 (-0.4/+0.2)	-0.1 (0.0/-0.2)	-0.6 (-0.9/+0.2)	-0.3 (-0.5/+0.2)	+0.3 (-0.2/+0.6)	+0.1 (-0.2/+0.5)
CDDm (nd)	3.8	+0.0 (-0.2/+0.2)	+0.0 (-0.1/+0.3)	-0.1 (-0.2/+0.2)	+0.0 (-0.3/+0.2)	-0.1 (-0.2/+0.3)	+0.0 (-0.2/+0.2)	+0.0 (-0.3/+0.2)	+0.0 (-0.2/+0.2)	-0.1 (-0.4/+0.2)	+0.1 (-0.4/+0.2)	+0.1 (-0.2/+0.4)	+0.1 (-0.2/+0.4)
SPI-36	0.0	+0.8 (+0.1/+1.5)	+1.0 (+0.2/+1.6)	+1.0 (+0.3/+1.7)	+1.1 (+0.4/+1.8)	+1.1 (+0.5/+1.9)	+1.4 (+0.7/+2.2)	+1.7 (+0.9/+2.5)	+1.7 (+1.1/+2.6)	+1.5 (+0.9/+2.3)	+2.0 (+1.3/+2.8)	+2.4 (+1.7/+3.2)	+2.9 (+2.1/+3.7)
SPEI-36	0.0	+0.1 (-0.6/+0.5)	+0.3 (-0.5/+0.7)	+0.3 (-0.4/+0.6)	+0.2 (-0.6/+0.7)	+0.0 (-0.8/+0.7)	+0.0 (-0.8/+0.3)	+0.2 (-0.6/+0.3)	+0.1 (-0.8/+0.7)	+0.3 (-0.4/+0.5)	+0.2 (-0.7/+0.8)	0.0 (-1.1/+1.1)	+0.1 (-1.6/+1.5)
Wind indicators													
EWG (km/h)	74	-6% (-20/+6)	-2% (-14/+2)	-11% (-23/+9)	-11% (-21/+4)	-13% (-26/+10)	-8% (-23/+6)	-8% (-19/+3)	-7% (-20/+3)	-8% (-21/+3)	-7% (-18/+5)	-6% (-21/+6)	-7% (-19/+11)

5.2. Dynamical downscaling outputs

It is important to note that the results analysed below **display a part of the available data and is not by all means complete**. After completion of the climate projections, **hourly values for different parameters (temperature, precipitation, wind, cloud cover, radiation, humidity, geopotential, pressure,...)** are available, allowing the detailed analysis of different time scales (f.i. hourly / 3 hourly etc). In total, there are 24 files per day, for 119 years (1981 - 2100), which amounts to **more than 1 million output files**. The analysis needed for the case studies will be defined in the upcoming weeks, depending on stakeholder communication needs and damage assessment models.

5.2.1. The South Aegean Region

Thermal indicators

The WRF results of the South Aegean region display an increase in yearly mean temperatures of about 2°C until the end of the century in the SSP126 and up to 5°C within SSP585.

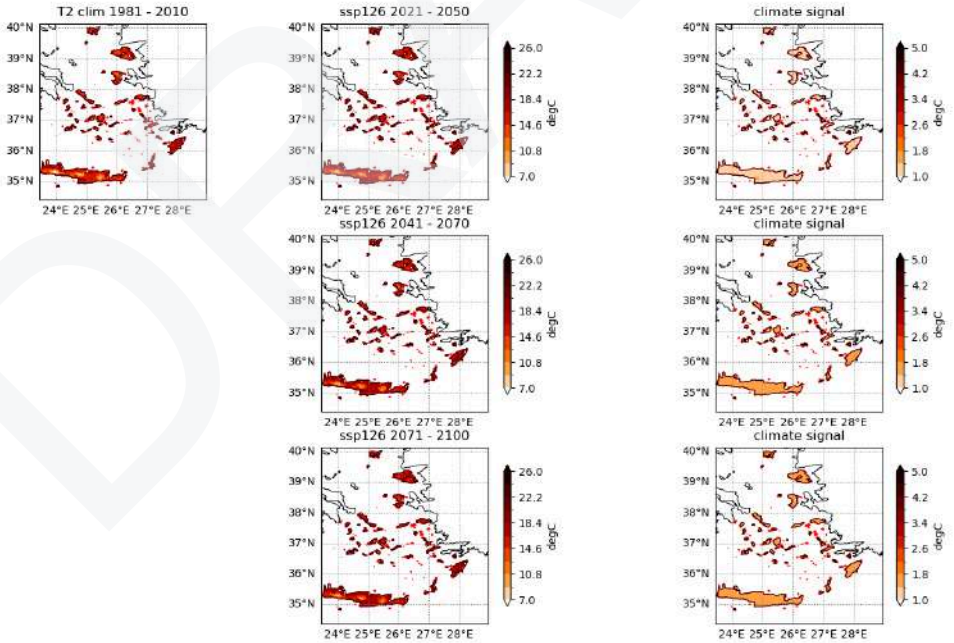

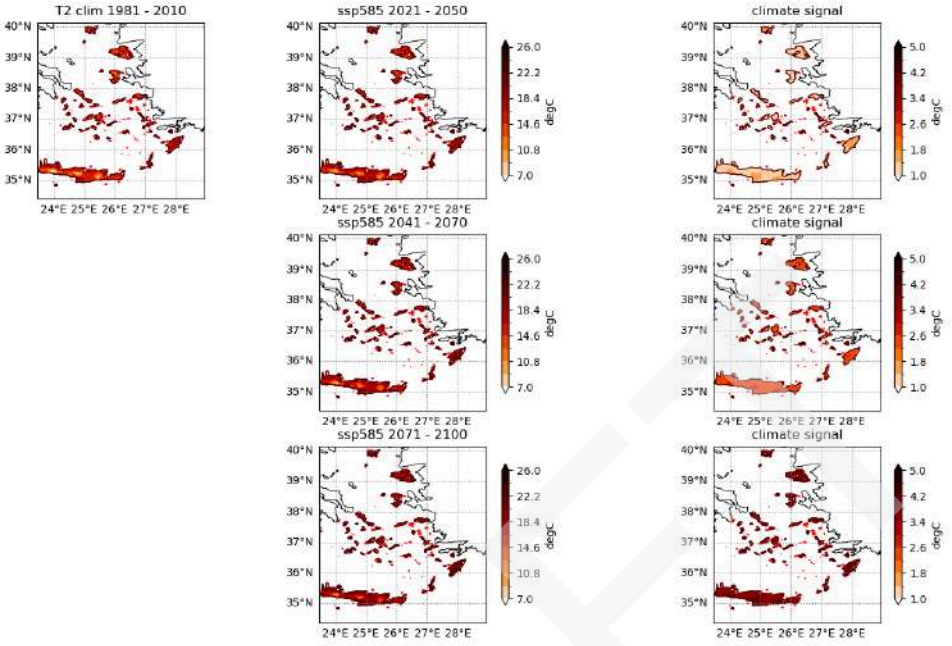

Figure 58: yearly mean temperatures as simulated by WRF for SSP126 (top) and SSP585 (bottom): clim corresponds to past period, middle column displays absolute values of simulations, right column the difference between the mid century and the reference period (respectively).

Regarding the yearly maximum temperatures, a similar magnitude is computed as for the yearly mean temperatures within SSP126 and SSP585. Further, it's important to note that within SSP126 the increase in temperature is the same for the mid to late century (whereas SSP585 strongly increases towards 2100), highlighting the need for climate mitigation measures!

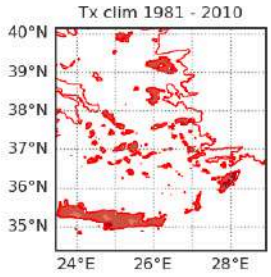
Tx clim 1981 - 2010
40°N
39°N
38°N
37°N
36°N
35°N
24°E
26°E
28°E

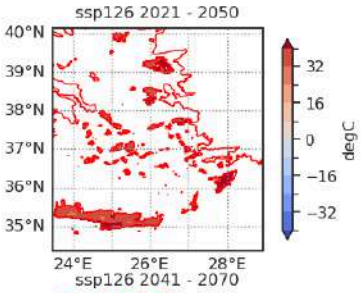
ssp126 2021 - 2050
40°N
39°N
38°N
37°N
36°N
35°N
24°E
26°E
28°E
32
16
0
−16
−32
degC

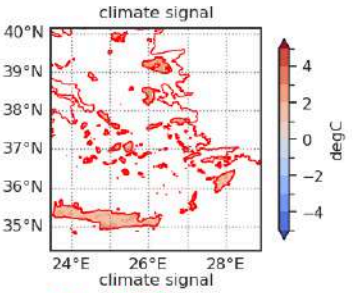
climate signal
40°N
39°N
38°N
37°N
36°N
35°N
24°E
26°E
28°E
4
2
0
−2
−4
degC

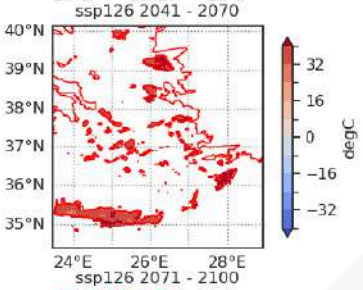
ssp126 2041 - 2070
40°N
39°N
38°N
37°N
36°N
35°N
24°E
26°E
28°E
32
16
0
−16
−32
degC

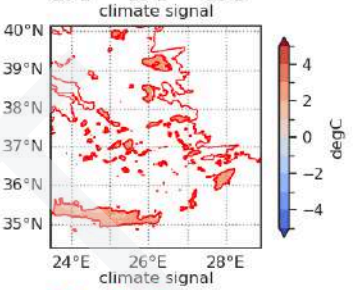
climate signal
40°N
39°N
38°N
37°N
36°N
35°N
24°E
26°E
28°E
4
2
0
−2
−4
degC

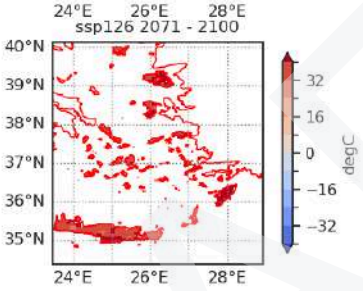
ssp126 2071 - 2100
40°N
39°N
38°N
37°N
36°N
35°N
24°E
26°E
28°E
32
16
0
−16
−32
degC

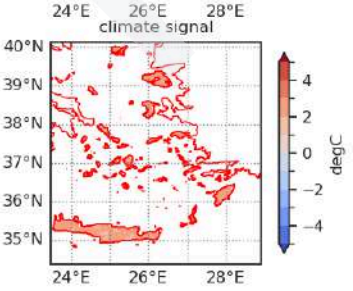
climate signal
40°N
39°N
38°N
37°N
36°N
35°N
24°E
26°E
28°E
4
2
0
−2
−4
degC

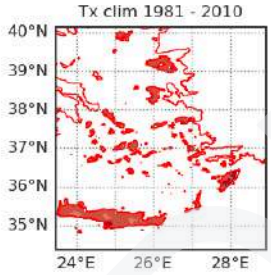
Tx clim 1981 - 2010
40°N
39°N
38°N
37°N
36°N
35°N
24°E
26°E
28°E

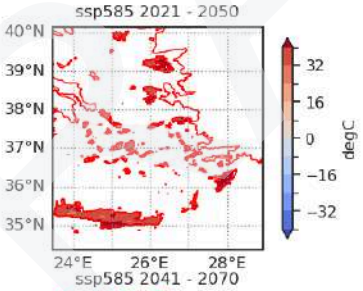
ssp585 2021 - 2050
40°N
39°N
38°N
37°N
36°N
35°N
24°E
26°E
28°E
32
16
0
−16
−32
degC

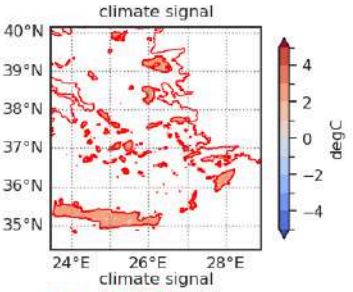
climate signal
40°N
39°N
38°N
37°N
36°N
35°N
24°E
26°E
28°E
4
2
0
−2
−4
degC

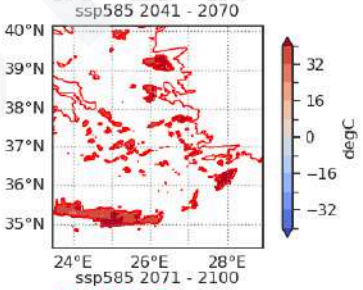
ssp585 2041 - 2070
40°N
39°N
38°N
37°N
36°N
35°N
24°E
26°E
28°E
32
16
0
−16
−32
degC

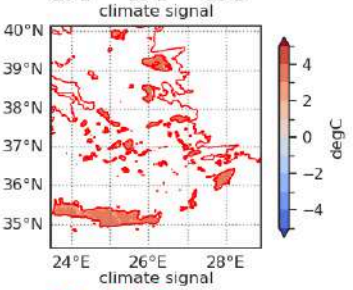
climate signal
40°N
39°N
38°N
37°N
36°N
35°N
24°E
26°E
28°E
4
2
0
−2
−4
degC

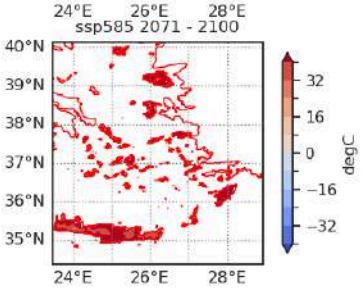
ssp585 2071 - 2100
40°N
39°N
38°N
37°N
36°N
35°N
24°E
26°E
28°E
32
16
0
−16
−32
degC

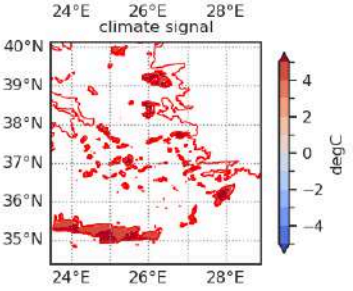
climate signal
40°N
39°N
38°N
37°N
36°N
35°N
24°E
26°E
28°E
4
2
0
−2
−4
degC

Figure 59: yearly mean temperatures as simulated by WRF for SSP126 (top) and SSP585 (bottom): clim corresponds to past period, middle column displays absolute values of simulations, right column the difference between the mid century and the reference period (respectively).

The change in yearly mean and maximum temperature relate to an increase in tropical nights (tmin > 20°C) by up to 20 nights in SSP126, while an increase by more than 40 can be expected within the high emission scenario. Added to the already occurring high number of tropical nights (70-90 in the historical period), this corresponds to 3-4 months of continuous high nighttime temperatures.

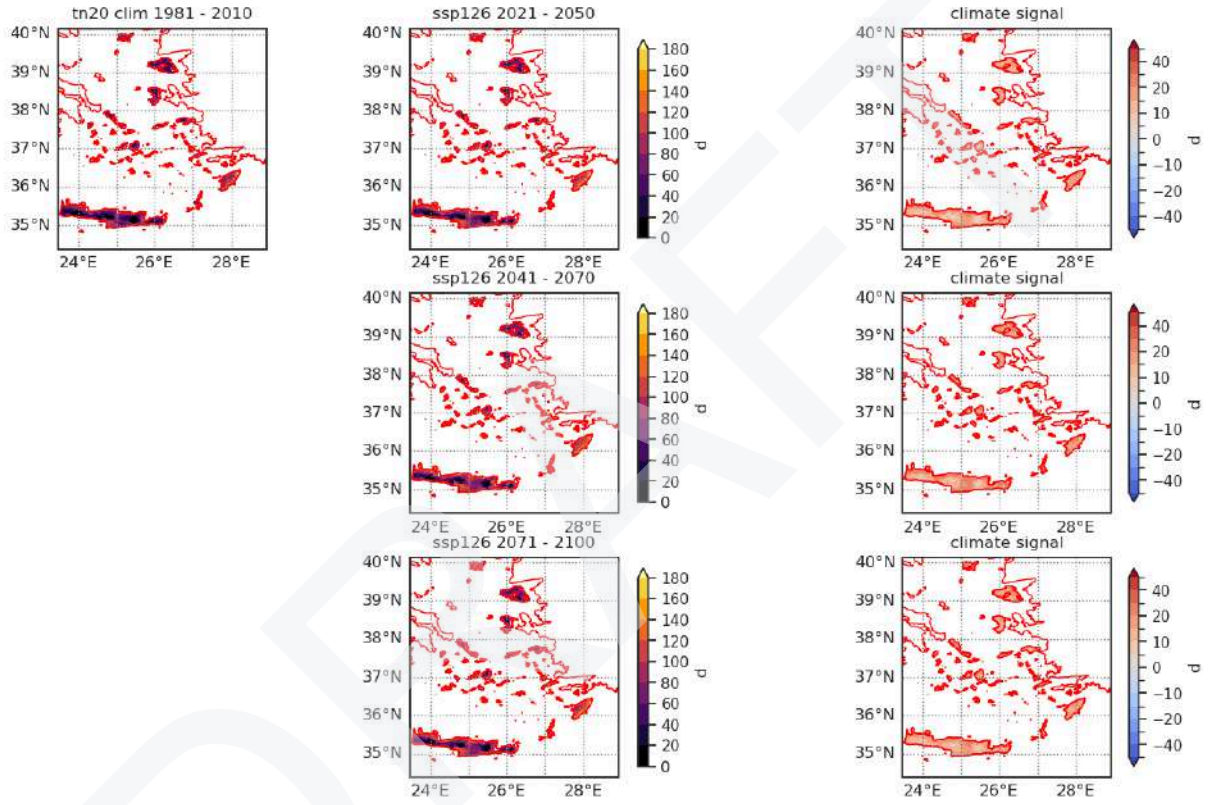

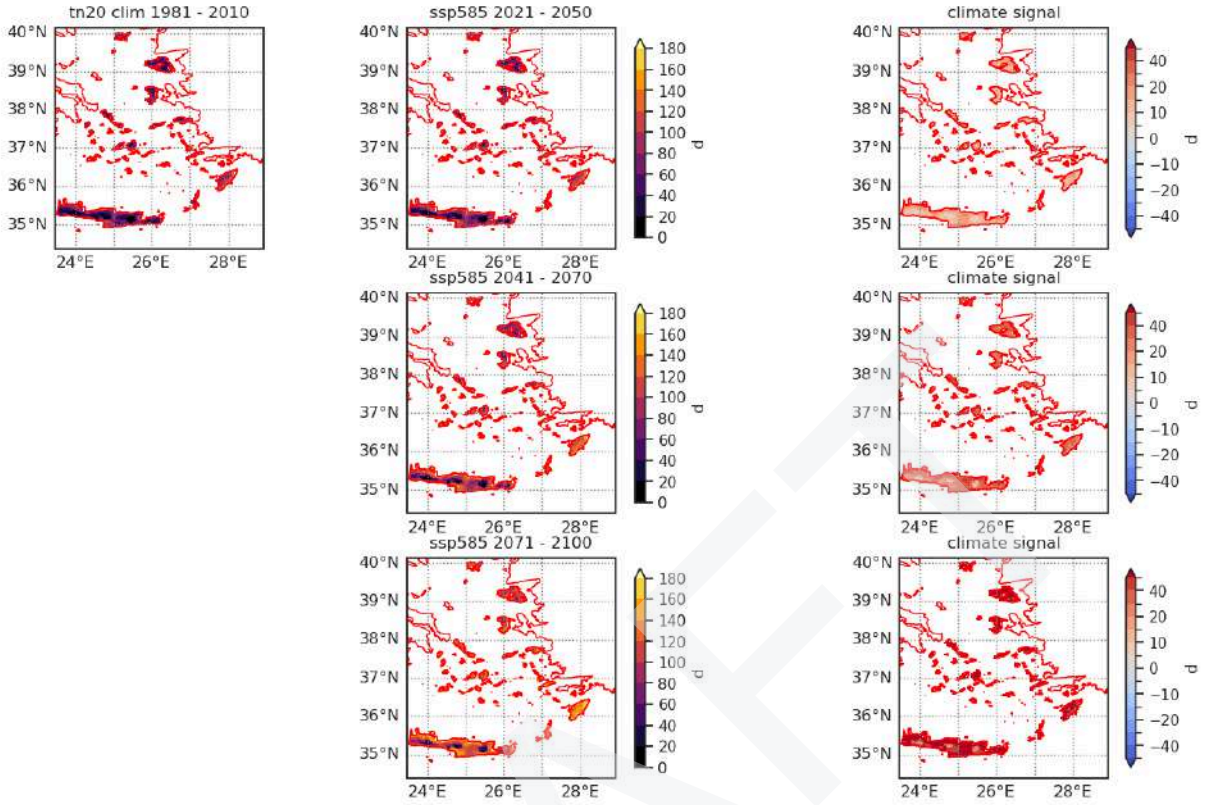

Figure 60: number of tropical nights as simulated by WRF for SSP126 (top) and SSP585 (bottom): clim corresponds to past period, middle column displays absolute values of simulations, right column the difference between the mid century and the reference period (respectively).

Not only the number of tropical nights, but also the number of days with maximum temperatures above 30°C is increasing over the summer period with the same magnitude .

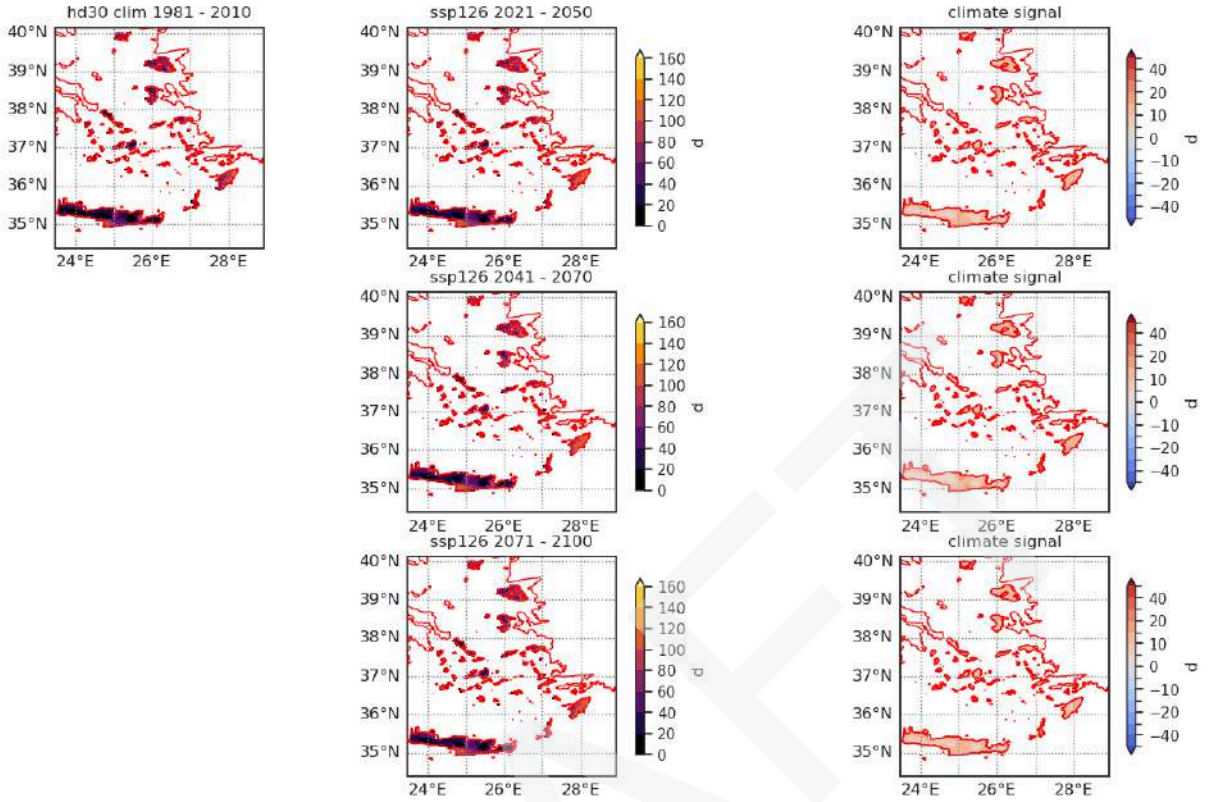
hd30 clim 1981 - 2010
ssp126 2021 - 2050
climate signal
ssp126 2041 - 2070
climate signal
ssp126 2071 - 2100
climate signal
40°N
39°N
38°N
37°N
36°N
35°N
24°E
26°E
28°E
d
160
140
120
100
80
60
40
20
0
40
20
10
0
−10
−20
−40

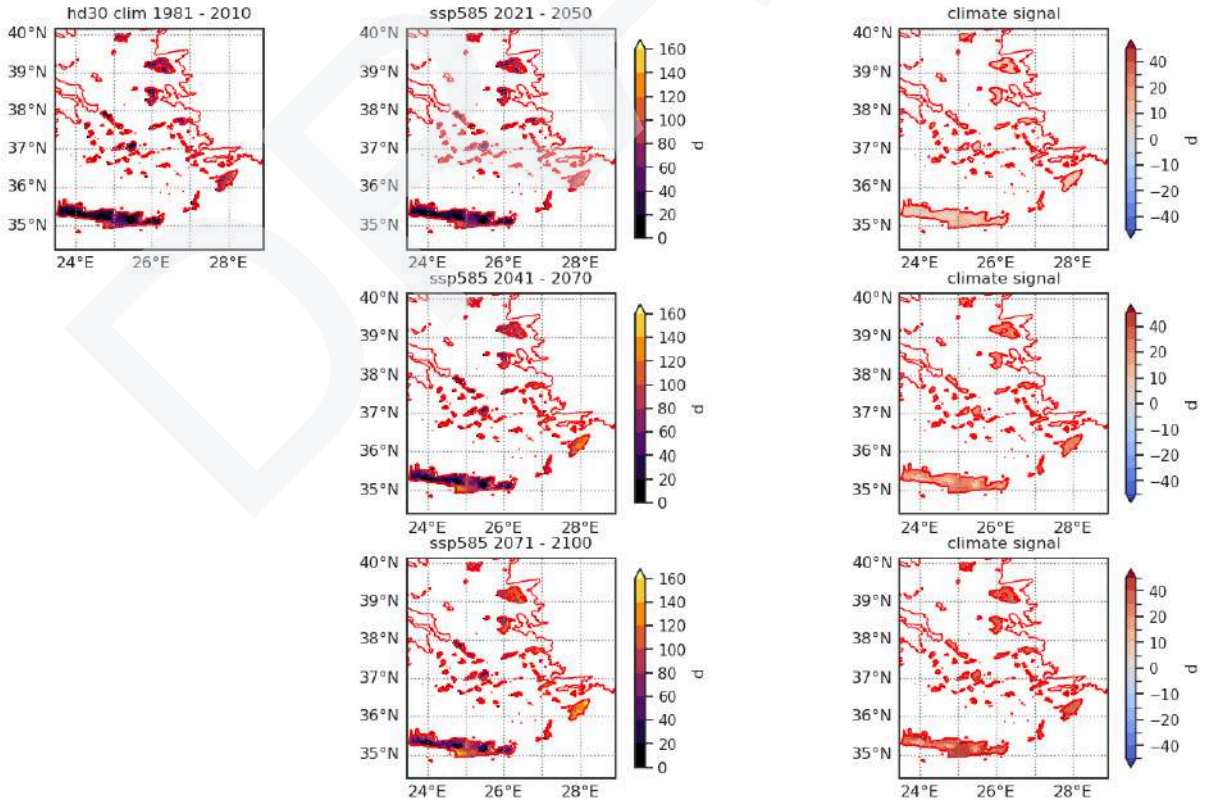
hd30 clim 1981 - 2010
ssp585 2021 - 2050
climate signal
ssp585 2041 - 2070
climate signal
ssp585 2071 - 2100
climate signal
40°N
39°N
38°N
37°N
36°N
35°N
24°E
26°E
28°E
d
160
140
120
100
80
60
40
20
0
40
20
10
0
−10
−20
−40

Figure 61: number of heat day (tmay > 30°C) as simulated by WRF for SSP126 (top) and SSP585 (bottom): clim corresponds to past period, middle column displays absolute values of simulations, right column the difference between the mid century and the reference period (respectively).

Precipitation indicators

The annual mean precipitation rate is slightly decreasing within SSP126 as simulated by WRF, but especially SSP585 indicates a strong drop for the South Aegean islands by mid-century, intensifying until 2100.

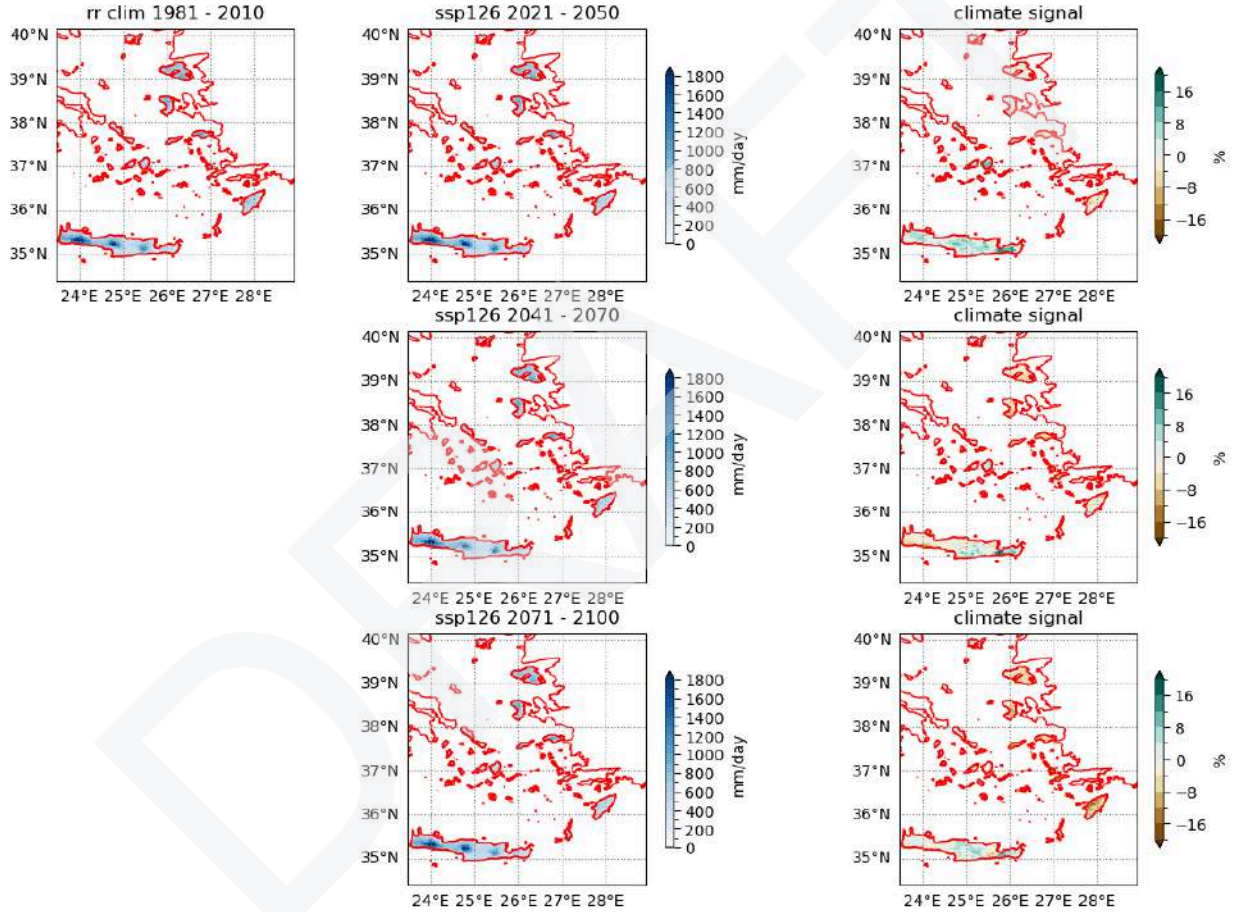

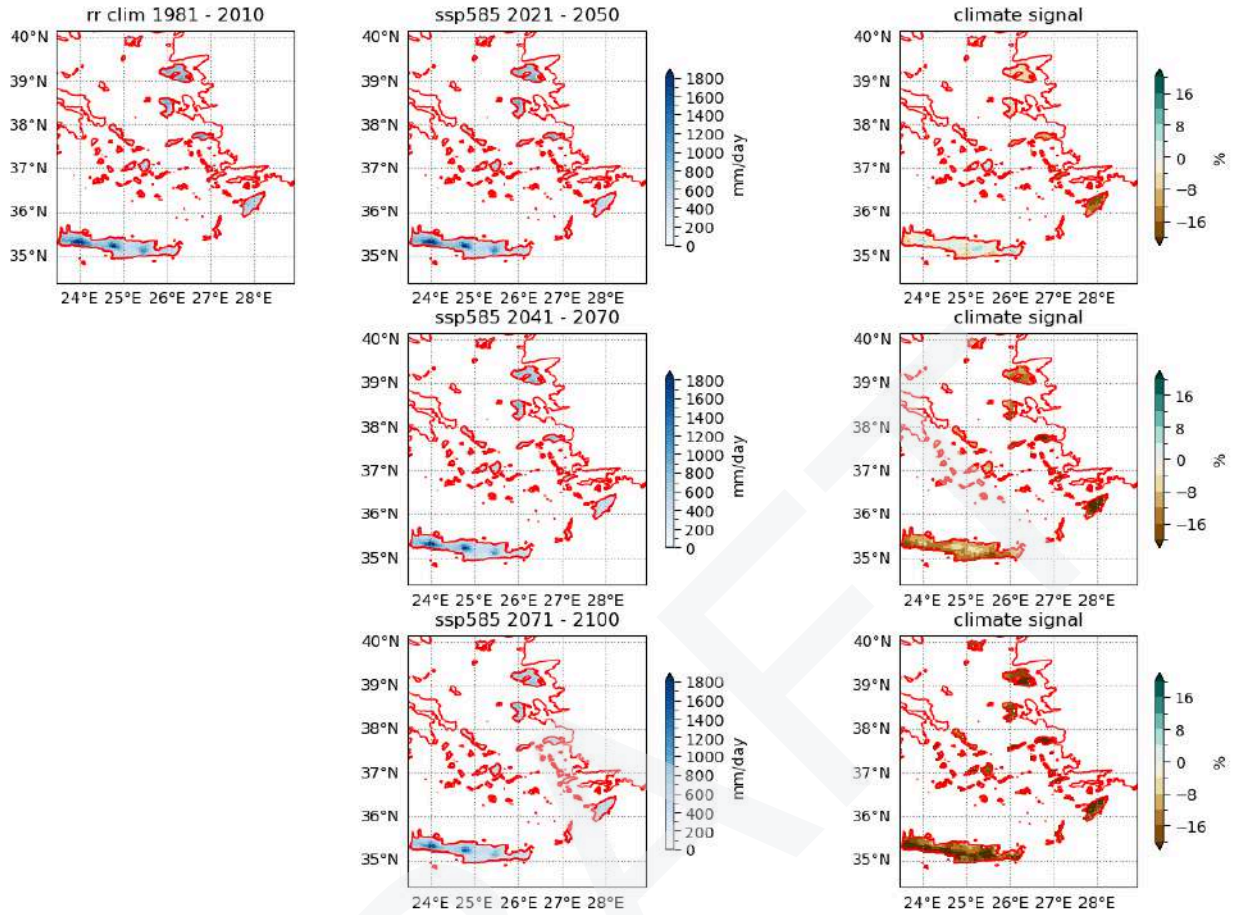

Figure 62: annual mean precipitation rate as simulated by WRF for SSP126 (top) and SSP585 (bottom): clim corresponds to past period, middle column displays absolute values of simulations, right column the difference between the mid century and the reference period (respectively).

To understand future drought risks, the indicator of maximum consecutive dry days reveals important information. Until 2050 especially the eastern part of the South Aegean region is expected to experience a prolongation of droughts. This pattern is intensified and extended over the whole simulated area until the mid century, especially in SSP585.

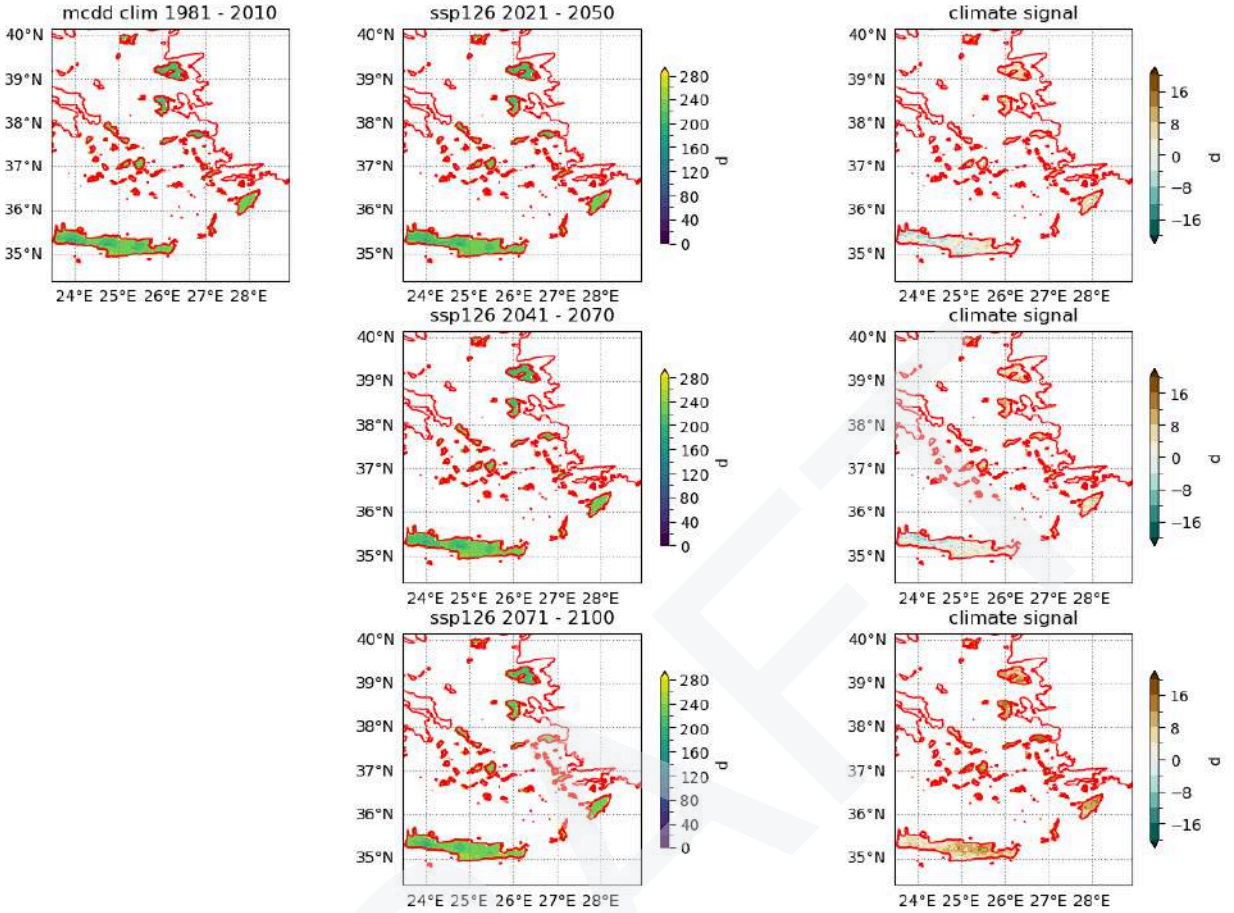
mcdd clim 1981 - 2010
ssp126 2021 - 2050
climate signal
ssp126 2041 - 2070
climate signal
ssp126 2071 - 2100
climate signal
40°N
39°N
38°N
37°N
36°N
35°N
24°E 25°E 26°E 27°E 28°E
d
280
240
200
160
120
80
40
0
16
8
0
−8
−16

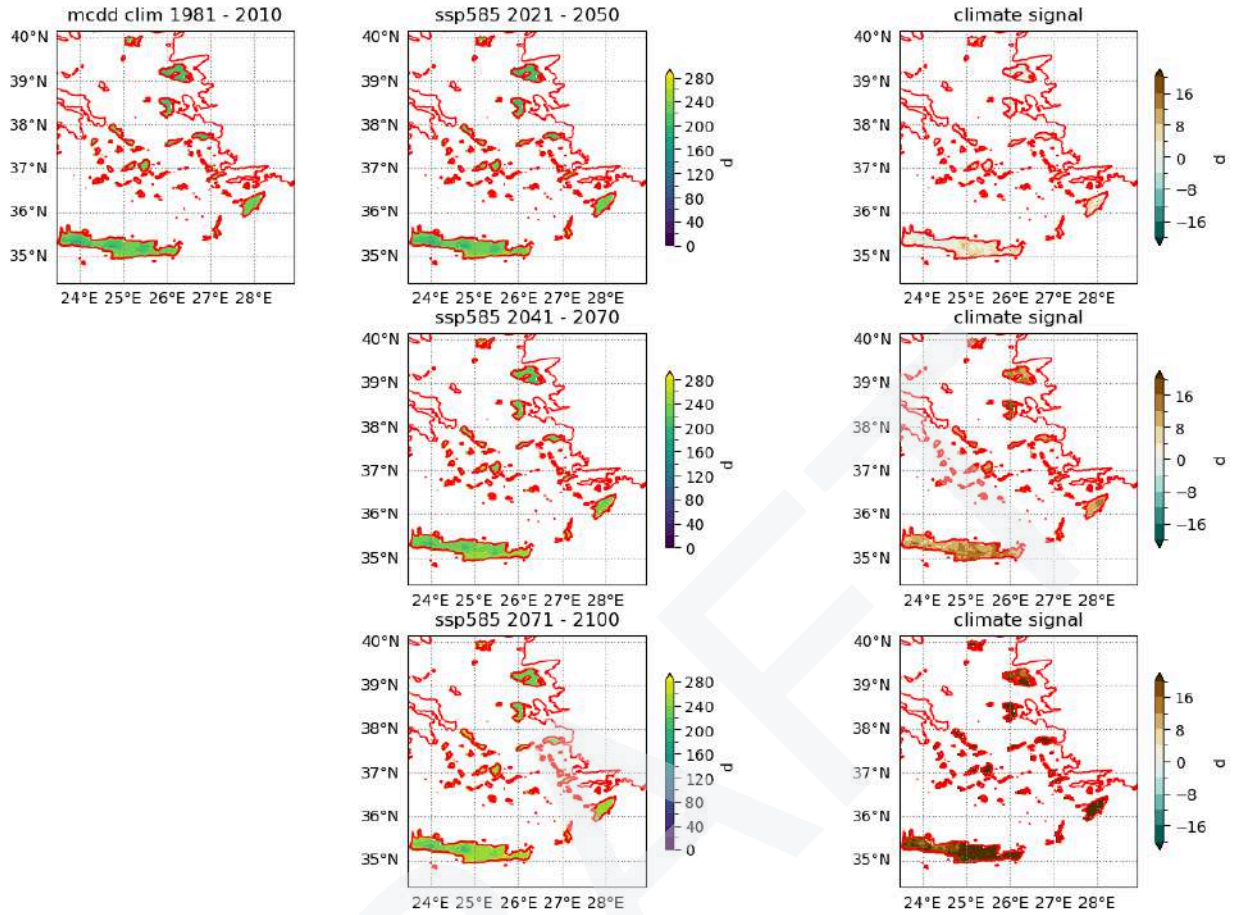

Figure 63: maximum number of consecutive dry days as simulated by WRF for SSP126 (top) and SSP585 (bottom): clim corresponds to past period, middle column displays absolute values of simulations, right column the difference between the mid century and the reference period (respectively).

In contrast to extreme drought, extreme precipitation amounts within a short time period, e.g. 1 day, also challenge critical infrastructure. For Syros there is a slight increase in intensities until 2050 simulated, whereas the signal for Rhodes is not significant within SSP126. For SSP585 Rhodes is to be expected to decrease intensities.

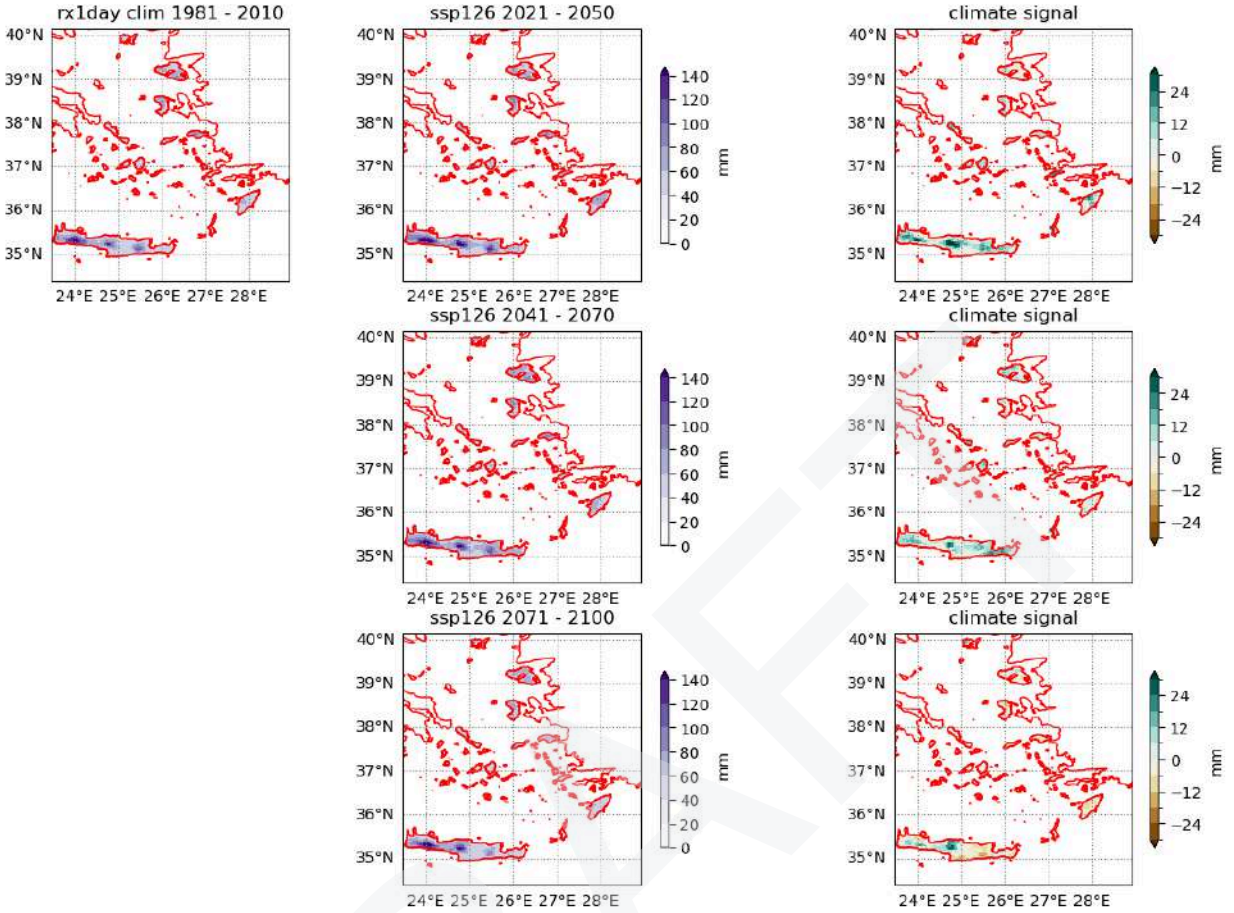
rx1day clim 1981 - 2010
ssp126 2021 - 2050
climate signal
ssp126 2041 - 2070
climate signal
ssp126 2071 - 2100
climate signal
40°N
39°N
38°N
37°N
36°N
35°N
24°E 25°E 26°E 27°E 28°E
140
120
100
80
60
40
20
0
24
12
0
−12
−24
mm

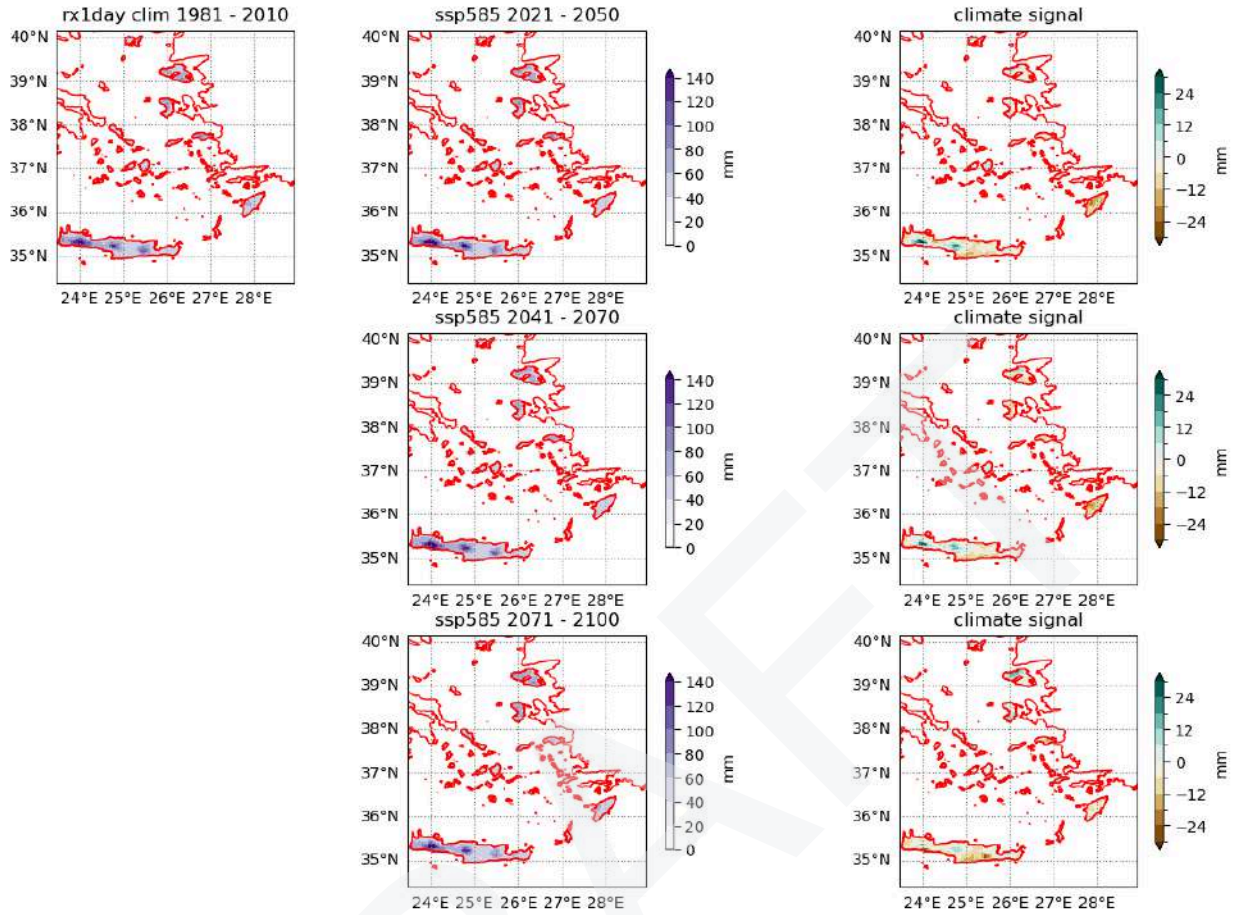

Figure 64: maximum rain rate within 1 day as simulated by WRF for SSP126 (top) and SSP585 (bottom): clim corresponds to past period, middle column displays absolute values of simulations, right column the difference between the mid century and the reference period (respectively).

Table 21. Summary table for expected changes in future climate variables and extreme indicators from AIT's dynamical downscaling for WRF model in SAR. Changes are for the mean and percentile 10/percentile 90 of

futures expected values for each considered SSP and time period with respect to the historical median reference value for the period 1981-2010.

WRF	period	1981 - 2010	21 - 50		41 - 70		71 - 100		units
	scenario	hist	ssp126	ssp585	ssp126	ssp585	ssp126	ssp585	
		Precipitation Indices							
rr	mean	588.6	3.5	-4.0	-1.1	-11.9	-3.0	-18.3	%
	10p	479.4	0.8	-7.0	-14.0	-10.7	-14.3	-39.4	
	90p	754.9	20.2	-1.4	-2.3	-14.6	5.8	-4.5	
mcdd	mean	224.0	1.6	2.4	2.9	11.8	8.4	22.3	d
	10p	208.0	8.2	7.5	6.1	21.2	10.9	20.7	
	90p	237.7	-0.9	-1.5	0.0	4.9	7.7	25.1	
rx1day	mean	50.8	11.8	-3.4	8.3	-3.8	-1.9	-2.9	%
	10p	44.2	2.4	2.6	-2.3	1.4	-5.2	-14.6	
	90p	58.1	12.5	-4.7	12.5	-4.9	7.2	5.2	
rx5day	mean	88.0	8.1	-4.5	1.1	-7.8	-4.6	-11.7	%
	10p	75.7	-1.9	-2.4	-1.9	-5.8	-6.3	-31.4	
	90p	99.2	9.6	-7.5	4.5	-8.6	5.4	-6.4	
		Temperature Indices							
T2	mean	17.1	0.9	0.9	1.1	1.9	1.1	3.3	°C
	10p	16.2	1.4	1.2	1.6	1.9	1.5	3.2	
	90p	17.9	0.8	0.7	0.9	2.4	1.1	3.7	
Tx	mean	32.0	1.0	1.1	1.2	2.0	1.3	3.7	°C
	10p	30.6	1.3	1.2	1.3	1.9	1.1	4.1	
	90p	33.2	1.7	1.9	1.7	2.3	2.0	4.2	
Tn	mean	0.8	1.5	1.1	1.5	2.1	2.0	4.0	°C
	10p	-1.7	0.7	1.5	1.0	2.5	2.3	4.1	
	90p	3.3	1.3	0.8	2.3	1.9	0.7	4.2	
hd30	mean	20.8	10.0	8.4	11.8	22.0	9.9	37.6	d
	10p	15.2	9.7	10.9	12.8	23.0	10.0	37.6	
	90p	25.0	14.6	8.1	15.3	30.8	14.1	41.8	
su25	mean	74.6	14.2	11.1	14.8	28.6	13.8	45.4	d
	10p	57.1	17.0	6.9	17.0	32.7	16.7	44.6	
	90p	88.4	17.7	14.9	17.7	31.9	18.9	42.7	
id	mean	2.4	-0.7	-0.6	-0.7	-0.9	-0.8	-1.3	d
	10p	1.1	-0.2	-0.2	-0.3	-0.3	-0.2	-0.5	
	90p	4.6	-1.6	-1.7	-1.4	-2.1	-2.3	-2.7	
tn20	mean	107.7	17.0	14.9	19.4	33.9	16.9	55.2	d
	10p	96.0	22.8	20.0	23.0	36.2	22.9	51.6	
	90p	118.6	18.9	11.2	18.9	41.8	17.9	55.7	
fd	mean	11.6	-2.9	-2.6	-3.2	-3.8	-3.5	-5.8	d
	10p	7.8	-1.4	-1.4	-1.9	-2.2	-1.2	-3.0	
	90p	16.3	-5.4	-5.3	-5.3	-7.0	-7.1	-9.1	
hwf	mean	1.2	1.0	0.7	1.1	2.0	1.0	3.2	n
	10p	0.8	0.7	0.9	0.9	1.9	1.2	3.6	
	90p	1.7	1.1	0.5	1.1	2.7	1.3	3.5	
		Wind Indices							
wspd	mean	6.3	0.1	0.1	0.1	0.1	0.1	0.1	m/s
	10p	6.1	0.1	0.2	0.1	0.1	0.1	0.2	
	90p	6.6	0.1	0.1	0.1	0.1	0.1	0.1	
wspdx	mean	19.8	0.4	0.5	0.3	0.3	-0.3	-0.4	m/s
	10p	18.8	0.7	0.8	0.7	0.7	0.1	0.2	
	90p	20.6	0.3	0.4	0.0	0.3	-0.4	-0.8	

5.2.2. The Salzburg Region

Since Salzburg is a highly heterogeneous region with lower parts and high mountains, the results are on the one hand displayed as spatial plots, as well as analysed for three different height levels (Figure 65) to account for and better represent the changes within the different heightlevels.

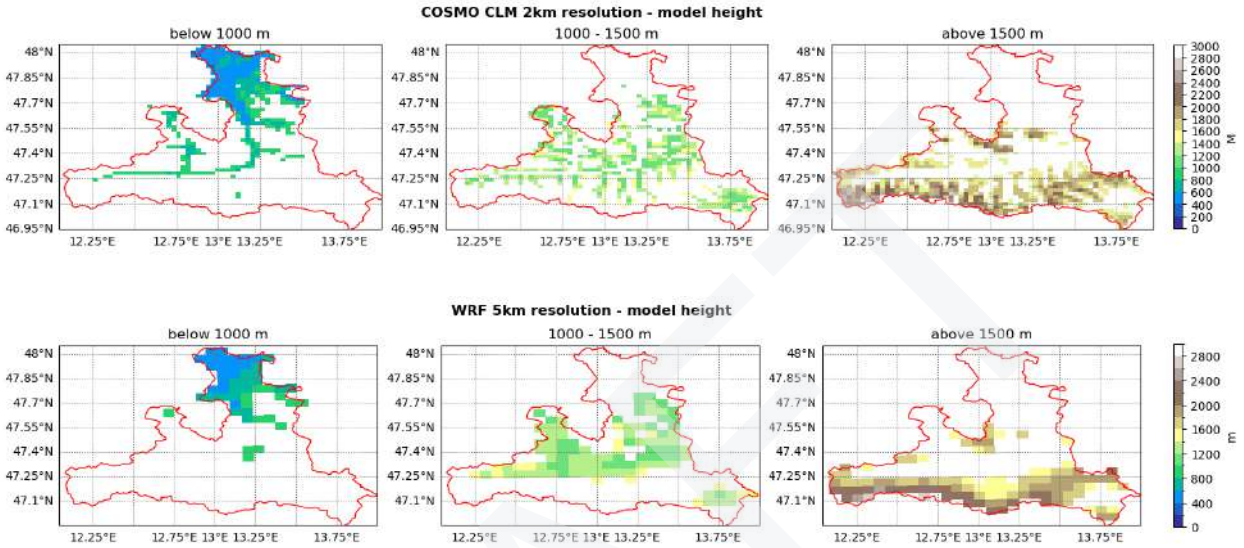

Figure 65: height areas within CCLM, WRF below 1000m, 1000 < x < 1500, >1500m; the different spatial resolutions (CCCLM 2 x 2km vs WRF 5 x 5km) is also clearly visible, as within CCLM the valley structure is well represented with CCLM (below 1000m), whereas not seen within WRF

Thermal indicators

The change in yearly mean temperature for the Salzburg region as computed by **CCLM** for the mid to late century displays no significant change for SSP126, but around 3°C for the mid and up to 5°C for the late century in the SSP585 scenario.

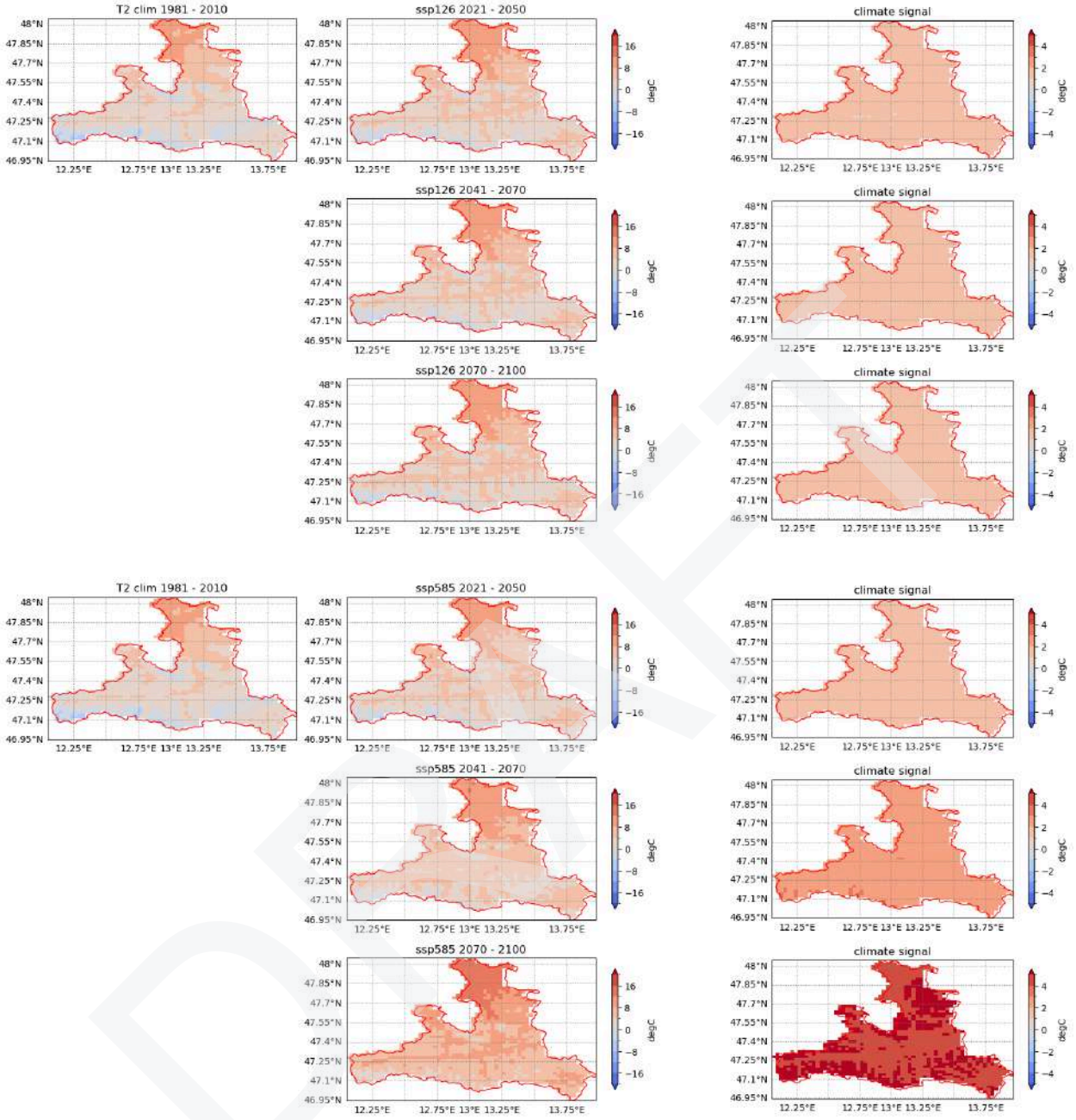

Figure 66: yearly mean temperatures as simulated by CCLM for SSP126 (top) and SSP585 (bottom): clim corresponds to past period, middle column displays absolute values of simulations, right column the difference between the mid- or late century and the reference period (respectively).

WRF displays similar results for SSP126, but a different structure in temperature increase in SSP585, as for the mid century the south of Salzburg region is experiencing an increase of about 3°C, whereas most northern areas are within the range of 1-2°.

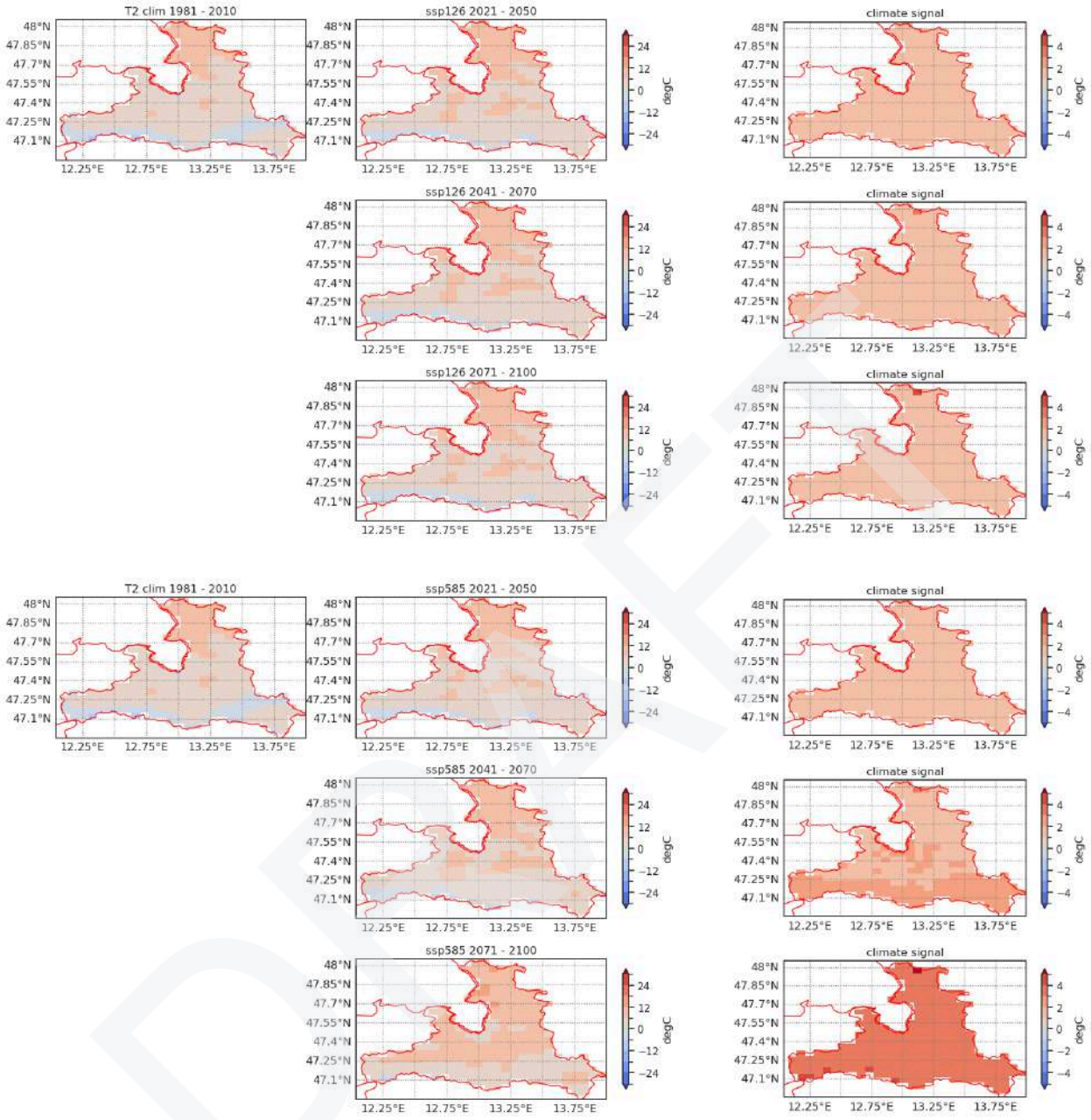

Figure 67: yearly mean temperatures as simulated by WRF for SSP126 (top) and SSP585 (bottom): clim corresponds to past period, middle column displays absolute values of simulations, right column the difference between the mid- or late century and the reference period (respectively).

Regarding the change in maximum temperatures the signal is a similar to the yearly mean temperature, with no significant change in SSP125, but a clear signal by the mid century in SSP585 of similar magnitude in CCLM and WRF, with WRF displaying a more structured change (up to 3°), whereas CCLM simulates this structure towards the end of the century (up to 7°C increase, Figure 67).

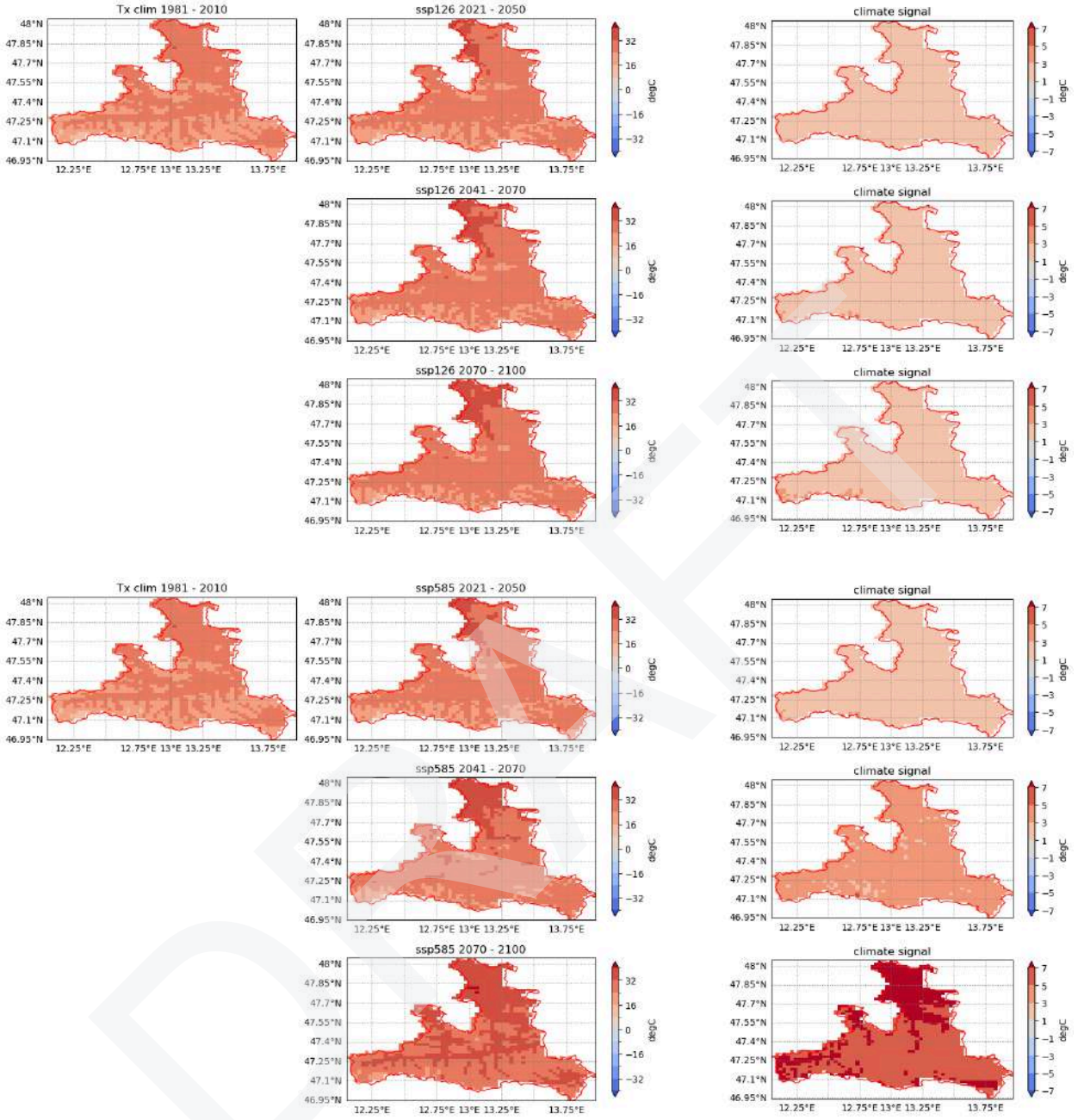

Figure 68: yearly maximum temperatures as simulated by CCLM for SSP126 (top) and SSP585 (bottom): clim corresponds to past period, middle column displays absolute values of simulations, right column the difference between the mid- or late century and the reference period (respectively).

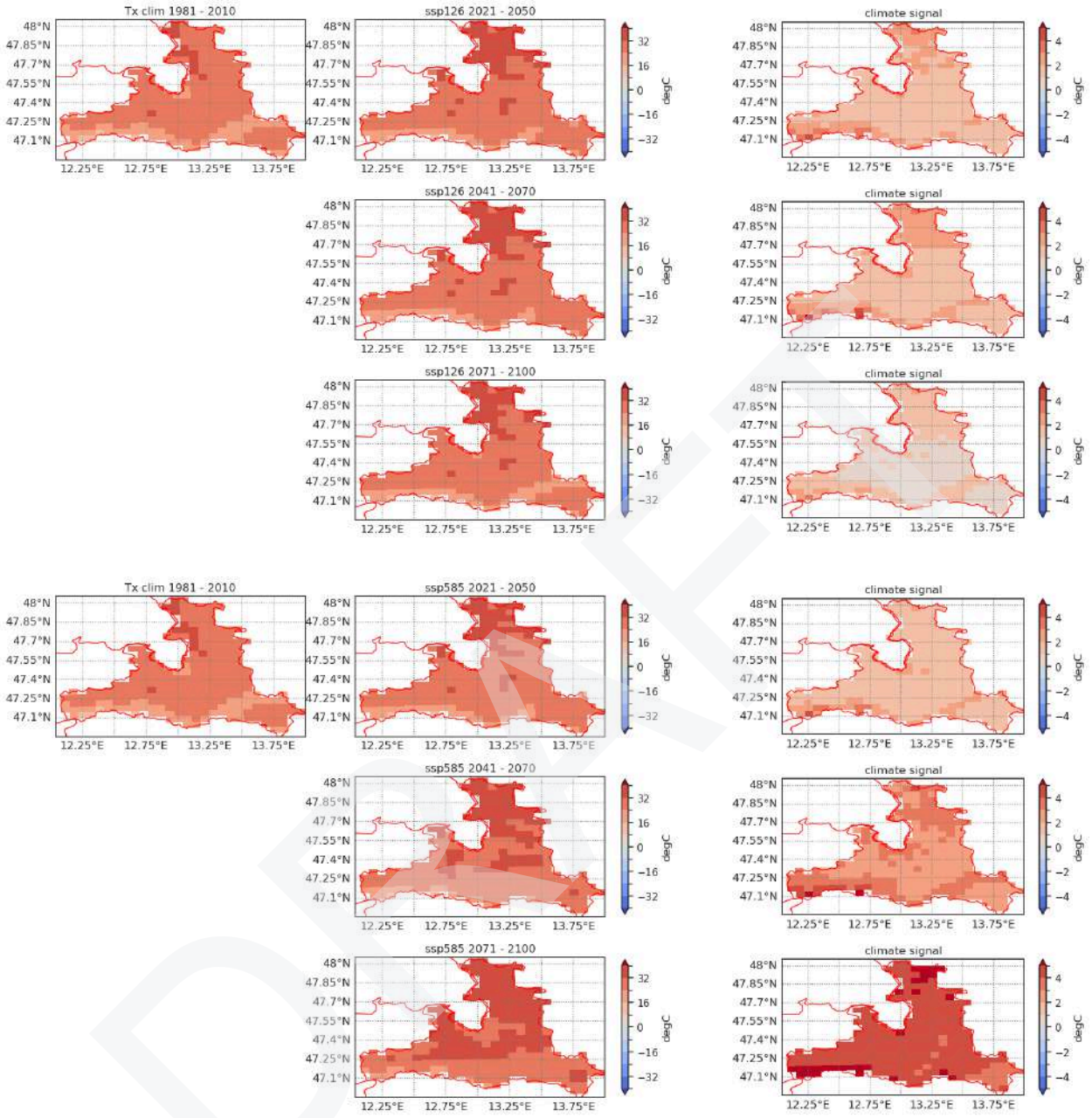

Figure 69: yearly maximum temperatures as simulated by WRF for SSP126 (top) and SSP585 (bottom): clim corresponds to past period, middle column displays absolute values of simulations, right column the difference between the mid- or late century and the reference period (respectively).

For the mountainous region Salzburg the yearly mean minimum temperatures doesn't depict a significant change in SSP126, whereas within SSP585 both models display a clear increase in minimum temperature, even though the magnitude of change is comparable, the structure differs with

CCLM displaying a change in the lower regions first whereas WRF shows higher response in the topographic areas (Figure 70)

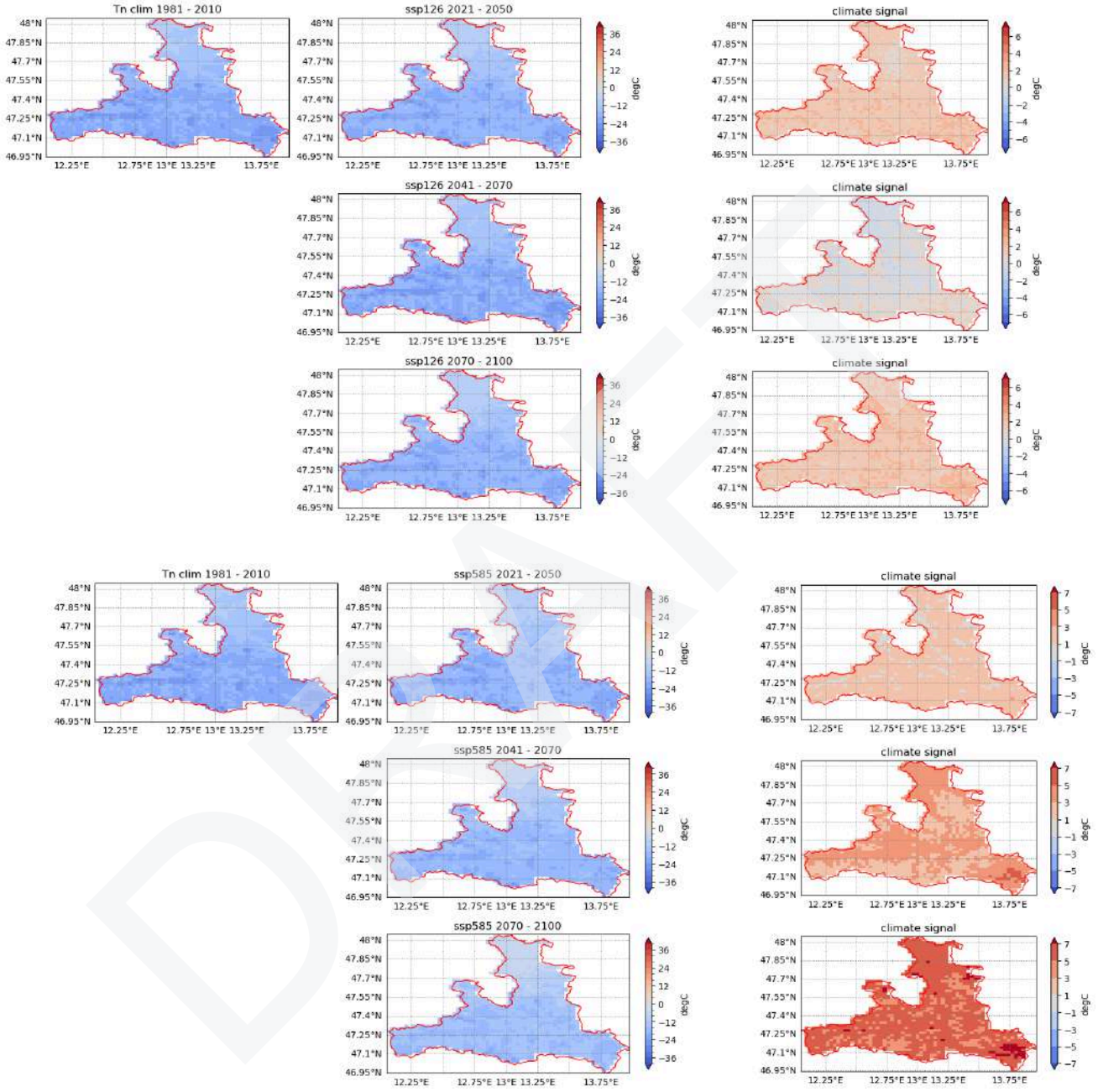

Figure 70: minimum temperature as simulated by CCLM for SSP126 (top) SSP585 (bottom): clim corresponds to past period, middle column displays absolute values of simulations, right column the difference between the mid- or late century and the reference period (respectively).

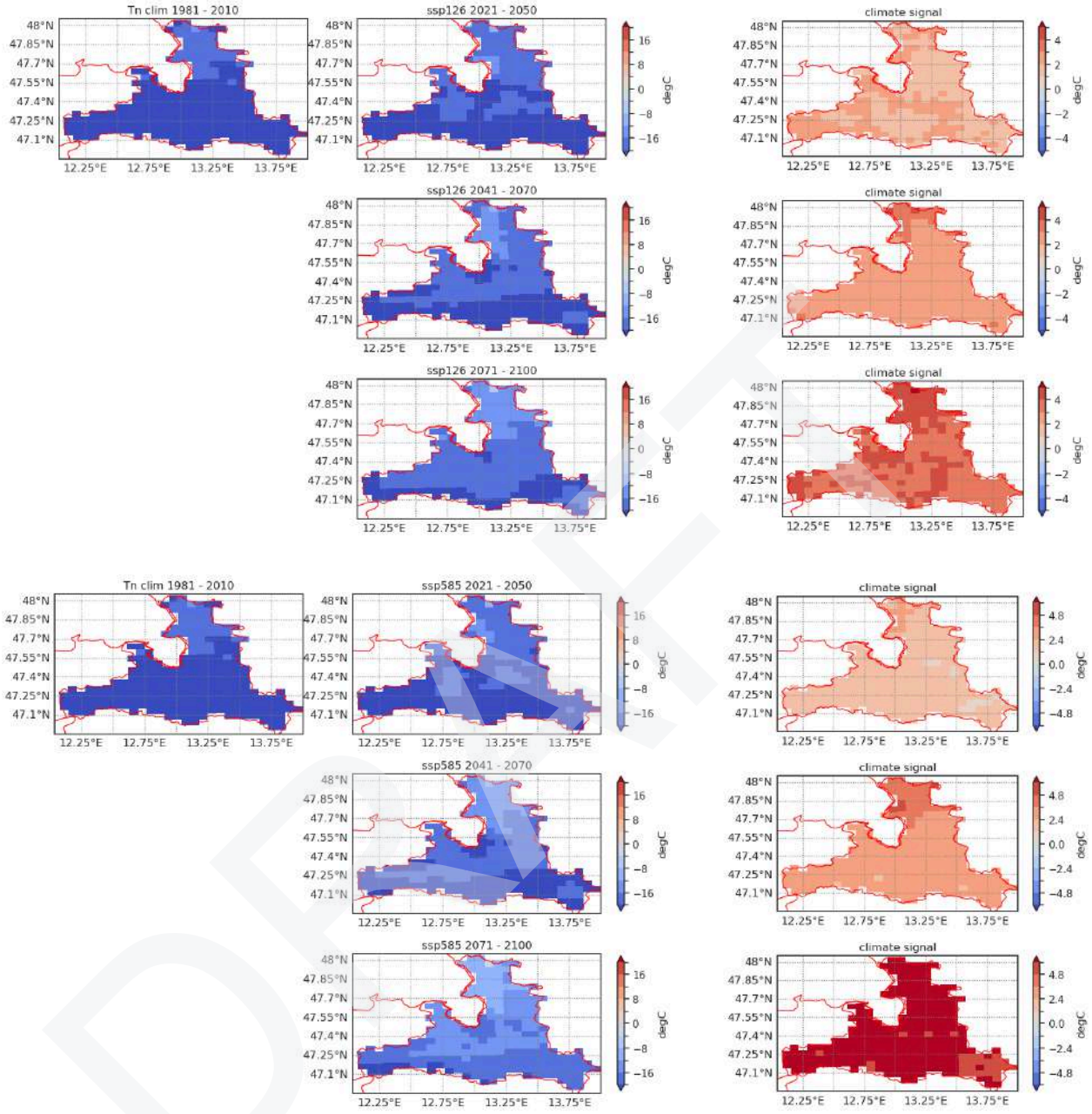

Figure 71: minimum temperature as simulated by WRF for SSP126 (top) SSP585 (bottom): clim corresponds to past period, middle column displays absolute values of simulations, right column the difference between the mid- or late century and the reference period (respectively).

For the mountainous regions not only change in maximum temperature, or related heat indices such as number of heatdays have important consequences, but also indicators representing cold conditions, such as frost or ice days, since these impact the prevailing permafrost, which in turn stabilises slopes. As an example the change in frost days (minimum temperature <0°C) is shown. All models and simulations display a decreasing number. However, as can also be seen from the boxplots (Figure 71) SSP126 relates to a stronger decrease by 2050 than SSP585 within WRF. In CCLM the

change is comparable and of much lesser spread within the 30 years considered. These discrepancies could be due to the different GCMs used for the initialization and of course the different model physics. The fact that SSP126 results in "warmer" conditions, thus less frost days, than SSP585 by 2050 can be explained with the different aerosol distributions considered within the SSPs (Rao et al., 2017), but needs further investigation.

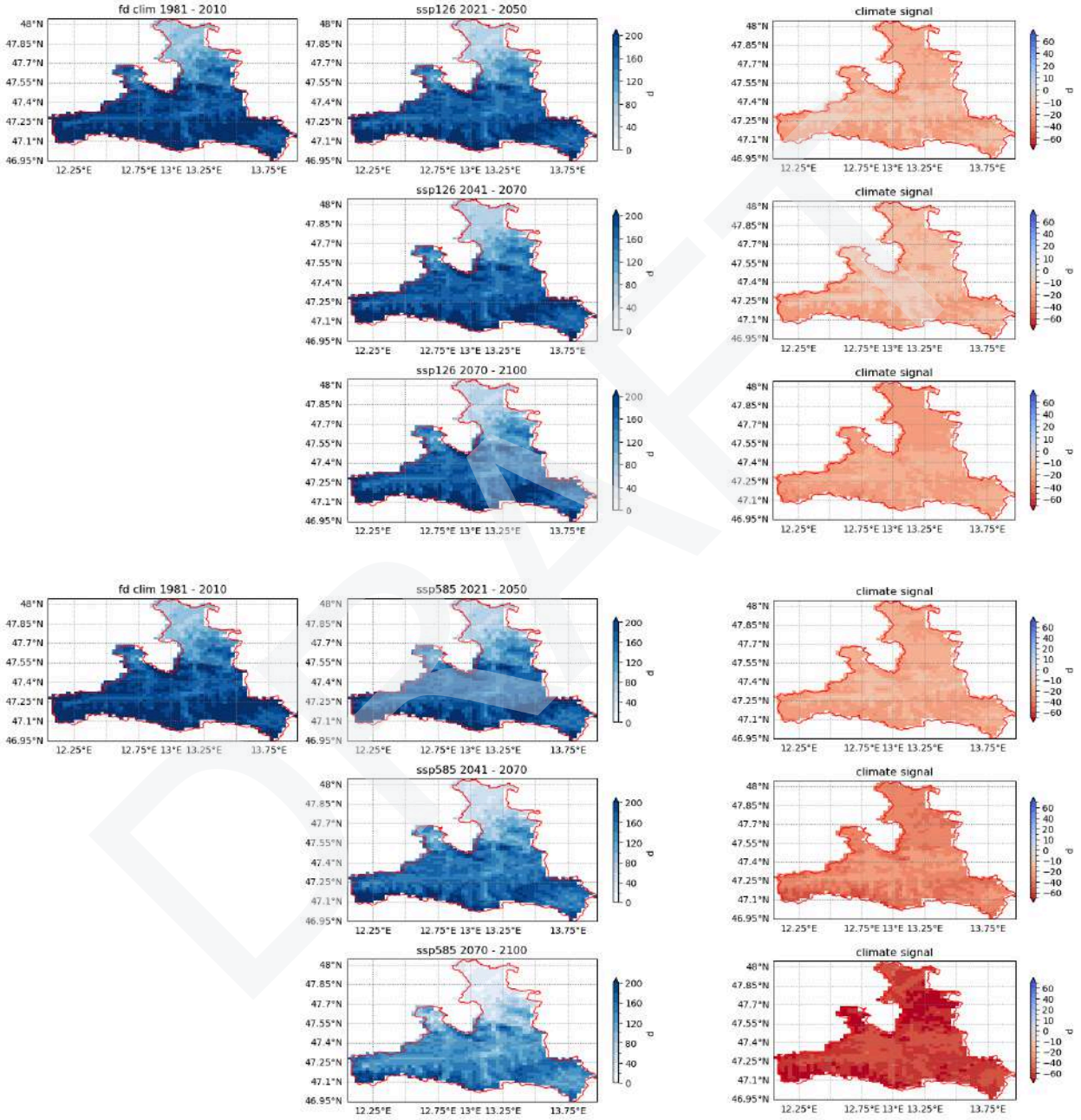

Figure 72: number of frost days (tmin < 0°C) as simulated by CCLM for SSP126 (top) SSP585 (bottom): clim corresponds to past period, middle column displays absolute values of simulations, right column the difference between the mid- or late century and the reference period (respectively).

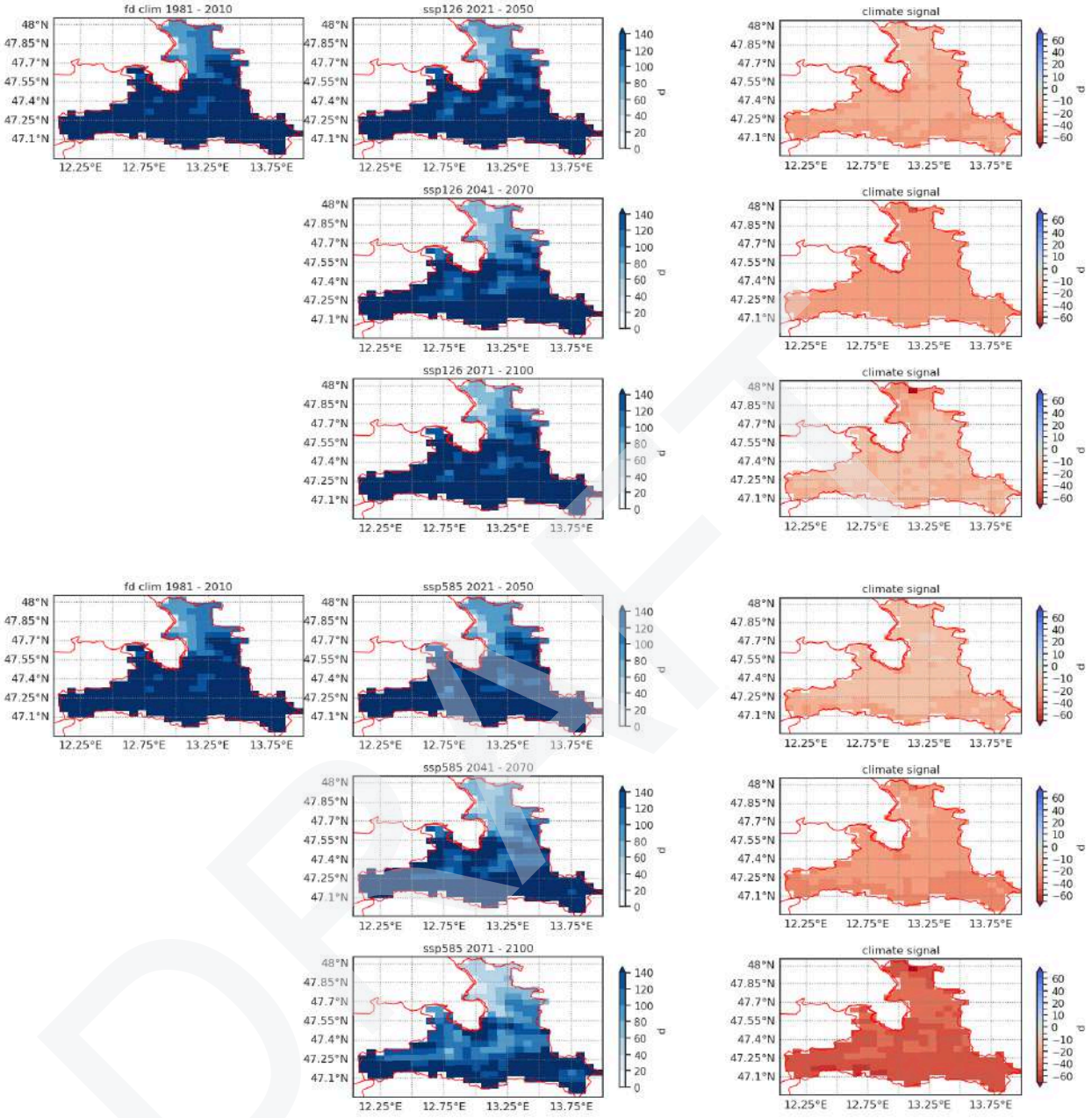

Figure 73: number of frost days (tmin < 0°C) as simulated by WRF for SSP126 (top) SSP585 (bottom): clim corresponds to past period, middle column displays absolute values of simulations, right column the difference between the mid- or late century and the reference period (respectively).

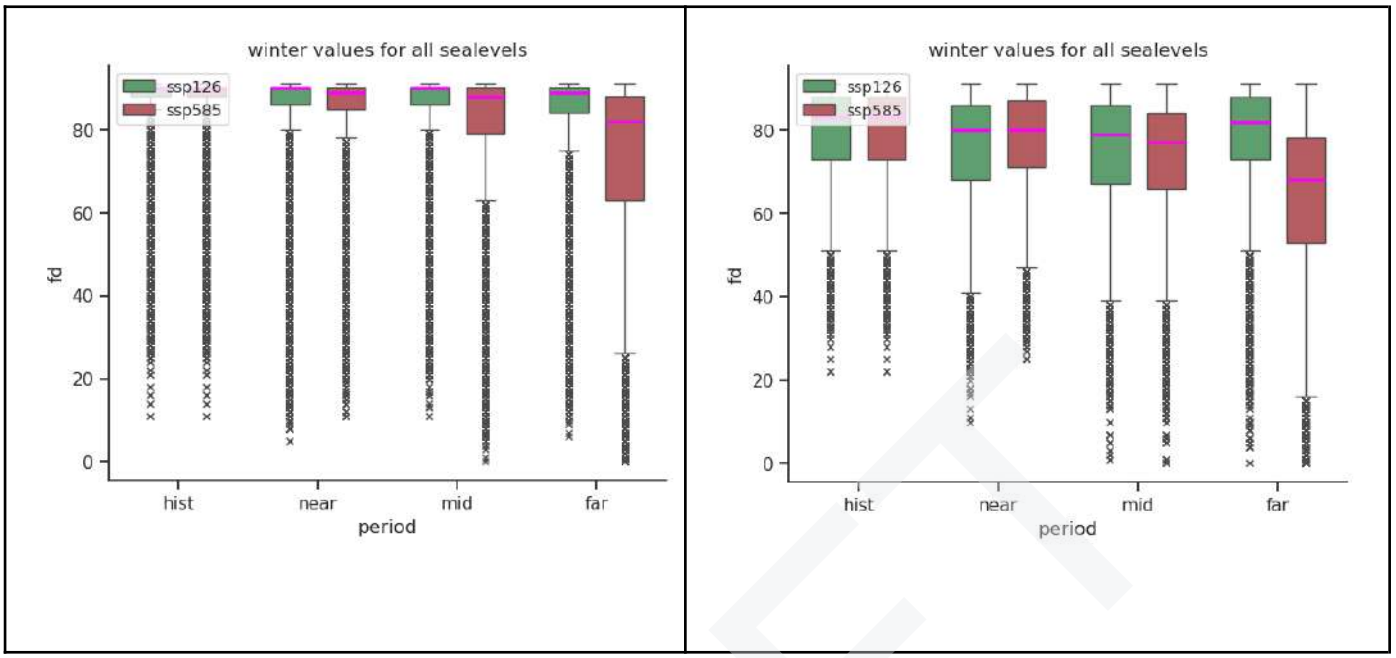

Figure 74: boxplots of number of frost days (tmin < 0°C) for CCLM (left) and WRF (rigth) for the winter (DJF) season

Precipitation indicators

Regarding the annual mean rain rate the signal from the dynamical simulations display different signals, with CCLM showing an increase of more than 12% until 2050, a smaller increase until 2070 and a decrease until the end of the century, especially in SSP585. WRF on the contrary displays areas of slight increase and decrease, in both scenarios. The different signals and amplitudes of change highlight the uncertainties related to model simulations and the involved complexity related to precipitation.

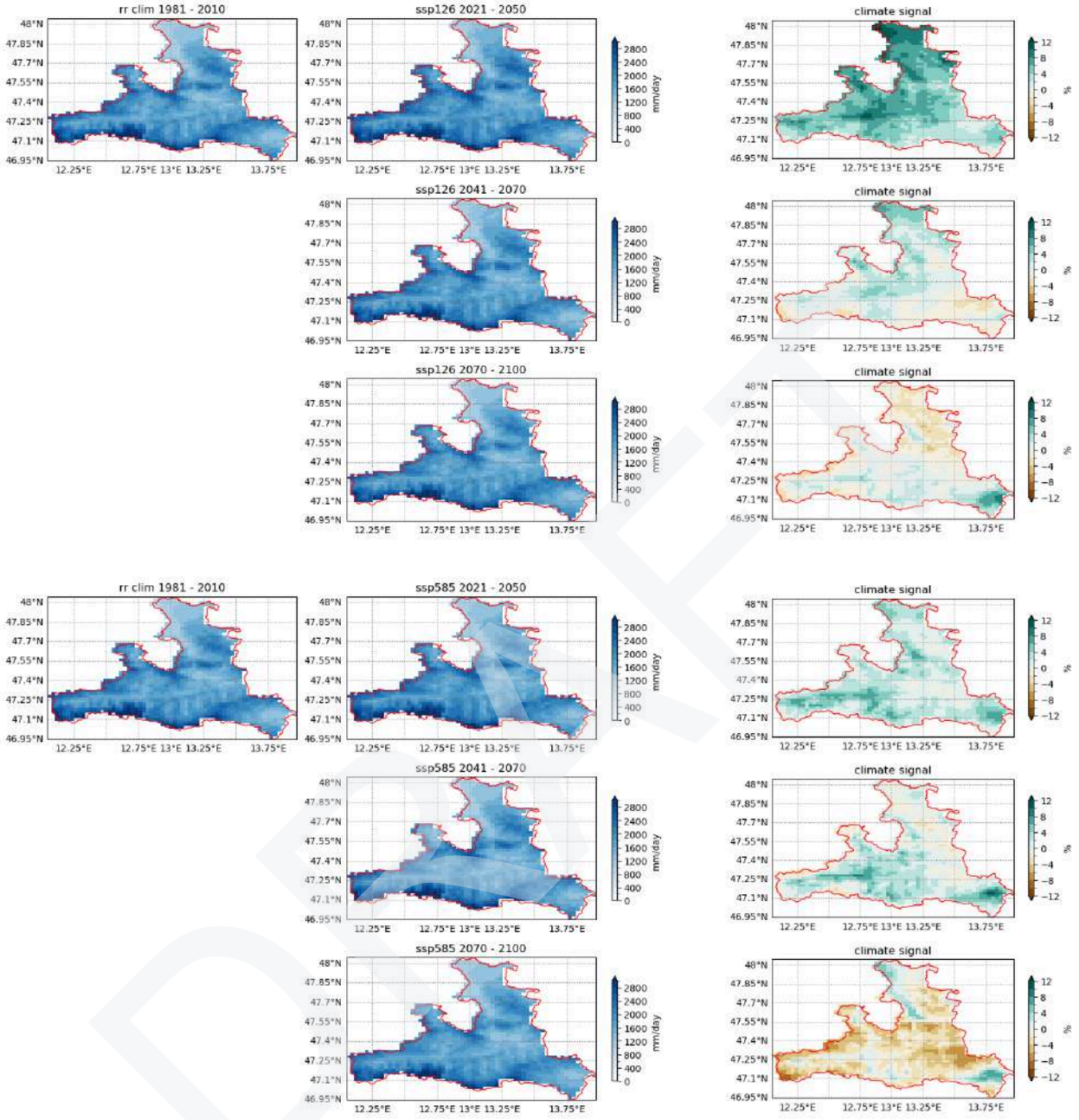

Figure 75: mean annual rain rate as simulated by CCLM for SSP126 (top) SSP585 (bottom): clim corresponds to past period, middle column displays absolute values of simulations, right column the difference between the mid- or late century and the reference period (respectively).

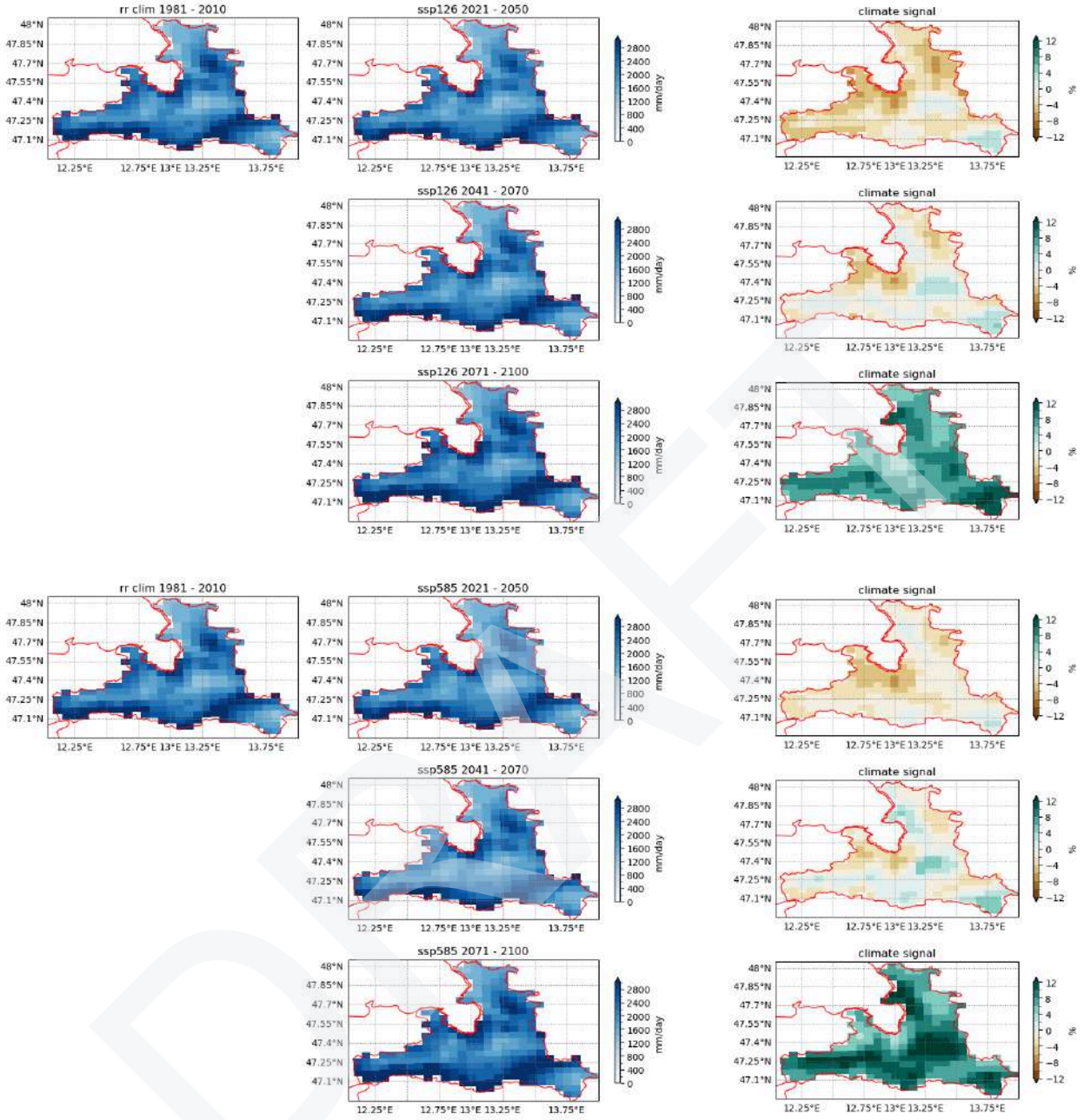

Figure 76: mean annual rain rate as simulated by WRF for SSP126 (top) SSP585 (bottom): clim corresponds to past period, middle column displays absolute values of simulations, right column the difference between the mid- or late century and the reference period (respectively).

Regarding extreme precipitation events that have caused extensive damage in the past, the change in maximum intensities (rx1day) over 1 day has been analysed (Figure 76). Both models and scenarios display an increase of up to 30% in the eastern part of the region. The signal is not as clear for the other regions.

Apart from the mean climatological change, the boxplots of rx1day (Figure 79) clearly display the intensities of extreme events reach unprecedented values of precipitation falling within 1 day during the summer season.

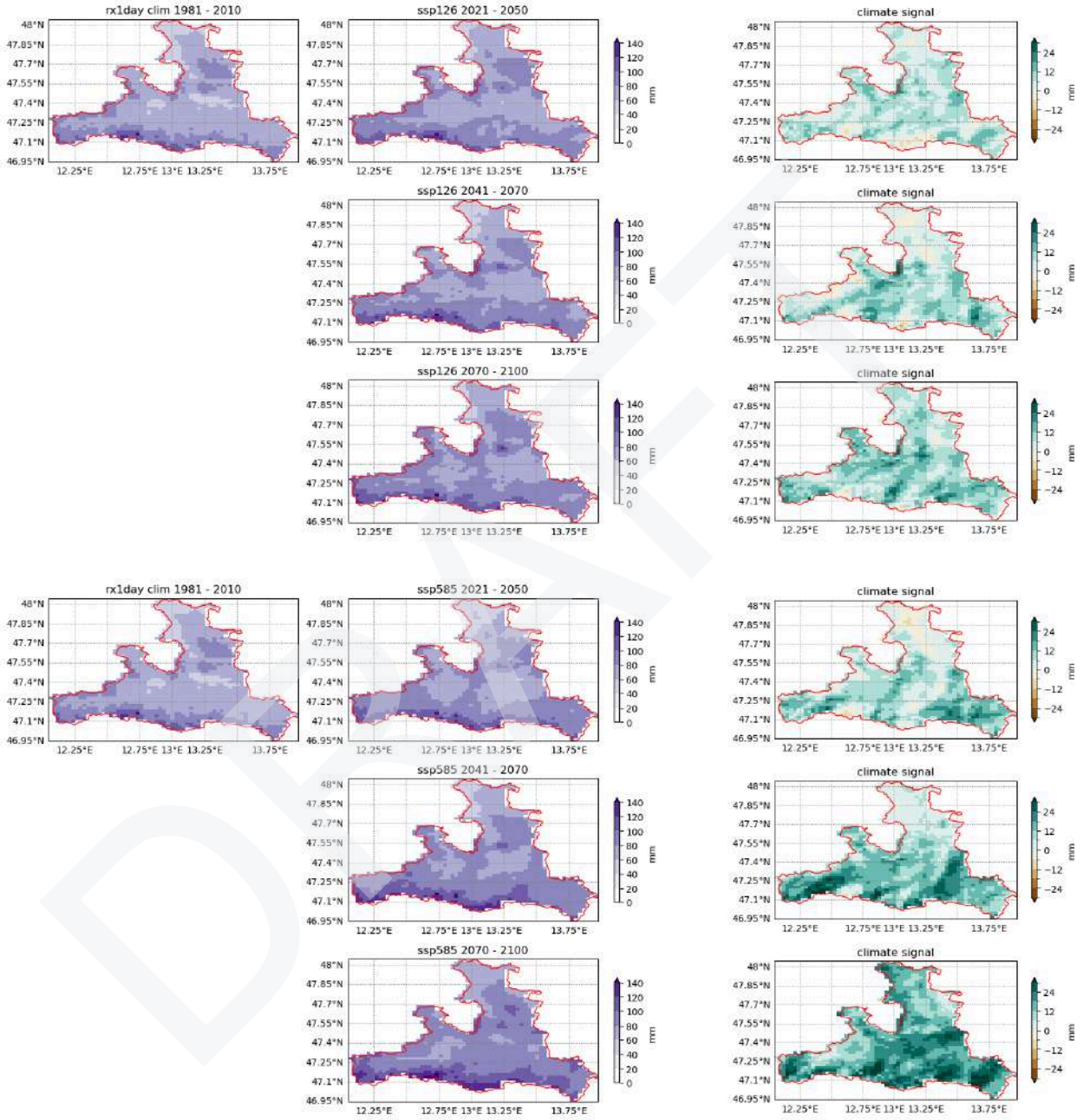

Figure 77 maximum amount of precipitation over 1 day as simulated by CCLM for SSP126 (top) SSP585 (bottom): clim corresponds to past period, middle column displays absolute values of simulations, right column the difference between the mid- or late century and the reference period (respectively).

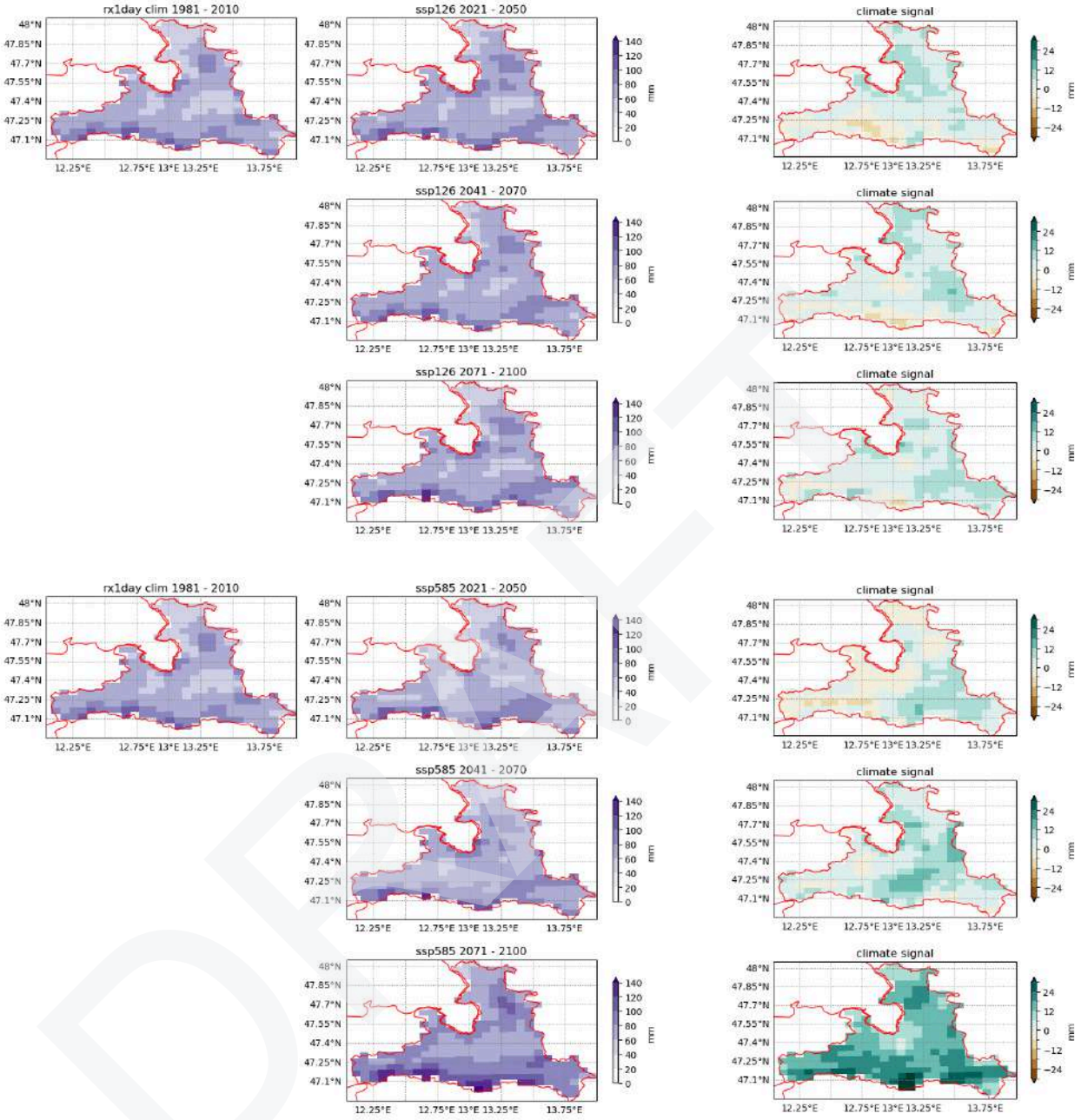

Figure 78: maximum amount of precipitation over 1 day as simulated by WRF for SSP126 (top) SSP585 (bottom): clim corresponds to past period, middle column displays absolute values of simulations, right column the difference between the mid- or late century and the reference period (respectively).

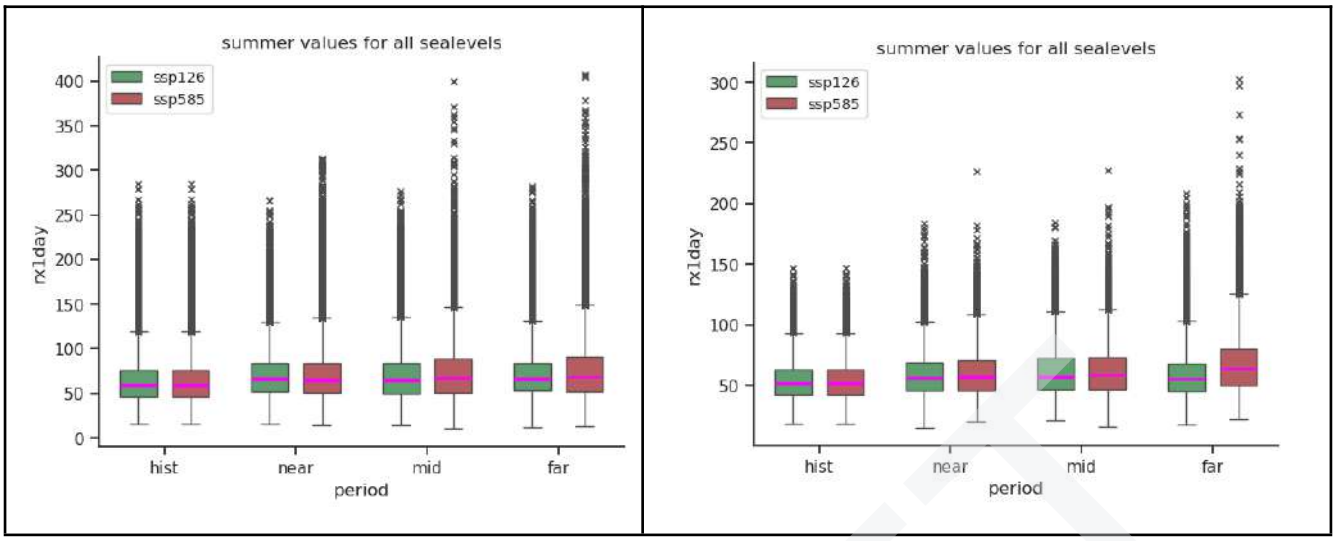

Figure 79: boxplots of max precipitation intensities over 1 day for CCLM (left) and WRF (rigth) for the summer (JJA) season

Wind indicators

As storm events also pose a threat to the infrastructure within Salzburg, change in maximum wind speed has been looked at. For most areas the change is not significant for SSP126, as well as SSP585, yet, for the northern part of the region there is a clear indication that maximum wind speed is increasing within the mountainous regions.

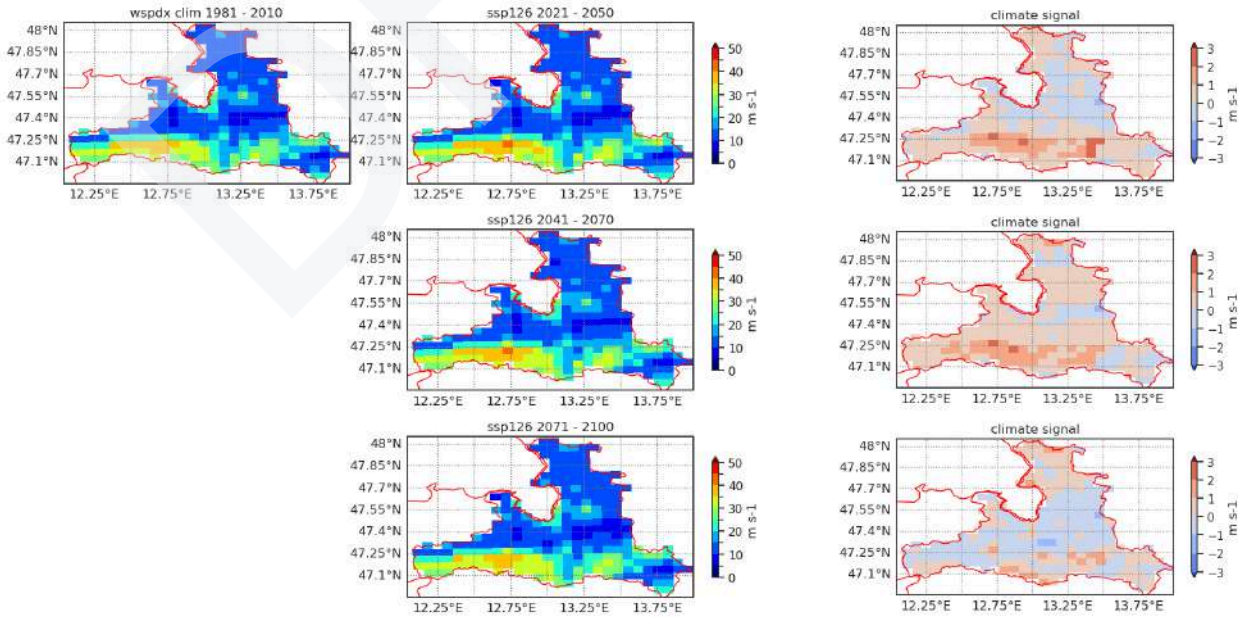

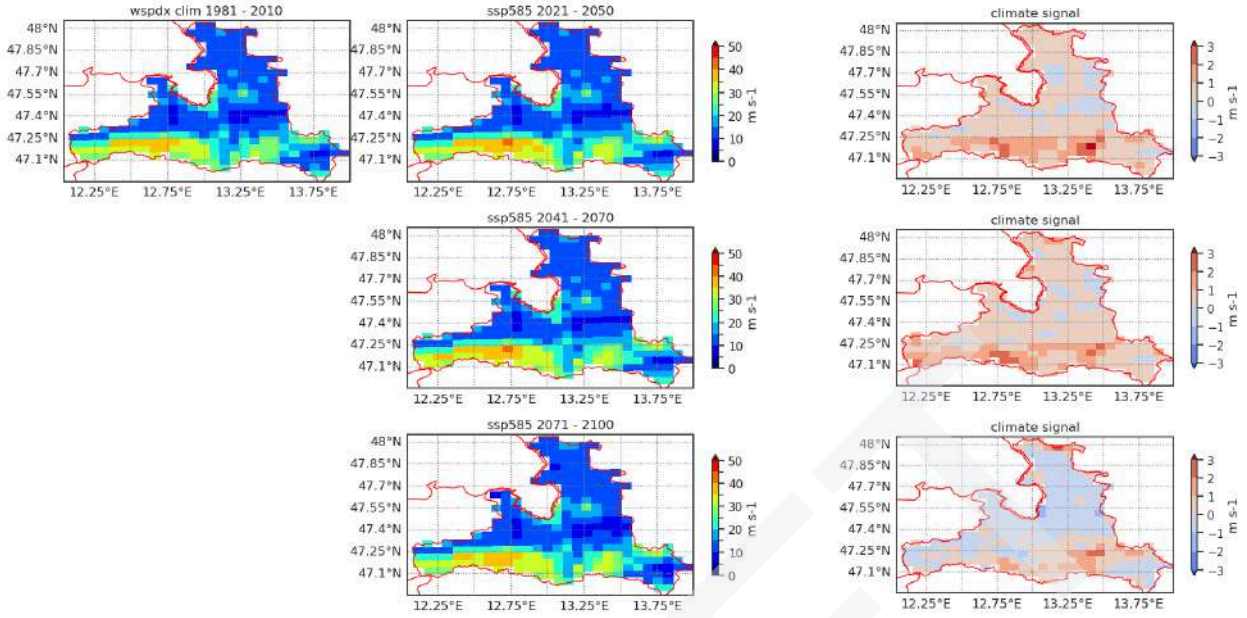

Figure 80: maximum wind speed as simulated by WRF for SSP126 (top) SSP585 (bottom): clim corresponds to past period, middle column displays absolute values of simulations, right column the difference between the mid- or late century and the reference period (respectively).

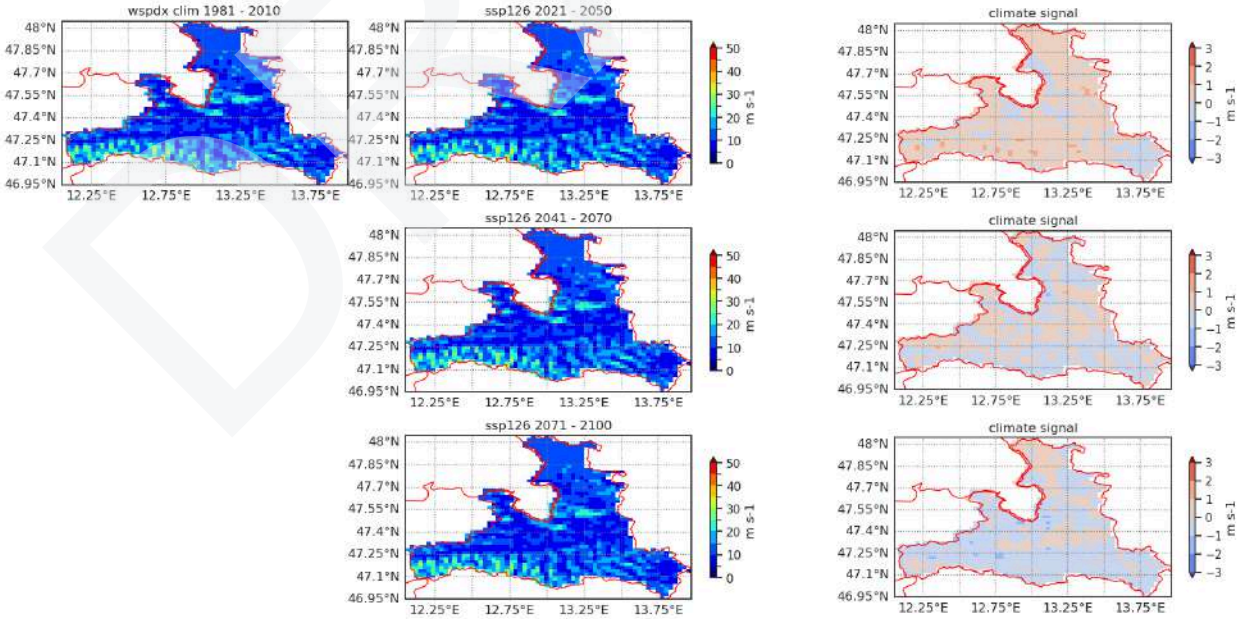

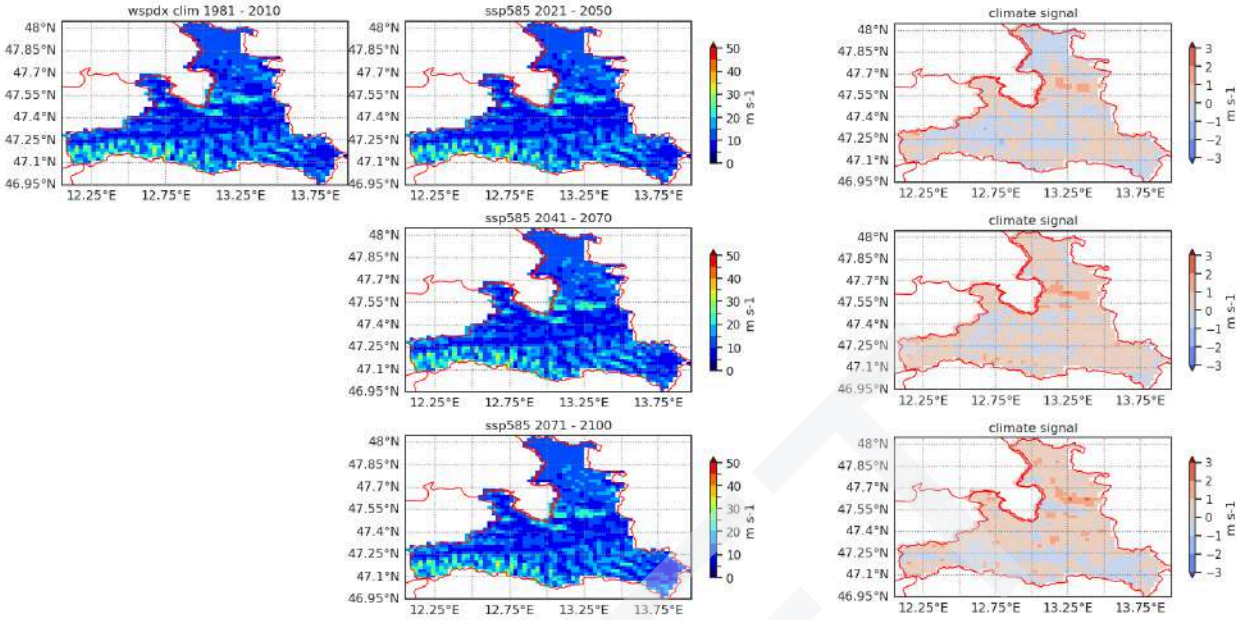

Figure 81: maximum wind speed as simulated by CCLM for SSP126 (top) SSP585 (bottom): clim corresponds to past period, middle column displays absolute values of simulations, right column the difference between the mid- or late century and the reference period (respectively).

Table 22. Summary table for expected changes in future climate variables and extreme indicators from AIT's dynamical downscaling of WRF model in SLZ. Changes are for the mean and percentile 10/percentile 90 of futures expected values for each considered SSP and time period with respect to the historical median reference value for the period 1981-2010.

WRF	period	1981 - 2010	21 - 50		41 - 70		41 - 70		units
	scenario	hist	ssp126	ssp585	ssp126	ssp585	ssp126	ssp585	
		Precipitation Indices							
rr	mean	2241.2	-2.9	-1.9	-1.2	-0.6	7.5	8.5	%
	10p	1957.2	-3.1	-1.8	-3.5	-1.1	10.0	8.9	
	90p	2466.6	1.4	2.3	3.2	5.1	15.1	10.2	
mcdd	mean	69.4	4.2	3.9	4.2	3.8	-0.5	3.0	d
	10p	56.4	5.8	5.0	6.6	1.5	-0.5	1.1	
	90p	86.4	4.4	5.7	-4.4	4.9	-2.4	-0.9	
rx1day	mean	69.8	4.5	2.9	4.2	8.3	5.7	23.7	%
	10p	57.0	9.4	-1.3	1.8	5.2	7.8	16.7	
	90p	80.3	11.8	8.2	2.8	18.3	15.9	23.2	
rx5day	mean	152.4	-1.3	0.7	0.1	1.8	4.3	15.9	%
	10p	128.1	-6.3	-4.6	-1.1	2.3	-4.6	3.8	
	90p	176.0	7.1	5.8	7.4	-0.3	7.6	39.9	
		Temperature Indices							
T2	mean	2.9	1.4	1.2	1.7	2.0	1.3	3.8	°C
	10p	1.8	1.6	1.6	1.9	1.6	1.1	3.4	
	90p	3.8	1.3	0.8	1.7	2.3	1.4	4.2	
Tx	mean	26.9	1.8	1.7	1.9	3.0	1.1	4.6	°C
	10p	25.2	1.3	0.4	1.4	2.5	0.1	3.9	
	90p	28.8	1.6	1.7	2.7	3.9	1.4	5.1	
Tn	mean	-22.4	1.8	1.7	2.7	3.1	4.0	6.5	°C
	10p	-27.2	2.9	2.9	3.2	3.1	4.5	7.2	
	90p	-17.4	1.6	0.2	1.7	2.8	2.5	6.1	
hd30	mean	0.7	1.6	1.3	1.5	2.8	1.0	5.1	d
	10p	0.1	0.2	0.1	0.4	0.5	0.1	1.9	
	90p	1.5	3.8	3.6	3.7	5.1	2.4	8.8	
su25	mean	8.9	6.1	5.8	6.4	10.5	4.9	18.7	d
	10p	4.5	2.1	0.9	2.8	2.2	2.2	12.0	
	90p	14.9	10.1	9.3	10.1	13.8	6.9	24.0	
id	mean	98.1	-15.5	-12.9	-19.7	-20.3	-15.3	-38.9	d
	10p	80.0	-13.6	-5.5	-21.5	-18.3	-11.7	-38.4	
	90p	118.2	-22.5	-22.1	-21.7	-21.2	-18.6	-42.5	
tn20	mean	0.6	0.8	1.0	1.1	2.2	0.8	4.6	d
	10p	0.1	0.2	0.0	0.5	0.4	0.2	2.6	
	90p	1.3	1.9	3.0	2.6	3.3	1.5	7.2	
fd	mean	177.3	-18.8	-13.8	-22.8	-27.5	-15.7	-51.0	d
	10p	158.3	-21.4	-10.4	-21.4	-26.5	-11.3	-57.4	
	90p	196.4	-19.3	-17.8	-26.4	-27.3	-15.5	-48.1	
hwf	mean	0.0	0.0	0.0	0.0	0.1	0.0	0.2	n
	10p	0.0	0.0	0.0	0.0	0.0	0.0	0.0	
	90p	0.0	0.1	0.1	0.1	0.2	0.1	0.6	
		Wind Indices							
wspd	mean	4.3	-0.1	0.0	0.0	-0.1	0.1	-0.1	m/s
	10p	4.1	0.0	0.0	-0.1	0.0	0.1	0.0	
	90p	4.5	0.0	0.1	0.0	0.0	0.1	-0.1	
wspdx	mean	18.0	0.3	0.5	0.4	0.6	-0.2	0.0	m/s
	10p	17.1	0.3	-0.4	0.1	-0.2	-0.1	-0.1	
	90p	19.2	0.2	0.8	0.5	0.7	-0.4	0.6	

Table 23. Summary table for expected changes in future climate variables and extreme indicators from AIT's dynamical downscaling of CLM model in SLZ. Changes are for the mean and percentile 10/percentile 90 of futures expected values for each considered SSP and time period with respect to the historical median reference value for the period 1981-2010.

CLM	period	1981 - 2010	21 - 50		41 - 70		71 - 100		units
	scenario	hist	ssp126	ssp585	ssp126	ssp585	ssp126	ssp585	
		Precipitation indices							
rr	mean	1886.6	5.3	2.5	1.1	1.6	-0.1	-2.6	%
	10p	1430.3	17.8	7.0	8.2	4.5	5.4	5.1	
	90p	2253.2	7.9	10.4	0.5	10.4	3.7	-2.5	
	mean	87.7	5.5	5.4	3.0	12.0	5.7	19.6	

5.3. Comparison of future climate states: statistical & downscaling

Within ICARIA two methodologies are applied: statistical and dynamical downscaling. By using the same CMIP6 models (EC-EARTH-Veg3, MPI-ESM) within both methodologies and applying these to two very different regions, general outcomes and differences can be discussed. Within the prevailing deliverable first insights with respect to Salzburg are provided, an in-depth study, also taking into account the South Aegean region will be presented within a scientific publication.

As the main hazards identified relate to temperature and precipitation, within this first comparison we focus on these two parameters.

One indicator of interest to the different regions are heat days. Within the statistical downscaling, a general increase in the number of heat days is seen from the mid century on. Depending on the emission scenario the increase stabilizes (SSP126) or increases to up to 50 days until the end of the century. When comparing these results with the RCMs, it is quite striking as CCLM only displays up to 10 heat days until the end of the century within SSP585, WRF exhibits slightly more, but much less pronounced than the statistical downscaling. This discrepancy is due to the fact that the boxplots of the RCMs are a spatial mean of various heights, whereas the statistical downscaling results represent 44 stations with a mean height of about 800m. Therefore, the same plot was produced for RCM results below 1000m (Figure 82).

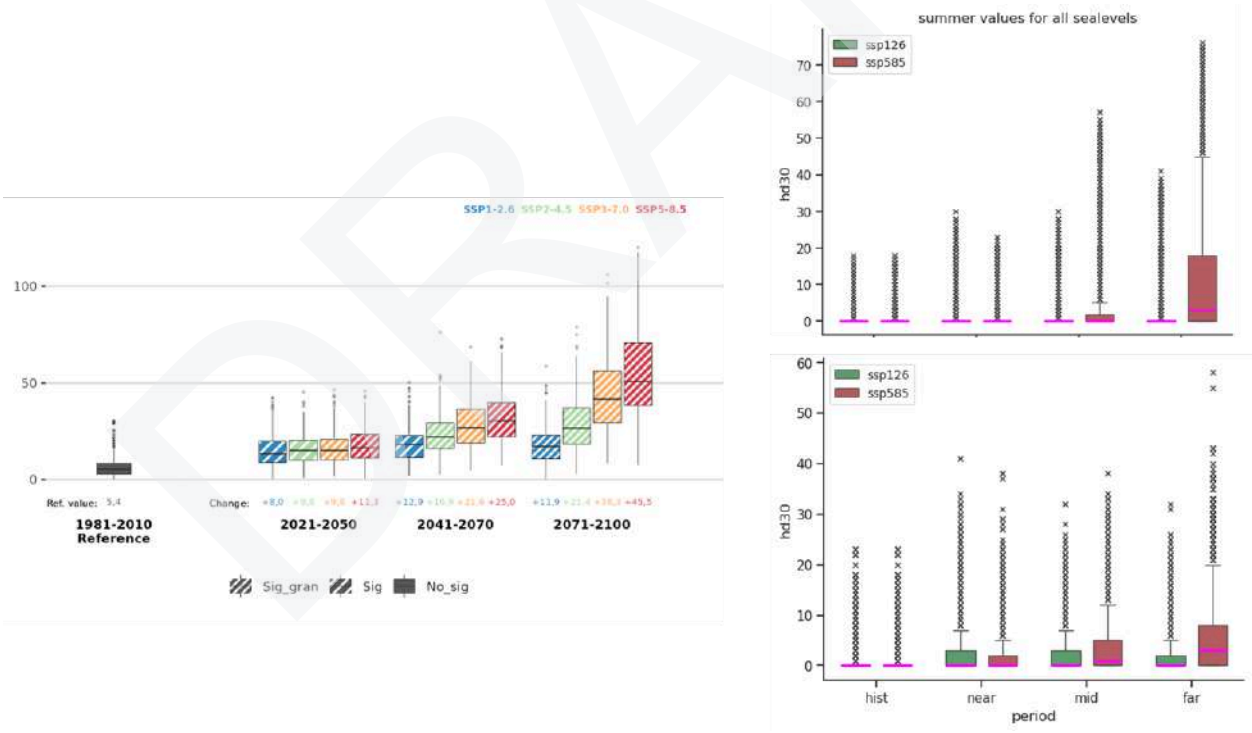

Figure 82: evolution of heat days until 2100 within the different emission scenarios; left: FICLIMA results, right: CCLM top, WRF bottom

When only looking at areas below 1000m, the number of heat days increases within both RCMs, yet, not reaching the same magnitude as within the statistical downscaling. Further, WRF displays more heat days for the historical period and the mid century, but represents less heat days at the end of the century.

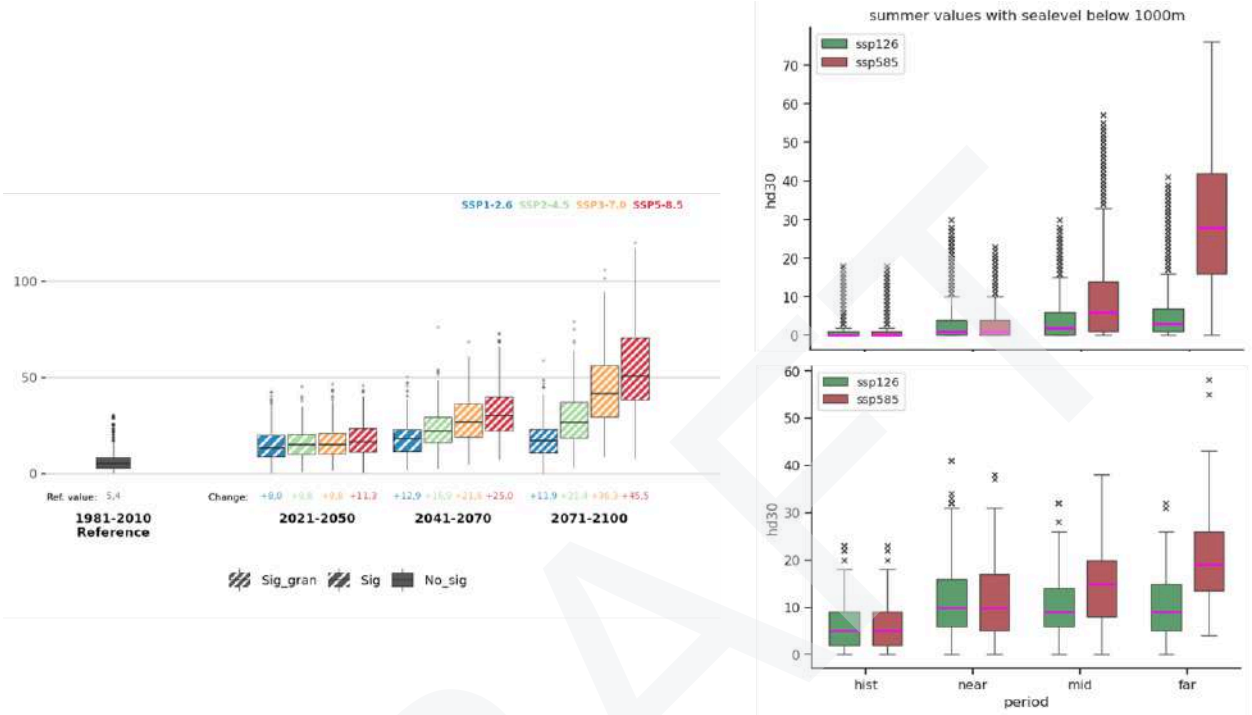

Figure 83: evolution of heat days until 2100 within the different emission scenarios; left: FICLIMA results, right: CCLM top, WRF bottom

The annual cumulative precipitation rate is displayed differently than the heat days, because within this parameter different interesting aspects arise. First, the statistical downscaling results in a slight increase until the end of the century, with the biggest signal within SSP585. Also the RCMs display a similar magnitude within the climate change signal of about 10%, yet, the direction of change (increase / decrease) is reversed within CCLM and WRF. CCLM displays an increase in both SSP scenarios until the mid century and a decrease afterwards. For SSP126 this signal is also seen within the statistical downscaling, for SSP585 however the decrease is not represented. Within WRF the signal is reversed, showing a decrease until the near future (2050), a mixed signal over Salzburg until mid century and an increase thereafter. The reason behind this difference needs to be further analysed.

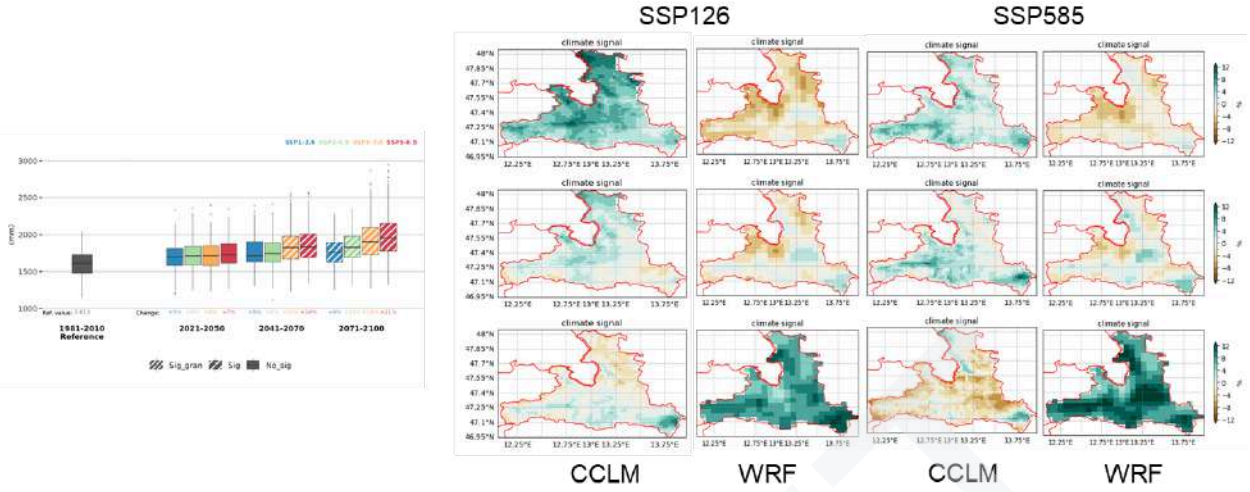

Figure 84: evolution of cumulative precipitation until 2100 within the different emission scenarios; left: FICLIMA results, right: CCLM top, WRF bottom

Conclusions

Extensive work related to downscaling of CMIP6 state of the art global climate projections was carried out within ICARIA. Building upon the two common methods (statistical and dynamical) the weaknesses and strengths became apparent within the production and will be further investigated with respect to their output.

Within the dynamical downscaling the extensive computational resources and hardware failures have led to delayed output, which is much less the case for statistical downscaling. Yet, the produced data sets for Salzburg and South Aegean region present the opportunity to assess climate change impacts on hourly time- and up to convection permitting spatial scale.

Furthermore, using physics aware ML techniques, an output dataset consisting of the GCM, RCM and - if feasible - spatially interpolated statistical downscaled fields, will be established to reduce model related uncertainties. The chosen approach is depicted within this deliverable.

Within the statistical downscaling, daily series of climate change projections have been produced covering a wide spectrum of climate variables and extreme indicators, covering the AMB case study and also for SAR and SLZ like the dynamical one. Taking into account the quickness of production of this method, a total of 10 GCMs and the 4 Tier 1 SSPs were used to develop the projections.

The regions of interest (AMB, SAR, SLZ) experience different magnitudes of climate change impacts due to their geographical location and typology (urban, islands, mountain region). The overall trends with respect to temperature, precipitation and wind evolution are similar within the statistical and dynamical downscaling and a first comparison is provided. Yet, only first insights were given as an in depth analysis will be presented within a scientific publication.

In general terms, both methodologies depict a climate future that aligns with the already existing climate trends within the present climate warming and the expected future one. All the temperature-related variables show, in different degrees depending on the case study and the indicator, a coherent and consistent increase in their values, larger the further we move into the future and also, normally, the worse the emission scenario we consider. This change is remarkable for both maximum temperatures (like for heat days) and minimum temperature (like for tropical nights). Regarding precipitation, slight to non-significant decreases are expected in the Mediterranean case studies, although an increase in the evapotranspiration and the number of dry days is foreseen. The contrary is expected in Salzburg, with slight to moderate significant increases in the future. Changes in wind and other variables tend to be more unpredictable, with large uncertainties associated, and require a specific case-by-case check or a more in-depth analysis.

ANNEXES

1. Data Management Statement

Table A1.1. Data used in preparation of ICARIA Deliverable 1.2

Dataset name	Format	Size	Owner and re-use conditions	Potential Utility within and outside ICARIA	Unique ID
AEMet weather observations	TXT	54 MB	AEMet - lent to FIC for research purposes	Used for their correction and as input in FICLIMA method	-
SMC weather observations	CSV	10 GB	SMC - lent for ICARIA for research purposes	(same)	-
BCASA weather observations	TXT	2.5 MB	BCASA - lent for RESCCUE for research purposes	(same)	-
PdE ocean observations	CSV	578 MB	PdE - Open Access	(same)	https://portus.puertos.es
DWD weather observations	TXT	5 MB	DWD - Open Access	(same)	https://opendata.dwd.de
ZAMG weather observations	CSV	2 GB	ZAMG - Open Access	(same)	https://data.hub.geosphere.at/
NOAA CDO weather observations	CSV	10 MB	NOAA - Open Access	(same)	https://www.ncdc.noaa.gov/cdo-web/

NOA-Meteogr weather observations	TXT	17 MB	NOA - Open Access	(same)	https://meteosearch.meteo.gr/
ERA5-Land reanalysis	NetCDF	3.1 TB	C3S - Open Access	Used for verification and statistical downscaling	DOI 10.24381/cds.e2161bac
ERA5 reanalysis	NetCDF	2.4 TB	C3S - Open Access	Used for statistical downscaling	DOI: 10.24381/cds.bd0915c6
ACCESS-CM2	NetCDF	1.4 TB	ESGF - Open Access	(same)	https://aims2.llnl.gov/search
BCC-CSM2-MR	NetCDF	3.5 TB	ESGF - Open Access	(same)	(same)
CanESM5	NetCDF	0.55 TB	ESGF - Open Access	(same)	(same)
CMCC-ESM2	NetCDF	2.8 TB	ESGF - Open Access	(same)	(same)
CNRM-ESM2-1	NetCDF	2.2 TB	ESGF - Open Access	(same)	(same)
EC-EARTH3	NetCDF	7.8 TB	ESGF - Open Access	(same)	(same)
EC-EARTH3-Veg	NetCDF	-	ESGF - Open Access	Used for dynamical downscaling	(same)
MPI-ESM1-2-HR	NetCDF	3.2 TB	ESGF - Open Access	Used for both downscalings	(same)
MRI-ESM2-0	NetCDF	2.6 TB	ESGF - Open Access	Used for statistical downscaling	(same)

NorESM2-MM	NetCDF	2.9 TB	ESGF - Open Access	(same)	(same)
UKESM1-0-LL	NetCDF	1.2 TB	ESGF - Open Access	(same)	(same)
CHELSA	NetCDF	-	ISIMIP - Open Access	verification	https://doi.org/10.48364/ISIMIP.836809.2

Table A1.2. Data produced in preparation of ICARIA Deliverable 1.2

Dataset name	Format	Size	Owner and re-use conditions	Potential Utility within and outside ICARIA	Unique ID
AMB corrected observations	ZIP (TXT)	14.2 MB	FIC - Open Access	Consultation and input for other modelling	DOI: 10.5281/zenodo.10964398
SAR corrected weather observations	ZIP (TXT)	0.5 MB	FIC - Open Access	Consultation and input for other modelling	(same)
SLZ corrected weather observations	ZIP (TXT)	4.1 MB	FIC - Open Access	Consultation and input for other modelling	(same)
FICLIMA climate change projections at local scale	ZIP (TXT)	2.9 GB	FIC - Open Access	Outcome. Input for other modelling and further replicability.	(same)
FICLIMA climate change spatial projections	TIF	TBD	FIC -Open Access	Outcome for stakeholders. Input to ICARIA's DSS.	ICARIA DSS [future Zenodo]
[AIT]spatially downscaled climate projections (2 RCMs)	NETCDF	? Terabyte	AIT- open access	Outcome for stakeholders. Input to ICARIA's DSS.	ICARIA DSS [future Zenodo]

2. Quality control of weather observations

2.1. Quality control

Before starting ICARIA's tasks of developing future climate change scenarios in the three CS (AMB, SAR and SLZ), it was mandatory to first gather multiple weather observations at the study regions and perform a check of their quality. This is, a previous study has been carried out of the provided observed data in CS areas to ensure that the quality of those data is good enough for subsequent studies and conclusions – that's what a Data Quality Control process involves.

Conducting quality control on a time series of records involves the implementation of a battery of tests aimed at ensuring data consistency within the analyzed series. **This annex section focuses on the critical climatic variables, specifically precipitation and temperature, with similar findings extending to other variables (RH, wind)**.

It is essential to note that the testing procedures must be designed to accommodate varying outcomes across different datasets. Each dataset represents the local climate of the observed area, necessitating a consistent theoretical approach to testing across all observatories, while acknowledging that the acceptable range is context-dependent. For instance, when examining the average temperature within a dataset, a daily maximum temperature of 40°C would be deemed acceptable in a series with an average temperature of 35°C but noteworthy in a series with a maximum average of 20°C. Identifying a noteworthy value does not imply automatic rejection; rather, it underscores the need for a thorough investigation into its origin to verify accuracy.

The primary automated controls employed for quality assurance include:

1. Basic Consistency Checks: Direct elimination of evident incorrect values, such as negative precipitation values.
2. Identification of Atypical Values or 'Outliers': Recognition of values within the dataset that significantly deviate, either originating from different data sources or generated differently from the rest of the dataset. The challenge in recognizing such values lies in defining "atypical," with practical identification often linked to values exhibiting an unusually high absolute magnitude.

Temperature

Basic consistency

Concerning temperature, we've conducted basic consistency checks by examining daily values where the recorded maximum temperature is lower than the minimum temperature. An illustrative real-life example of such cases is presented in Table A2.1, which is derived from observed data.

There are two common scenarios leading to these instances:

1. Misrecorded Missing Values: In some instances, missing temperature values are not appropriately marked as missing. Depending on the source, these values might be recorded as "NA" (Not Available) or "-9999," but they end up being recorded as 0. In such cases, we promptly dismiss maximum temperature values if we can verify that 0°C is not a plausible value after scrutinizing the dataset.

2. Internal Inconsistency: Another situation arises when a temperature value, while internally consistent, becomes inconsistent when compared with the concurrent daily temperature value. The table's last two lines provide an example of this scenario: either of the two values could be incorrect. Consequently, we opt to reject both values.

Table A2.1.Examples of real daily temperature data observed where maximum temperature is lower than minimum temperature. These values are given as an example of possible detected situations and they come from several different meteorological stations.

Year	Month	Day	Maximum temperature (°C)	Minimum temperature (°C)
1977	11	13	0	15
1978	1	11	0	13
2000	10	25	20.7	22.7
2009	12	2	22.5	23.5

Outliers

As mentioned earlier, identifying an atypical value hinges on the theoretical definition of "atypical." Taking as an example one of the stations considered for ICARIA, depicted in the figure below (Figure A2.1): a series of maximum temperature values exceeding 70°C appears blatantly unusual, not only for this specific observatory but on a global scale. However, it prompts us to ponder: Why is a value of 94°C considered self-evident as an outlier for us? Would it still be self-evident if the value were 50°C? What about 40°C?

From a theoretical standpoint, determining whether a value is atypical involves assessing how much it deviates from the typical values in our dataset. The formal procedure for this test involves gauging the distance of a value from the mean of the observed series, with the unit of measurement for this distance being the standard deviation of the series.

Consequently, our tests need to ascertain the following:

1. The mean and standard deviation of each meteorological station.

2. A threshold value, expressed in units of standard deviation (added to the mean), beyond which a daily value can be classified as atypical.

3. A comprehensive analysis of values identified as outliers in the previous step to verify their accuracy. This analysis aids in determining whether these values should be rejected or if a new threshold value needs to be assigned, prompting a repeated analysis.

After this first introduction to the general methodology applied in these types of temperature quality tests, hereafter are facilitated some examples of real stations considered within ICARIA that failed to pass these controls and were either corrected (if possible) or removed.

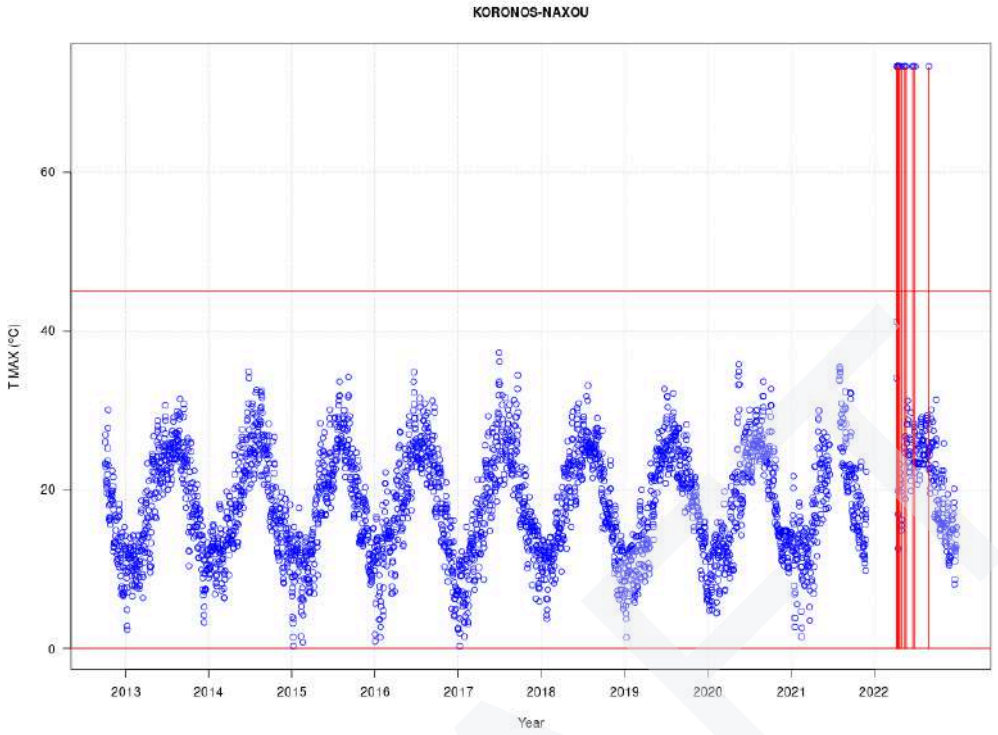

Figure A2.1. Observed series of maximum temperatures for a real weather station, in this case corresponding to SAR CS station "Koronos-Naxou". Values of more than 70ºC are registered.

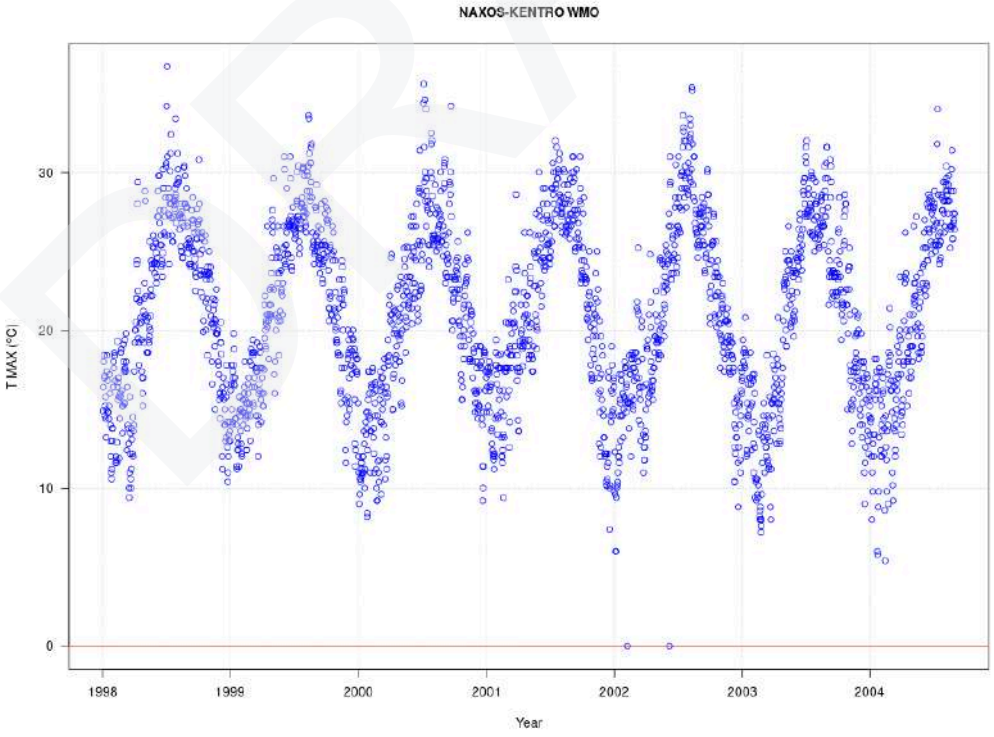

Figure A2.2. Observed series of maximum temperature for a weather station corresponding to SAR CS station "Naxos-Kentro WMO". Abnormal maximum values of 0ºC are registered.

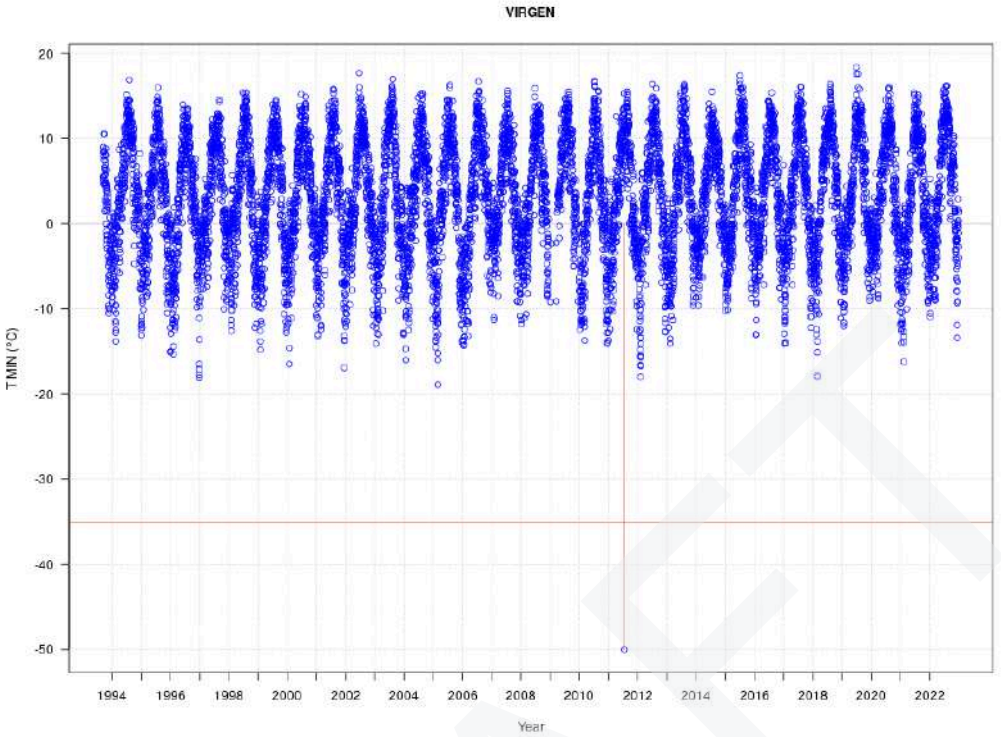

Figure A2.3. Observed series of maximum temperatures for a weather station corresponding to SLZ CS station "Virgen" and ID "11252". Abnormal minimum values of -50ºC are registered.

Precipitation

Basic consistency

In the case of precipitation, basic consistency tests are associated with the search of negative daily records - some real examples of these cases (based on real data from real weather stations) are shown in the table below (Table A2.2).

Table A2.2. Samples of real data where daily observed precipitation is negative (shown for illustrative purposes – not stations provided for this study).

Year	Month	Day	Precipitation
1986	8	31	-1.0 mm
2003	9	21	-8.0 mm

Due to the self-evident error of these values, every detected case is directly marked as wrong and immediately rejected.

Outliers

Regarding precipitation, like before with temperature, an odd value is identified when it surpasses a specified multiple of the series mean. However, due to the intrinsic characteristics of this

meteorological variable, detecting an outlier does not automatically result in its direct rejection This is because really heavy rain can be rare but not impossible. Therefore, a meticulous analysis of the climatology specific to the area is imperative.

For example, places hit by hurricanes might have daily rainfall records that seem odd, but they could be totally fine given the hurricane conditions. So, checking strange rainfall values needs a close and careful look, considering that extreme weather events might be normal for some places.

Like in the previous section, now with precipitation methodology described, hereafter are facilitated some examples of stations considered within ICARIA that failed to pass these controls and were either corrected (if possible) or removed.

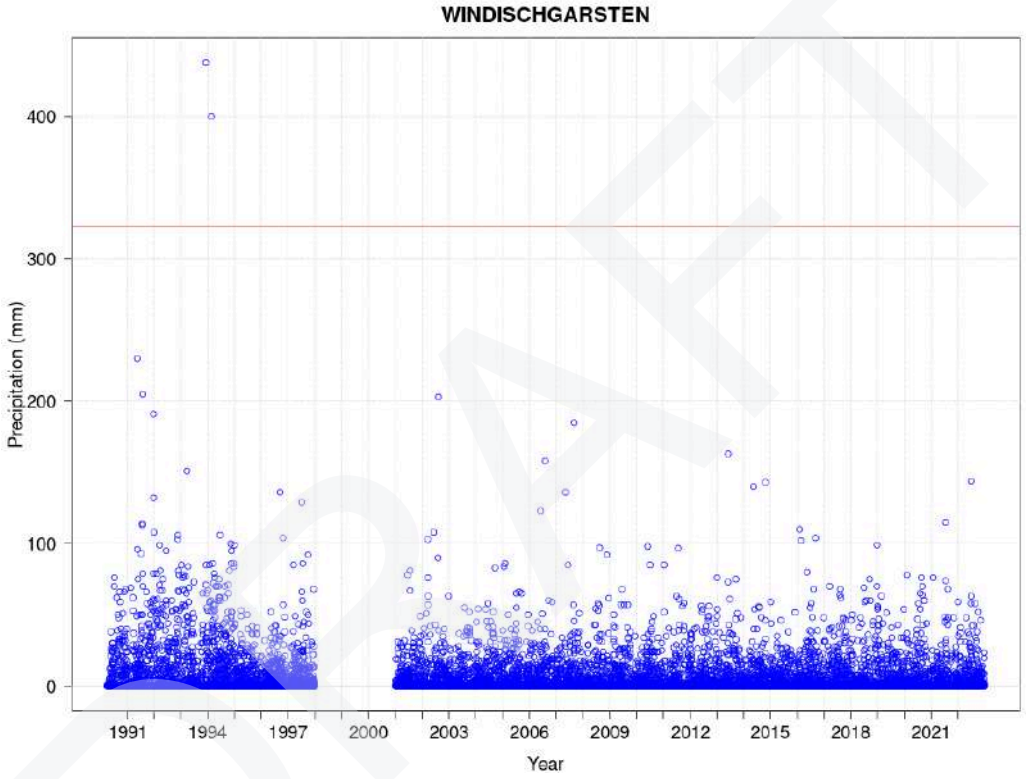

Figure A2.4. Observed series of 24-h precipitation accumulations for a weather station corresponding to SLZ CS station "Windischgarsten" and ID "11355". Abnormal rainfall gauged values of >400mm are registered, considered as outliers for this area's climate.

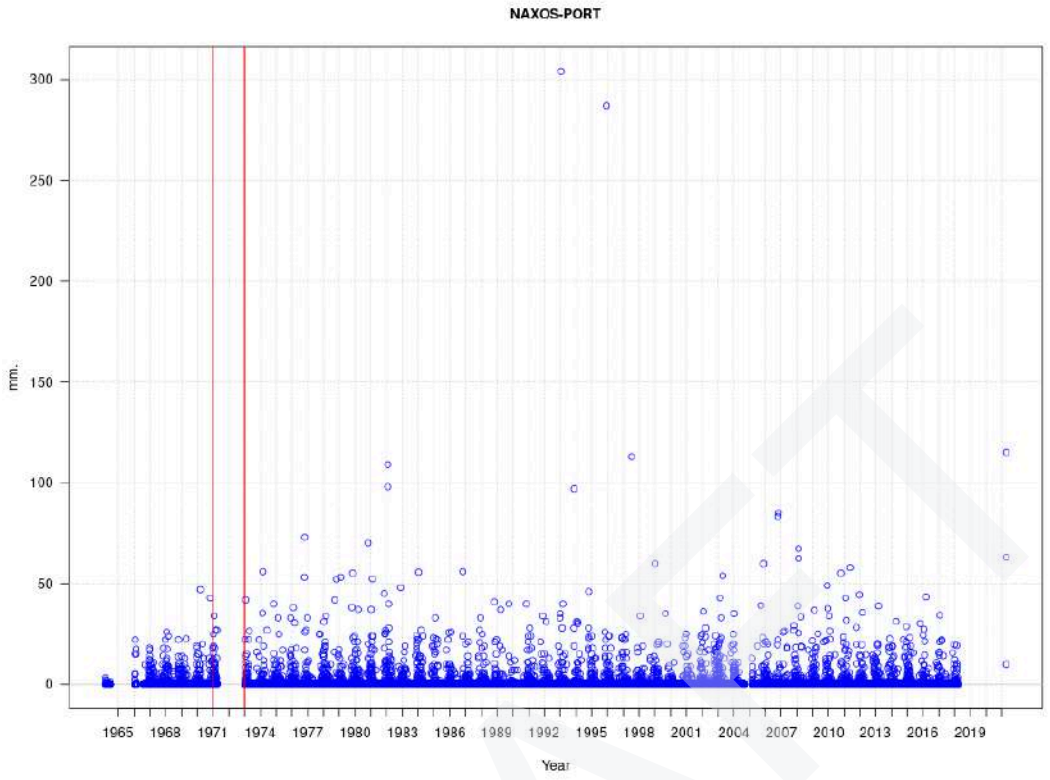

Figure A2.5. Observed series of 24-h precipitation accumulations for a weather station corresponding to SAR CS station "Naxos-Port". A gap of missing values was identified.

2.2. Homogenization

The homogenization of a time series is related to the quality control of data aligned with the chronological order of the series. Essentially, homogenization checks the consistency of data presentation. Although preceding tests may be employed for series analysis, they do not provide insights into the temporal variability of the data, particularly concerning the annual cycle.

It's worth noting that homogenization is part of the bigger process of quality control for a series. I'm mentioning it separately just to stress how crucial it is and what it reveals.

Refer to Figure A2.6 below, illustrating the maximum temperature from an actual weather station.

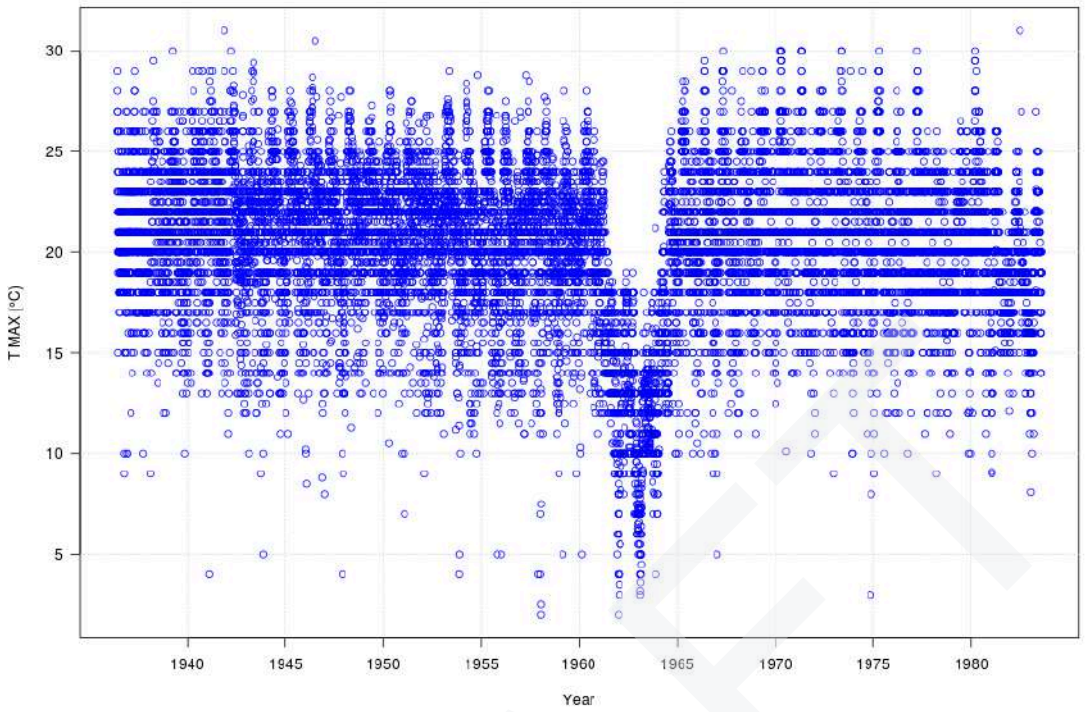

Figure A2.6. Another observed series of maximum temperatures for a real weather station (showed for illustrative purposes – not a station provided for this study).

The observed maximum temperature behavior of this station exhibits erratic tendencies during the period from 1961 to 1964. While these values display erraticism concerning the preceding and subsequent temperature patterns, they are not inherently irrational. This practical example aids in comprehending the objective of homogenization tests: identifying temporal segments within a series where data deviates from the overall pattern. In fact, the series presented here as an illustration was identified through these tests. The formal execution of homogenization tests poses challenges rooted in defining the similarity between a segment of the series and the rest of the dataset.

The homogeneity test methodology employed here is based on the approach developed by Monjo et al. (2013):

1. To measure the similarity between data from one year and another, a distribution comparison test utilizing the Kolmogorov-Smirnov (KS) test is applied. This non-parametric statistical test, not assuming distributions of the studied variable, yields a p-value serving as a metric for the similarity between two years. Figure A2.7 illustrates the "Control Analysis" graph, showcasing the logarithmic p-value comparison between each year and the subsequent year for the given example (maximum temperature of the studied station). Values close to 0 signify highly similar value distributions between two consecutive years, indicating no discernible inhomogeneity. A lower Log(KS) value implies a higher probability of inhomogeneity between two consecutive years. This initial phase assesses similarities solely between adjacent years, establishing a preliminary condition for potential inhomogeneity.
2. If a specific year is flagged as a potential indicator of inhomogeneity, it undergoes another test ("Similarity between years," Figure A2.7). The p-value of each year relative to the selected years is computed (represented by the red and blue lines in the graph). The presence of a distinct jump or break in these p-values indicates a true inhomogeneity across the entire series.

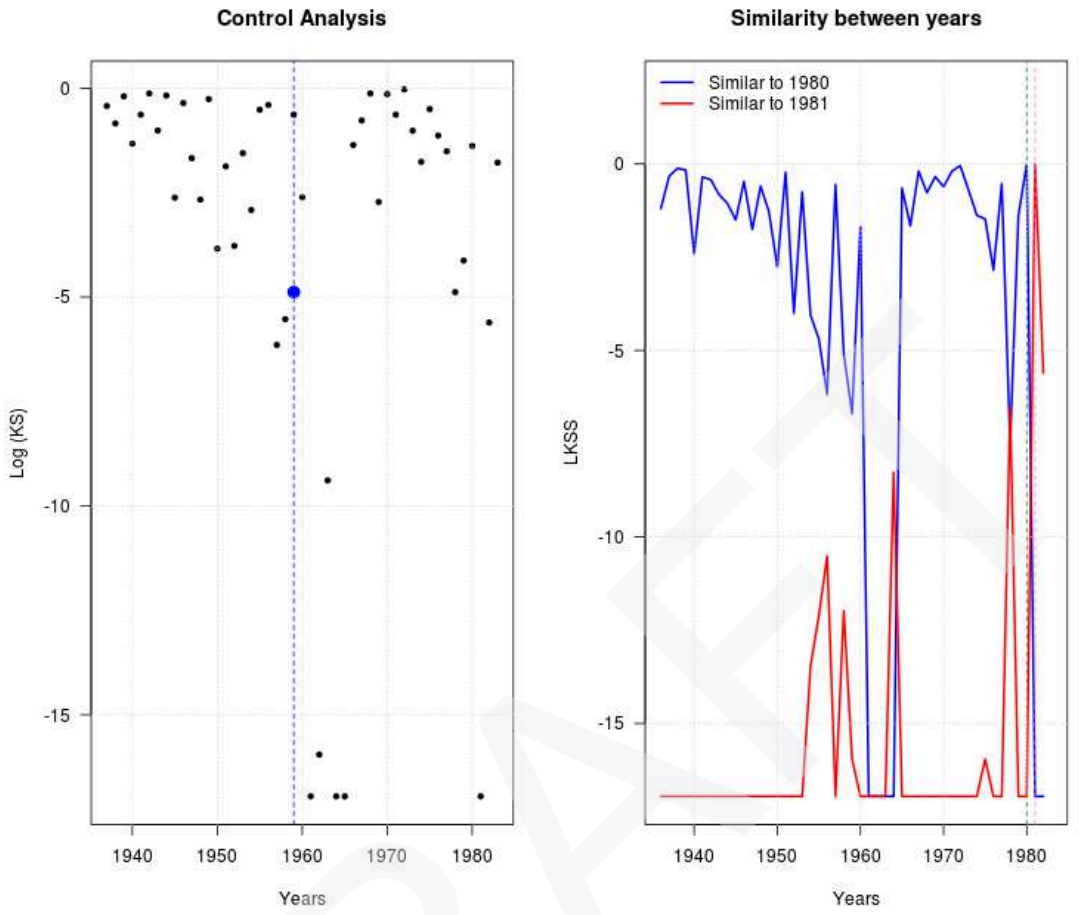

Figure A2.7. Logarithm of KS test p-value used in the homogenisation process for daily data. The case selected belongs to the maximum temperature of a real meteorological station whose daily data are represented in Figure A2.6.

This procedure enables the identification of years exhibiting inhomogeneity in a series. Since determining the threshold for a sufficiently small p-value to indicate potential inhomogeneity is contingent on our criteria, the same test is iterated with varying threshold p-values, ranging from strongly negative to close to zero. This iterative approach aims to enhance the objectivity of the criterion. If a genuine inhomogeneity exists, it should manifest when the majority of tests are conducted.

It is crucial to emphasize that there is no automated process dictating the appropriate action to be taken regarding a series (whether removal or adjustment). Given that these actions become necessary when dealing with a substantial number of observatories, a visual inspection is invariably required after conducting the tests to validate the correctness of the final series.

Now with the methodology for homogenization explained, we attach below some examples that serve as proof of some ICARIA's observations that failed to pass these controls and were either corrected (if possible) or removed. Furthermore, a detailed set of tables (Table A2.3 to Table A2.7) are also provided as summary of the total number of stations treated (with positive or negative outcomes) by CS and the variable of interest.

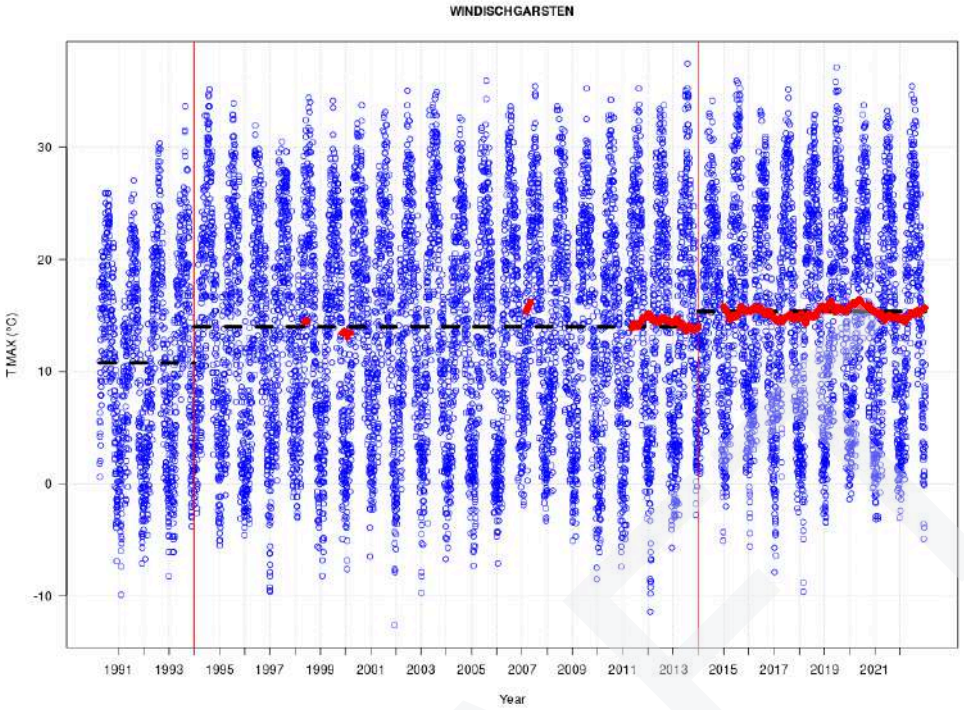

Figure A2.8. Observed series of maximum temperatures for SLZ CS weather station "Windischgarsten", ID "11355". Two sudden different changes (jumps) in the mean trend of the station are observed.

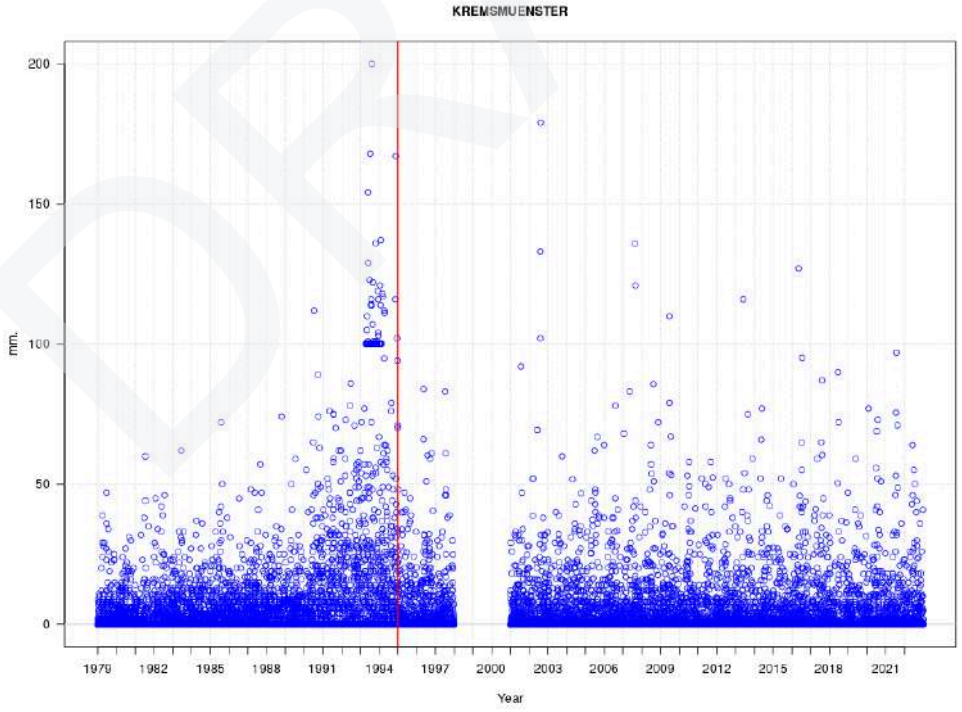

Figure A2.9. Observed series of 24-h precipitation accumulations for SLZ CS weather station "Kremsmuenster", ID "11012". An abnormal data cluster of ~100mm is observed.

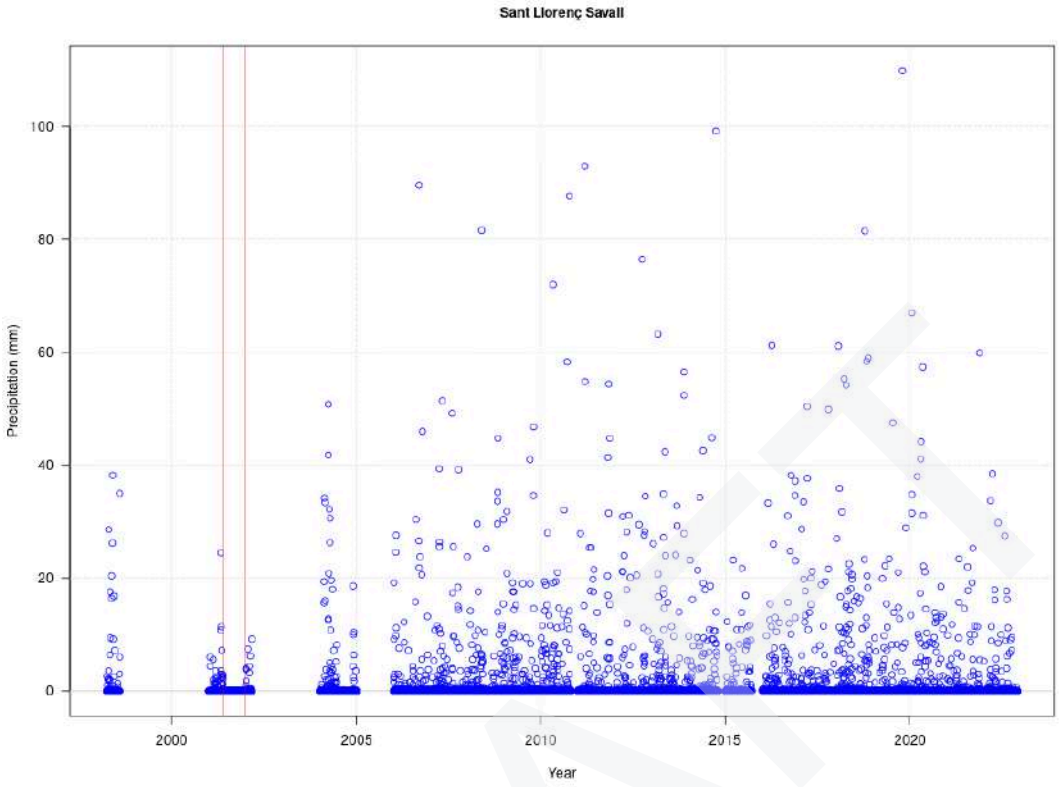

Figure A2.10. Observed series of 24-hour precipitation accumulations for AMB CS weather station "Sant Llorenç Savall". A period of odd zero values was identified.

Table A2.3. Summary of temperature weather observations before and after the quality control.

Case study	Retrieved observations	Dismissed observations	Final accepted observations
AMB	168	15	153
SAR	19	2	17
SLZ	61	4	57

Table A2.4. Summary of precipitation weather observations before and after the quality control.

Case study	Retrieved observations	Dismissed observations	Final accepted observations
AMB	225	13	212
SAR	19	5	14
SLZ	61	3	58

Table A2.5. Summary of wind weather observations before and after the quality control

Case study	Retrieved observations	Dismissed observations	Final accepted observations
AMB	66	9	57
SAR	17	0	17
SLZ	55	4	51

Table A2.6. Summary of RH weather observations before and after the quality control.

Case study	Retrieved observations	Dismissed observations	Final accepted observations
AMB	171	58	113
SAR	17	1	16
SLZ	59	15	44

Table A2.7. Summary of oceanic (weaves + sea level) weather observations before and after the quality control.

Case study	Retrieved observations	Dismissed observations	Final accepted observations
AMB	12	0	12

3. Quality control of downscaling methodologies. Uncertainty analysis.

Before simulating the future climate, it is necessary to verify that the tools used for this purpose work properly in the study area by correctly simulating the observed past climate. For this purpose, it is necessary to carry out a complete and robust verification analysis of the downscaling methodologies used in ICARIA and how these affect the GCMs to be downscaled so as to assess properly the uncertainty introduced in the outcomes. For the different variables, the errors with which the methodology and each GCM simulate the observed climate at each location must be known. In this Annex section, a more in-depth description of the procedures used will be provided for each downscaling method applied.

3.1. Statistical downscaling - FICLIMA

In the case of the statistical downscaling applied in ICARIA, coming from the FICLIMA method, the quality control has the peculiarity of consisting of two steps. The FICLIMA method is a statistical procedure that takes as input local weather observations to analyze local climate signals and introduce them into the GCMs projections. Being so, and after the quality control of weather data, a first verification of the ERA5-Land reanalysis that is used for the search of analogue days is done against weather data. Then, a validation of the application of the downscaling for each GCM is performed using its historical experiment and the reanalysis. Here below more information is provided.

Verification of the methodology

The verification process commences by employing the downscaling methodology on atmospheric reanalyses, which represent the state of the atmosphere (the predictors) on each day within a specified reference period (e.g., from 1981 to 2010). While the latest ERA5-Land reanalyses boast detailed resolutions of approximately 9 km, it would be counterproductive for a tool to yield satisfactory outcomes with such high-resolution predictors if it is subsequently applied to Global Climate Model (GCM) outputs characterized by lower resolution (around 100 km). Therefore, it becomes necessary to adjust the spatial and temporal resolution of the reanalyses to align with that of the GCMs to ensure compatibility and accuracy in the downscaling process.

Thorough verification is essential, extending beyond mean values to include extremes and covering all time scales, including daily intervals. The emphasis on daily verification is particularly significant. If the tool correctly simulates changes from one day to the next, it indicates an effective capture of the underlying physical connections between predictors and predictands. These physical links remain relatively consistent, even in the face of climate change (as opposed to purely empirical relationships that might shift). In essence, this approach theoretically addresses the primary challenge in statistical downscaling known as the non-stationarity problem. This problem questions the stability of predictor/predictand relationships established in the past, probing whether these relationships will persist in the future.

As previously mentioned, we assess the method's performance by comparing observed and ERA5-Land reanalysis simulated time series for a historical reference period (1981-2010). The mean absolute error

(MAE) and mean relative error (MRE) serve as key metrics for most climate variables, offering a primary measure of the method's efficacy in replicating day-to-day weather variability. This analysis is crucial as it gauges the method's ability to accurately capture the physical forcings influencing each climate variable, enabling the detection of potential changes in their intensity or frequency.

Subsequently, the Kolmogorov-Smirnov (KS) test is employed to evaluate the statistical significance of the simulated probability distributions compared to the observed ones (Marsaglia et al., 2003). This test proves valuable in assessing the method's capability to replicate not only the mean distribution but also extreme values. Additionally, the KS test is applied to ascertain the effectiveness of bias correction, ensuring a comprehensive evaluation of the method's overall performance.

Results coming from the verification processes all across ICARIA's three case studies are completely satisfactory, and pretty similar from one case to another. As a matter of fact, considering the previous statement and for the sake of clarity and space, hereafter are displayed only the results for the verification at the AMB case study (which happens to be the one with more weather data as basis). Results are shown for temperature, precipitation and wind.

Precipitation

Verification results concerning the precipitation are shown here for all stations considered in AMB. Figures displayed showcase the results of the KS-test before and after the correction (Figure A3.1), as well as the distribution of mean monthly values and days with precipitation, before and after correction (Figure A3.2).

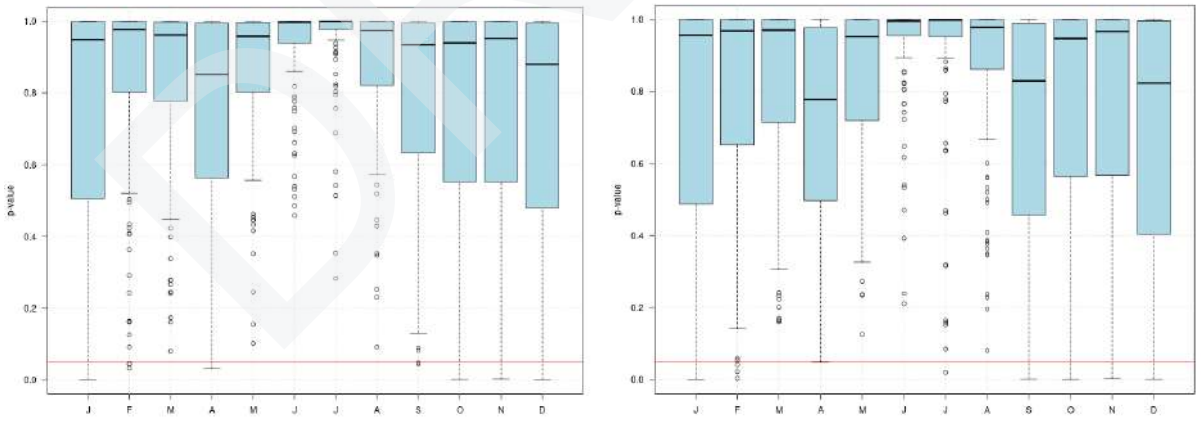

Figure A3.1. Verification results for the application of the KS-test before (left) and after (right) correction. P-value threshold at 0.05. Check Y-axis for more detail on scales.

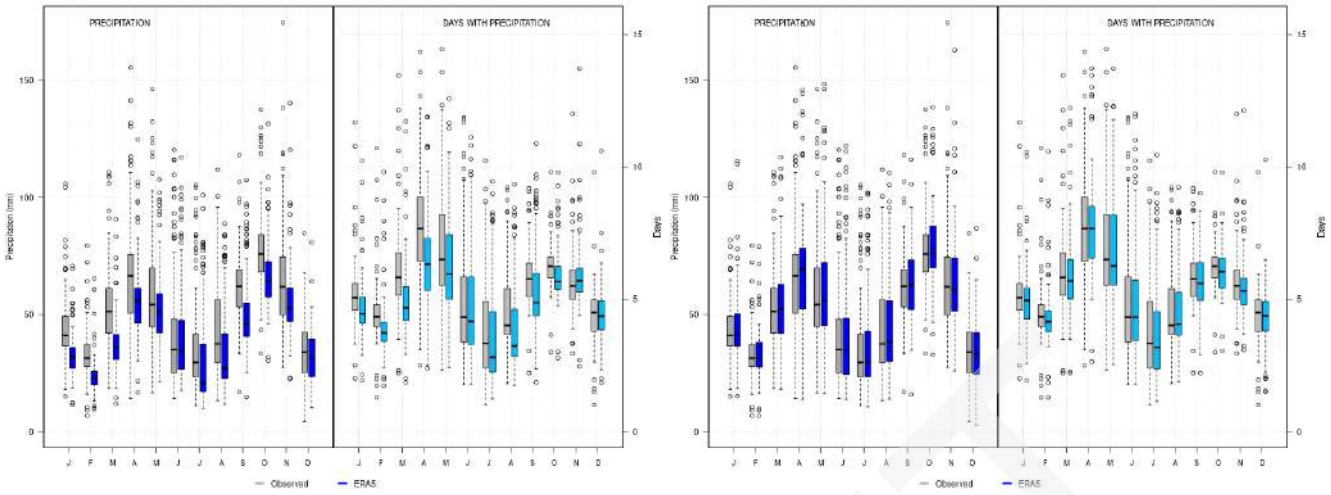

Figure A3.2. Verification results at monthly scale after the correction of ERA5-Land values from weather data, displayed at mean values and days with precipitation before (left) and after (right) correction.

Temperature

Verification results concerning the temperature are shown here for all stations considered in AMB (same results for SAR and SLZ). Figures displayed showcase the results of the BIAS and MAE statistics (Figure A3.3), as well as KS-test before and after the correction (Figure A3.4). Also, the distribution of mean monthly values is shown (Figure A3.5).

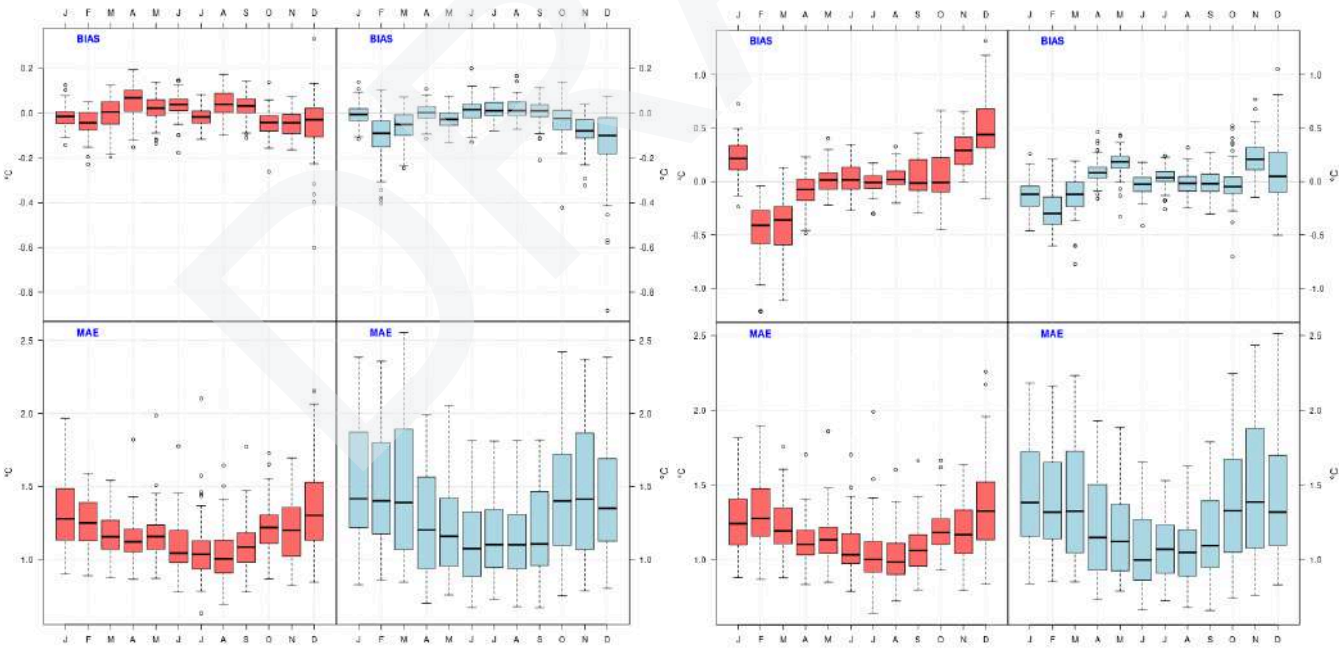

Figure A3.3. Verification results of maximum temperature (red) and minimum temperatures (blue) after the calculation of BIAS (upper row) and MAE (bottom row) statistics before (left picture) and after (right picture) correction. Check Y-axis for more detail on scales.

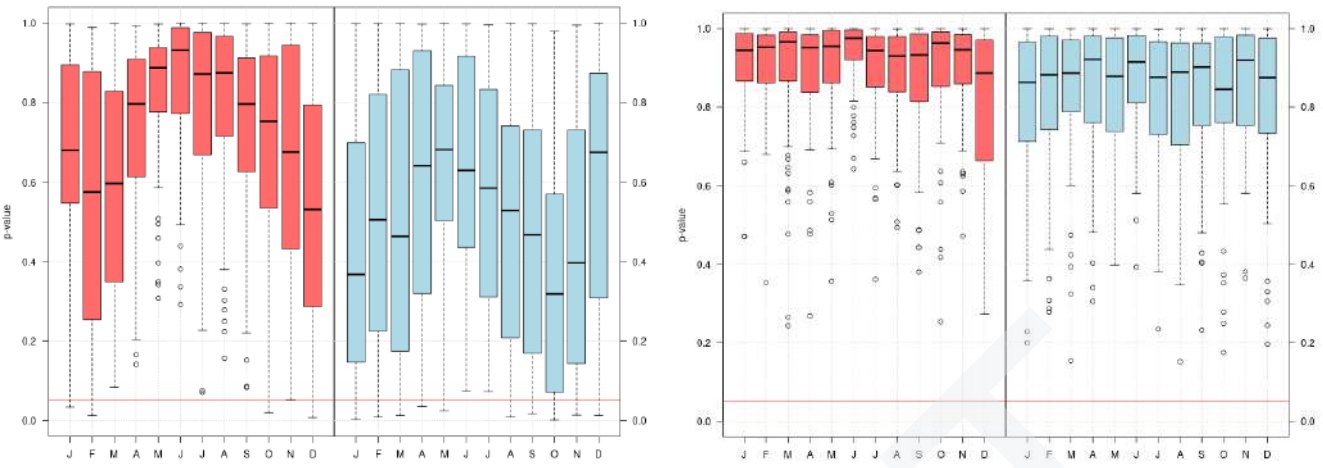

Figure A3.4. Verification results of maximum temperature (red) and minimum temperatures (blue) for the application of the KS-test before (left) and after (right) correction. P-value threshold at 0.05. Check Y-axis for more detail on scales.

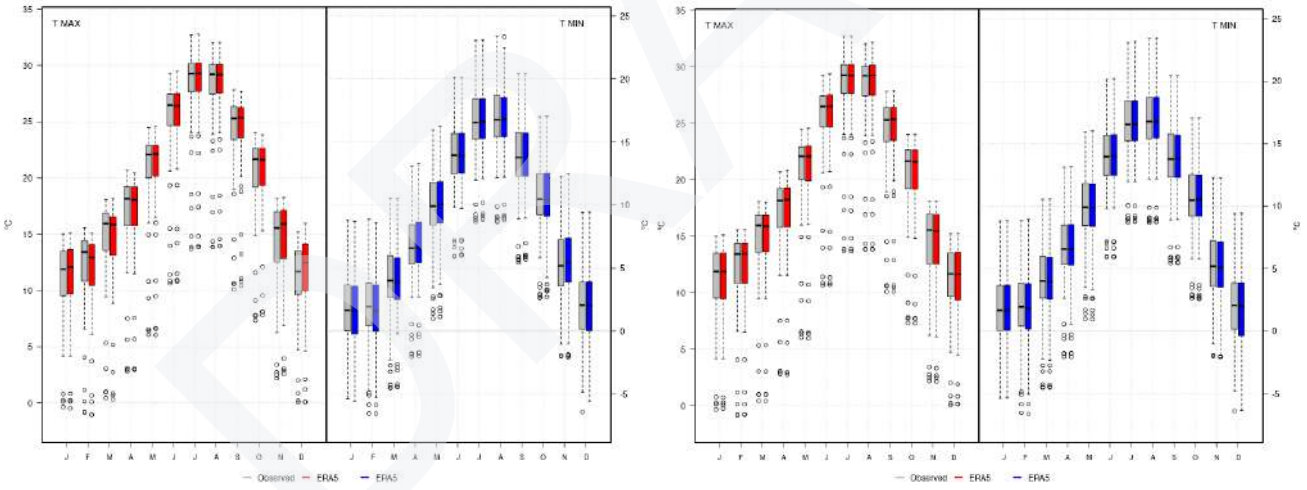

Figure A3.5. Verification results of Maximum Temperature monthly values after the correction of ERA5-Land values from weather data, displayed at mean values before (left) and after (right) correction.

Wind gust

Verification results concerning wind gusts are shown here for all stations considered in AMB, since outcomes for SAR and SLZ are similar. Considering the particular nature of wind gusts, tests applied differ slightly from those of precipitation and temperature, being checked the extremest percentile (P99 and P100), thresholds and their behaviour. Figure A3.6 showcases the results of the verification for specific thresholds, and in Figure A3.7 can be found as well as the distribution of mean monthly values for the P99 percentile.

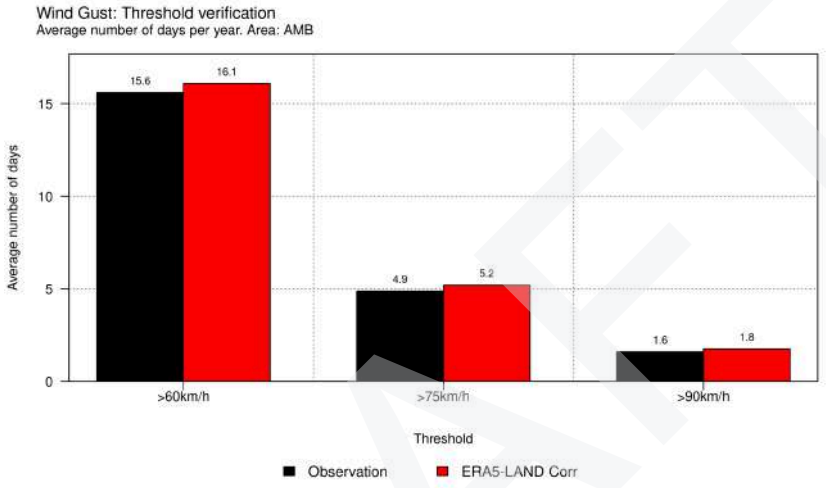

Figure A3.6. Verification results at specific wind gust thresholds after the correction of ERA5-Land values from weather data, displayed at number of days above the thresholds.

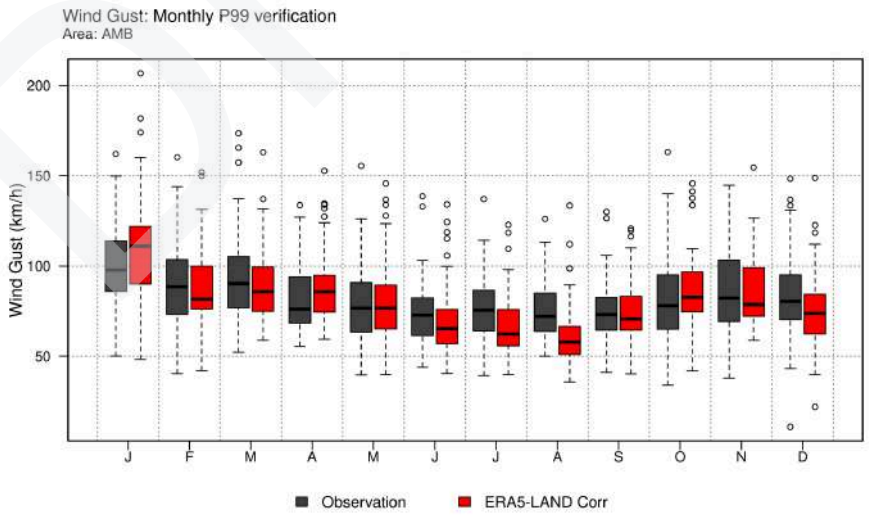

Figure A3.7. Verification results at monthly scale for the P99 percentile of wind gust values after the correction of ERA5-Land values from weather data.

Validation for the CMIP6 models

Once the successful verification of the downscaling methodology is accomplished, each Global Climate Model (GCM) slated for regionalization undergoes validation through the downscaling of its control outputs, referred to as Historical (covering the period 1960-2015, for instance). This involves comparing the simulations derived from these outputs with the observed climate to gauge the extent to which the GCM accurately represents the observed climate. Notably, this validation is not only conducted at a global scale but also at the local scale, recognizing that certain GCMs may perform well in one area of a region but not in another. The outcomes of this validation, assessed for each GCM, variable, and geographical point, play a pivotal role in quantifying uncertainties. A GCM with more favourable validation results corresponds to lower uncertainties in its simulations.

The validation process involves assessing the performance of applying the chosen method to each climate model. Unlike reanalyses, a *historical experiment* of a climate model aims to simulate climate variability at a daily scale rather than replicating the actual day-to-day weather evolution in the reference period. Consequently, errors obtained from day-to-day comparisons between time series (such as MAE, MRA, and RPS) are not meaningful. Instead, other statistics are commonly employed to evaluate the model's ability to reproduce climate averages and variability effectively.

One key statistic for a model is the bias of the mean and the standard deviation, calculated as the average of the total error for each station across each climate variable. The bias is crucial because a model should accurately reproduce the spatial distribution of climate averages. High dispersion in bias across a set of observatories may imply a distortion of regional variability and, consequently, an unrealistic portrayal of key climatic features.

However, evaluating a climate model goes beyond climatic averages; climate variability should also be assessed through additional statistics. In this regard, the non-parametric Kolmogorov-Smirnov (KS) test proves useful for measuring the distance between two probability distributions, considering the entire distribution. The KS p-value indicates whether two distributions are indistinguishable, with a preferred threshold typically set at p-value > 0.05.

The results obtained from the validation processes in ICARIA's three case studies are entirely satisfactory in the cases of precipitation and temperature, exhibiting a consistent pattern across all cases, with no notable exceptions worth highlighting. **There is however a remarkable situation for wind due to the complexity of working with it, and depending on the CS there are some models that can be seen to not properly represent a correct distribution for wind behaviour and shall be not considered for the delivery of results**. In light of this, and considering clarity and brevity, only the verification results for the AMB case study are presented in the temperature and precipitation sections, with a more detailed discussion on wind for other CS. The displayed results encompass assessments for temperature, precipitation, and wind variables.

Precipitation

Validation results concerning the precipitation are shown here for all stations considered in AMB. Figures displayed showcase results of the SD difference (Figure A3.8), the KS-test (Figure A3.9), as well as the

distribution of mean monthly values for each model considered before and after correction and application of FICLIMA method (Figure A3.10).

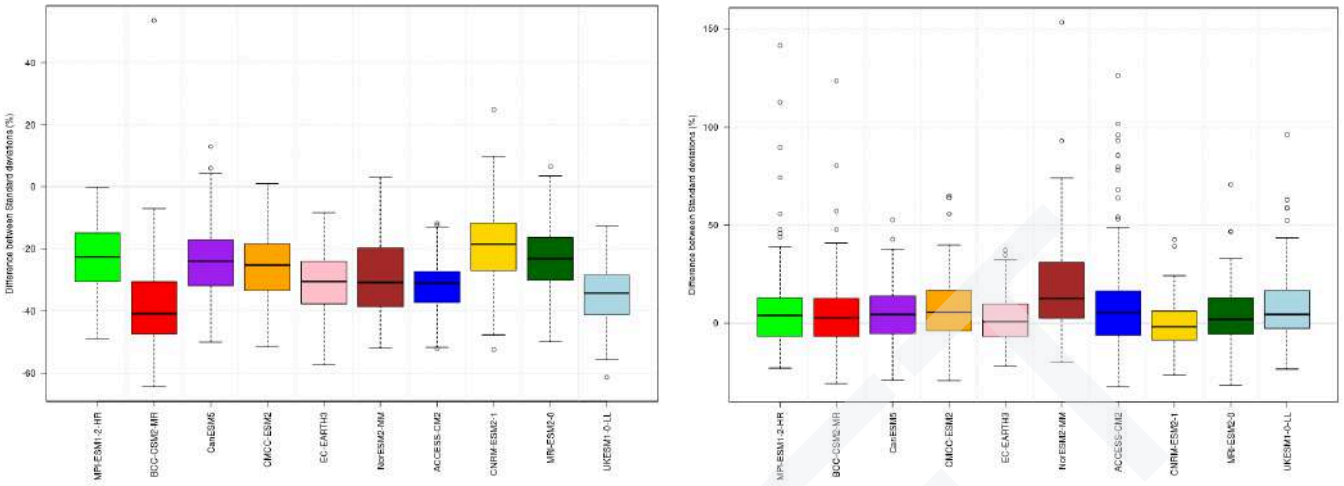

Figure A3.8. Validation results of difference between Standard Deviation (SD) statistic to Maximum Temperature values before (left) and after (right) the correction of the 10 CMIP6 models considered and the application of FICLIMA method. Check Y-axis for more details on scale.

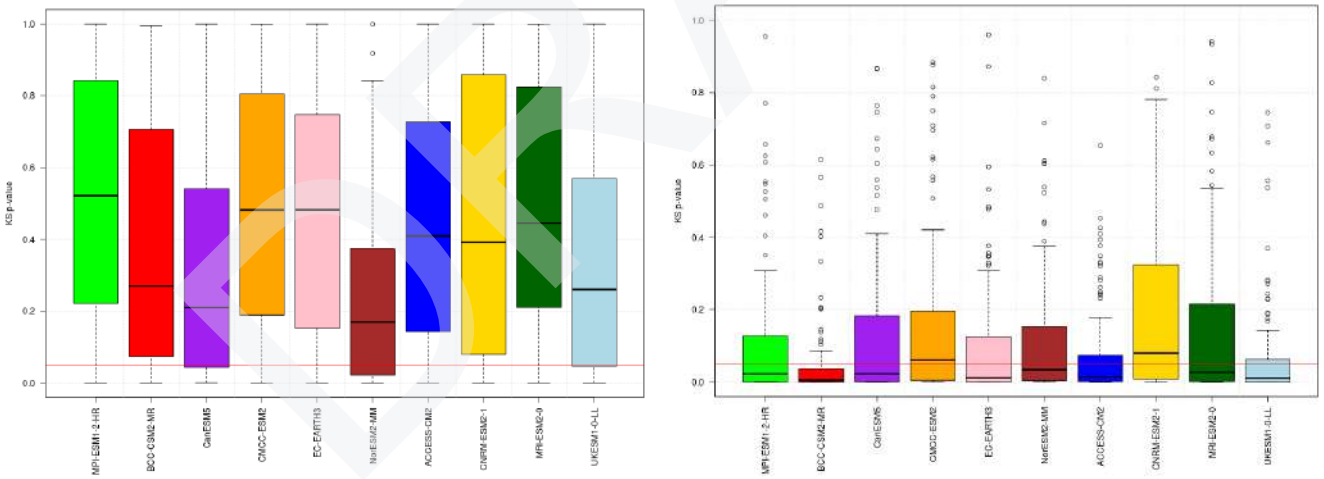

Figure A3.9. Validation results, for precipitation, of the application of the Kolmogorov-Smirnov (KS) test values before (left) and after (right) the correction of the 10 CMIP6 models considered and the application of FICLIMA method. P-value threshold set at 0.05. Check Y-axis for more details on scale.

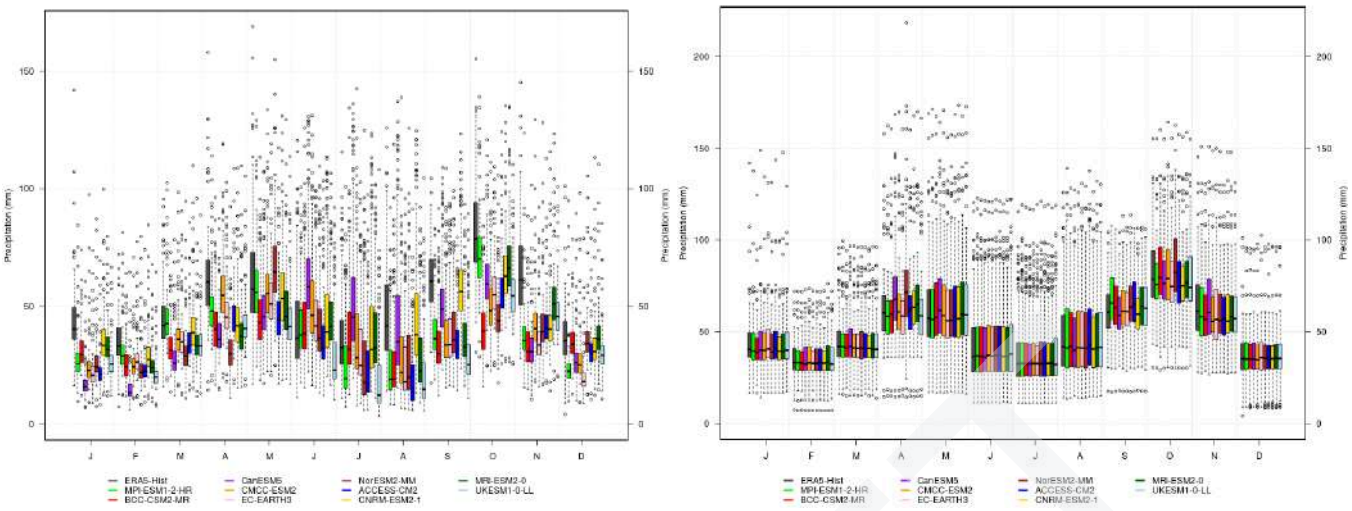

Figure A3.10. Validation results of precipitation monthly values before (left) and after (right) the correction of the 10 CMIP6 models considered and the application of FICLIMA method. Check Y-axis for more details on scale.

Temperature

Validation results concerning temperature are shown here for all stations considered in AMB (same results for SAR and SLZ). Figures displayed showcase results of the SD difference (Figure A3.11), the KS-test (Figure A3.12), as well as the distribution of mean monthly values for each model considered before and after correction and application of FICLIMA method (Figure A3.13.

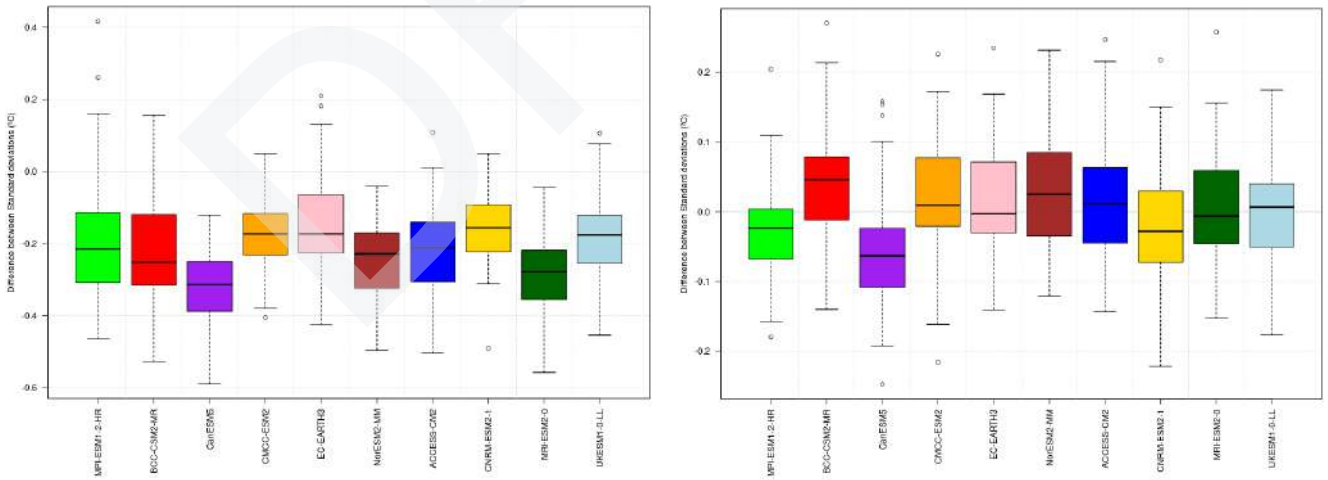

Figure A3.11. Validation results of difference between Standard Deviation (SD) statistic to Maximum Temperature values before (left) and after (right) the correction of the 10 CMIP6 models considered and the application of FICLIMA method. Check Y-axis for more details on scale.

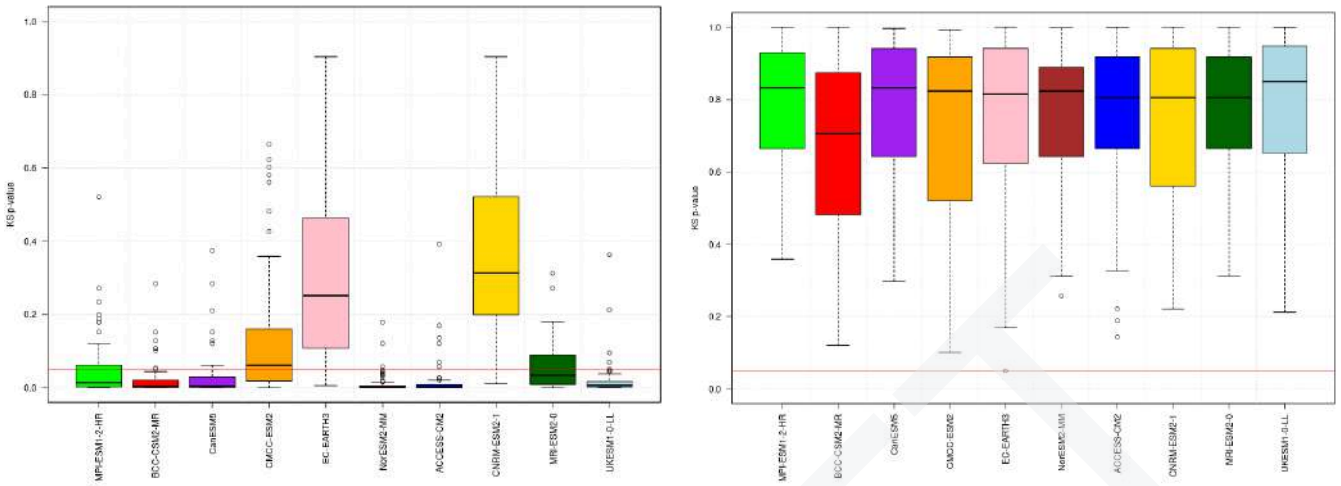

Figure A3.12. Validation results for Maximum Temperature of the application of the Kolmogorov-Smirnov (KS) test values before (left) and after (right) the correction of the 10 CMIP6 models considered and the application of FICLIMA method. P-value threshold set at 0.05. Check Y-axis for more details on scale.

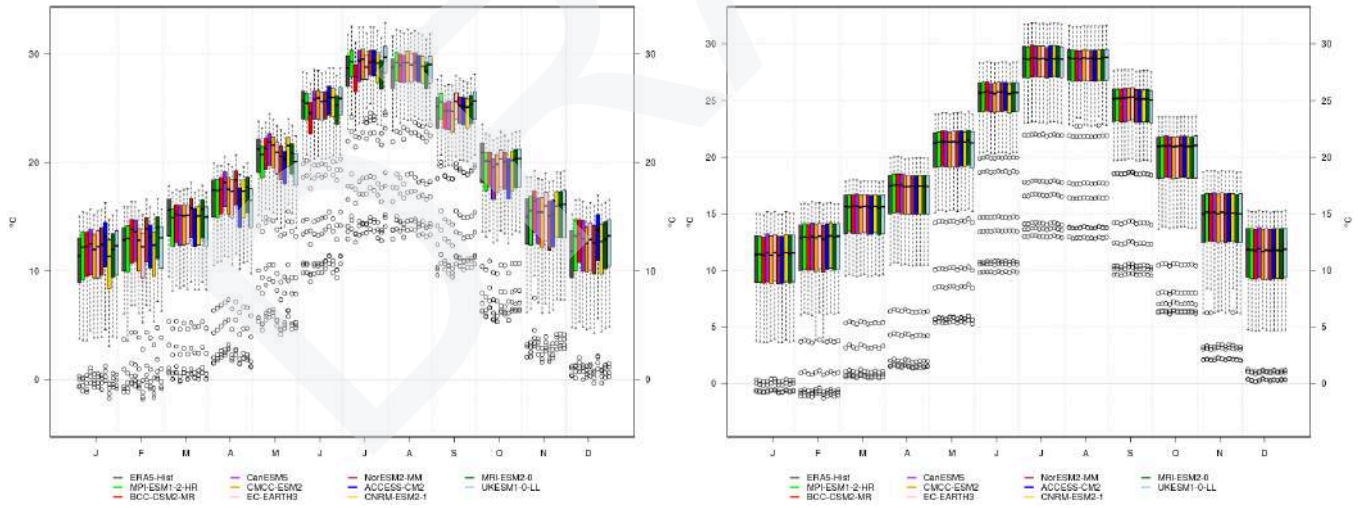

Figure A3.13. Validation results of Maximum Temperature monthly values before (left) and after (right) the correction of the 10 CMIP6 models considered and the application of FICLIMA method. Check Y-axis for more details on scale.

Wind gust

Validation results concerning wind gusts are shown here. It is in this case, unlike those of precipitation and temperature, to be remarked that validation tests have indeed shown a case for discussion. In this case of wind gust, validation results show different conclusions for each of the CS, and while for SAR the outcome is positive in general, for AMB and SLZ there are problems in the performance of some models. **This is the reason why here figures for AMB and SLZ are shown**. As it can be seen in the figures, especially in Figure A3.15 at monthly scale for AMB, there are a couple of models, namely ACCESS-CM2 and MRI-ESM2-0, that can be seen to not properly represent a correct distribution for wind behaviour; in Figure A3.18 for the case of SLZ it is MPI-ESM1-2-HR the one that off-performs; these models shall be not considered for the delivery of results. Depending on the CS, these models have been removed from the results and are therefore not considered in the ensemble strategy, **limiting for the wind variable the results to a total of 5-7 CMIP6 models.** A summary of the results is displayed in Table A3.1.

Figures displayed showcase results of the MAE statistic (Figure A3.14 and A3.17), and of an evaluation of model behaviour around percentiles at monthly scale (Figure A3.15 and A3.18) as well as their distribution around other percentiles or fixed wind thresholds at annual scale (Figure A3.16 and A3.19) after correction and application of FICLIMA method.

Table A3.1. Validation results for all three ICARIA's CS of wind gust variable considering the performance from each of the 7 models used. After evaluation of the models performance from MAE and monthly bias, the final assessment of those used is presented. Green means "ok", yellow "good but use with care" and red "dismissed".

Models	Validation results for wind gust in each case study		
	AMB	SAR	SLZ
ACCESS-CM2			
CanESM5			
CMCC-ESM2			
CNRM-ESM2-1			
EC-EARTH3			
MPI-ESM1-2-HR			
MRI-ESM2-0			

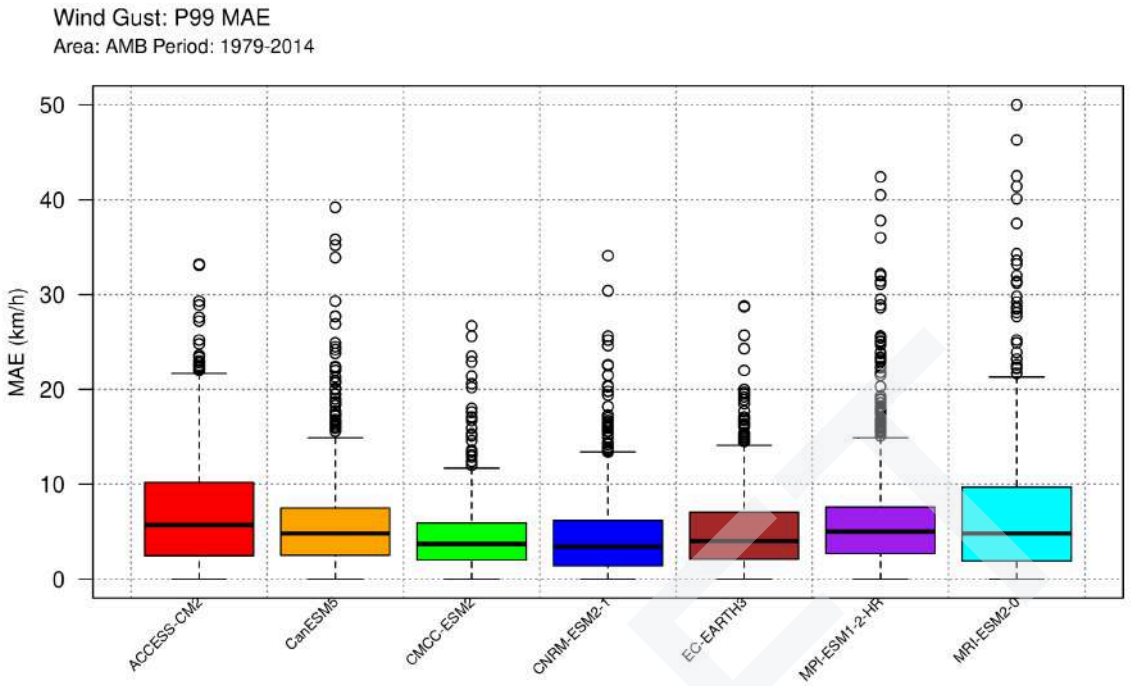

Figure A3.14. Validation results for **AMB** of wind gust considering the statistical MAE value before after the correction of the 7 CMIP6 models considered and the application of FICLIMA method.

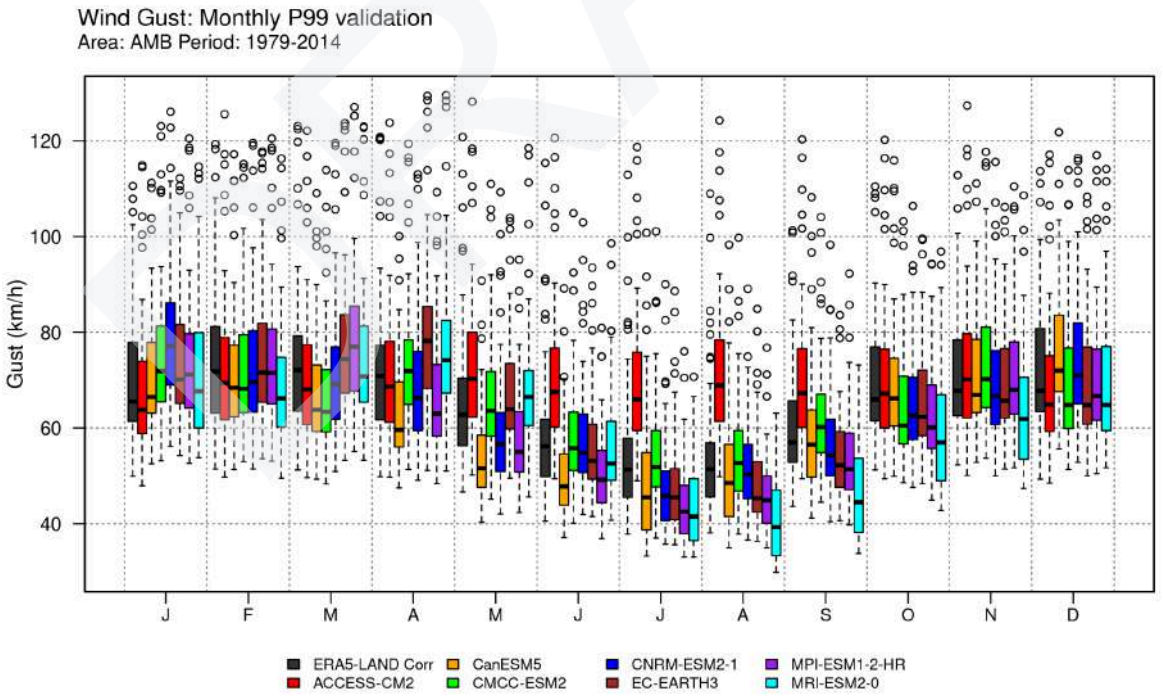

Figure A3.15. Validation results for **AMB** of monthly wind gust percentile 99th values after the correction of all the 7 CMIP6 models considered and the application of FICLIMA method.

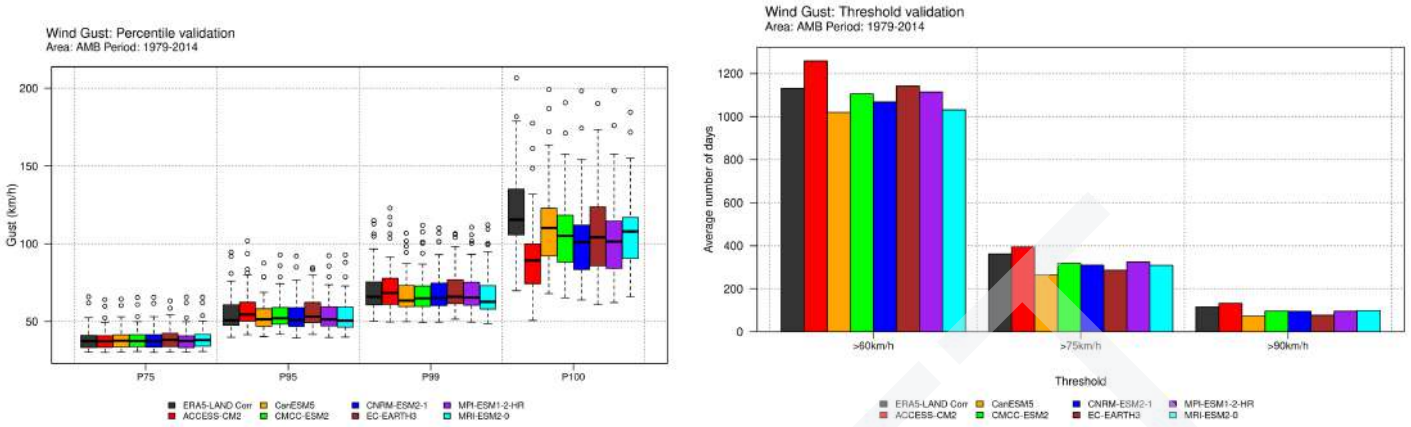

Figure A3.16. Validation results for **AMB** of several wind gust percentiles and threshold values after the correction of all the 7 CMIP6 models considered and the application of FICLIMA method.

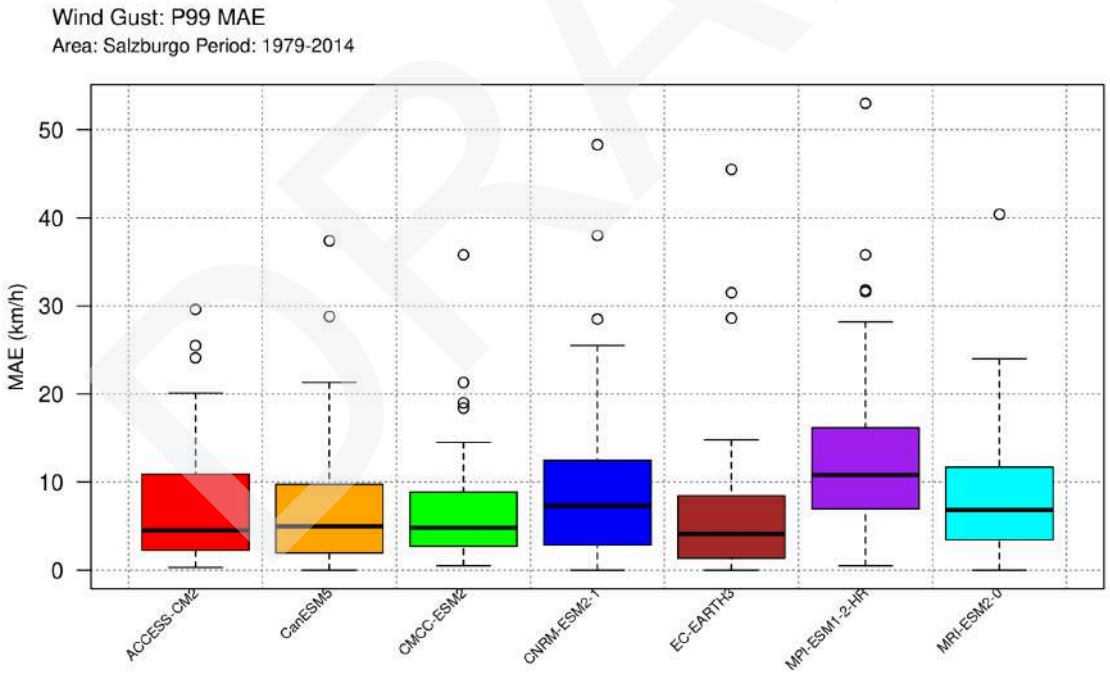

Figure A3.17. Validation results for **SLZ** of wind gust considering the statistical MAE value before after the correction of the 7 CMIP6 models considered and the application of FICLIMA method.

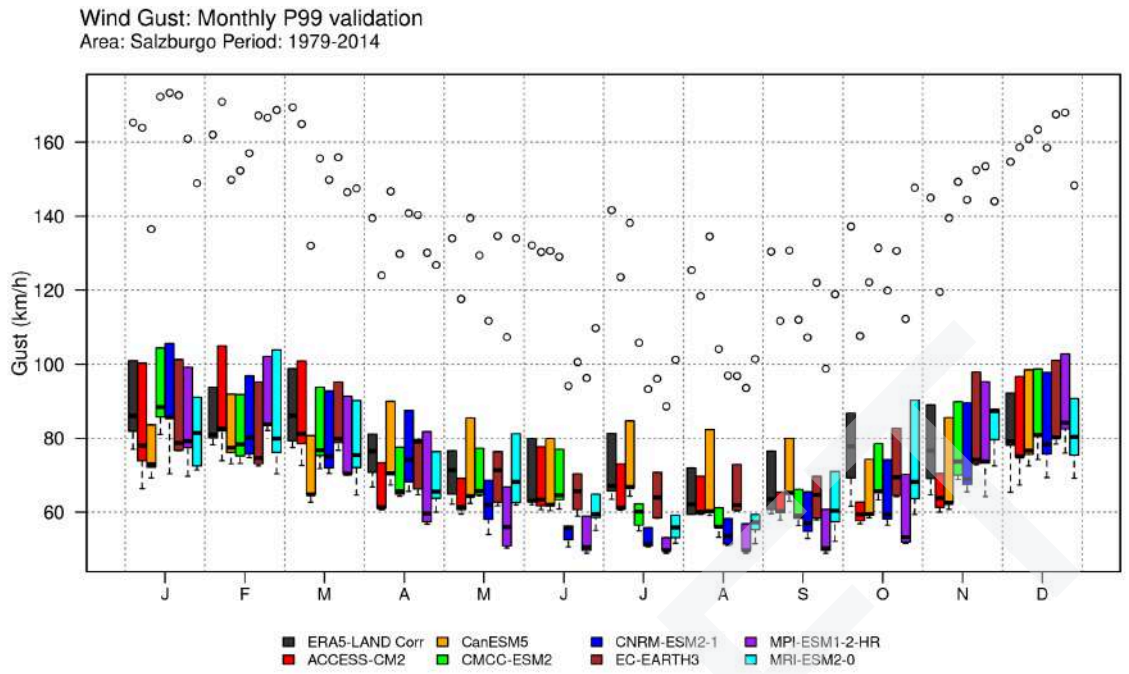

Figure A3.18. Validation results for **SLZ** of monthly wind gust percentile 99th values after the correction of all the 7 CMIP6 models considered and the application of FICLIMA method.

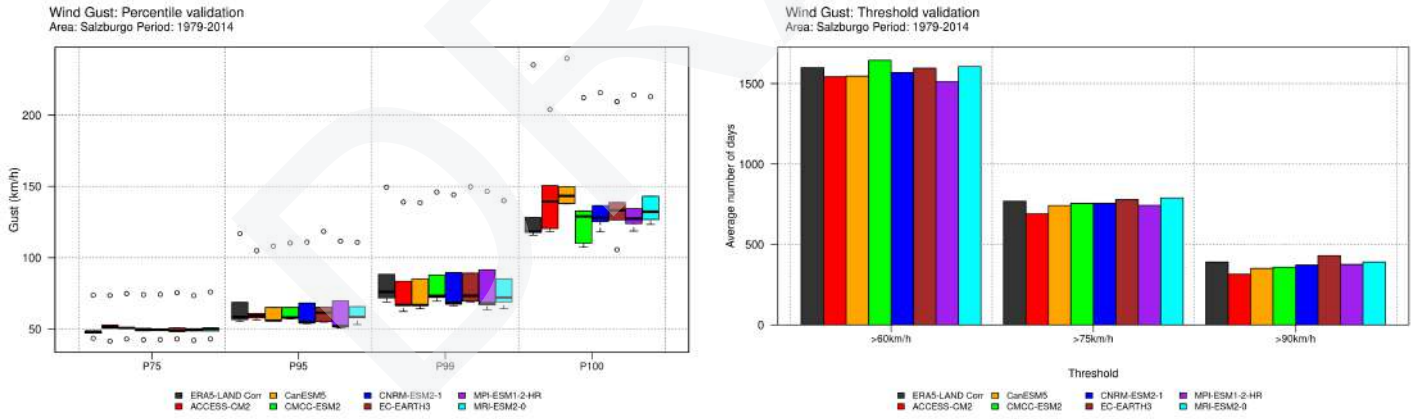

Figure A3.19. Validation results for **SLZ** of several wind gust percentiles and threshold values after the correction of all the 7 CMIP6 models considered and the application of FICLIMA method.

Projection uncertainty

The cascade of uncertainties in climate simulation at the local scale within ICARIA's FICLIMA method stems from four primary sources: (1) the employed statistical downscaling method (verification process), (2) the selection of models/runs and the performance of the method/models (validation processes), (3) the inclusion of SSP scenarios, and (4) the inherent natural variability in climate.

The last two sources of uncertainty are addressed through the implementation of an ensemble strategy. Following bias correction across all models, an ensemble is created by combining these models, providing an estimation of the uncertainty attributed to both past and future climate variability. This ensemble is executed for each SSP scenario to assess the impact of potential future economic conditions. All climate projections are conducted for yearly averages, considering both absolute and relative changes when necessary.

It's important to note that climate projections are not regarded as forecasts because they are simulated under various SSP scenarios, the likelihood of which is contingent upon decisions made by politicians and citizens.

The ensemble of climate projections is visually represented through uncertainty areas, specifically considering the 10th–90th percentile values and the median value for each year horizon. These values are calculated based on all stations and models validated for each climate variable, as illustrated in Figure A3.20.

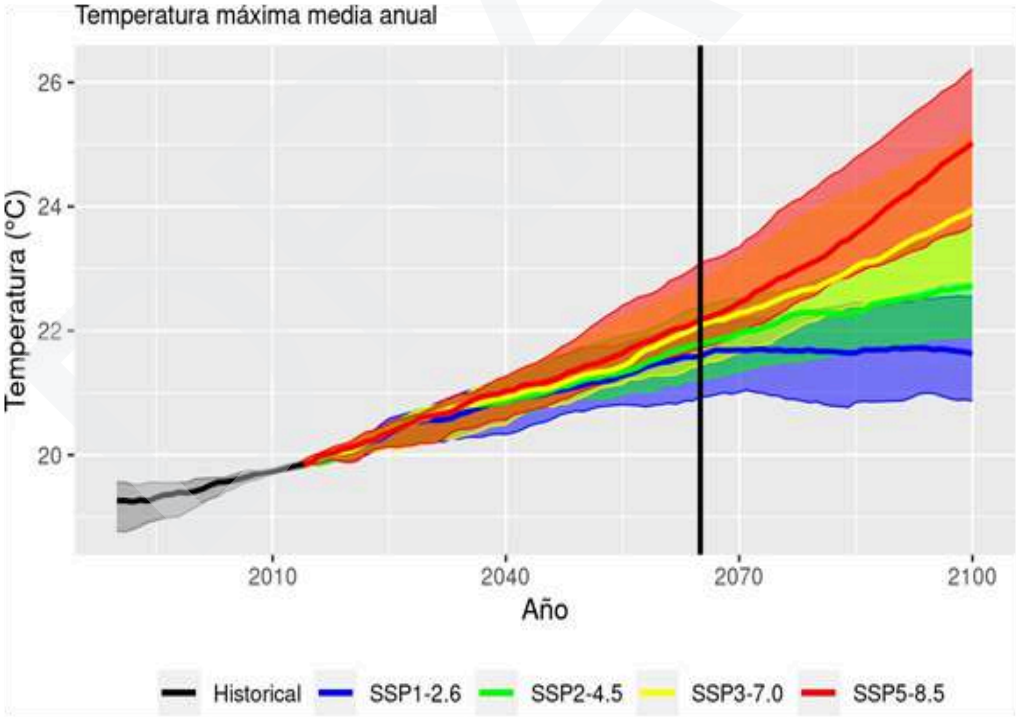

Figure A3.20. Example of ensemble strategy. Figure shows climate projections of changes in maximum annual temperature for a random city. The ensemble median (solid lines) and the 10th–90th percentile values (shaded areas) are displayed. Gray area represents the Historical data up to year 2015. Vertical black line shows in this particular example a moment of increase in uncertainty.

3.2. Verification of Dynamical downscaling - AIT

To verify the quality of the used regional climate models, so-called hindcast simulations (1980 - 2014), where ERA5 is used to initialize the RCMs, were performed. This approach allows the comparison of the RCM output with observation based re-analysis data. Within ICARIA the 1km² data set CHELSA (Karger et al., 2021) is used.

The description of the dataset is taken from ISIMIP[12]:

The CHELSA-W5E5 dataset was created to serve as observational climate input data for the impact assessments carried out in phase 3a of the Inter-Sectoral Impact Model Intercomparison Project (ISIMIP3a).

Version 1.0 of the CHELSA-W5E5 dataset covers the entire globe at 30 arcsec horizontal and daily temporal resolution from 1979 to 2016. Data sources of CHELSA-W5E5 are version 1.0 of WFDE5 over land merged with ERA5 over the ocean (W5E5; Lange, 2019; Cucchi et al., 2020), the ERA5 global reanalysis (Hersbach et al. 2020) and the Global Multi-resolution Terrain Elevation Data 2010 (GMTED2010; Danielson and Gersch, 2011).

Variables (with short names and units in brackets) included in the CHELSA-W5E5 dataset are Daily Mean Precipitation (pr, kg m-2 s-1), Daily Mean Surface Downwelling Shortwave Radiation (rsds, W m-2), Daily Mean Near-Surface Air Temperature (tas, K), Daily Maximum Near Surface Air Temperature (tasmax, K), Daily Minimum Near Surface Air Temperature (tasmin, K), Surface Altitude (orog, m), and the CHELSA-W5E5 land-sea mask (mask, 1). Version 1.0.1 of this dataset resolved the caveat described at https://data.isimip.org/caveats/6/. Version 1.0.2 added data with coarser resolution (90 arcsec = 1.5 arcmin, 360 arcsec = 6 arcmin, 1800 arcsec = 30 arcmin = 0.5°), which were generated from version 1.0.1 of the 30 arcsec data via spatial aggregation.

Methods:

CHELSA-W5E5 v1.0 is a downscaled version of the W5E5 v1.0 dataset, where the downscaling is done with the CHELSA v2.0 algorithm (Karger et al. 2017, Karger et al. 2021). In the following we outline how this algorithm works. The CHELSA algorithm applies topographic adjustments based on the surface altitude, orog, from GMTED2010. Since it does not add any value over the ocean, all values over the ocean are masked. The CHELSA algorithm is applied day by day. CHELSA-W5E5 tas is obtained by applying a lapse rate adjustment to W5E5 tas, using differences between CHELSA-W5E5 orog and W5E5 orog in combination with temperature lapse rates from ERA5. Those lapse rates are calculated based on atmospheric temperature, ta, at 950 hPa and 850 hPa, and the geopotential height, zg, of those pressure levels. The lapse rate used for the adjustment is calculated as the daily mean of hourly values of (ta_850-ta_950)/(zg_850-zg_950). The variables tasmax and tasmin are downscaled in the same way, using the same lapse rate value.

Precipitation downscaling uses daily mean zonal and meridional wind components from ERA5 to calculate the orographic wind effect and combines that with the height of the planetary boundary layer to approximate the total orographic effect on precipitation intensity. Using that, precipitation from W5E5 is

[12] https://data.isimip.org/10.48364/ISIMIP.836809.2

downscaled such that precipitation fluxes are preserved at the original 0.5° resolution of W5E5. More details are given in Karger et al. (2021).

Surface downwelling shortwave radiation, rsds, at 30 arcsec resolution is strongly influenced by topographic features such as aspect or terrain shadows, that are less pronounced at 0.5° resolution. The downscaling algorithm combines such geometric effects with orographic effects on cloud cover for an orographic adjustment of rsds. Geometric effects are considered by computing 30 arcsec clear-sky radiation estimates using the method described in Böhner and Antonic (2009) and a simplified, uniform atmospheric transmittance of 80 %. These effects include shadowing from surrounding terrain, diffuse radiation based on reflectance from surrounding terrain, and terrain aspect. To include how orographic effects on cloud cover influence rsds, the clear-sky radiation estimates are adjusted using downscaled ERA5 total cloud cover. The cloud cover downscaling uses ERA5 cloud cover at all pressure levels and the orographic wind field. For details see Karger et al. (2022, in preparation). Finally, the clear-sky radiation estimates adjusted for cloud cover are rescaled such that they match W5E5 rsds, B-spline interpolated to 30 arcsec.

For brevity reasons, only the verification results for Salzburg for selected indicators are displayed. Within a planned publication, the results for both Salzburg and the South Aegean region will be presented.

The mean monthly temperatures for CHELSA and CLM, as well as for heights below and above 1500m are displayed below. CLM captures well the overall structure of warmer or colder months, but displays overall slightly lower temperatures than CHELSA, with the differences being more pronounced during the winter months. A similar distribution is seen within WRF (Figure A3.22). Overall, is the performance of the models with respect to the mean monthly temperature satisfactory.

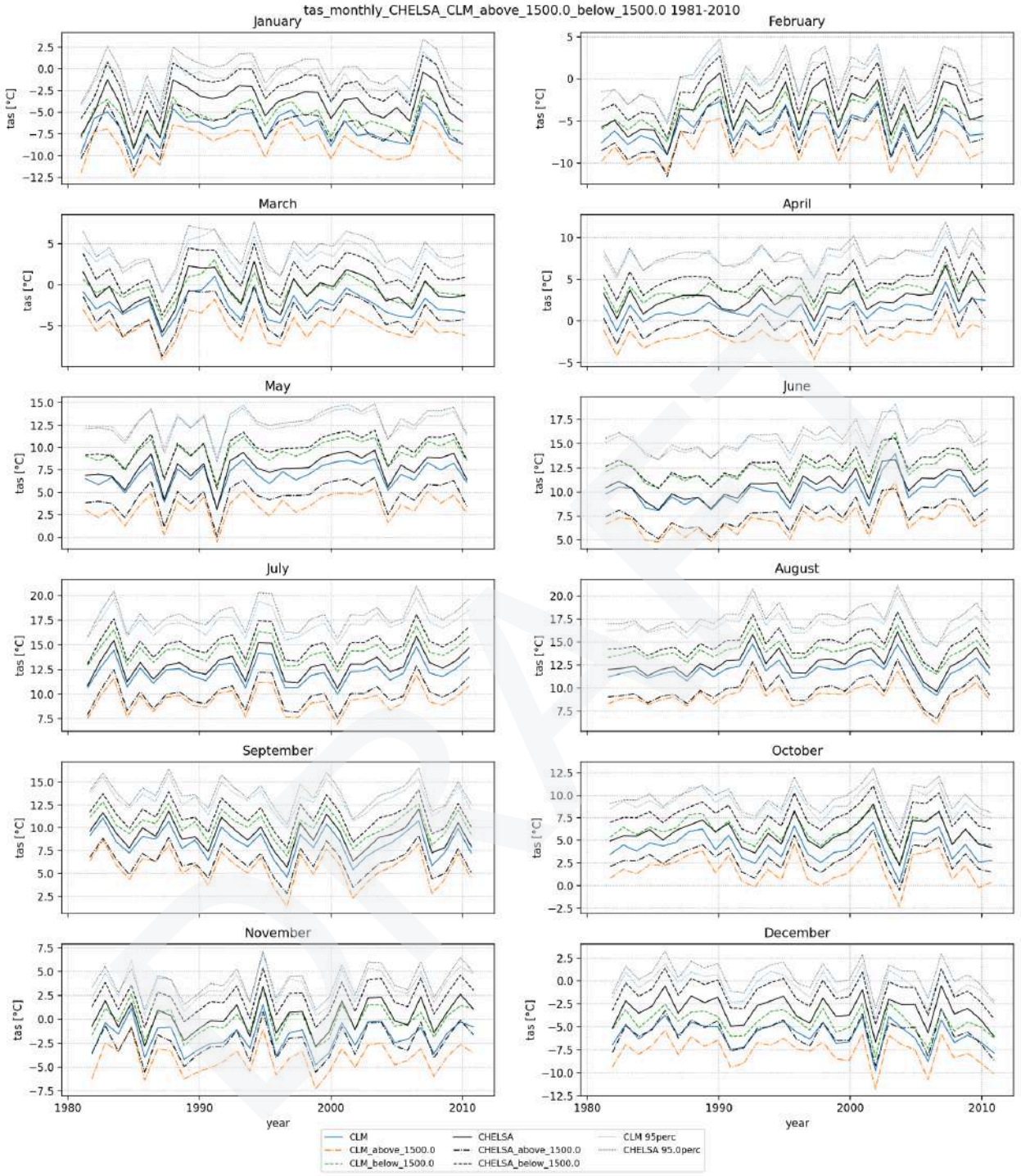

Figure A3.21: spatial average: monthly mean temperature of CHELSA (black) and CLM (blue) above (orange) and below (green)

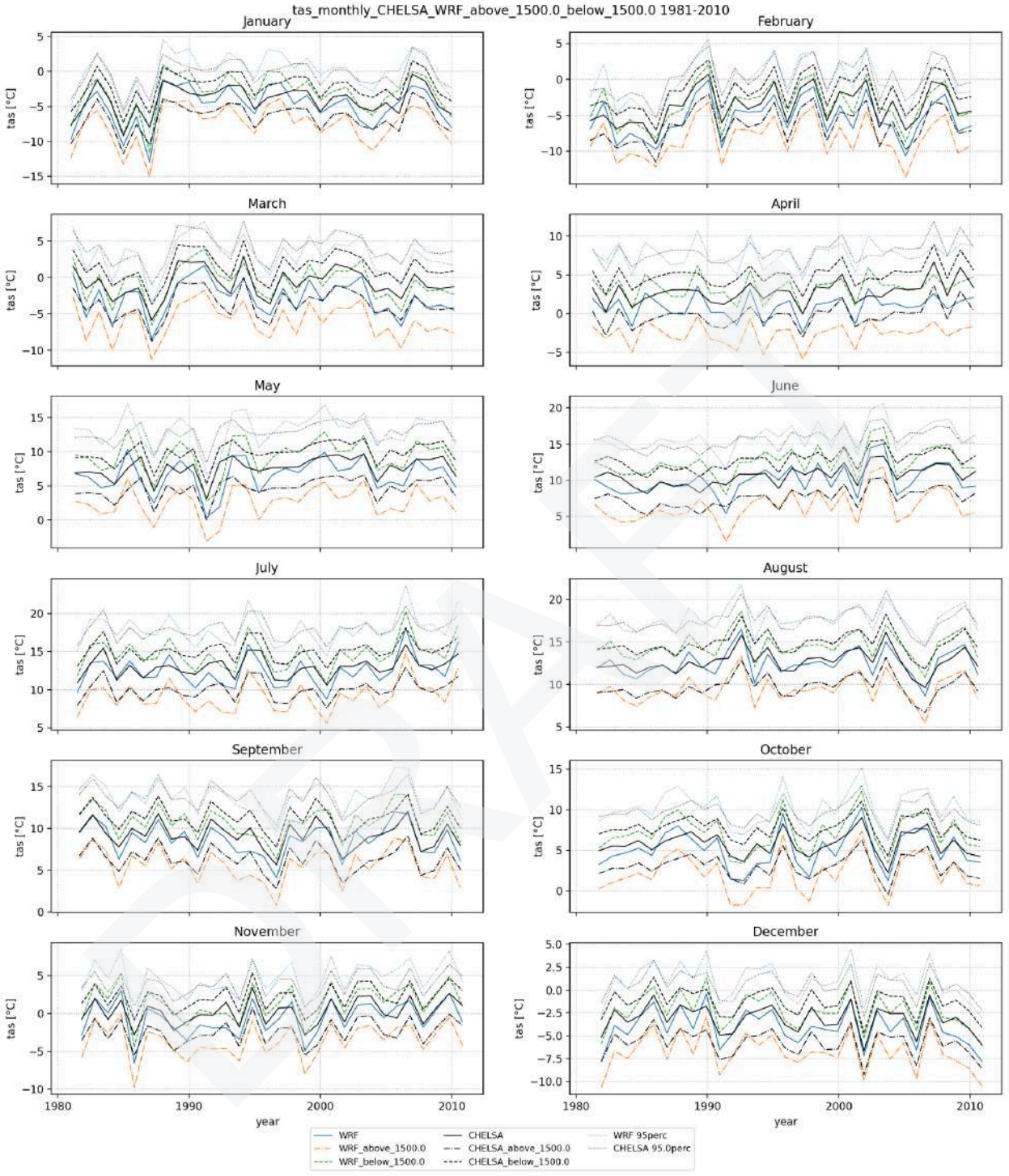

Figure A3.22: spatial average: monthly mean temperature of CHELSA (black) and WRF (blue) above (orange) and below (green)

Apart from the mean monthly temperatures, the models' ability to represent heat or drought are crucial.

To better analyse spatial (in)consistencies between models and verification database, the monthly mean temperatures are displayed. WRF better represents the spatial distribution of mean monthly temperature in January than CCLM as displayed in Figure A3.23. This is also depicted within the bias and RMSE, where the underestimated temperatures within the valleys in CCLM are apparent.

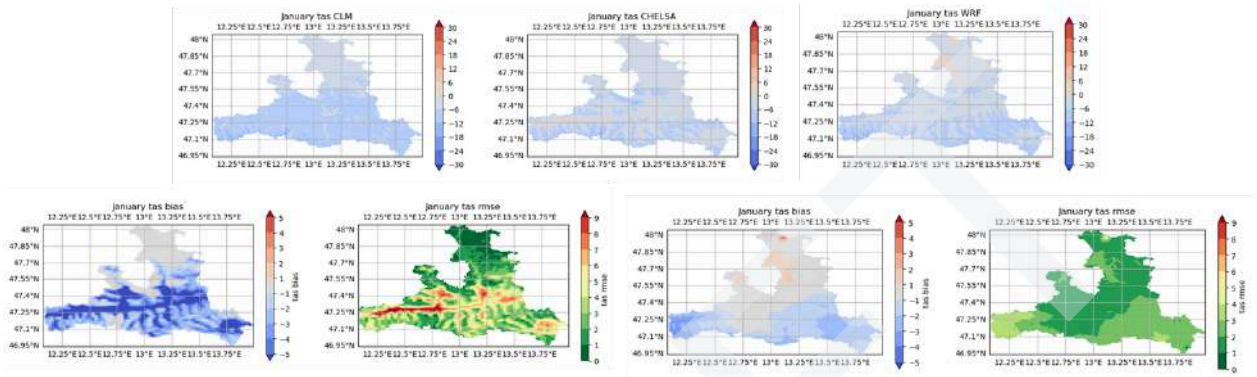

Figure A3.23: mean January temperature (1981 - 2010) top row: CCLM, CHELSA, WRF; bottom row: BIAS CCLM-CHELSA left, WRF - CHELSA right

The analysis of the July mean temperatures display similar characteristics within CCLM and WRF, both models underestimating the summer temperatures within the higher altitudes and mainly underestimating it within the other areas. WRF displays higher error values than CCLM.

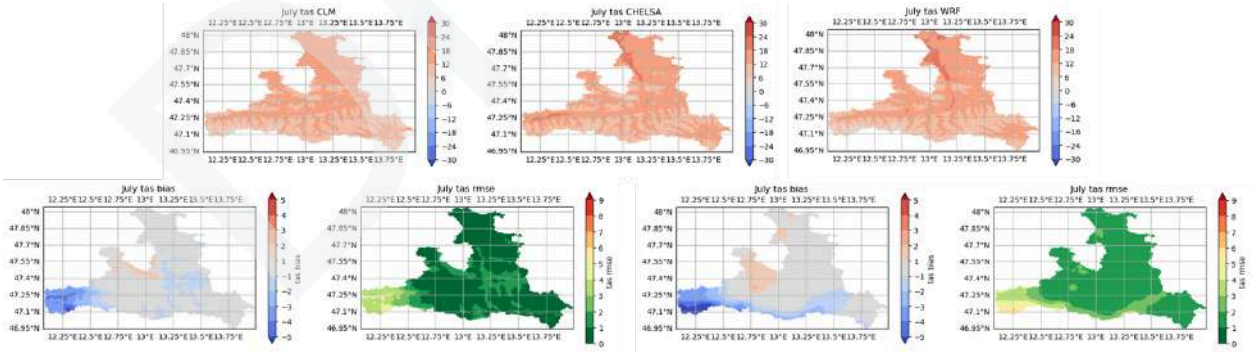

Figure A3.24: mean July temperature (1981 - 2010) top row: CCLM, CHELSA, WRF; bottom row: BIAS CCLM-CHELSA left, WRF - CHELSA right

When looking at the July precipitation rate, the cold bias within the south of Salzburg relates to a strong overestimation of rain rates. Yet, it is important to consider that observations within steep topography are prone to errors, thus CHELSA might underestimate the actual rain rates.

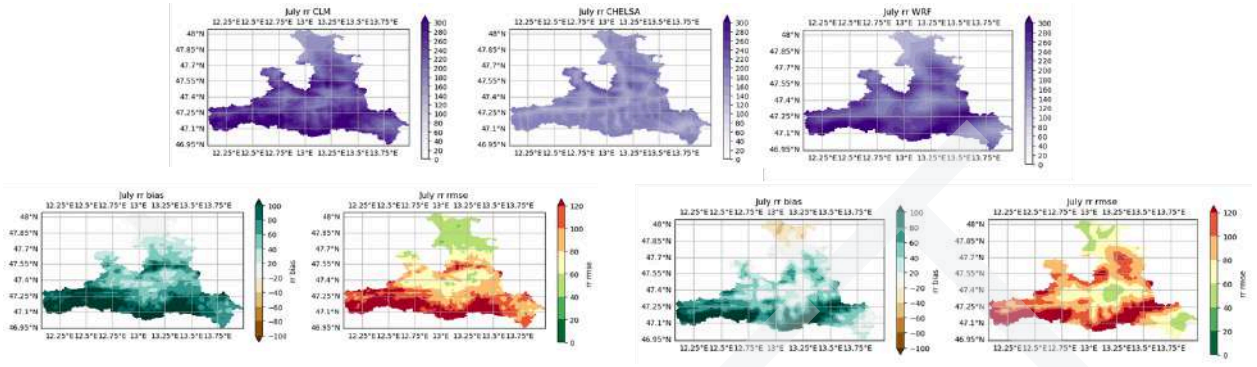

Figure A3.25: mean July precipitation rate (1981 - 2010) top row: CCLM, CHELSA, WRF; bottom row: BIAS CCLM-CHELSA left, WRF - CHELSA right

The monthly skill to simulate the rain rate of CCLM and WRF in comparison to CHELSA and distinguished between height is shown below. Both models capture the pattern of the precipitation (years with a lot or less precipitation), yet, the absolute values are overestimated, especially within WRF.

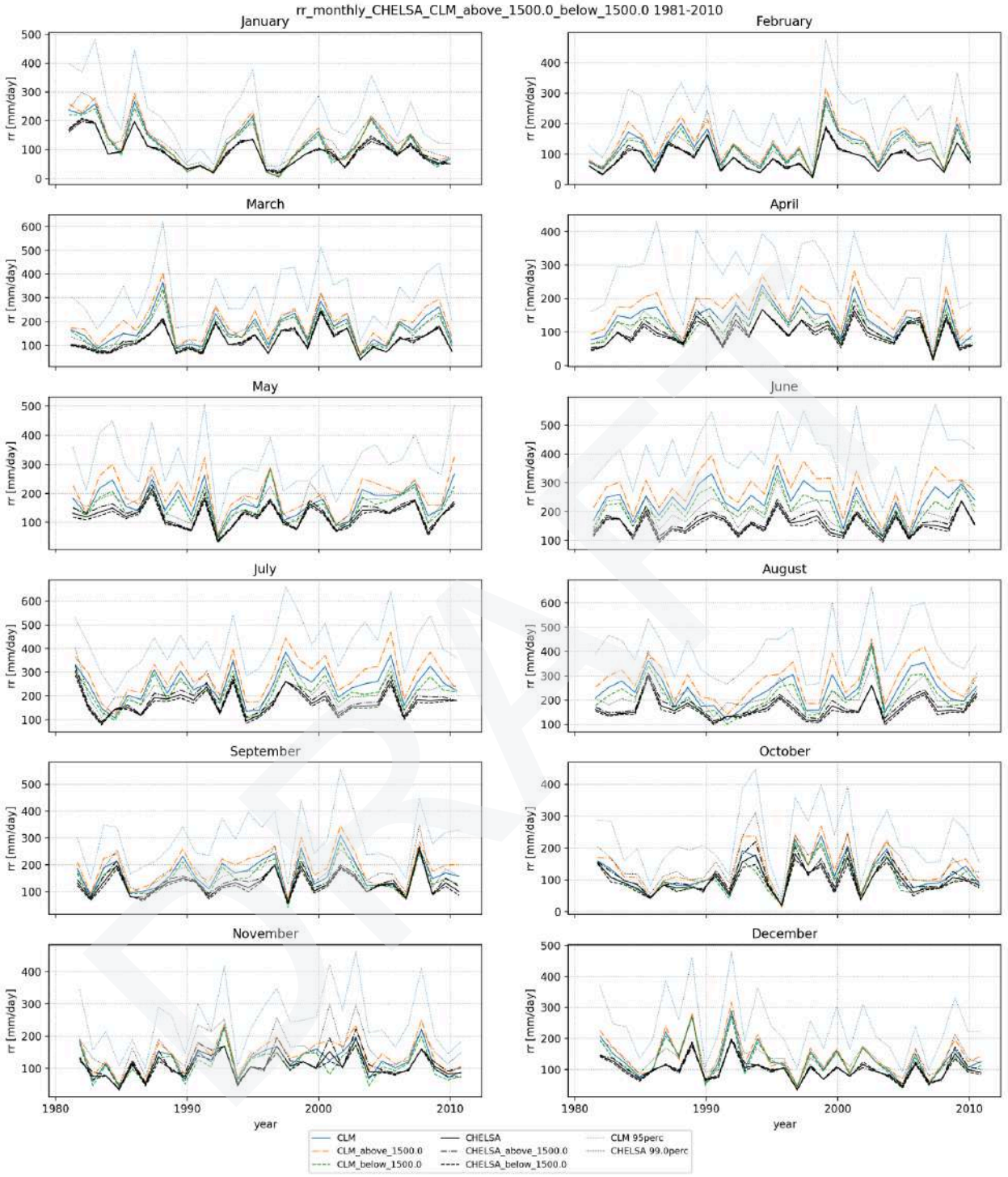

Figure A3.26: spatial average: monthly mean precipitation rate of CHELSA (black) and CCLM (blue) above (orange) and below (green)

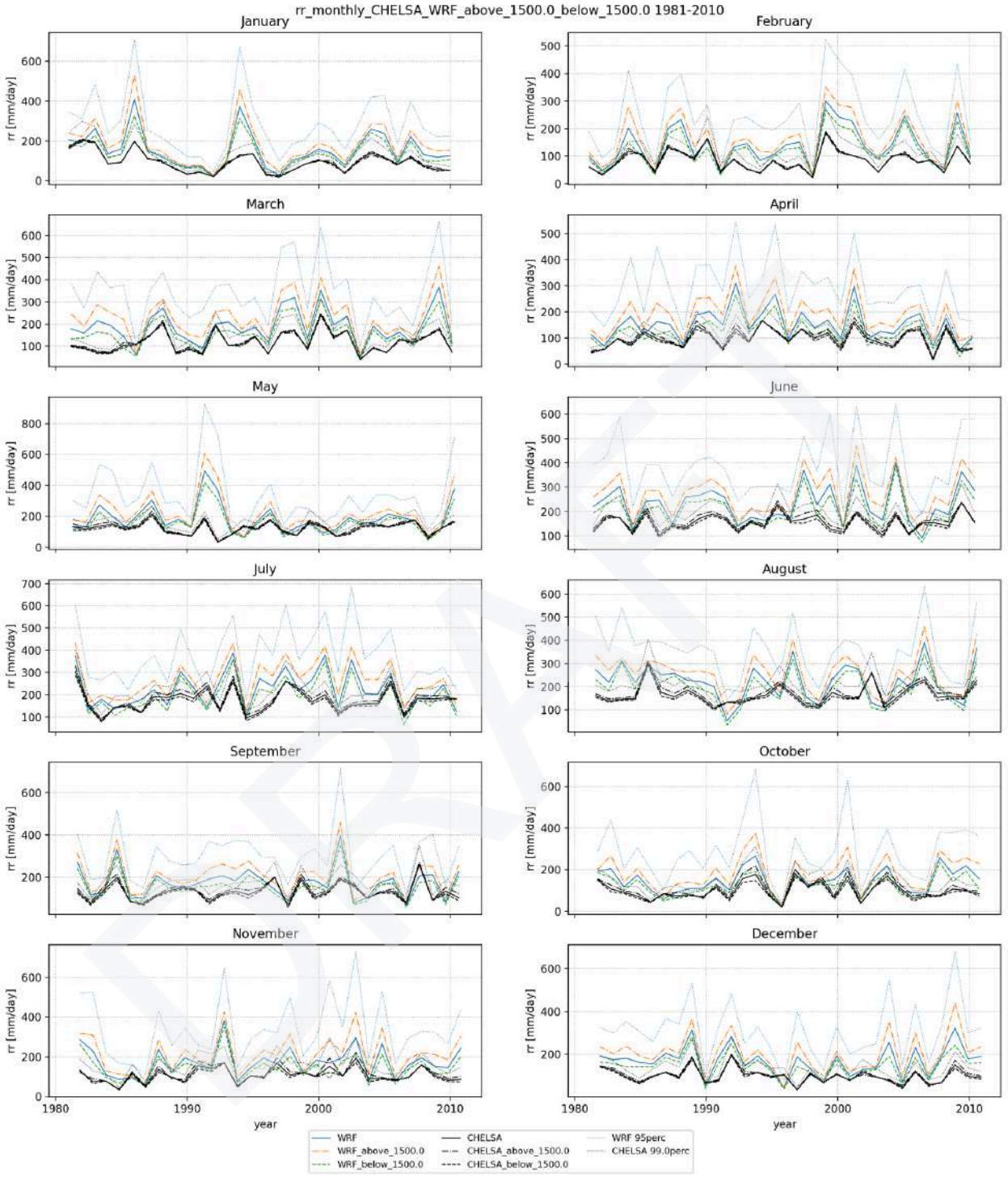

Figure A3.27: spatial average: monthly mean precipitation rate of CHELSA (black) and WRF (blue) above (orange) and below (green)

4. Definition of climate change extreme indicators

In this annex, all the indicators that have been calculated and analysed to characterise future climate and also extreme events changes, and that were first mentioned in section 4 and listed in Table 10 ant Table 11, are described hereafter.

Thermal indicators

1) Warm/cold days

The definition of warm/cold days is taken after a quantile analysis of the local climate data, defining it as a day whose maximum/minimum value goes beyond the 90%/10% quantile of its historical values for that precise climate day. This indicator has the potential to be applied anywhere since its core definition relies on the local climate by using an empirical threshold instead of a fixed temperature value; this is, the threshold would vary depending on the place considered.

2) Heat day

A heat day (and the number of them of the indicator) is defined as a day whose maximum temperature reaches or exceeds the 30ºC threshold. This indicator is based on a fixed value, being therefore an indicator that relies on the known impact of this temperature threshold and does not depend on local climate. It is scalability is not appropriate but has a great value in certain climate areas of the world.

3) Extreme heat day

A heat day (and the number of them of the indicator) is defined as a day whose maximum temperature reaches or exceeds the 35ºC threshold. This indicator is based on a fixed value, being therefore an indicator that relies on the known impact of this temperature threshold and does not depend on local climate. It is scalability is not appropriate but has a great value in certain climate areas of the world.

4) Tropical nights

The number of tropical nights per year has been obtained as the sum of the number of days in which the daily minimum temperature is greater than or equal to 20ºC for each year of the period in question. For example, for the reference period 1981-2010, for each of the 30 years considered, the number of times that the daily minimum temperature exceeds or equals 20ºC is counted.

5) Equatorial nights

The number of equatorial nights per year has been obtained as the sum of the number of days in which the daily minimum temperature is greater than or equal to 25ºC for each year of the period in question. For example, for the reference period 1981-2010, for each of the 30 years considered, the number of times that the daily minimum temperature exceeds or equals 25ºC is counted.

6) Infernal nights

The number of infernal nights per year has been obtained as the sum of the number of days in which the daily minimum temperature is greater than or equal to 30ºC for each year of the period in question. For example, for the reference period 1981-2010, for each of the 30 years considered, the number of times that the daily minimum temperature exceeds or equals 30ºC is counted.

7) Frost days

The number of frosts days (strictly speaking, the number of frost nights) has been obtained as the sum of the number of days in which the daily minimum temperature is less than or equal to 0ºC for each year of the period in question. For example, for the reference period 1981-2010, for each of the 30 years considered, the number of times that the daily minimum temperature equals or falls below 0ºC is counted.

8) Maximum spell length of thermal indicators

For all the previous indicators (from 1-7), aside from the number of days that fall within the description given for each year, an additional step has been added by calculating the maximum number of consecutive days (spell) that each indicator applies. Here is therefore possible to assess the worst-case scenario of not just suffering this event but also its persistence in time within an area.

9) Number of events of thermal indicators

For all the previous single indicators (from 1-7), aside from the number of days that fall within the description given for each year, an additional step has been added by calculating the number of events that each indicator applies. An event has been defined as a spell of at least 3 consecutive days where the indicator is valid. Here is therefore possible to assess a scenario of not just suffering this event but also its persistence in time and the frequency of these events impact within an area.

10) Mean maximum temperature

The mean maximum temperature for each period and time range - where the time ranges considered have been both annual and seasonal - has been obtained by calculating the average of the daily maximum temperatures for each year of the specific time range of the period in question. For example, for the reference period 1981-2010, for each of the 30 years considered, the daily maximum temperature data associated with the time range of interest (annual or seasonal) is taken, and the average is calculated.

11) Mean minimum temperature

The mean minimum temperature for each period and time range - where the time ranges considered have been both annual and seasonal - has been obtained by calculating the average of the daily minimum temperatures for each year of the specific time range of the period in question. For example, for the reference period 1981-2010, for each of the 30 years considered, the daily minimum temperature data associated with the time range of interest (annual or seasonal) is taken, and the average is calculated.

12) Mean temperature

The Mean temperature for each period and time range - where the time ranges considered have been both annual and seasonal - has been obtained by calculating the average of the daily mean temperatures for each year of the specific time range of the period in question. For example, for the reference period 1981-2010, for each of the 30 years considered, the daily mean temperature data associated with the time range of interest (annual or seasonal) is taken, and the average is calculated

13) Heat waves

A heat wave is meant to be an extremely high-temperature event that poses a risk for the human health, infrastructure and other critical assets. For a temperature event like this, in order to consider it extreme enough to be classified as a hazard and affect the normal development of local activities, it should cover a set of requirements such as:

- High intensity. Temperature values need to be extremely high related to what is common in the local climate. This is to suppose a risk for the way infrastructure was previously designed and to what human bodies are normally used to deal with. With this, values need to be above the average maximum values registered in the warmest period of the year, i.e. summer.
- Low frequency. Linked to the previous point, a heat wave should be rare to suppose an event extreme as a definition linked to a probability distribution of the local climate. Percentiles are therefore a good approach in this sense.
- Certain duration in time. For a temperature-related event, it is proved that the impact and risk grow bigger the more time it lasts rather than a great intensity event of some hours of duration. This is so since a long-time event will have the time to impact infrastructure (materials, thermal isolation…) and activities (leisure, outside labour) as well as the health of the population (worse rest, thermal shock…).

Following these points, and including the particularities of the climate distributions of the case studies, an agreement was made to adapt the Heat Wave definition made by the Spanish AEMet to apply it to ICARIA, being this as:

Heat wave: *a temperature-related episode of at least three consecutive days where the weather observations considered register maximum temperatures above the 95% percentile of their daily maximum temperature records for the months of June to September of the 1981-2010 period.*

A heat wave episode is analysed based on several characteristics for each of which a different indicator has been defined:

13.1. Average length of Heat waves

The average length of a heat wave episode is defined as the number of consecutive days in which the maximum temperature is above the set threshold. It is calculated for each of the 30 years of each period in question. In the case of more than one heat wave in the same year, the value is obtained as the average of all cases.

13.2. Average intensity of Heat Waves

The average intensity of a heat wave episode is the average of the maximum temperature values recorded on the days constituting the heat wave episode. It is calculated for each of the 30 years of each period in question. If more than one heat wave in the same year, the value is the average of all.

13.3. Maximum intensity of Heat Waves

The maximum intensity of a heat wave episode is the most extreme value of the maximum temperature values recorded on the days constituting the heat wave episode. It is calculated for each of the 30 years of each period in question. If more than one heat wave in the same year, the value is the average of all.

13.4. Number of Heat Waves

The average number of heat waves per year makes it possible to analyse possible trends in the increase or decrease in the occurrence of this type of phenomena. It is calculated for each of the 30 years of each period in question.

13.5. Number of days with maximum temperatures over Heat Wave threshold

The number of days with Tmax > T(P95) (1981-2010 JJAS) expresses the number of days per year where the daily maximum temperature is higher than the 95th percentile obtained for the reference period 1981-2010 between the months of June to September (inclusive). In this way, it is possible to quantify the number of days in which the temperature threshold necessary to consider a Heat Wave episode is exceeded, although it is not considered as such because it does not reach the minimum number of consecutive days with a maximum temperature above the established threshold value.

14) Heat Index (HI)

As a plus to considering heatwaves for temperature events, and under requirements from some of the attendees, a step beyond this work was agreed to be made in order to consider also the Heat Index, being acknowledged that in northern countries (such as Austria), heat waves tend to happen linked to relatively high relative humidity values, which add on to pose greater stress and risk for human bodies. In this sense, the standardized USA's NWS Heat Index[13] definition during Heat Wave events will be used, being for degrees Celsius (º C) this:

$$\mathrm{HI} = c_1 + c_2 T + c_3 R + c_4 T R + c_5 T^2 + c_6 R^2 + c_7 T^2 R + c_8 T R^2 + c_9 T^2 R^2$$

using the following coefficients (T=air temperature ºC, R=relative humidity in %):

$$\begin{aligned} c_1 &= -8.784\,694\,755\,56, & c_2 &= 1.611\,394\,11, & c_3 &= 2.338\,548\,838\,89, \\ c_4 &= -0.146\,116\,05, & c_5 &= -0.012\,308\,094, & c_6 &= -0.016\,424\,827\,7778, \\ c_7 &= 2.211\,732 \times 10^{-3}, & c_8 &= 7.2546 \times 10^{-4}, & c_9 &= -3.582 \times 10^{-6}. \end{aligned}$$

[13] https://www.weather.gov/ama/heatindex

HEAT INDEX CHART

AIR TEMPERATURE (°C)	RELATIVE HUMIDITY								
	10%	20%	30%	40%	50%	60%	70%	80%	90%
26	25	25	26	26	27	27	27	28	28
27	26	26	26	27	27	28	29	30	31
28	27	27	27	28	28	29	31	32	34
29	27	27	28	29	30	31	33	35	37
30	28	28	29	30	31	33	35	38	41
31	29	29	30	31	33	35	38	41	45
32	30	30	31	32	34	37	40	44	49
33	31	31	32	34	36	40	43	48	54
34	31	32	33	35	38	42	47	52	> 54
35	32	33	35	37	41	45	50	> 54	> 54
36	33	34	36	39	43	49	54	> 54	> 54
37	34	35	38	41	46	51	> 54	> 54	> 54
38	35	37	39	43	49	> 54	> 54	> 54	> 54
39	36	38	41	46	52	> 54	> 54	> 54	> 54
40	37	39	43	48	> 54	> 54	> 54	> 54	> 54
41	38	41	45	51	> 54	> 54	> 54	> 54	> 54
42	39	42	47	54	> 54	> 54	> 54	> 54	> 54
43	40	44	49	> 54	> 54	> 54	> 54	> 54	> 54
44	41	46	52	> 54	> 54	> 54	> 54	> 54	> 54
45	42	47	54	> 54	> 54	> 54	> 54	> 54	> 54
46	43	49	> 54	> 54	> 54	> 54	> 54	> 54	> 54
47	44	51	> 54	> 54	> 54	> 54	> 54	> 54	> 54
48	45	53	> 54	> 54	> 54	> 54	> 54	> 54	> 54
49	47	> 54	> 54	> 54	> 54	> 54	> 54	> 54	> 54
50	48	> 54	> 54	> 54	> 54	> 54	> 54	> 54	> 54

Figure A4.1. Example of a Heat Index chart with the estimated values of HI with Celsius ºC.

15) Universal Thermal Climate Index (UTCI)

The Universal Thermal Climate Index (UTCI) serves as a bioclimatic indicator to characterize the physiological comfort of the human body in specific meteorological situations (Bröde et al., 2012). The UTCI is defined as the air temperature (Ta) of the reference condition causing the same model response as the actual condition. The discrepancy, or offset, between UTCI and air temperature depends on the actual values of air temperature, mean radiant temperature (Tr), wind speed (va), and humidity, expressed as either water vapour pressure (pa) or relative humidity (RH), as shown below:

$$UTCI(Ta,Tr,va,pa) = Ta + Offset(Ta,Tr,va,pa)$$

16) Urban Heat Island effect (UHI)

The intensity of the heat island is the temperature difference between the warmest sector of the city and the non-urban space surrounding the city at a given time of the city and the non-urban space surrounding the city at a given time. Formally,

$$\Delta Tu\text{-}r = Tu - Tr$$

where ΔTu-r is the intensity of the heat island, Tu is the temperature of a point in the (warm) center of the city and Tr is the temperature of a point in the center of the city (warm) point of the city and Tr , the temperature of a rural or non-urban point close to the city. These places are selected as AEMet Vila Olimpica de Barcelona (0201D) station and Barcelona Airport (0076) station. In order to work in future times, the mean of daily values obtained from the calculation of UHI is done at annual and seasonal scale.

Drought indicators

17) Dry spell duration

This indicator simply comes to define as a "dry spell" the amount of consecutive days in which the amount of precipitation registered at a certain point does not exceed 1mm. To improve the detail of the information provided, two sub-indicators were defined based on the previous definition, which are the maximum length of this spell, and its mean duration.

18) Standardised Precipitation Index (SPI)

The Standardized Precipitation Index (SPI, Standard Precipitation Index) (McKee et al.,1993) is defined as a numerical value representing the number of standard deviations of the precipitation falling over the accumulation period in question, with respect to the mean, once the original distribution of precipitation has been transformed to a normal distribution.

In this way, a scale of values is defined which is grouped in sections related to the character of the precipitation (Table AX). It has the advantage of being able to work on temporal scales by identifying different types of droughts and their responses to different natural systems. It is based on two assumptions:

1) The variability of precipitation is greater than that of temperature and potential evapotranspiration (PET).

2) All other variables are stationary over time. It is one of the most widely used indices in recent decades as it has a solid, robust and versatile basis. It can be calculated at different scales, so that the SPI at 3 months will represent the short and medium term, e.g. seasonal precipitation; at 6 months it represents the medium term, e.g. potential precipitation deficit; and at 12, 24 and 60 months it represents long-term precipitation patterns with impact on water supplies.

Table A4.1. Climate classification depending on the Standardized Precipitation Index (SPI).

Climate type SPI	Thresholds
Extremely wet	SPI ⩾ 2.0
Severely wet	1.50 ⩽ SPI < 2.00
Moderately wet	0.50 ⩽ SPI < 1.50
Normal	-0.50 ⩽ SPI < 0.50
Moderately dry	-1.50 ⩽ SPI < -0.50
Severely dry	-2.00 ⩽ SPI < -1.50
Extremely dry	SPI < -2.00

19) Standardized Precipitation Evapotranspiration Index (SPEI)

The Standardized Precipitation Evapotranspiration Index (SPEI, proposed by Vicente-Serrano et al., -2010-) is a variant of the SPI. It has a higher potential as it is sensitive to the impact of climate change by considering the water balance as the difference between monthly precipitation and potential evapotranspiration (calculated according to Thorntwaite). As with the SPI, a scale of values is defined and grouped into tranches (Table AX).

Table A4.2. Climate classification depending on Standardized Precipitation Evapotranspiration and Precipitation Index (SPEI).

Climate type SPI	Thresholds
Extremely wet	SPEI ⩾ 2.0
Severely wet	1.50 ⩽ SPEI < 2.00
Moderately wet	0.50 ⩽ SPEI < 1.50
Normal	-0.50 ⩽ SPEI < 0.50
Moderately dry	-1.50 ⩽ SPEI < -0.50
Severely dry	-2.00 ⩽ SPEI < -1.50
Extremely dry	SPEI < -2.00

Forest fire indicator

20) Canadian Fire Weather Index (FWI)

The occurrence of forest fires is extremely linked to both human actions and natural causes, with in some countries having around 80-90% (MITECO[14], Spanish Government; BML[15], Austrian Government) of total forest fires being provocated due to human negligence or conscious criminal action. Their occurrence can't be therefore predicted, but the likelihood of a fire set to evolve into a great wildfire can be approached through some indexes that gather surface and atmospheric conditions. For ICARIA it's been agreed that the already widely used Canadian Fire Weather Index (FWI, Stocks et al., 1989) will be taken into account.

The FWI allows us to know how likely it is for a fire to start and propagate considering aspects such as:

- the humidity of the air at the beginning of the afternoon (when it has its lowest value);
- the temperature in the middle of the afternoon (when it has its highest value);
- the 24-hour total precipitation (from noon to noon);
- the maximum speed of the average wind.

More details on the terminology, methodology and application can be found here[16]. The specific variations for the FWI presentation have been taken from the C3S portal app as they were obtained for CMIP5: https://climate.copernicus.eu/fire-weather-index

Table A4.3. FWI classified in 6 classes of danger accordingly to EFFIS[17] danger class levels definition. Fire danger is mapped in 6 classes (very low, low, medium, high, very high and extreme). The fire danger classes are the same for all countries.

Fire Danges Classes	FWI ranges (upper bound excluded)
Very low	< 5.2
Low	5.2 - 11.2
Moderate	11.2 - 21.3
High	21.3 - 38.0
Very high	38.0 - 50.0
Extreme	>= 50.0

[14]https://www.miteco.gob.es/es/biodiversidad/temas/incendios-forestales/estadisticas-datos.aspx
[15]https://info.bml.gv.at/en/topics/forests/forest-and-natural-hazards/forest-fires/forest-fires-in-austria.html
[16] https://doi.org/10.5558/tfc65450-6
[17] http://effis.jrc.ec.europa.eu/about-effis/technical-background/fire-danger-forecast

Precipitation indicators

21) Number of heavy precipitation days

This indicator is defined to assess rainfall days with a remarkable accumulation, with a threshold defined as 24h accumulations of >20mm.

22) Days with extreme heavy rain

This indicator has been taken into consideration after a specific request from AMB CS, being actually defined by them following their interests and previous work done (AMB et. al, 2017). This indicator is defined to assess the extreme rainfall days, very common at the Mediterranean shores, with two thresholds defined to account for different magnitudes of events: total rainfall accumulations (24h) of >50mm, and of >100mm.

23) Yearly and seasonal rainfall absolute change

The accumulated precipitation for each period and time range - where the time ranges considered have been both annual and seasonal - has been obtained by calculating the sum of the daily precipitation for each year of the specific time range of the period in question. For example, for the reference period 1981-2010, for each of the 30 years considered, the daily precipitation data associated with the time range of interest (annual or seasonal) are taken, and the sum is calculated. The results are presented in "mm", accounting for the absolute change regardless of the mean climate rainfall of the area of interest.

24) Yearly and seasonal rainfall relative change

The accumulated precipitation for each period and time range - where the time ranges considered have been both annual and seasonal - has been obtained by calculating the sum of the daily precipitation for each year of the specific time range of the period in question. For example, for the reference period 1981-2010, for each of the 30 years considered, the daily precipitation data associated with the time range of interest (annual or seasonal) are taken, and the sum is calculated. The results are presented in a relative change "%", accounting for the total rainfall change with regard of the actual mean climate rainfall of the area of interest.

25) Climate Change Factor (CCF)

The CCF (or Climate Change Factor) of the IDF (Intensity Duration Frequency) curves is the ratio between the projected SSP IDF scenario (2015-2100) and the historical IDF curves (1951-2014). The IDF curves are obtained by calculating the following: First, the return periods for each observatory and the amount of precipitation associated with each of them by performing a Gumbel distribution (or generalized extreme value distribution). Second, the precipitation intensity factor, calculated using the n index (Monjo, R. 2016) for each time scale. Third, and due to the lack of data (the availability of high temporal resolution is scarce and limited to a few observatories), an extrapolation of the temporal ratio between the high temporal resolution (up to one minute) and the daily resolution of the n-index has been performed. Once all the parameters are calculated for a given duration and return period or frequency, the specific intensity is obtained.

Oceanic indicators

26) Storm surge

The storm surge is calculated by disaggregating the total sea level into three components: the astronomical tide, the mean sea level and the meteorological tide. The meteorological tide represents the residual component of the total sea level itself, and is projected into the future using the analog method carried out by FIClima. From the projections, the return periods corresponding to the extreme events are extracted for each specific period of each climate scenario, which will provide us with a picture of the evolution of the hazard in the coastal area.

27) Significant and maximum wave height

The Significant Wave Height is determined statistically by calculating the average of approximately one-third of the highest waves in a representative sample. This measure is used to characterise the overall state of the sea, considering multiple waves rather than focusing on a single one.

The Maximum Wave Height is defined as the vertical distance between the crest and trough of an individual wave. This parameter is measured under ideal conditions, from the base to the peak of the wave. It is a point metric that highlights the maximum amplitude of a specific wave at a given moment.

Wind indicators

28) Extreme wind gusts

In order to analyze the wind gust extremes, a selection of quantiles was made for each time range to extract the values that can be considered as peaks in the entire data series. This allows us to determine each percentile for each time period and obtain the values in the future.

References

- AEMet 2020, https://aemetblog.es/2020/07/03/noches-muy-calidas-en-las-ciudades-mediterraneas/

- AMB, Altava-Ortiz V, Barrera-Escoda A, Amaro J, Cunillera J, Prohom M, Sairouni A. 2017. Escenaris climàtics futurs a l'àrea metropolitana de Barcelona. Direcció de Serveis Ambientals de l'Àrea Metropolitana de Barcelina (AMB).

- AMB, Metrobs, 2015. Javier Martín-Vide, Víctor M. Artola, Mª José Cordobilla i Mª Carmen Moreno. Barcelona Regional (BR): https://www3.amb.cat/repositori/CANVICLIMATIC/METROBS/METROBS_UHI.pdf

- Arnbjerg-Nielsen, K. (2012) Quantification of climate change effects on extreme precipitation used for high resolution hydrologic design. Urban Water Journal, 9, 57–65. Available from: https://doi.org/10.1080/1573062X.2011.630091

- Baldauf, M., Seifert, A., Förstner, J., Majewski, D., Raschendorfer, M., & Reinhardt, T. (2011). Operational convective-scale numerical weather prediction with the COSMO model: Description and sensitivities. Monthly Weather Review, 139(12), 3887-3905.

- Barr, L., & Nider, S. (2015). Critical Infrastructure & Climate Adaptation. The CIP Report, 20th August 2015. Available at: https://cip.gmu.edu/2015/08/20/critical-infrastructure-climate-adaptation/ (17/06/2023).

- Bentsen, Mats; Oliviè, Dirk Jan Leo; Seland, Øyvind; Toniazzo, Thomas; Gjermundsen, Ada; Graff, Lise Seland; Debernard, Jens Boldingh; Gupta, Alok Kumar; He, Yanchun; Kirkevåg, Alf; Schwinger, Jörg; MülleTjiputra, Jerry; Aas, Kjetil Schanke; Bethke, Ingo; Fan, Yuanchao; Griesfeller, Jan; Grini, Alf; Guo, Chuncheng; Ilicak, Mehmet; Karset, Inger Helene Hafsahl; Landgren, Oskar Andreas; Liakka, Johan; Moseid, Kine Onsum; Nummelin, Aleksi; Spensberger, Clemens; Tang, Hui; Zhang, Zhongshi; Heinze, Christoph; Iversen, Trond; Schulz, Michael (2019). NCC NorESM2-MM model output prepared for CMIP6 ScenarioMIP. Version YYYYMMDD[1]. Earth System Grid Federation. doi: 10.22033/ESGF/CMIP6.608.

- Bi, Daohua, Dix, Martin, Marsland, Simon, O'Farrell, Siobhan, Sullivan, Arnold, Bodman, Roger, Law, Rachel, Harman, Ian, Srbinovsky, Jhan, Rashid, Harun A., Dobrohotoff, Peter, Mackallah, Chloe, Yan, Hailin, Hirst, Anthony, Savita, Abhishek, Dias, Fabio Boeira, Woodhouse, Matthew, Fiedler, Russell, Heerdegen, Aidan, 2020: Configuration and spin-up of ACCESS-CM2, the new generation Australian Community Climate and Earth System Simulator Coupled Model. Journal of Southern Hemisphere Earth Systems Science, 70, 225, doi:10.1071/es19040.

- Böhner, J. and Antonic, O. (2009). Land-Surface Parameters Specific to Topo-Climatology. In T. Hengl, & H. I. Reuter (Eds.), GEOMORPHOMETRY: CONCEPTS, SOFTWARE, APPLICATIONS (pp. 195-226). Elsevier Science., in: in T. Hengl, & H. I. Reuter (eds.) Geomorphometry: Concepts, Software, Applications, Elsevier Science, 195–226, 2009. https://doi.org/10.1016/S0166-2481(08)00008-1

- Bröde, P., Fiala, D., Błażejczyk, K., Holmér, I., Jendritzky, G., Kampmann, B., ... & Havenith, G. (2012). Deriving the operational procedure for the Universal Thermal Climate Index (UTCI). International journal of biometeorology, 56, 481-494.

- Brohan, P., Kennedy, J. J., Harris, I., Tett, S. F., & Jones, P. D. (2006). Uncertainty estimates in regional and global observed temperature changes: A new data set from 1850. Journal of Geophysical Research: Atmospheres, 111(D12). https://doi.org/10.1029/2005JD006548

- Bryant, K. M., & Akbar, M. (2016). An exploration of wind stress calculation techniques in hurricane storm surge modeling. *Journal of Marine Science and Engineering*, *4*(3), 58.

- C3S, 2019. https://doi.org/10.24381/cds.e2161bac

- Cowtan, K., & Way, R. G. (2014). Coverage bias in the HadCRUT4 temperature series and its impact on recent temperature trends. Quarterly Journal of the Royal Meteorological Society, 140(683), 1935-1944. https://doi.org/10.1002/qj.229

- Cucchi, M., Weedon,G. P., Amici A., Bellouin, N., Lange, S., Müller, H., Schmied, Hersbach, H., and Buontempo, C. (2020) WFDE5: bias adjusted ERA5 reanalysis data for impact studies, Earth System Science Data https://doi.org/10.5194/essd-12-2097-2020

- Danielson, J. J. and Gesch, D. B.: Global multi-resolution terrain elevation data 2010 (GMTED2010), US Geological Survey, 2011. https://doi.org/10.3133/ofr20111073

- Doms, G., J. Förstner, E. Heise, H.-J. Herzog, M. Raschendorfer, T. Reinhardt, T. Ritter, R. Schrodin, J.-P. Schulz, and G. Vogel (2011), A description of the nonhydrostatic regional COSMO model. Part II: Physical parameterization, 153 pp., Deutscher Wetterdienst.

- Döscher, R., Acosta, M., Alessandri, A., Anthoni, P., Arneth, A., Arsouze, T., ... & Zhang, Q. (2021). The EC-earth3 Earth system model for the climate model intercomparison project 6. Geoscientific Model Development Discussions, 2021, 1-90.

- Eyring, V., Bony, S., Meehl, G. A., Senior, C. A., Stevens, B., Stouffer, R. J., and Taylor, K. E. (2016). Overview of the Coupled Model Intercomparison Project Phase 6 (CMIP6) experimental design and organization, Geosci. Model Dev. 9: 1937-1958. doi:10.5194/gmd-9-1937-2016.

- EC-Earth Consortium (EC-Earth) (2019). EC-Earth-Consortium EC-Earth3-Veg model output prepared for CMIP6 Scenario MIP. Earth System Grid Federation. doi:10.22033/ESGF/CMIP6.727.

- Giorgi, F. (2019). Thirty years of regional climate modeling: where are we and where are we going next?. Journal of Geophysical Research: Atmospheres, 124(11), 5696-5723.

- Good P., Sellar A., Tang Y., Rumbold S., Ellis R., Kelley D., Kuhlbrodt T. (2019). MOHC UKESM1.0-LL model output prepared for CMIP6 ScenarioMIP ssp245. 1]. Earth System Grid Federation. doi:10.22033/ESGF/CMIP6.6339.

- Hersbach, H, Bell, B, Berrisford, P, et al. The ERA5 global reanalysis. Q J R Meteorol Soc. 2020; 146: 1999– 2049. https://doi.org/10.1002/qj.3803

- Huber García, V., Meyer, S., Kok, K., Verweij, P., & Ludwig, R. (2018). Deriving spatially explicit water uses from land use change modelling results in four river basins across Europe. Science of the Total Environment, 628–629, 1079–1097. https://doi.org/10.1016/j.scitotenv.2018.02.051

- Jendritzky, G., de Dear, R., & Havenith, G. (2012). UTCI—why another thermal index?. International journal of biometeorology, 56, 421-428. DOI: https://doi.org/10.1007/s00484-011-0513-7

- Karger, D. N., Lange, S., Hari, C., Reyer, C. P., Conrad, O., Zimmermann, N. E., & Frieler, K. (2022). CHELSA-W5E5: Daily 1 km meteorological forcing data for climate impact studies. Earth System Science Data Discussions, 2022, 1-28.

- Karger, D. N., Conrad, O., Böhner, J., Kawohl, T., Kreft, H., Soria-Auza, R. W., ... & Kessler, M. (2017). Climatologies at high resolution for the earth's land surface areas. Scientific data, 4(1), 1-20.

- Cherchi, A., Fogli, P.G., Lovato, T., Peano, D., Iovino, D., Gualdi, S., Masina, S., Scoccimarro, E., Materia, S., Bellucci, A. and Navarra, A., 2019. Global mean climate and main patterns of variability in the CMCC–CM2 coupled model. Journal of Advances in Modeling Earth Systems, 11(1), pp.185-209. https://doi.org/10.1029/2018MS001369.

- Lenssen, N. J. L., Schmidt, G. A., Hansen, J. E., Menne, M. J., Persin, A., Ruedy, R., & Zyss, D. (2019). Improvements in the GISTEMP uncertainty model. Journal of Geophysical Research: Atmospheres, 124 (12), 6307-6326. Retrieved from https://agupubs.onlinelibrary.wiley.com/doi/abs/10.1029/2018JD029522

- Marsaglia G, Tsang WW, Wang J. 2003. Evaluating Kolmogorov's distribution. J Stat Softw 8:18. DOI: 10.18637/jss.v008.i18

- Martin-Vide, J., & Moreno-Garcia, M. C. (2020). Probability values for the intensity of Barcelona's urban heat island (Spain). *Atmospheric Research, 240,* 104877. DOI: https://doi.org/10.1016/j.atmosres.2020.104877

- McKee TBN, Doesken J, Kleist J, 1993. The relationship of drought frequency and duration to time scales. In Proceedings of the 8th Conference of Applied Climatology, 17-22 January, Anaheim, CA. American Meterological Society, Boston, MA. 179-184

- Meinshausen, M., Nicholls, Z.R., Lewis, J., Gidden, M.J., Vogel, E., Freund, M.B., Beyerle, U., Gessner, C., Nauels, A., Bauer, N., Canadell, J.G., Daniel, J., John, A., Krummel, P.B., Luderer, G., Meinshausen, N., Montzka, S.A., Rayner, P.J., Reimann, S., Smith, S.J., van den Berg, M., Velders, G.J., Vollmer, M.K., & Wang, H.J. (2019). The SSP greenhouse gas concentrations and their extensions to 2500. Geoscientific Model Development Discussions, 1-77.DOI:10.5194/gmd-2019-222

- Merrifield, A. L., Brunner, L., Lorenz, R., Medhaug, I., and Knutti, R.: An investigation of weighting schemes suitable for incorporating large ensembles into multi-model ensembles, Earth Syst. Dynam., 11, 807–834, https://doi.org/10.5194/esd-11-807-2020, 2020.

- Monjo, R. (2016). Measure of rainfall time structure using the dimensionless n-index. Climate Research, 67(1), 71-86.

- Monjo R, Caselles V, Chust G. 2014. Probabilistic correction of RCM precipitation in the Basque Country (Northern Spain). Theoretical and Applied Climatology 117: 317-329. DOI: 10.1007/s00704-013-1008-8.

- Monjo R, Gaitán, E., Pórtoles, J., Ribalaygua, J., & Torres, L. (2016). Changes in extreme precipitation over Spain using statistical downscaling of CMIP5 projections. International Journal of Climatology, 36(2), 757-769. DOI: https://doi.org/10.1002/joc.438

- Monjo R, Pórtoles J, Ribalaygua J. 2013. Detection of inhomogeneities in daily data: a test based in the Kolmogorov-Smirnov goodness-of-fit test. 9th Data Management Workshop of EUMETNET, El Escorial (Madrid), 6th-8th November.

- Morice, C. P., Kennedy, J. J., Rayner, N. A., & Jones, P. D. (2012). Quantifying uncertainties in global and regional temperature change using an ensemble of observational estimates: The HadCRUT4 data set. Journal of Geophysical Research: Atmospheres, 117(D8). https://doi.org/10.1029/2011JD017187

- Müller, W. A., Jungclaus, J. H., Mauritsen, T., Baehr, J., Bittner, M., Budich, R., ... & Marotzke, J. (2018). A higher–resolution version of the max planck institute earth system model (MPI–ESM1. 2–HR). Journal of Advances in Modeling Earth Systems, 10(7), 1383-1413.

- NWS (National Weather Service), 1994: Excessive heat watch, warning and advisory heat index criteria. Regional Operations Manual Letter E-5-94, Eastern Region, NWS, Bohemia, NY. 3 pp.

- O'Neill, B. C., Kriegler, E., Ebi, K. L., Kemp-Benedict, E., Riahi, K., Rothman, D. S., ... & Solecki, W. (2017). The roads ahead: Narratives for shared socioeconomic pathways describing world futures in the 21st century. Global environmental change, 42, 169-180. DOi: https://doi.org/10.1016/j.gloenvcha.2015.01.004

- Patz, J. A., Campbell-Lendrum, D., Holloway, T., & Foley, J. A. (2005). Impact of regional climate change on human health. Nature, 438(7066), 310-317.DOI: https://doi.org/10.1038/nature04188

- Prein, Andreas F., et al. "A review on regional convection–permitting climate modeling: Demonstrations, prospects, and challenges." Reviews of geophysics 53.2, 323-361, (2015).

- Rao, S., Klimont, Z., Smith, S. J., Van Dingenen, R., Dentener, F., Bouwman, L., ... & Tavoni, M. (2017). Future air pollution in the Shared Socio-economic Pathways. Global Environmental Change, 42, 346-358

- Ribalaygua J, Torres L, Pórtoles J, Monjo R, Gaitán E, Pino MR. (2013). Description and validation of a two-step analogue/regression downscaling method. Theoretical and Applied Climatology, 114: 253-269. doi:10.1007/s00704-013-0836-x.

- Rockel, B., Will, A., & Hense, A. (2008). The regional climate model COSMO-CLM (CCLM). Meteorologische zeitschrift, 17(4), 347.

- Seferian R. (2019). CNRM-CERFACS CNRM-ESM2-1 model output prepared for CMIP6 AerChemMIP hist-1950HC. Version YYYYMMDD[1].Earth System Grid Federation. doi:10.22033/ESGF/CMIP6.4041.

- Sengupta, Ushnish, Matt Amos, J. Scott Hosking, Carl Edward Rasmussen, Matthew Juniper, and Paul J. Young. "Ensembling Geophysical Models with Bayesian Neural Networks," 2020. https://doi.org/10.48550/ARXIV.2010.03561.

- Skamarock, W. C., Klemp, J. B., Dudhia, J., Gill, D. O., Liu, Z., Berner, J., ... & Huang, X. Y. (2019). A description of the advanced research WRF version 4. NCAR tech. note ncar/tn-556+ str, 145.

- Slater, L. J., Arnal, L., Boucher, M.-A., Chang, A. Y.-Y., Moulds, S., Murphy, C., Nearing, G., Shalev, G., Shen, C., Speight, L., Villarini, G., Wilby, R. L., Wood, A., and Zappa, M.: Hybrid forecasting: blending climate predictions with AI models, Hydrol. Earth Syst. Sci., 27, 1865–1889, https://doi.org/10.5194/hess-27-1865-2023, 2023.

- Stocks, B. J., Lawson, B. D., Alexander, M. E., Wagner, C. V., McAlpine, R. S., Lynham, T. J., & Dube, D. E. (1989). The Canadian forest fire danger rating system: an overview. The Forestry Chronicle, 65(6), 450-457. DOI: https://doi.org/10.5558/tfc65450-6

- Sun, Xia, Lian Xie, Shahil Umeshkumar Shah, and Xipeng Shen. "A Machine Learning Based Ensemble Forecasting Optimization Algorithm for Preseason Prediction of Atlantic Hurricane Activity." Atmosphere 12, no. 4 (April 20, 2021): 522. https://doi.org/10.3390/atmos12040522.

- Swart N. C., Cole J. N. S., Kharin V. V., Lazare M., Scinocca J. F., Gillett N. P., Anstey J., Arora V., Christian J. R., Hanna S., Jiao Y., Lee W. G., Majaess F., Saenko O. A., Seiler C., Seinen C., Shao, A., Sigmond M., Solheim L., von Salzen K., Yang D. and Winter B. (2019). The Canadian Earth System Model version 5 (CanESM5.0.3), Geosci. Model Dev., 12, 4823–4873, doi:10.5194/gmd-12-4823-2019.

- Thornthwaite CW. 1948. An approach toward a rational classification of climate. Geographical Review 38: 55-94, doi:10.2307/210739

- Vicente-Serrano, S. M., Beguería, S., & López-Moreno, J. I. (2010). A multiscalar drought index sensitive to global warming: the standardized precipitation evapotranspiration index. Journal of climate, 23(7), 1696-1718. DOI: https://doi.org/10.1175/2009JCLI2909.1

- Wilcke, R.A.I. and Bärring, L., 2016: Selecting regional climate scenarios for impact modelling studies. Environmental Modelling & Software 78, 191-201 http://dx.doi.org/10.1016/j.envsoft.2016.01.002

- Wu T., Lu Y., Fang Y., Xin X., Li L., Li W., Jie W., Zhang J., Liu Y., Zhang L., Zhang F., Zhang Y., Wu F., Li J., Chu M., Wang Z., Shi X., Liu X., Wei M., Huang A., Zhang Y. and Liu, X. (2019). The Beijing Climate Center Climate System Model (BCC-CSM): the main progress from CMIP5 to CMIP6 , Geosci. Model Dev. 12, 1573–1600. doi:10.5194/gmd-12-1573-2019, 2019.

- Yukimoto S., Koshiro T., Kawai H., Oshima N., Yoshida, K., Urakawa S.; Tsujino H., Deushi M., Tanaka T., Hosaka M., Yoshimura H., Shindo E., Mizuta R., Ishii M., Obata A., Adachi, Y. (2019). MRI MRI-ESM2.0 model output prepared for CMIP6 CMIP. Earth System Grid Federation. doi:10.22033/ESGF/CMIP6.621.

- Zhang X, Alexander L, Hegerl GC, Jones P, Tank AK, Peterson T, Trewin B, Zwiers F. 2011. Indices for monitoring changes in extremes based on daily temperature and precipitation data. WIREs Climate Change, doi: 10.1002/wcc.147.

- Zorita E, Hughes J, Lettenmaier D, Storch Hv. 1993. Stochastic downscaling of regional circulation patterns for climate model diagnosis and estimation of local precipitation. Max Planck Institute for Meteorology Technical Report 109.

ICARIA
Improving climate resilience of critical assets

More info: **www.icaria-project.eu**

This project has received funding from the European Union's Horizon Europe research and innovation programme under grant agreement No. 101093806. The publication reflects only the authors' views and the European Union is not liable for any use that may be made of the information contained therein.